THE UNIVERSITY *of* EDINBURGH

The Interaction of Light and Temperature on the Phytochrome:PIF Signalling Complex

J R Hemsted

PhD

The University of Edinburgh

2012

Contents

List of Figures

List of Tables

Abbreviations

χ^2	*Chi squared* Goodness of Fit
Δ	The Cost Function
$\sigma_{fr\lambda}$	Absorbance of P_r at wavelength λ
$\sigma_{r\lambda}$	Absorbance of P_r at wavelength λ
k_1	Light dependent phyB activation
k_2	Light dependent phyB deactivation
N_λ	Fluence rate at wavelength λ
P_{fr}	Active phytochrome
P_r	Inactive phytochrome
R_c	Constant Red Light
R_p	Pulsed Red Light
Arabidopsis	*Arabidopsis thaliana (L.) Heynh*
BCA	Bicinchoninic Acid Assay
bHLH	basic helix loop helix
BL	Brassinolide
BR	Brassinosteroid
BZR1	BRASSINAZOLE-RESISTANT 1

CCA1	CIRCADIAN CLOCK ASSOCIATED 1
CO	CONSTANS
Col	*Columbia*
COP1	CONSTITUTIVE PHOTOMORPHOGENIC 1
Cry	Cryptochrome
ELF3	EARLY FLOWERING 3
ELIP2	EARLY LIGHT INDUCIBLE PROTEIN 2
EOD	End of Day
FLC	FLOWERING LOCUS C
FLM	FLOWERING LOCUS M
FR	Far Red
FT	FLOWERING LOCUS T
GA	Gibberellic Acid
GFP	Green Fluorescent Protein
GI	GIGANTEA
HFR1	LONG HYPOCOTYL IN FAR-RED
HIR	High Irradiance Response
HMR	HEMERA
HY5	ELONGATED HYPOCOTYL 5
HYH	HY5 HOMOLOGUE
LD	Long Day
Ler	*Landsberg erecta*

LFR	Low Fluence Response
LHY	LATE ELONGATED HYPOCOTYL
LUC	Luciferase
MS	Murashige & Skoog medium
PAC	Paclobutrazol
PAR	Photosynthetically Active Radiation
Phot	Phototrophins
Phy	Phytochrome
PIF	Phytochrome Interacting Factor
pifq	*pif1pif3pif4pif5*
PNBs	Phytochrome Nuclear Bodies
R	Red
SAM	Shoot Apical Meristem
SVP	SHORT VEGETATIVE PHASE
TOC1	TIMING OF CAB EXPRESSION 1
VLFR	Very Low Fluence Response
WT	Wild Type
Y2H	Yeast 2 Hybrid
YFP	Yellow Fluorescent Protein
ZTL	ZEITLUPE

Acknowledgements

Firstly I would Like to thank Karen Halliday for her excellent supervision of this project. To Ramon Grima for his co-supervision and to Christian Fleck for his supervision during my time in Freiburg. To all the members of the Halliday Lab, in particular Henrik Johansson who has answered a great deal of my questions and Kelly Stewart who was willing to share her Technical expertise. To Richard and Lloyd from workshop who spent a lot of their time making sure the growth rooms were working properly. To Ferenc Nagy and Stefan Kircher for providing seeds used in this study. To the University Triathlon Club who provided challenging form of stress relief in addition to the great socials. To my friends, family and housemates and in particular to my parents, who's continued support has been invaluable throughout my PhD. Finally to Bradley Wiggins and the Members of Team GB who have made the writing process far more bearable.

Declaration

I declare that the work in this Thesis was carried out in accordance with the regulations of the University of Edinburgh. The work is original, except where indicated by specific reference in the text. This Thesis is all my own work except where explicitly stated and no part of the Thesis has previously been submitted for any other academic award.

Joseph Hemsted

31st August 2012

Abstract

Light and temperature are two of the most important non-biological signals that plants must be able to sense and respond to. However, it is not just the individual signals, but the interaction between them that is important. In the dark, Arabidopsis has strongly reduced temperature plasticity. The red light photoreceptor phyB and the PIF family of transcription factors have previously been identified as key regulators of this response. Computer modelling was used to study the interaction between the proteins, to explain counter-intuitive behaviour at certain light conditions. A fluence rate dependent response to temperature was uncovered, where high temperature causes a reversal of the normal seedling response to light. In a PIF and phyB dependent manner, increasing light intensity in the warm can lead to an increase in hypocotyl elongation, the opposite of what has been previously published. This was shown to be dependent on an apically derived response to high fluence rates, independent of the Phytochromes. To extend the analysis beyond the seedling stage, the adult phenotypes of light signalling mutants were subsequently characterised at different temperatures. The temperature dependent control of flowering time and leaf growth were both dependent on Phytochrome and the PIFs, but in apparent opposite directions. This demonstrates that the light signalling system in plants is a complex network of signalling factors, affecting each other in a dynamic process to respond to light and temperature.

Chapter 1

Introduction

As sessile organisms, the ability to sense the local conditions is crucial to flowering plants. Plants must be able to coordinate growth and stress responses with the current environment and a plant with a well adapted pathway, transducing external signals into gene expression and physiological outputs, is much more likely to survive. As autotrophs, plants rely on light as their energy source, and the composition of light can give the plant information such as what time of year it is and how strongly it is competing with nearby vegetation.

Temperature is an important parameter for all living organisms. Plants must be able to cope with the problems of freezing and enzyme denaturation at extreme temperatures [1, 2], but they must also be able to respond across a more ambient range. The loss of water through transpiration is a significant danger at warm temperatures but more generally, the chemical reactions characteristic of life are strongly temperature dependent and plants need to balance these. Being unable to control their internal temperature, plants change their growth architecture to minimise these effects.

The model plant *Arabidopsis thaliana* contains three distinct families of photoreceptor. The UVA and Blue Light absorbing phototrophins (phot) and cryptochromes (cry) and the red light absorbing phytochromes (Phy) [3, 4, 5]. The most important light to plants is the Blue and Red light wavelengths that make up the Photosynthetically Active Radiation (PAR). However, any light conditions provide the plant with

information and *Arabidopsis* can respond to green light [6, 7].

1.1 The Phytochrome Family of Red Light Photoreceptors

1.1.1 Phytochrome is a Dynamically Reversible Molecule

Arabidopsis *thaliana* senses red light through a family of 5 photoreceptors called the Phytochromes. These are divided into the light labile phyA and the relatively light stable phyB-phyE [8]. Phytochrome B (phyB) is the most important member of this family in seedling photomorphogenesis, the change of architecture in the juvenile plant in response to light [9]. These responses include the repression of hypocotyl elongation and the opening of the embryonic leaves called the cotyledons. The light sensing function of Phytochrome comes from its ability to reversibly switch between two conformers with different absorption spectra (Figure 1.1). These are the red light absorbing P_r form and the far red light absorbing P_{fr} form [10, 11, 12]. NMR analysis found structural loops of the bilin binding region were rotated upon light absorption. It was therefore suggested that the P_r and P_{fr} conformers differed in their orientation of the bilin chromophore [13].

The P_r form of Phytochrome is most sensitive to red light (666nm) and the P_{fr} form is most sensitive to far red light (720nm). However, absorption of both conformers occurs at all wavelengths of light and phytochrome also has blue light effects (Figure 1.2) [14]. The conversion rate from P_r to P_{fr} (k_1) is faster than the reverse reaction (k_2) at red wavelengths, so a red light pulse results in the majority of phyB existing in its active P_{fr} form. The opposite is true for a far red light pulse which results in virtually all phytochrome returning to the inactive P_r form [10]. Also observed is a light independent conversion from P_{fr} to P_r, termed dark reversion [15] (Figure 1.1). Therefore at the end of a photoperiod all the active P_{fr} is converted back to P_r with an *in vivo* half life of approximately 60 minutes [16, 17] and a faster *in vitro* half life of approximately 20 minutes [18] when expressed in transgenic yeast. This slow process means Phytochrome is still active in the early part of the night, taking a few hours to revert back to its inactive state [19].

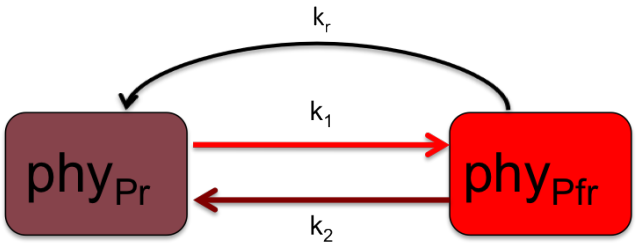

Figure 1.1: Phytochrome is a Reversible Signalling Molecule

Phytochrome will reversibly convert between its inactive (P_r) form and its active (P_{fr}) form based on rates dependent on the wavelength (Figure 1.2). Dark reversion (k_r) is a light independent relaxation to the inactive state.

1.1.2 The N Terminus of Phytochrome is Critical for Light Signalling

Phytochrome is divided into an N terminal region containing the chromophore and a C terminal region required for phytochrome dimerisation and nucleus localisation (Figure 1.3) [21, 20, 22]. Within the N terminal region, the PAS and GAF domains are those most critical to light signalling of the photoreceptor, particularly the light-sensing knot which lies at the N terminal of the PAS domain but passes through a loop of the GAF domain. This region of the protein has also been identified as important for binding the PIF (Phytochrome Interacting Factor) family of bHLH transcription factors [23, 20].

Also contained in the N terminal region is the PHY domain, thought to be important for stabilising the photoreceptor in its active form. The Tongue section of this region interacts with the chromophore and seems particularly important to this role. It has been postulated that it is through the tongue that the chromophore acts to transduce the light signal, changing the structure of the protein [24]. A mutation in this region can lead to the phyB-401 mutant (G564E) which has significantly reduced capacity for phytochrome B deactivtion [25]

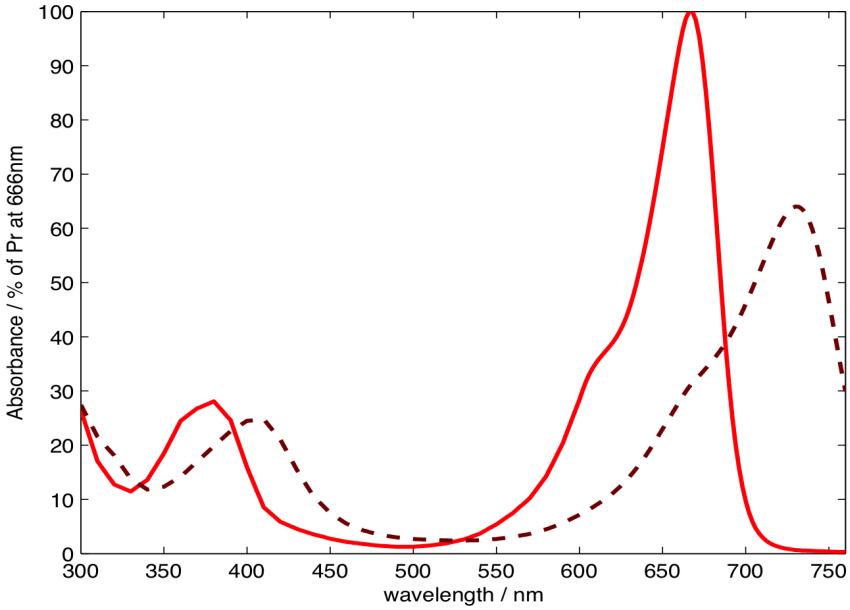

Figure 1.2: The Phytochrome Absorption Spectrum

Absorption of inactive (P_r) and active (P_{fr}) Phytochrome at different wavelength of light as calculated previously [12]

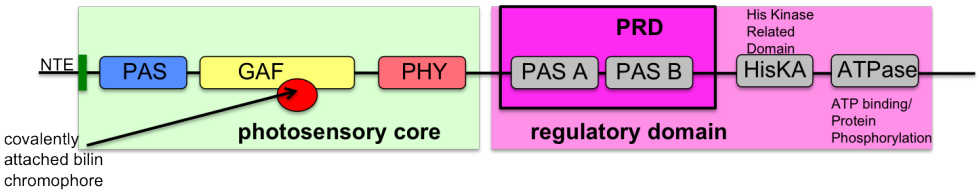

Figure 1.3: Phytochrome Structure

Diagram showing different regions of phytochrome. For a thorough review see [20]

1.1.3 Functional Diversity in the Phytochrome Family

The Phytochrome family of photoreceptors consists of five members labeled phy(A-E). Phytochrome B, D and E are more closely evolutionarily related, with only phyA, B and C conserved across angiosperms [26, 27]. However, phyA is functionally different from the other photoreceptors. It is the most abundant phytochrome in dark grown seedlings but in response to light, autophosphorylates and is rapidly degraded [28]. Despite being very similar structurally to the other Phytochromes, phyA is most active in far red Light ($730nm$), where there is virtually no other Phytochrome activity. Phytochrome A behaves either with a Very Low Fluence Response (VLFR) at any wavelength of low intensity light or a High Irradiance Response (HIR) in high intensity far red light [29]. The anomalous nature of phyA was found to be related to its nuclear shuttling by the carrier proteins FHY1 and FHL which it must dissociate from in the nucleus. This means in order to transduce its signal, phyA must undergo at least one reverse reaction ($P_{fr} \rightarrow P_r$), making it more active in far red light [30].

Phytochromes are involved in a myriad of responses, relating to both the development and mature physiology of the plant [31]. Phytochrome activity is linked to Seedling germination [32], shade avoidance [33], flowering [34, 35], cellulose synthesis [36] and the entrainment of the plant circadian clock [37]. The different Phytochromes having separate but overlapping function [38], with a level of redundancy in Phytochrome signalling. A quintuple *phyAphyBphyCphyDphyEft* will not germinate without exogenous GA in any light condition but the *phyBphyCphyDphyEft* can survive to flowering [39]. The control of hypocotyl growth by phytochrome B is so well established that this phenotype is often used as a marker of phyB activity [40, 41, 42], with short hypocotyls equating to high levels of active photoreceptor. PhyB will delay flowering largely by suppressing levels of *CONSTANS* (*CO*) in the morning, but phyA will accelerate flowering by stabilising CO protein [43, 44]. The phytochromes are able to exist as either homo or heterodimers [45] although the majority of molecules at any one time are in a homodimer formation. Phytochrome A is currently thought only to form homodimers [45, 46] but phytochrome heterodimers have been found in seed extracts [45] and evidence suggests all phyC and phyE is present in heterodimers with

phyB and phyD [47].

1.1.4 Phytochrome Moves into the Nucleus in Response to Light, Localising in Nuclear Bodies

Once activated, phytochrome moves to the nucleus leading to changes in gene expression [48, 49, 50]. PhyA achieves this through the transport proteins FHY1 and FHL [51, 52], with a *fhy1/fhl* double mutant showing no nuclear phyA in high FR [53]. PhyB was originally thought to contain a native NLS [54], but it was recently found that PIF3, and possibly the other PIF proteins act to transport phyB to the nucleus [55]. Phytochrome is not uniformly spread throughout the nucleus, but is instead present in localised foci [56, 57, 58], since termed Phytochrome nuclear bodies (PNBs) [59]. There are two types of nuclear bodies, early and late, which form 2-3 minutes and 4-6 hours after red light induction respectively [56]. The size and number of NBs has been shown to be dependent on the fluence rate of light [60] and PIF3 was found to be necessary for early but not late phyB:GFP speckle formation [61]. Mutants of phytochrome, deficient in signalling, show light dependent nuclear import but do not form speckles [58]. It therefore appears that these speckles are sites of Phytochrome:PIF3 interaction and important to phytochrome function. PhyB derivatives have however been known to trigger the phyB response without forming NBs [62] suggesting they are not absolutely necessary for photomorphogenesis. Necessary to form NBs is the phytochrome signalling component HEMERA (HMR). *hmr* mutants do not form large phyB NBs, and the degradation of PIF1 and PIF3 is impaired [63]. HMR protein binds preferentially to activated phytochrome and accumulates in the light, showing the phytochrome control of PIF degradation is not based solely on the proteins interacting [64].

1.1.5 Phytochrome Signals in Different Modes Dependent on the Quality and Quantity of light

Phytochrome has previously been described as signalling through three distinct mechanisms; the Very Low Fluence Response (VLFR), the Low Fluence Response (LFR)

and the High Irradiance Response (HIR) [65]. Once phytochrome is activated, it takes some time to relax back to its inactive state through dark reversion (Figure 1.1) [16] so a short pulse of light can establish a concentration of active phytochrome able to affect downstream gene regulation. If a physiological response can be achieved through short pulses of light then it is either a VLFR or an LFR. The difference between the VLFR and LFR is based on how much phytochrome must be activated to induce the response. A VLFR only requires a very small P_{fr} % and can be induced by any wavelength of light [66, 30]. An LFR requires a higher proportion of P_{fr} and therefore is typically reversible by far red light [65]. Characteristic of the LFR is that it obeys the Bunsen-Roscoe law of reciprocity [67]. This states that light dependent effects can be induced with hourly light pulses of the same wavelength with the same total fluence as constant light. When this law fails, the extra effect of constant light is defined as an HIR. An HIR has previously only been reported in phyA with constant FR reducing hypocotyl elongation in a manner that can not be recreated by pulses [68]. This is likely to be significant beyond hypocotyl elongation as constant FR has a very strong effect on the induction of several genes such as the Carbon fixing protein Rubisco [69].

$$\begin{aligned} VLFR &= \text{An effect that can be established by pulses of any wavelength of light} \\ LFR &= \text{An effect that can be established by pulses of Red Light. R/FR Reversible} \\ HIR &= \text{An effect that can only be established by Constant Irradiation} \end{aligned} \tag{1.1}$$

1.2 The PIF Family of Transcription Factors

1.2.1 The PIFs are bHLH Transcription Factors that Interact with phyB in Response to Light

The PIF (Phytochrome Interacting Factor) Proteins were identified in a Yeast 2 Hybrid (Y2H) screen for binding partners to Phytochrome B [70]. The strongest binding of these proteins, PIF3, was shown to interact preferably with the P_{fr} form of phyB, providing a mechanism for photoreceptor signal transduction. This binding is reversibly

induced by light. Such that, a far red light pulse inactivating phyB would have the effect of separating PIF3 from the photoreceptor [71]. This action of PIF3 has since been discovered in all other PIFs (PIF1, PIF4, PIF5, PIF6, PIF7, PIF8)[72, 73, 74, 42, 75]. The PIFs are also characterised as a subfamily of the bHLH family of transcription factors; a set of transcription factors which bind to G-Box (CACGTG) motifs [76, 72, 77, 19, 78]. PIF3 can form both homodimers and heterodimers with other PIF family transcription factors and their non DNA binding homolog LONG HYPOCOTYL IN FAR-RED (HFR1) and all combination of PIF heterodimers are thought to be possible [77, 79, 80].

1.2.2 PIFs are Degraded in Response to Red Light in a Phytochrome Dependent Manner

In response to both red and far red light PIF3 is rapidly degraded by the concerted activity of phyA, phyB and phyD [61, 81, 82]. In red light, PIF3 is known to be phosphorylated [83], ubiquitinated and degraded by the 26S proteosome, leading a light steady state level 20% of the dark in a manner independent of CONSTITUTIVE PHOTOMORPHOGENIC 1 (COP1) [81, 84]. A similar behaviour has been seen for the other PIFs [85, 86, 87], with the exception of PIF7 which is thought to be stable in red light [42]. The PIFs have therefore been described of as transiently active transcription factors, working in the dark. Upon light induction, phyB is activated, moves to the nucleus and promotes PIF degradation, transferring the plant to its photomorphgenic state (Figure 1.4) [88].

1.2.3 Transcription of PIF4 & 5 is Regulated by Light, Temperature and the Circadian Clock

The majority of the PIFs have a transcription rate independent of the clock and only weakly dependent on light [89, 19]. However *PIF4* and *PIF5* mRNA is circadian regulated, with levels repressed by the circadian clock at the beginning of the night [90]. In long days, *PIF4* & *PIF5* mRNA is most expressed in the light, so virtually no hypocotyl elongation is observed [91]. In short days, transcription is maximal at the end of the night and during the day. In the light, PIF protein is degraded by phyB, so the only

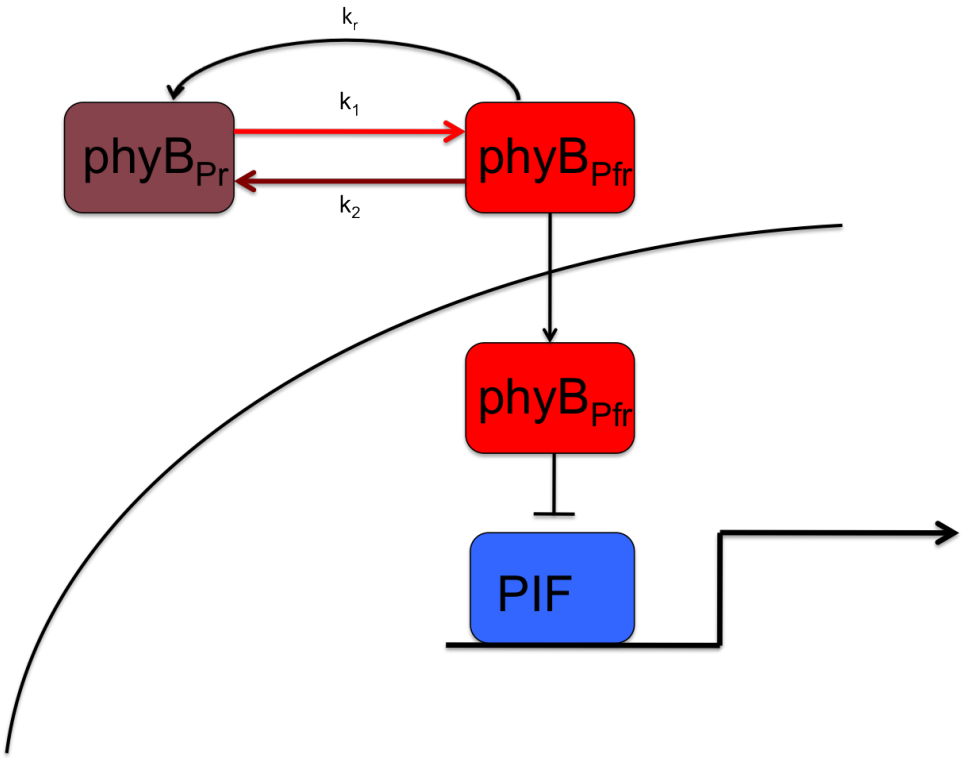

Figure 1.4: Cartoon of Degradation of PIF by Active phyB

Representation of the current paradigm. Active Nuclear phyB degrades nuclear PIF

time of the day that PIF4 and PIF5 protein is present is just before dawn, and this is time of increased hypocotyl elongation [85]. In mutants overexpressing the circadian clock component *CIRCADIAN CLOCK ASSOCIATED 1* (*CCA1*) the transcription of *PIF4* and *PIF5* does not follow a rhythmic pattern, with transcript maintained throughout the subjective night [85]. As a result the protein levels at night are higher, leading to increased hypocotyl and petiole elongation and larger leaf area [92].

Transcription of *PIF4* and *PIF5* is also sensitive to the transfer from darkness to light. While there is no noticeable increase in *PIF3* mRNA, *PIF4* and *PIF5* show increased transcript for 3 hours following transfer to white light [89]. A similar behaviour is seen with high temperature. In hypocotyls both *PIF4* and *PIF5* show an increase in transcript after an increase from 20 to 29°C and in cotyledons, an increase of *PIF4* is also observed [93].

1.2.4 The PIFs Act to Degrade Active PhyB in a COP1 Dependent Manner

PhyB degrades slowly in constant red light with a half life of around 8 hours [16, 84]. This is much more stable than phytochrome A, which has a half life of approximately 30 minutes in normal intensity red light [41]. PIF3, PIF4, PIF5 and PIF7 have been shown to contribute to phyB degradation in a COP1 dependent manner [40, 42, 74, 84]. In addition, the effect of PIFs is additive, in that the *pif3pif7* mutant has higher levels of phyB than *pif7*, and *pif3pif4pif7* has higher levels still. This led to the theory that the PIFs could control hypocotyl length through modulation of phyB levels. The difference in hypocotyl length between WT and *pif3* only becomes apparent 2-3 days after induction of constant red light (R_c) where as statistically different increases in phyB levels in *pif3* are observed after 36 hours [16, 42]. This suggested it is more likely to be the activation of phyB that leads to hypocotyl shortening, rather than the destruction of the PIFs. This idea was supported by the observation that PIF3 affects hypocotyl length by binding to phyB, but not to DNA [40].

1.2.5 P_{fr} Affects PIF Activity in Addition to Protein Levels

Phytochrome B binds to PIF3 at the active phytochrome binding (APB) site [23]. This binding site is necessary for both phyB led PIF3 and PIF3 led phyB degradation [40]. Mutant PIF3 without this binding site was indistinquishable from the null mutant when grown in R_c both in terms of phyB levels and hypocotyl length. *mAPBmAPA*-PIF3 (which is unable to bind phyA or phyB) [23] is significantly more stable than WT PIF3 in red light [42, 83]. A number of mutations in the light-sensing knot of phyB at the junction of the PAS and GAF domains have also been identified with reduced capacity to bind PIFs (Figure 1.3) [94, 95].

mAPBmAPA-PIF3 still promotes the induction of *EARLY LIGHT INDUCIBLE PROTEIN 2* (*ELIP2*) in response to 1 hour red or far red Light [40], but shows a hypocotyl phenotype closer to *pif3* than WT in constant red light. In contrast, PIF3 unable to bind DNA, had no noticeable effect on the hypocotyl phenotype. This suggests the PIFs mediate their effects through the modification of active phyB rather than as transcriptional targets. However, the *pif1pif3pif4pif5* (*pifq*) mutant is constitutively photomorphogenic, so the degradation of PIF proteins by P_{fr} is a significant factor in photomorphogenesis.

PhyB is also able to affect PIF activity through the suppression of the phytohormone Gibberellic Acid (GA). Activated phytochrome has been shown to promote the induction of GA catabolic genes and the repression of GA biosynthetic genes [96, 75]. GA is strongly associated with the control of plant growth, with GA deficient mutant plants dwarf, late flowering and infertile [97]. The DELLA proteins function as a key repressor of GA mediated growth, accumulating in the nucleus and are rapidly degraded in response to GA [98]. DELLA proteins RGA and GAI have been shown to interact with PIF3 and PIF4, suppressing their transcriptional activity [99, 100]. The activation of phyB therefore can lead indirectly to PIFs being sequestered from DNA.

The blue light photoreceptors, cryptochromes interact directly with E3 ubiquitin ligase, COP1, to promote photomorphogenesis [101, 102]. COP1 is also deactivated by

red light, in a manner predicted to be due to phyB [75]. COP1 is the most important factor in skokomorphogenesis, degrading a suite of transcription factors that promote photomorphogenesis, and is predicted to increase PIF stability [88].

PhyB likely interacts with the circadian clock through the evening complex, as complex component EARLY FLOWERING 3 (ELF3) has been shown to contribute to phyB signalling [103, 104, 105, 106]. This complex has recently been shown to control *PIF4* and *PIF5* expression and hypocotyl elongation, providing a further way that phyB can affect the PIFs [90].

1.3 The Regulation by Light on Seedling and Adult Plant Architecture

1.3.1 From Skokomorphogenesis to Photomorphogenesis

Upon initial exposure to light, seedlings signalling undergos a change, from skotomorphogenesis (the dark grown response) to photomorphogenesis, the developmental light response [107]. In the dark, the majority of a seedlings resources are used on hypocotyl elongation as it attempts to reach light. In the natural environment, the developmental change corresponds to a seedling emerging out of the soil. Once the seedling has reached light, photomorphogenesis is the process of reallocating these resources to maximise the quantity of light it receives. This involves the repression of hypocotyl elongation, unfolding of the apical hook to open the cotyledons and the production of chlorophyll [108]. Once the seedling is photosynthetically active, it enters the vegetative stage of growth, producing new leaves and gaining biomass. This is to ensure the plant is in the healthiest possible state for the reproductive stage, where it produces flowers and then seeds.

A number of genes important for photomorphogenesis have been discovered but perhaps the most important is *COP1*. A mutant with reduced *COP1* activity (*cop1-6*) looks photomorphogenic in the dark, with short hypocotyls and open cotyledons [109]. *COP1* encodes an E3 Ubiquitin Ligase, which is nuclear localised in darkness and acts to degrade positive factors of photomorphogenesis such as HY5 and HYH

[110, 111, 112]. It has however also been proposed that COP1 might promote PIF protein accumulation [88]

phyB mutants show the opposite phenotype to *cop1-6*, with mutants looking more dark grown in red light, particularly with regard to hypocotyl phenotype [41]. In response to light, a reduction of nuclear COP1 is observed [113]. The cryptochromes have been shown to deactivate COP1 in blue light [101, 102], and it is predicted that the deactivation of COP1 in red light is due to phyB [75, 114]. However, phyB is known to affect photomorphogenesis through the degradation of the PIFs. Mutants of the PIF proteins show increased sensitivity to light, in an additive manner such that the *pifq* quadruple mutant has a constitutive photomorphogenic phenotype [88]. Suppression of photomorphogenesis in darkness also requires the four-member SUPPRESSOR OF PHYTOCHROME A (SPA) gene family. Seedlings of the *spa1spa2spa3spa4* quadruple mutant exhibit constitutive photomorphogenesis that is very similar to that of *cop1* mutants [115].

The Hypocotyl length of *Arabidopsis* seedlings has long been seen as a read out of phyB activity, there is a very strong correlation between phyB quantity and hypocotyl length of *Arabidopsis* seedlings [42]. Although phyB is known to cause PIF degradation upon activation [87], there has also been the suggestion that PIFs regulate growth through modulation of phyB levels [42]. However, in short days PIF levels appear to directly regulate growth, with maximal growth rates corresponding to maximal PIF protein levels [19, 85]. These changes in PIF levels are controlled by degradation through the phytochromes, and in the case of PIF4 & 5, transcription by the clock.

1.3.2 *Arabidopsis* Responds to the Quality and Quantity of Light

The fluence response curve is a key tool in understanding the adaption of plants to light. Seedlings respond to different intensities of light gradually, with photomorphogenesis occurring faster the more light is present. Seedlings of the same age therefore show hypocotyl elongation inversely related to fluence rate [116]. Given a certain level

of light, far lower than what seedlings would experience in bright sunlight, this fluence rate saturates, with seedlings undergoing maximum photomorphogenesis. The point at which this happens depends on the light conditions, with different responses seen in white, red and blue light [64, 107, 117].

The fluence response of hypocotyl elongation under red light is strongly controlled by phyB [118]. In blue light, cry1 is most important, with separate roles for cry2, phyA and HFR1 [119, 120]. PhyA is the only light receptor to respond to far red light, with *phyA* mutants, or a mutant deficient in phyA nuclear transport *fhy1fhl* appearing virtually blind to FR [52, 121]. While the PIFs are generally associated with red light signalling, blue light will induce the degradation of PIF1, and mutant analysis has identified a function for PIF4 [122, 123]. PHYB is the most important regulator of adult plant growth in long term Red Light, with the other phytochromes acting redundantly [116].

Shade conditions delay germination, cause extended hypocotyls and petioles and early flowering [124]. The sensing of shade in *Arabidopsis* is not based on absolute light levels, but the ratio of red to far red Light. As vegetation absorbs red light more efficiently, conditions under canopy will be highly supplemented with far red light [33]. Even if *Arabidopsis* is not in direct shade, the reflection of far red light by surrounding vegetation can partially invoke a Shade Avoidance Response. Shade is sensed primarily by phytochrome B, although there is involvement of other phytochromes [125]. The Red/Far Red reversibility of phyB allows the R:FR ratio to be detected as the phyB P_{fr} % [126]. In high far red conditions, phyB will be primarily in its deactivated P_r state, leading to responses similar to low level light conditions. The long hypocotyls, stems and petioles, characteristic of shade grown plants are an attempt to reach better light conditions. Plants also flower early to avoid potentially worse shade if an overhead canopy closes above them [33]. The responses to shade in *Arabidopsis* are similar to those of high temperature [127, 128], leading to the hypothesis they may be controlled through similar pathways [129].

1.3.3 Different Photoperiods Affect Plant Development

Critical to a plants reproductive success is its ability to flower at the right time of year. *Arabidopsis* is able to sense the seasons through the relative lengths of day compared to night. It is a facultative long-day plant so flowers earlier under long days (LDs) of 16 h of light characteristic of late spring and summer. Using an external coincidence mechanism between its circadian clock and the external light conditions, the plant shows accelerated flowering in long days and severely reduced flowering in short days [130]. *CONSTANS* (*CO*) mRNA in controlled by the clock but its protein is degraded in the night. During long days, the peak of *CO* mRNA expression coincides with the light, allowing CO to promote the induction of *FLOWERING LOCUS T* (*FT*) [131]. phyB will degrades *CO* in the morning, acting to delay flowering, while phyA promotes flowering by stabilising CO [43, 44, 130].

The growth rate of seedlings is also dependent on the photoperiod. There is a relationship between the length of the days and the extent of hypocotyl elongation, dependent on the PIFs. In arhythmic clock mutants hypocotyl length is directly related to the length of the photoperiod. However, if WT *Arabidopsis* seedlings receive more than 12 hours white light in a day, there is virtually no hypocotyl elongation [91]. This is due to repression of elongation by the clock, which together with the phytochromes regulates hypocotyl elongation in an external coincidence model [85]. Although PIF3 is not under transcriptional control, it is under diurnal regulation by phytochrome and has been shown to be the most important PIF in hypocotyl elongation under short days [19].

1.4 Temperature Control on Seedling and Adult Plant Development

1.4.1 The Temperature Effect on Plant Architecture is Light Dependent

An increase in temperature leads to increased seedling elongation, but this is only observed in the light, with temperature having no effect on the hypocotyl length of dark grown seedlings [127]. Adult plants show reduced biomass when grown in the warm and this is strongly dependent on the phyB photoreceptor. Four week old *phyB* mutant

plants show significantly reduced biomass at high temperature, relative to wild type [132]. This is exacerbated in an *hfr1* background and partly rescued in a *pif4* background, suggesting this temperature effect of phyB is based on its control of PIF4. In blue light, HFR1 has a role in temperature compensation, with *hfr1* mutants looking long in the warm. This growth is dependent on light, with no phenotype seen when the temperature rise is given at night [132]. HFR1 is a PIF-like bHLH transcription factor, that does not bind to DNA [80]. Its major effect is in FR light but also has a function in blue light. Increased temperature is known to have a greater effect on biomass when given during the day in a *SPATULA* dependent manner [133].

1.4.2 Temperature Induced Seedling Growth is Hormonally Dependent

Auxin was the first plant hormone to be identified and its activity is present throughout the plant [134]. Auxin increases expression of some genes and decreases others [135] and exogenous auxin can lead to an increase or decrease in growth, dependent on its concentration and the tissue measured [136]. Auxin signalling is known to contribute to temperature dependent hypocotyl elongation. The *tir1-3* mutants, lacking auxin receptors show a highly reduced warm hypocotyl response, and the *axr1-12* mutant, which is largely resistant to auxin signalling, shows an almost complete loss of temperature response in white light [127]. Microarray analysis has previously identified significant overlap between genes regulated by auxin and PIF4 & 5 [136].

Adding Paclobutrazol to warm grown seedlings abolishes the temperature effect, showing the response is also dependent on Gibberellic Acid (GA) [93], likely through the suppression of DELLA proteins [137]. The biosynthesis of GA is dependent on both phyB, and temperature [93] and the phytohormone is also required for sucrose induced hypocotyl elongation, with the effect diminished in increasing concentrations of the GA biosynthesis inhibitor Paclobutrazol (PAC) [138]. However, auxin and brassinosteroids (BR) also suppress temperature dependent growth in a DELLA independent way, as DELLA quintuple mutants both respond to inhibitors of auxin transport (NPA) and of BR biosynthesis (BRZ) [93].

The Brassinosteroid (BR) activated transcription factor BZR1 has since been shown to interact with PIF4, and synergistically regulate a suite of target genes [139]. These include the PRE family of transcription factors involved in the promotion of cell elongation and suppression of chloroplast development. Indeed, GA, BR and PIF signalling has all been shown to be interdependent on the control of hypocotyl elongation [140]. Ethylene has been found to suppress hypocotyl elongation in darkness [141] while promoting it in light [142, 143] and PIF3 has been implicated in the system [144]. However no temperature effect has been described.

1.4.3 PIF4 & 5 are Temperature Regulated and are Important for Temperature Plasticity

PhyB's light independent deactivation (dark reversion) has been shown to be temperature dependent [145], but the majority of data on temperature inputs into the red light signalling pathway have come through the transcription factor PIF4, and partly PIF5. *PIF4* and *PIF5* RNA accumulate in seedlings following a temperature rise [93, 146]. The protein also accumulates more in the warm, and there is evidence of a temperature dependent phosphorylation [132]. PIF4 is also sequestered and deactivated in a temperature dependent way by HFR1 and DELLA proteins [126, 132, 137]. Recently, PIF4 was also found to bind promoters in a temperature dependent way, due to chromatin modification at high temperatures, so temperature appears to affect PIF4 activity at every level [78, 137].

As a result, an *Arabidopsis pif4* mutant has severely reduced response to temperature. Hypocotyl length, petiole length and leaf angle are virtually indistinguishable in the mutant between $22°C$ and $28°C$ when seedlings are grown on soil [129]. In short days, *pif4* also shows a near complete loss of flowering time response to temperature [137]. PIF4 is necessary for the greatly induced expression of some auxin response genes in high temperatures [129, 147, 148], and has been shown to bind the promoter of IAA29 [80]. It is also however necessary for the temperature increase in auxin biosynthesis [146], so the effect on auxin response genes may be downstream of this.

PIF4 interacts with BR to signal at high temperatures. PIFs and BRASSINAZOLE-RESISTANT 1 (BZR1) act interdependently in promoting hypocotyl elongation [139, 140]. The control of PIF activity is also strongly dependent on GA, due to its suppression of the DELLA proteins [99, 100]. The DELLAs will sequester the PIF proteins, preventing them from binding DNA. This contributes to the suppression of PIF activity at low temperatures [137].

1.4.4 Temperature Control of Flowering Time is Day Length Dependent

Under 12:12 or long day photoperiods, flowering time is relatively insensitive to temperature, with the days to flowering and rosette number only slightly increased in the warm [149]. However, in short days, flowering time is very strongly delayed and this can be overcome by increased temperature. An increase in temperature from $23°C$ to $27°C$ in short day plants is as effective at inducing flowering as moving them to long days [128]. The *phyB* mutant shows an early flowering phenotype at $22°C$ that is completely abolished at $16°C$. The early flowering phenotype seen at $22°C$ is additive with multiple phytochrome mutants showing increasing effects. This is achieved through the regulation of FT expression, which is increased in phytochrome mutants at $22°C$ but not at $16°C$ [35].

It was recently shown that the temperature induction of flowering in short days is strongly dependent on PIF4, with the *pif4* mutant showing severely delayed flowering in the warm [137]. PIF4 shows greatly increased binding to the promoter of FT in high temperatures, with this dependent on nucleosome modification [78]. In addition, the strong repression of flowering was found to be dependent on the DELLA induced suppression of PIF4 and therefore also on GA. These results correlate well with the observed phyB phenotype and may suggest that phyB affects flowering time primarily through PIF4 degradation. If PIF4 does not bind to FT in the cool then the *phyB* mutant would have little effect. However, in warmer temperatures the increased PIF4 levels in a *phyB* background could lead to increased FT promotion and dramatically accelerated flowering.

Other temperature control of flowering may come from the floral repressor *FLOWERING LOCUS C* (*FLC*) and its close homologue *FLOWERING LOCUS M* (*FLM*). Mutants in the autonomous pathway *fca*, *fve*, *fy*, known to regulate FLC show no flowering response to temperature. However the *flc-3* knockout mutants themselves still respond to temperature [150], and it has been suggested *FLC* acts redundantly with FLM and *SHORT VEGETATIVE PHASE* (SVP), which have been shown to control FT transcription and are involved in the temperature response [151]. These regulators may coordinate with PIF4 or act in a separate pathway altogether.

1.4.5 Temperature Compensation on the Circadian Clock is Important for Maintaining Plant Architecture

The plant circadian clock is based on a series of transcriptional feedback loops that interact to produce an approximately 24 hour rhythm [106]. Genes *LATE ELONGATED HYPOCOTYL* (*LHY*) and *CIRCADIAN CLOCK ASSOCIATED 1* (*CCA1*) form part of a morning loop with the *PSEUDO RESPONSE REGULATORS* (*PRRs*). This loop represses *TIMING OF CAB EXPRESSION 1* (*TOC1*) and the evening complex such that the components expression pattern is close to 24 hours. This machinery helps to organise functions such as hypocotyl growth [85] and flowering [131]. A clock matching the external rhythms gives the plant a competitive advantage, increasing carbon fixation and growing faster [152, 92]. The clock is able to entrain to both external light conditions and temperature [153, 154]. Important to the clocks function is its ability to maintain 24 hour rhythms in varying conditions, including changes in temperature. This however is not a trivial task as reaction rates are strongly temperature dependent.

The central oscillator is not itself temperature compensated, but rather the associated genes that make up the clock circuit are [155, 156]. Components *GIGANTEA* (*GI*) and *ZEITLUPE* (*ZTL*) were found to be important components of temperature compensation [155], with *GI* critical for Robust rhythms in the clock at $12°C$ and $27°C$ [157]. However, there is also a role for the *PRRs*, with their negative expression

of *CCA1* and *LHY* varied in different temperatures to help maintain a constant rhythm [158, 159]. LHY and PRR7 show temperature dependent alternative splicing, which may also be significant for temperature compensation [160].

1.5 The Interaction of Light and Temperature

Light and Temperature are vital abiotic signals alone but the interaction between them provides more information than either of the signals in isolation. This interaction is sensed by *Arabidopsis*, with temperature responses in functions such as hypocotyl growth and flowering time gated by temperature. However, little is understood of how the plant integrates these signals and transduce them to a physiological response. In this thesis, I take a multi scale approach to the problem. Examining, in detail, the pathway most strongly implicated in this interaction, the Phytochrome regulation of PIFs. Using a computer modelling approach to explain counterintuitive phenotypes. The response of the seedling to light and temperature is then characterised in relation to this system, with close examination into how far the core phyB:PIF model can control Physiological output. The analysis is then extended to the adult plant, to investigate if the temperature dependent phenotypes of developed *Arabidopsis* can be explained by a system created from juvenile analysis.

Chapter 2

Methods

2.1 Plant Material and Growth Conditions

Plant Material

Unless otherwise stated, plants were in the *Columbia* ecotype and all material used previously described *phyB-9 phyA-211* [161], *pif4-101*, *pif5-3 (pil6-1)* & the cross of these two lines *pif45* [87, 162], *35S:PHYB:GFP* and *35S:PHYB-401:GFP* [163], *phyB-401* [25], *CCA1-OX* [164].

Seedling Growth Conditions

Seeds were surface sterilised and planted on $\frac{1}{2}$ Murashige & Skoog (MS) medium containing either 0.8% agar (Physiology Experiments) or 2% agar (Luciferase Assay, Immunoblotting and qPCR). Seeds were stratified in darkness for 3 days at $4°C$ before light pulsing for 2 hours at $22°C$ and moved to darkness for 22 hours at the same temperature. Seedlings were harvested after 6 days unless otherwise stated. For red light experiments climate controlled Sneijder cabinets were used in a controlled dark room. The peak of red light occurred at 658nm and the spread of the light at half light intensity was ±10.5nm (Figure 2.1). The radiant heat created by the LEDs was measured by HOBO Pendant Temperature/Light Data Logger. These were placed directly under the lights and measured at the highest possible intensity at 17 and $27°C$. In constant light, the cabinets are able to keep the temperature almost completely stable. Under hourly pulses, the temperature does fluctuate slightly, corresponding to the lights being

switched on and off but does not change by more than $0.5°C$ (Figure 2.2).

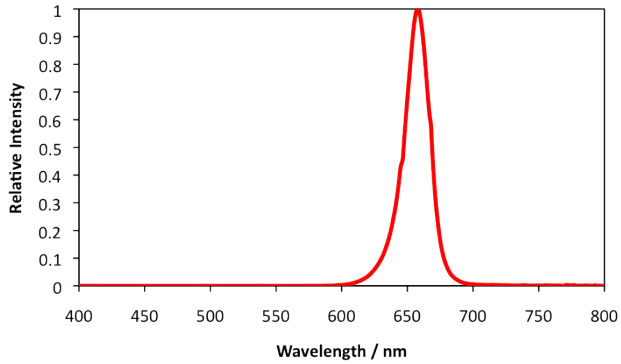

Figure 2.1: Spectrum of Red Light in Growth Cabinets

Fluence rates were measured with a Macam Q201 PAR Radiometer. The different fluence rates in the same experiments were obtained through use of grey filters by LEE. The strength of these are defined by 'STOPs' which reduce light intensity by approximately 50%. We found these reduced 658nm red light by approximately 57% for each 'STOP' and this was used to calculate the effective fluence rates of the covered plates (Figure 2.3).

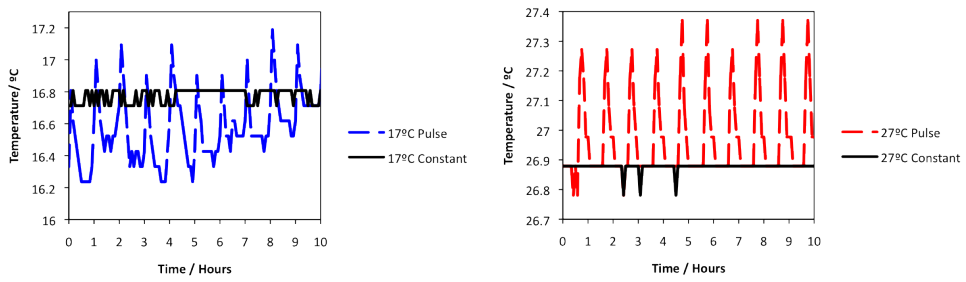

(a) $17°C$ **(b)** $27°C$

Figure 2.2: Temperature of Growth Cabinets Under High Intensity Pulsed (R_p) or Constant (R_c) Red Light

Adult Physiology Growth Conditions

After being established on 0.8 % agar for 7 days, seedlings were transferred to soil in trays containing 24 wells (6x4). Further into the study, plants were spread out to

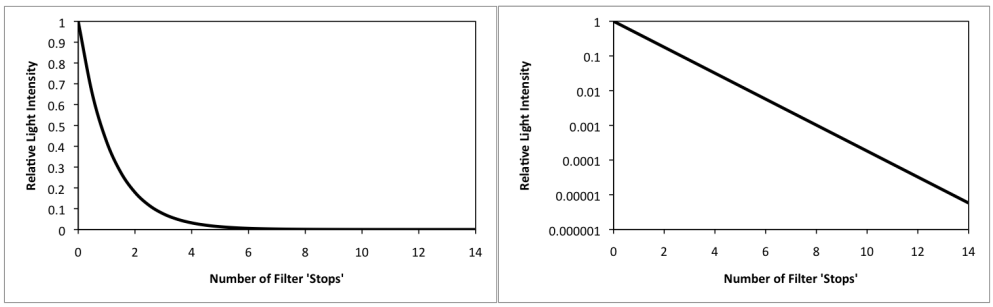

(a) Linear Scale **(b)** *Log* Scale

Figure 2.3: The Effect of Grey Filters on the Relative Fluence Rate

prevent shading as they increased in size. Two growth rooms were be set to short day 10:14 hour photoperiods with temperatures of $17°C$ and $27°C$. An even spread of white light is used with fluence rate of 100 $\mu molm^{-2}s^{-1}$. A slight fluctuation of temperature with day night cycles was observed, but this was relatively stable (Figure 2.4).

There were 12 plants of each mutant at each temperature to measure leaf emergence and flowering time. Eight representative samples were harvested for physiology analysis. At $17°C$ plants were harvested at bolting while at $27°C$ plants were harvested at the end of their life cycle. Leaves were cut and photographed to measure size and petiole length before being individually weighed with a precision balance. Three plants of each mutant had all the leaves weighed and the remaining 5 leaf size measurements were only taken for leaf number 20, 21, 22 (at $17°C$) and 5, 6, 7 (at $27°C$). Leaf number 20, 21 (at $17°C$) and 5,6 (at $27°C$) were individually wrapped in foil for dry mass analysis. The total above ground biomass was then measured. Then the foil wrapped plant was placed in an oven at $80°C$ for 3 days before re-measuring for dry mass.

Hypocotyl, Cotyledon and Rosette Leaf Measurement

For hypocotyl length measurements, seedlings were flattened on their agar plates to reveal the full extent of their hypocotyl phenotype, and images were taken using a digital camera. If cotyledons were to be measured, these were cut off and flattened before a second photograph was taken. Rosette Leaves were flattened with a microscope slide or transparent ruler before a photograph was taken. Measurements were taken using

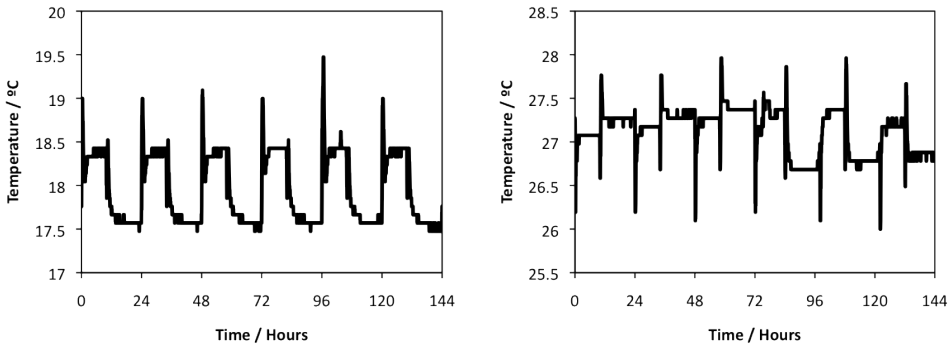

(a) 17 $^{\circ}C$ **(b)** 27 $^{\circ}C$

Figure 2.4: Temperature in Short Day Growth Rooms used for Physiology Experiments

the fiji package of ImageJ (http://fiji.sc/wiki/index.php/Fiji).

2.2 Experimental Techniques

Norflurazon and IAA Treatment

Norflurazon was added to the growth media (0.8% Agar) at a concentration of 50nM as described in [165]. IAA was dissolved in Ethanol and added to 1% Agar as previously described [166]. After 7 days of growth in Diurnal Red Dark Cycles (100 μmol), seedlings were moved onto plates containing either 5μmol IAA or ethanol control.

Extraction of RNA and qPCR

RNA extraction, cDNA synthesis, and qPCR were performed as described previously [132]. Primers used were IPP2 (GTATGAGTTGCTTCTCCAGCAAAG and GAGGATGGCTGCAACAAGTGT), IAA19 (TGGCCTTGAAAGATGGTGAC and TTGCATGACTCTAGAAACATCCC), IAA29(AAGCCCATTACTTCAGTGGTC and ATAAAGCACTGTTGGTACAAGG) HFR1 (AGAGAAGTTCCTTCAGTTACTCG and AACCTTGTCCGTCTTGTGAC).

Immunoblotting and Protein Extraction

Protein Extraction and Immunoblotting was performed as described previously [132]. The Luciferase (LUC) tag was detected by probing the membrane with mouse-anti-Luciferase produced by Sigma Aldrich (http://www.sigmaaldrich.com/catalog/product/sigma/l2164) at a dilution of 1:1000 followed by a HRP-conjugated rabbit-anti-mouse antibody from Agrisera (http://www.agrisera.com/en/artiklar/rabbit-anti-mouse-igg-hl-hrp-conjugated-.html). Loading was checked by reprobing membranes with an anti-UGPase antibody as previously described [132].

The Destructive Luciferase Assay

A Quantitative, Luciferase Assay based on harvested samples and measured by a plate reader has been developed by *Promega*. This allows measurement of LUC tagged proteins to be achieved in a much more accurate and directly quantifiable way than can be achieved with traditional Immunoblot. The readings are linear to the quantity of Luciferase (Figure 2.5). Seedlings are harvested into liquid nitrogen, ground to a fine powder in the cold before addition of *Cell Culture Lysis Reagent* and placed on a 96 well plate. A Luciferin based, *Reporter Lysis Buffer* is injected into the plate by a MicroLumatPlus LB96V Microplate Luminometer and Luminesence Measured.

Internal Protein Control is obtained by the BCA protein Assay. Samples must be first washed with *Compat-Able* Protein Assay Preparation Set .

http://www.promega.com/resources/protocols/technical-bulletins/0/luciferase-assay-system-protocol/
www.piercenet.com/instructions/2161308.pdf
www.piercenet.com/instructions/2161296.pdf

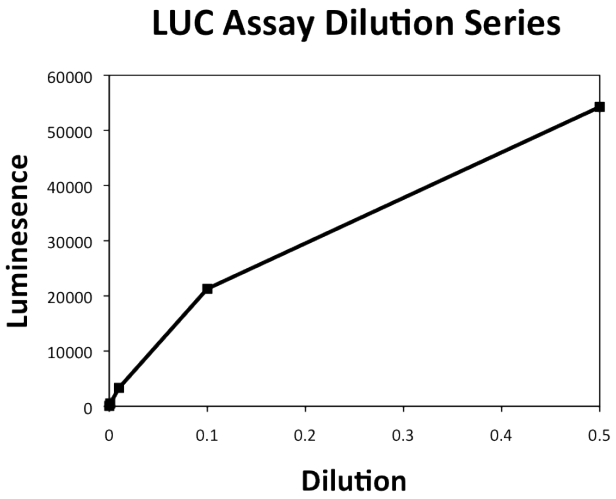

Figure 2.5: Dilution Curve of Destructive Luciferase Assay

An overexpressing 35S:LUC line is grown for 4 days before a serial dilution. The curve shows the assay is strongly linear up to 20,000 Units and is close to linear up to 50,000 units.

Chapter 3

Modelling Mutual Phytochrome and PIF Dependent Degradation

3.1 Introduction

3.1.1 PhyB and PIF Mutually Regulate Their Protein Levels

Key to the function of phytochrome is its ability to reversibly switch between its active and inactive forms (P_r & P_{fr} respectively) (Figure 1.1). In response to light, the protein will change conformation, leading to downstream events and ultimately changes in gene expression [10]. PhyB is maximally activated by red light ($\approx$ 660nm) and maximally deactivated by far red light ($\approx$ 720nm), but both these conversions can take place at any wavelength (Figure 1.2) [12, 167]. In the dark active phytochrome slowly relaxes back to the inactive form in a process termed dark reversion [15]. This process is relatively slow and therefore phyB remains active through a proportion of the night [16, 19]. PhyB can be deactivated before the night with the addition of an End of Day (EOD) Far Red Pulse. This treatment leads the plant to display a shade avoidance phenotype; early flowering and enhanced elongation of hypocotyls and petioles [34, 163, 168, 169].

The PIF family of proteins are highly unstable in response to light [61, 81]. Following the induction of red light, PIF3 will rapidly degrade with a half life of approximately 15 minutes before reaching a new steady state about 20% of its dark level. Other PIF

family members show the same general pattern of degradation [85, 86, 87]. The degradation of the PIFs is dependent on active phytochromes with a level of redundancy between phyB, phyA and phyD [61]. The PIFs have been shown to preferentially bind the active P_{fr} form of the photoreceptor which then targets them for degradation via the 26S proteasome [82]. This degradation is generally thought to be the cause of a change in PIF activity in the light, particularly regarding growth [19, 85]. As PIF3 is able to form dimers with light stable PIF7, as well as other light stable bHLH transcription factors this may be significant for PIF stability as a whole [77], but the significance of these dimers is not currently known.

Like the PIFs, phyB degrades in constant red light, but with a much longer half life of around 8 hours [16, 84] compared to 15 minutes for PIF3. This degradation has been found to be dependent on the PIFs [40], with PIF 3,4 and 5 degrading phyB additively in a COP1 dependent manner [84]. PhyB and PIF3 must form a complex in order to be subsequently degraded. A *pif3* mutant that is unable to bind phyB ($mAPAmAPB$) is relatively stable in red light [74] and has no affect on phyB degradation [40].

The general dogma has been that phytochrome controls growth through degradation of the PIFs [19, 85]. However, under some conditions, such as constant red light, PIFs appear to be controlling growth through regulation of phytochromes [42]. This dual action was described as *Mechanistic Duality* whereby PIF3 would act as a transcription factor normally, but then degrade phyB in long term constant red light [40]. These contrasting results however suggest a level of feedback, such that the light signalling mechanism is more accurately described as a system than a pathway. It is uncertain how such a system would fit together, but as the components are fairly well defined [8, 75] much can be learned from a modelling approach. The construction of a series of simulations will test what is necessary to achieve this level of mutual feedback.

The starting point for these models is that PIF3 and phyB must mutually regulate each others levels, either directly or indirectly. Through parameter search by a cost function, the ability of the model to recreate observed degradation dynamics is simulated. The models can then be tested through their behaviour under different

conditions and their ability to make new predictions. The abundance of both phyB and PIF3 changes drastically in response to light. This change in protein levels is the simplest way to explain changes in growth. The conflict in the literature can then hopefully be solved through this modelling approach, either giving a mechanism for how PIFs could control growth through phyB or give a reason for why it may appear that way.

3.2 Model Construction

3.2.1 Modelling Biological Systems as a Series of Ordinary Different Equations

This work was done while working with the Theoretical Lab of Dr Christian Fleck at the University of Freiburg

The Models were constructed as a series of ordinary differential equations (ODEs). Each component of the system is described by an individual ODE, as shown previously for the nuclear localisation of phytochrome [16]. The photoconversion of phytochrome between its P_r and P_{fr} forms has been well characterised over the entire spectrum [12, 167] and therefore these values are used for the light dependent activation of phyB k_1 ($P_r \rightarrow P_{fr}$) and the light dependent deactivation k_2 ($P_{fr} \rightarrow P_r$). Dark Reversion, the light independent relaxation of P_{fr} back to P_r is initially taken from published work [16], and is represented by the parameter k_r. This mathematical representation of phyB is consistent throughout the models and represented in equation (3.1) and Figure (3.1). Parameters j_s and j_d represent the synthesis and degradation of phytochrome respectively.

Table 3.1: Definition of Parameters Related to Phytochrome

Parameter	Definition
k_1	Light Dependent phyB activation
k_2	Light Dependent phyB deactivation
k_r	Dark Reversion (Light Independent phyB deactivation)
j_s	Phytochrome Synthesis
j_d	Phytochrome Degradation

$$\begin{aligned} \dot{P_r} &= j_s - (k_1 + j_d)\, P_r + (k_2 + k_r)\, P_{fr} \\ \dot{P_{fr}} &= k_1 P_r - (k_2 + k_d + k_r)\, P_{fr} \end{aligned} \tag{3.1}$$

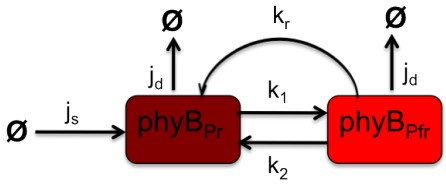

Figure 3.1: Cartoon of phyB Activity in Mathematical Models

In the mathematical models, inactive (P_r) and active (P_{fr}) are represented by individual Ordinary Differential equations. On activation of the protein, P_r levels are reduced and P_{fr} levels increase by the same amount.

The majority of work on PIF degradation mechanics has been on PIF3 [61, 81, 82]. In constant light we see an initial fast degradation, followed by stabilisation at a different steady state. A similar behaviour has also been described for PIF 1, 4 and 5 [86, 87] and the degradation of phyB is thought to be dependent on all the PIFs, independent of their stability [84]. PIF3 protein data will therefore initially be used as a proxy for the levels of the whole PIF subfamily. The models are calibrated towards a qualitative result; aiming to produce a system with rapid PIF degradation not leading to complete depletion [61, 81, 82] and a much slower degradation of phyB [75]. A representation of the optimal result is shown in Figure (3.2).

3.2.2 The Cost Function ($\triangle$) is Minimised to Fit the Data

The models were initially fitted to an optimal solution based upon the behaviour of phyB and PIF3 protein in etiolated seedlings moved into constant red light [61, 81, 82, 16]. PIF degradation is represented by a simple step function and PhyB degradation by exponential decay, assuming different rates for light dependent and independent degradation (σ & κ respectively). PhyB levels are calculated relative to their dark levels and represented by an exponential decay (3.2). Derivation of this equation is shown in (S1.1).

$$\begin{aligned} \kappa &= \text{light independent degradation} \\ \sigma &= \text{light dependent degradation} \\ t &= \text{time} \\ [\text{phyB}] &= \tfrac{\kappa}{\kappa+\sigma}\left(1+\tfrac{\sigma}{\kappa}e^{-(\kappa+\sigma)t}\right) \end{aligned} \tag{3.2}$$

The ideal solution has PIF levels to be 20% of their dark value after $\frac{1}{2}$ hour in red light (Figure 3.2). A cost function (Δ) minimises the difference between the optimal function (Figure 3.2) and simulated data. This cost function is used to fit parameters of the model. The differential equations were solved in MATLAB by the stiff solver *ode15s* and the cost function minimised by the parameter search technique *lsqnonlin*, which is based on an interior reflective Newton method [170, 171]. The output of the cost function is the reduced_χ^2 statistic. This gives a measurement of how closely the model can approximate the data, while punishing its complexity. With a large number of variable parameters a model may be able to fit a data set without bearing any relation to the true mechanism. In many cases the parameter sets proved to be non-identifiable, meaning the parameter set found by the cost function depends on the starting parameters. For this reason, the parameter search was performed many times, with different starting values from parameter space selected with Latin hypercubes of a minimum size of 10 [172]. This ensures the parameter space is well represented.

3.3 Results

3.3.1 A Binding Cofactor or Tagging Step is Necessary to Explain the Mutual Degradation of Phytochrome B and PIF

That a transcription factor (PIF) has post transcriptional control of a light receptor (phyB) [40] is not intuitive, going against the expected behaviour of signal cascades [10]. The relatively stable half life of phyB [16, 84] suggested that the system of degradation appeared more complex than a simple feedback loop, as PIF3 is affecting Phytochrome

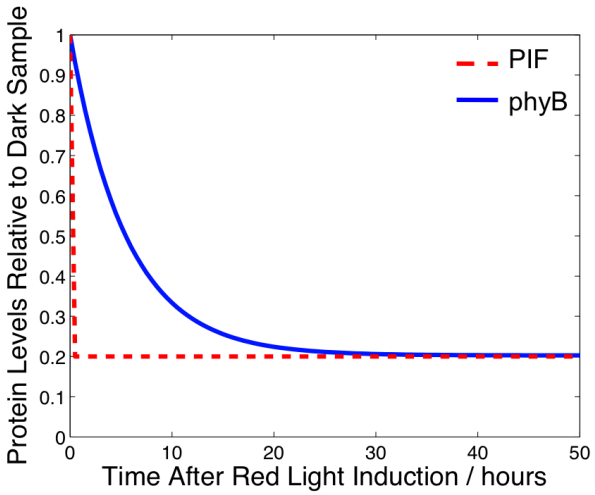

Figure 3.2: Optimal phyB and PIF Degradation Rates

Graphical representation of the optimal solution. Upon red light induction, phyB degrades as described in (3.2) with parameters κ and σ given as $0.00061 min^{-1}$ and $0.0024 min^{-1}$ respectively. PIF reaches a new steady state 20 % of its dark value after 30 minutes. The difference between this optimal solution and the simulated data is the cost function (Δ).

at a constant rate even though it is being degraded itself. Starting with the most simple possible model ((S1.2), Figure 3.3a), a series of possible explanations for the data were hypothesised and models constructed accordingly (Section S1). By building up iteratively from the most simple system we aim to find the minimal model able to describe the data. The degradation speeds of phytochrome and PIF were fitted to the ideal solution (Figure 3.2) through the cost function to test how accurately the models could explain the data. The exact definition of the parameters differs slightly with various models, but closely follows those shown (Table 3.2).

Some of the initial models were not able to accurately describe the data (Figure 3.4a, *Simple Mutual Degradation* (S1.2)) and could be dismissed immediately. Others were able to show the degradation effect but made clear qualitative errors such as the behaviour of a *pif3* mutant behaving in the opposite way to the literature (Figure 3.4b, *Indirect phyB Degradation* (S1.3)[40]). As these models are simplified to include only 1 species of PIF, the *pif* mutants should show no degradation of phyB at all, and this is true for all other models investigated. This model can therefore also be dismissed at this stage. Therefore, as expected, a larger number of components are needed in the

Table 3.2: Definition of the Parameters used in Section 3.3

Parameter	Definition
α	phyB synthesis rate
β	phyB dark degradation rate
k_s	PIF3 synthesis rate
k_d	PIF3 dark degradation rate
x_s	Synthesis of Protein 'x'
x_d	Degradation of Protein 'x'
k_1	Light Dependent phyB activation
k_2	Light Dependent phyB deactivation
k_r	Dark Reversion (Light Independent phyB deactivation)
μ	PIF3 Light degradation rate
ν	phyB Light degradation rate
γ	Complex Formation Rate
ρ	Complex Dissociation Rate
δ	PIF/ phyB tagging rate

system to explain the data.

However there are a number of different ways of achieving the desired phenotype of a large difference in degradation rate for the two proteins (Figure 3.4). These are dependent on a separate pool of either PIF or phyB with altered activity. Differential equations are given in Appendix S1 (*Double Tagging* S1.4, *PIF Protection* S1.5, *Phytochrome Support* S1.6, *PIF Heterodimers* S1.8). In particular a near perfect solution is found for the *Double Tagging* model (Figure 3.4c, S1.4). This provides initial evidence for the impact of separate proteins on the degradation mechanics.

Double Tagging

Prior to degradation, PIF3 is phosphorylated and ubiquitinated [83] and phyB undergoes ubiquitination in a PIF3 dependent manner [84]. In an extension to Simple Mutual Degradation (Figure 3.3a), PIF and active phyB catalyse each others tagging rather than their degradation (Figure 3.3c, (S1.4)). The *Double Tagging* model is able to recreate the degradation rates very accurately (Figure 3.4c).

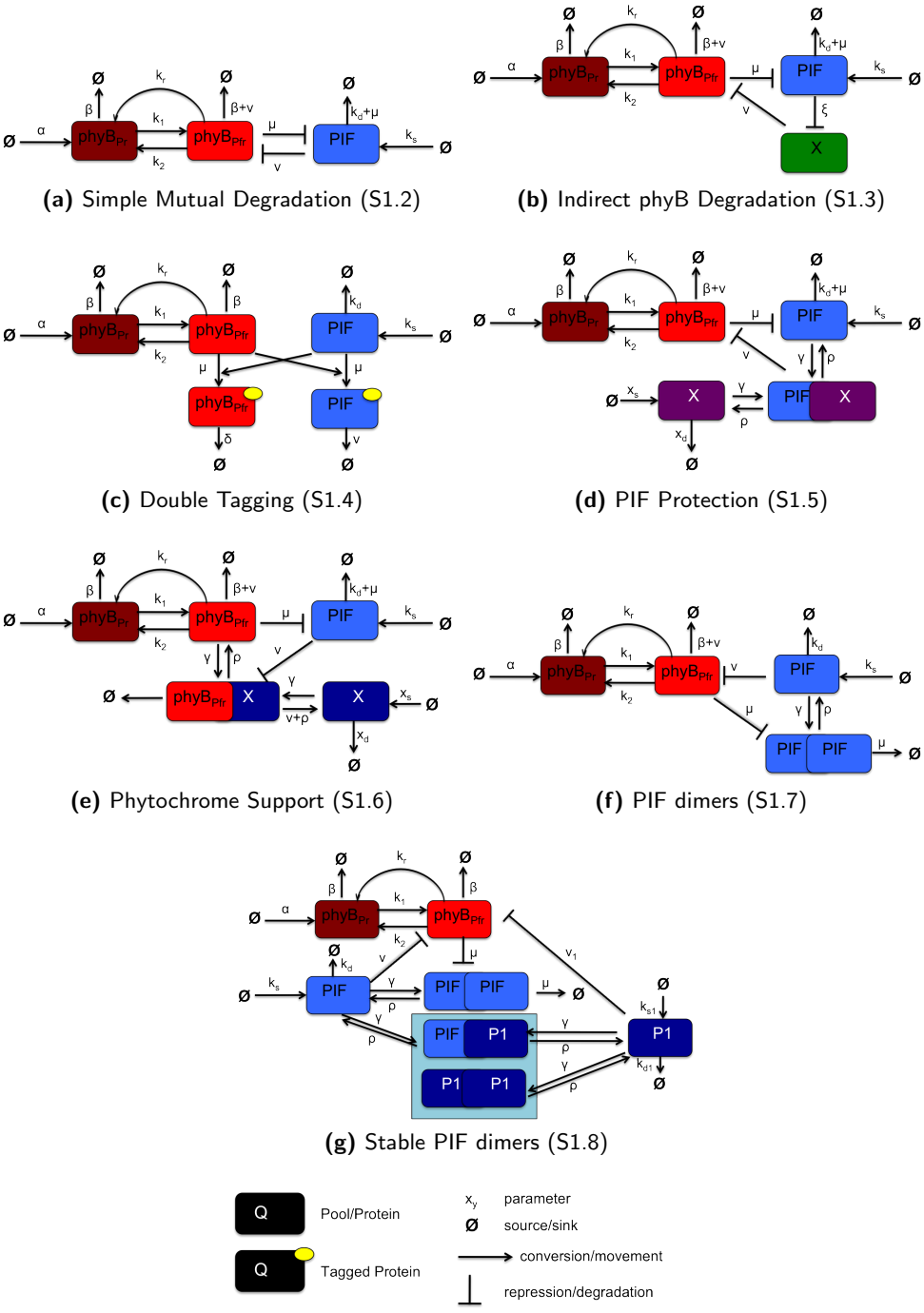

(a) Simple Mutual Degradation (S1.2)

(b) Indirect phyB Degradation (S1.3)

(c) Double Tagging (S1.4)

(d) PIF Protection (S1.5)

(e) Phytochrome Support (S1.6)

(f) PIF dimers (S1.7)

(g) Stable PIF dimers (S1.8)

Figure 3.3: Cartoon Representation of Models Discussed in Section 3.3 and Appendix S1

Cartoons showing models (S1.2, S1.3, S1.4, S1.5, S1.6, S1.7 & S1.8) The Labile PIF dimer model (S1.9) is too complicated to be shown in this form but is similar to The Stable PIF dimer (Figure 3.3g) with an added set of dimer permutations.

Protection & Support

A common way a biological molecule can change function is through binding to a co-factor. Models were constructed where an unknown molecule altered the activity of the $phyB : PIF$ complex.

In the *Protection* and *Support* models, formation of the $phyB : PIF$ complex normally results in the degradation of PIF. However if cofactor X is bound to this complex, phyB is degraded. Both these models make use of this mechanism, they only differ in the order of complex formation. PIF *Protection* (Figure 3.3d , (S1.5)), allows X to bind to PIF in the dark, meaning phyB cannot degrade this pool upon light activation. In phytochrome *Support* (Figure 3.3e , (S1.6)), X binds instead to activated P_{fr}. On initial light activation the PIF molecules are unbound and able to be degraded. It is only in longer term light that the cofactor is able to bind phyB, leading to its PIF dependent degradation.

Both these models allow for the difference in degradation times between the proteins (*Protection*, Figure (3.4d), *Support*, Figure 3.4e)). Neither of these are as accurate as the simulations seen with *Double Tagging* but estimate the ideal solution close enough that they could provide the correct mechanism.

PIF Dimers

PIF3 is able to form both homodimers and heterodimers with other PIFs and similar bHLH Transcription Factors such as HFR1 [77]. Three separate models, able to explain the data, rely on PIF monomers and dimers behaving differently when coming into contact with Phytochrome. The essence of these models is that a monomeric form of PIF is able to bind phyB on a separate part of the molecule, leading to degradation of the photoreceptor. When in its dimer formation, PIF is degraded by phyB in its normal way. If dimeric PIF would also bind to DNA, this could give an explanation for the *Mechanistic duality* described for some PIFs [40].

The simple model, only taking one type of PIF into account (Figure 3.3f, (S1.7))

can recreate a difference in degradation rates, but not enough to accurately match the data (Figure 3.4f). The addition of a light stable PIF (Figure 3.3g, (S1.8)) greatly improves the accuracy of the fit (Figure 3.4g). Further complicating the model with more light labile PIFs which do not contribute to the quantification (S1.9) does not further improve the fit and so this level of complication should be deemed unnecessary (Figure 3.4h).

3.3.2 Constrainment by Light Pulse Data aids Model Selection

Short pulses of light, activating phyB, are sufficient to affect growth [68] and it was confirmed by collaborators that PIF3 levels are also affected by a pulse. A 1 minute pulse of red light will lead to PIF3 degradation qualitatively similar to that observed for constant light. PIF3 rapidly degrades with a half life of around 15 minutes, resulting in a steady state 20% of the dark level and it does not start to re-accumulate until at least 60 minutes in darkness (Figure 3.5). With this added information, further constraints on the models can be included to take account of short light pulse conditions. The models must be able to recreate the observed PIF degradation after a short light pulse with the same parameter set that can explain constant light degradation. As the models are not being specifically fitted to this new data, only a qualitative response is looked for after a simulated 0.1hr (6 minute) red light pulse (Figure 3.6).

We see that the double tagging (Figure 3.6a) (equation (S1.4)) and protection (Figure 3.6b (equation S1.5)) models reproduce observed PIF3 behaviour following a light pulse. The previously calculated parameters show a fast degradation of PIF3 followed by a slow re-accumulation in the dark. However the phytochrome support model (Figure 3.6c, equaion S1.6) only shows a slow PIF3 degradation and therefore can be discounted at this stage.

The PIF dimer model (Figure 3.6d), may fit the data. This analysis however shows the double tagging and protection models performed the best, and therefore may provide the most accurate representation of the pathway. This demonstrates the impor-

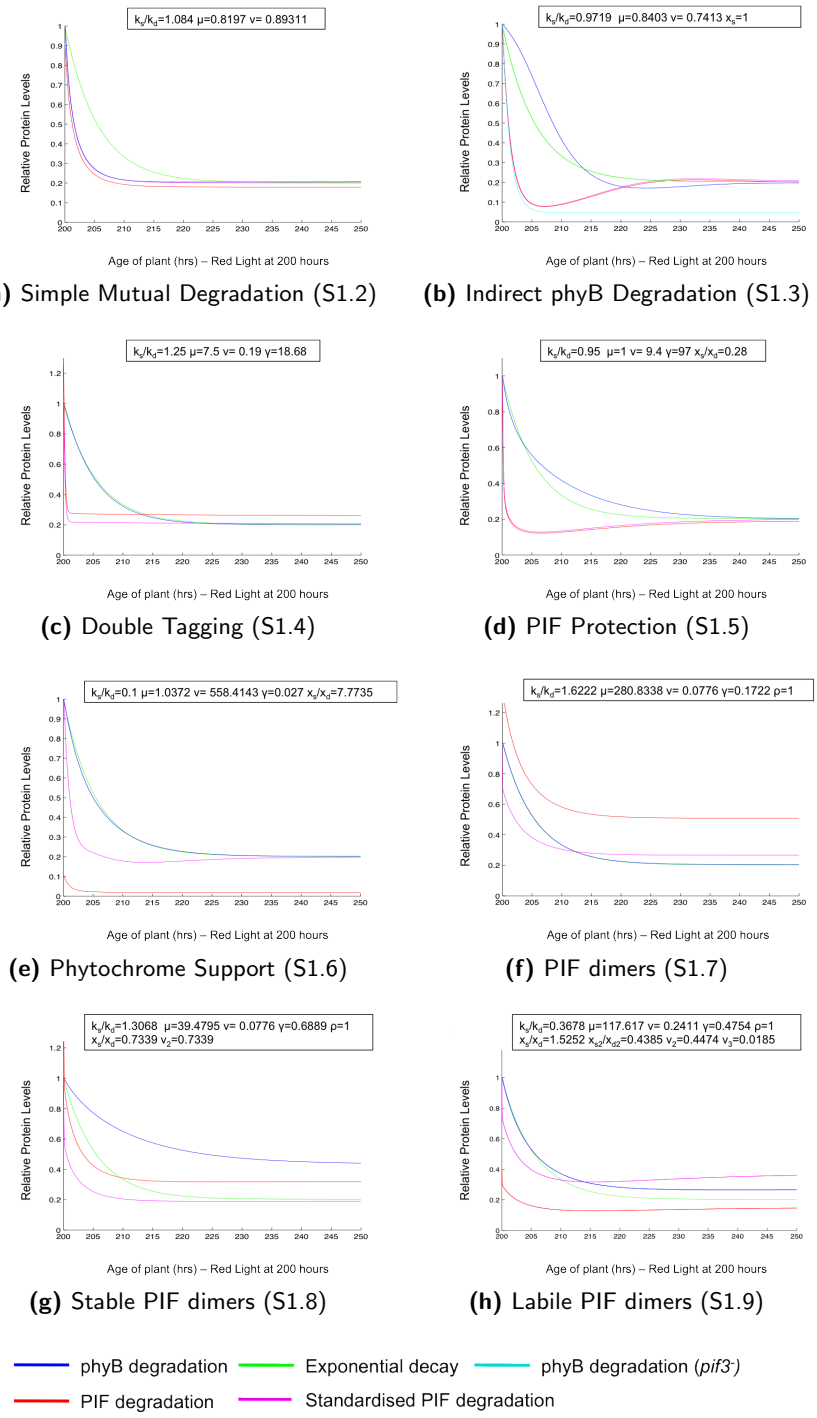

(a) Simple Mutual Degradation (S1.2) **(b)** Indirect phyB Degradation (S1.3)

(c) Double Tagging (S1.4) **(d)** PIF Protection (S1.5)

(e) Phytochrome Support (S1.6) **(f)** PIF dimers (S1.7)

(g) Stable PIF dimers (S1.8) **(h)** Labile PIF dimers (S1.9)

Figure 3.4: Simulated data from Models shown in Figure (3.3) After Parameter Fitting to Constant Light Conditions

Results from simulations of models (S1.2,S1.3, S1.4, S1.5, S1.6, S1.7, S1.8, S1.9) after fitting to the cost function described in (3.2.2) and shown graphically in Figure (3.2). Simple mutual degradation and Indirect phyB degradation (Figures 3.4a & 3.4b) are unable to describe the data but all other models are. Models are stabilised in darkness before being moved to constant red light at 200 hours.

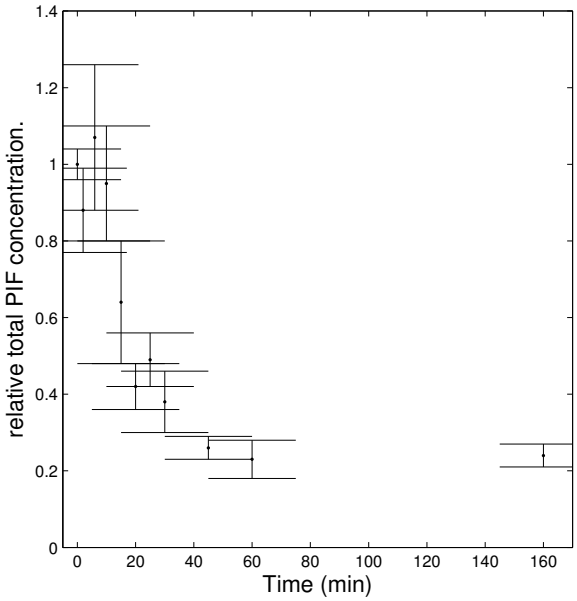

Figure 3.5: Quantified Levels of PIF3:LUC Following a Red Light Pulse

PIF3:PIF3:LUC seedlings are given a 1 minute pulse of red light and samples harvested at different times after movement to darkness. The data shows a rapid degradation of PIF3 followed by a new lower steady state, in the same pattern as previously reported for constant light [16, 61, 81, 82].
This Experiment was performed by Collaborators at the University of Freiburg

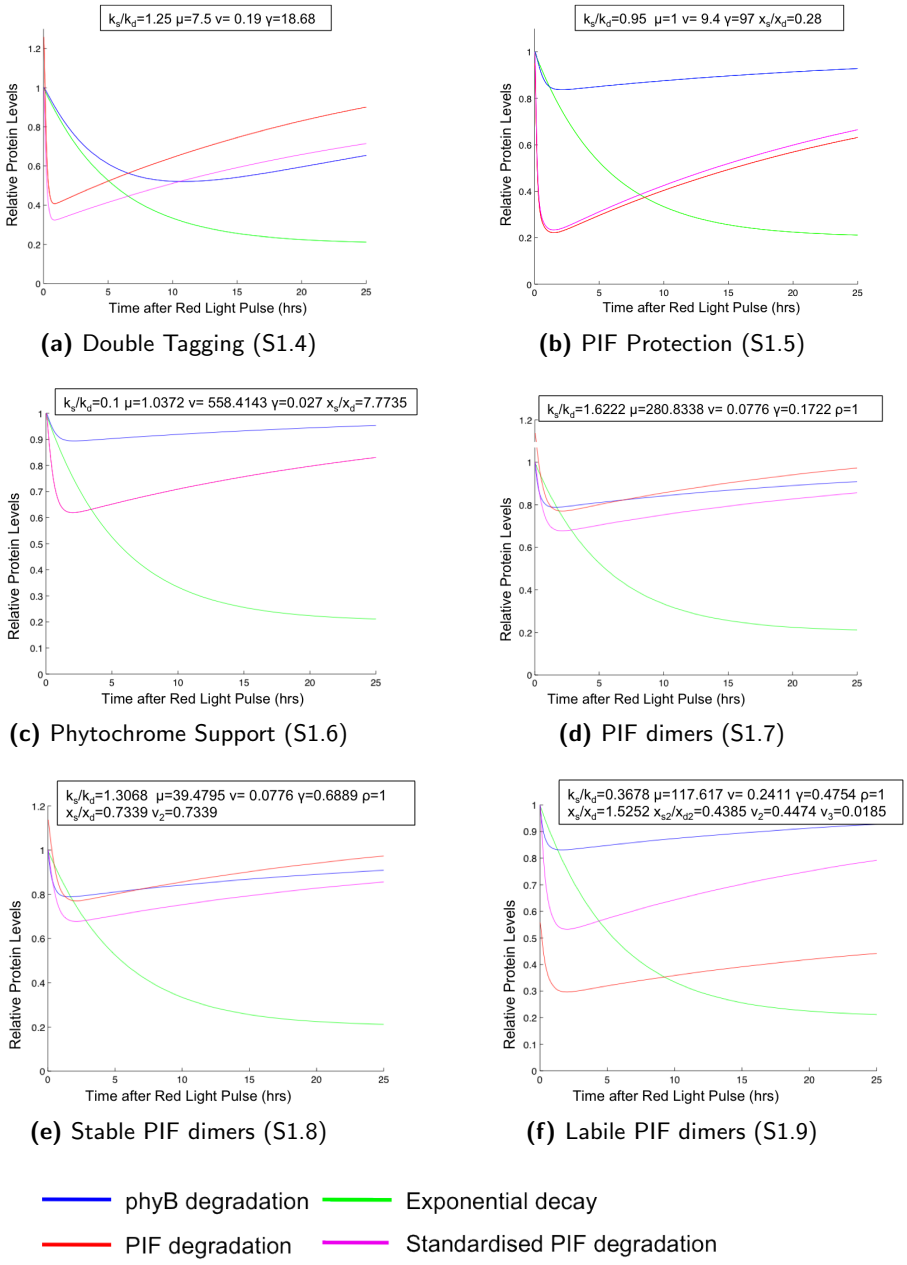

Figure 3.6: Behaviour of Models Following a 6 minute Red Light Pulse

Models found to accurately recreate degradation mechanics in constant light S1.4,S1.5,S1.6,S1.7,S1.8,S1.9 (Figure 3.4) were subjected to 0.1 hours of red light to see if experimental observations can also be recreated here

tance of high light sensitivity to the model. Phytochrome B is very sensitive to light and requires only a short pulse to cause PIF3 degradation. Only the double tagging and protection are able to provide that level of sensitivity (Figure (3.6a),(3.6b)).

3.4 Quantitative Data

A series of quantitive data was created at the University of Freiburg, subsequently allowing these models to be fitted to real results. Through the use of mutant lines where PIF3 is tagged with the reporter gene Luciferase (LUC) [173]. In addition to the time dependent degradation previously described (Figure 3.5), degradation of the protein in different wavelengths and light intensities were also tested (Figure (3.7b) & (3.7a)). A quantified phyB immunoblot also performed at Freiburg is also included here. This shows the degradation of phyB in constant red light (Figure 3.7d).

3.4.1 PIF3 Levels are More Sensitive to a Light Pulse than Constant Irradiation

The steady state behaviour of PIF was looked at in a number of different light conditions. Using results from [12, 167] the wavelength and intensity of light necessary to produce a given proportion of active phyB was calculated. *Arabidopsis* seedlings were then either treated with constant light for 60 minutes (Figure 3.7a), or given a 1 minute light pulse followed by 59 minutes of darkness (Figure 3.7b). The time of 60 minutes was chosen as initial results suggested this was the length of time required for PIF to reach steady state (Figure 3.5). The x axis represents the calculated proportion of active phyB (P_{fr}), and the y axis show the total levels of PIF3:LUC.

Interestingly these results indicate that a light pulse is more efficient at degrading PIF3 than constant light, in contrast to the idea that phyB becomes more active with increased light. A light pulse causing activation of only 20% of phyB is sufficient to degrade PIF3 to 20% of its starting value after an hour. However, the same phyB activation in constant light, only degrades half of PIF3 in the same time frame. This is a result to be investigated through the modelling approach

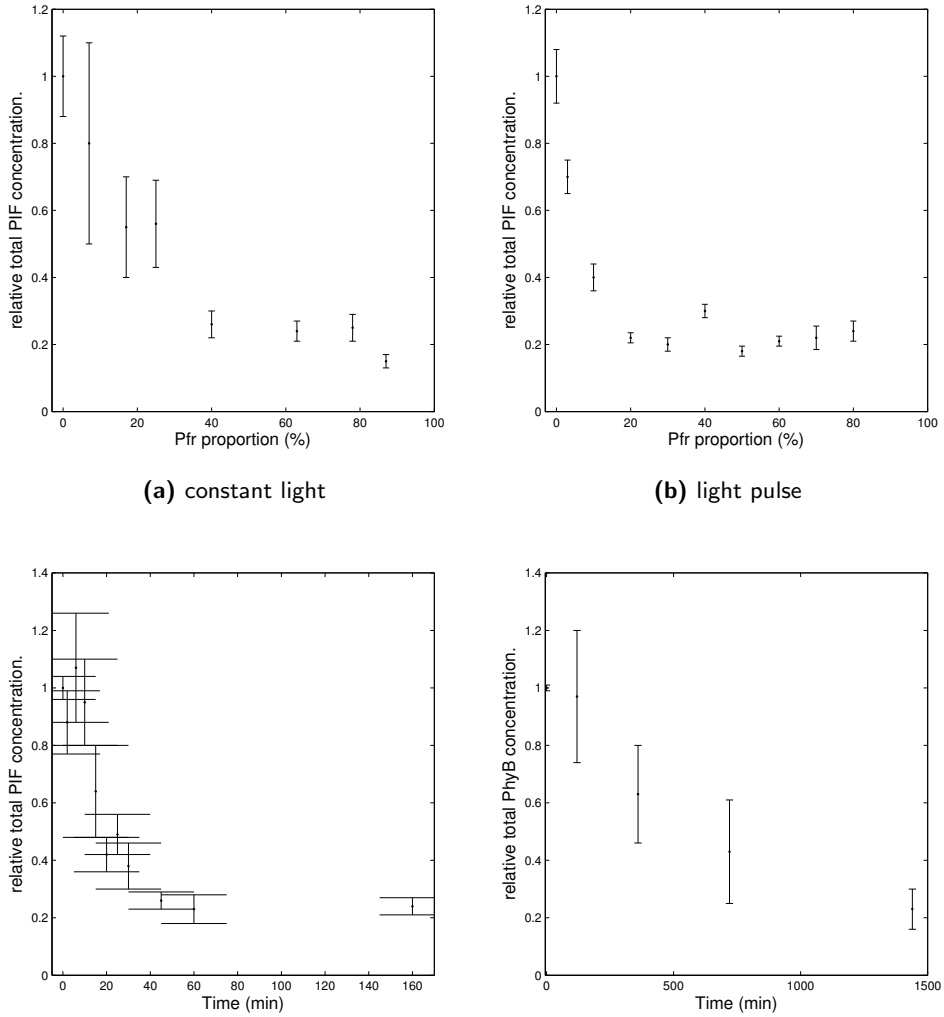

(a) constant light

(b) light pulse

(c) PIF degradation

(d) PhyB degradation

Figure 3.7: Quantified Levels of PIF3 and phyB Under Different Conditions, used to Parameterise the Models

(a-c) Quantitated Values of PIF3:PIF3:LUC taken from a Luciferase Assay.
(a) Levels of PIF3 in seedlings after an hour of constant light. Different wavelengths of light were used to create a different proportion of P_{fr} (Table S1.6). (b) Levels of PIF3 in seedlings following a 1 minute light pulse and 59 minutes of darkness. Different intensities of pulses created different proportions of P_{fr} (Table S1.7). (c) Degradation of PIF3 following a light pulse. Shown previously in Figure 3.5.
(d) Quantified Immunoblot of phyB levels of seedlings in constant light. Since published [16].
Error bars represent the standard error of the mean.
This Experiment was performed by Collaborators at the University of Freiburg

3.4.2 A Multi-Experiment Fit of the Models

For our models to represent the system they need to explain all the data and so a new multi-experiment fit is created which includes the data from Figure (3.7). The simple *Double Tagging* and *Protection* models were used to simulate the new available data. The equations were the same as used previously (S1.4 & S1.5 respectively) but the dark level of PIF3 was set to 1 and the parameters k_1 and k_2 allowed to vary based on experimental light conditions. Figures (3.8 & 3.9) shows these models were unable to recreate all the results.

Both models are able to recreate the behaviour seen in constant red light, which is not surprising as this had been shown before. However, both models fail to explain the behaviour that light pulses can be more efficient at degrading PIF3 than constant conditions, instead showing the more intuitive result that constant conditions would be more efficient. Both models show a response to increasing P_{fr} concentration in constant light but they fail to recreate degradation rates following a pulse of light. If their parameters are again allowed to vary, and the simple models are fitted to all quantitative data they can still not recreate the behaviour (Figure S1.1). This demonstrates that this response is due to a more complicated mechanism than previously described.

The *Double Tagging* model shows a more accurate fit than the *Protection* model overall. When the behaviour under a light pulse was looked at qualitatively (Figure 3.6b), the *Protection* model appeared to show the observed response to a pulse of red light (Figure 3.5). However when compared to quantitative data, it is shown that the model achieves this degradation under a pulse by being extremely sensitive to light. PIF3 does not continue to degrade in the dark, but instead degrades very quickly in the light. This is inconsistent with the behaviour of the system and so the *Double Tagging* model has the better overall fit to the data.

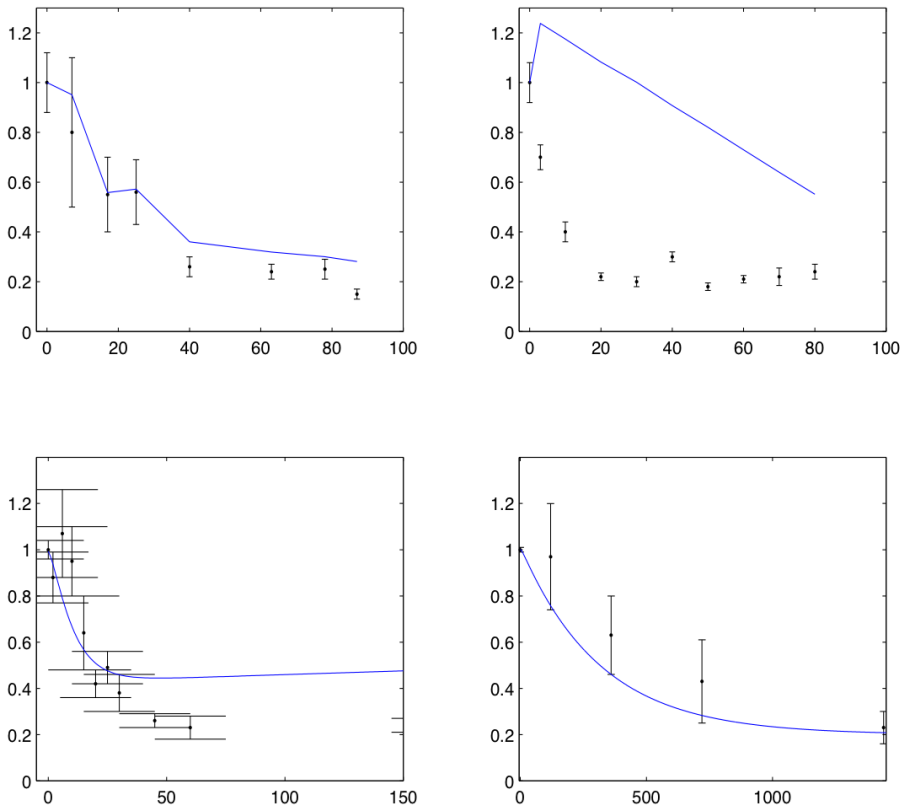

Figure 3.8: *Double Tagging* Model (S1.4) Compared to Quantitative Data

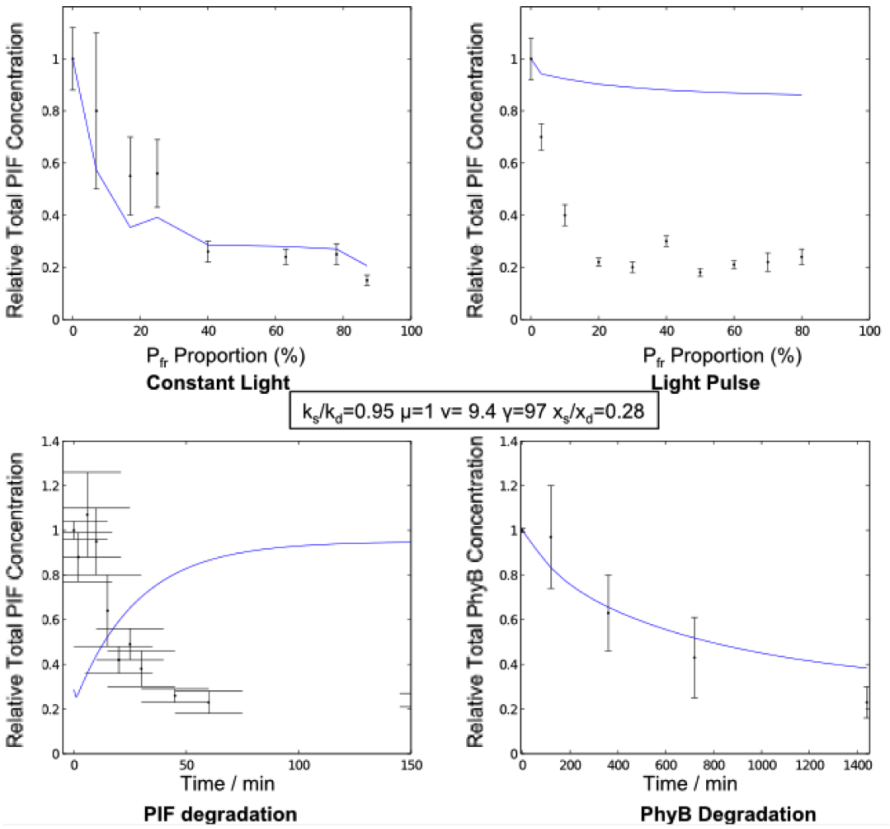

Figure 3.9: *Protection* Model (S1.5) Compared to Quantitative Data

3.5 Model Improvement through Mathematical Analysis

Following the rejection of the model with the addition of these new data, a different method is used. Instead of purely computational approach, the model will be built up gradually using mathematical analysis. In this sense the model will be kept as small as possible. Only bringing in extra steps if they are required to fit the data. In this section, parameter definitions are kept similar to those described previously (Table 3.2). A major difference is that dark PIF levels are defined as = 1 and so PIF synthesis and degradation have the same value (k_d).

Table 3.3: Definition of the Parameters used in Section 3.5

Parameter	Definition
k_1	Light Dependent phyB activation
k_2	Light Dependent phyB deactivation
k_r	Dark Reversion (Light Independent phyB deactivation)
γ	Complex Formation Rate
k_d	PIF synthesis & dark degradation rate
δ	PIF (and phyB where relevant) tagging rate
μ	Tagged PIF degradation rate
ν	Tagged phyB degradation rate
x	Dark Steady State phyB level (relative to PIF)
α	phyB synthesis rate
β	phyB dark degradation rate
x	phyB dark steady state $\left(\frac{\alpha}{\beta}\right)$

3.5.1 Describing Early PIF Degradation

In the first hour after light induction, the change in protein level of phyB is very small (Figure 3.7d). Following a light pulse, a constant pool of active P_{fr} is created, only reverting back to its inactive form very slowly. For the initial simple model we therefore assume active phyB is constant and only consider the different states of PIF (Table 3.4, Equation (3.3), Figure (3.10a)).

Table 3.4: Definition of PIF Component Used in Modelling (Section 3.5)

Parameter	Definition
Y	Free PIF
C	PIF:phyB complex
Y_t	PIF tagged for degradation
Y_{tot}	Total PIF

$$\begin{aligned} \dot{Y} &= 1 - Y - \gamma(x - C)Y \\ \dot{C} &= \gamma(x - C)Y - \delta C \\ \dot{Y_t} &= \delta C - \mu Y_t \end{aligned} \tag{3.3}$$

The analytical solution for (3.3) can not be solved due to the nonlinearity of the system. However, the steady state behaviour can be found by looking at the behaviour as $t \to \infty$ (setting the right hand side of the differential equations to zero). These are shown in (3.4) including the total PIF level ($Y_{tot} \equiv Y + C + Y_t$). This is significant as it corresponds to the measurable level of PIF3 seen in experiments.

$$\begin{aligned} \lim_{t\to\infty} Y &= \frac{-\delta+\gamma-\delta\gamma x+\sqrt{4\delta\gamma+(\delta-\gamma+\delta\gamma x)^2}}{2\gamma} \\ \lim_{t\to\infty} C &= \frac{1+\frac{\delta}{\gamma}+\delta x-\frac{\sqrt{4\delta\gamma+(\delta-\gamma+\delta\gamma x)^2}}{\gamma}}{2\delta} \\ \lim_{t\to\infty} Y_t &= \frac{1+\frac{\delta}{\gamma}+\delta x-\frac{\sqrt{4\delta\gamma+(\delta-\gamma+\delta\gamma x)^2}}{\gamma}}{2\mu} \\ \lim_{t\to\infty} Y_{tot} &= \frac{1}{2\delta\gamma\mu}[\gamma\mu - \delta^2(\mu-1)(1+\gamma x) - \delta\sqrt{4\delta\gamma+(\delta-\gamma+\delta\gamma x)^2} \\ &\quad -\mu\sqrt{4\delta\gamma+(\delta-\gamma+\delta\gamma x)^2} + \delta\mu\sqrt{4\delta\gamma+(\delta-\gamma+\delta\gamma x)^2} \\ &\quad +\delta(\mu+\gamma(\mu x+\mu+1))] \end{aligned} \tag{3.4}$$

The steady state value of Y_{tot} (3.4) is not intuitive but can be simplified by expansion around $\gamma = \infty$. Due to the quadratic term from (3.4) $\left(\sqrt{4\delta\gamma+(\delta-\gamma+\delta\gamma x)^2}\right)$ there are two different solutions to this expansion, depending on the value (δx). This

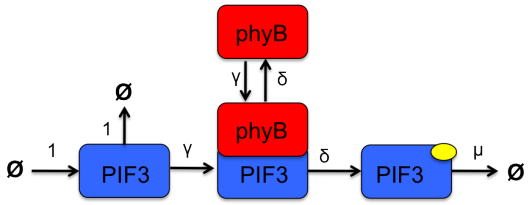

(a) Equation (3.3)

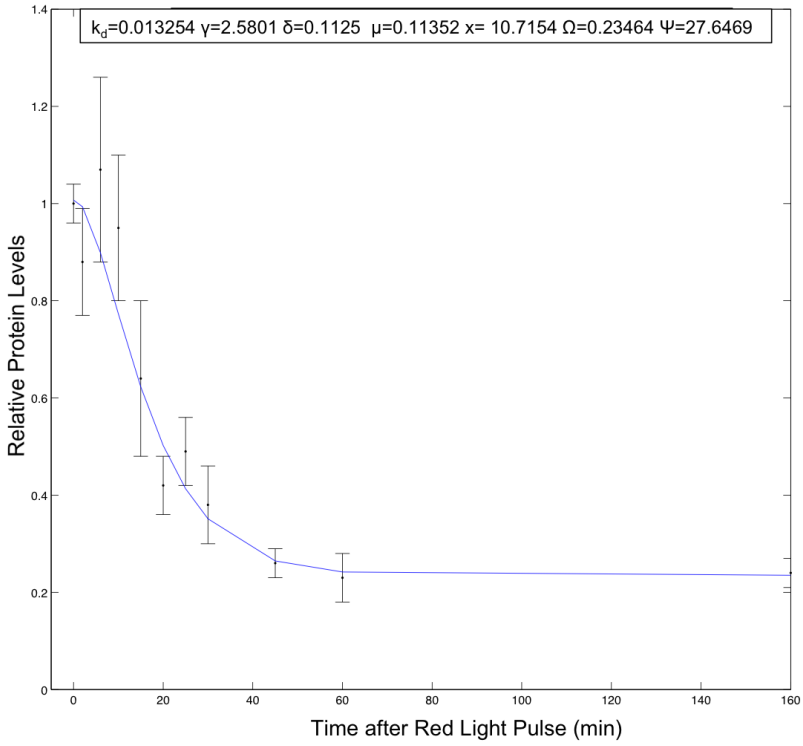

(b)

Figure 3.10: Early PIF Degradation Model Fitted to PIF3 Degradation Data (Figure 3.7c)

(a) Cartoon Representation of (3.3).
(b) Fit of (3.3) to PIF3 Degradation Data (3.7c). Fit of Model to Data Showing Degradation Following a Light Pulse. Here here is a large value of Ψ, meaning the value of the steady state closely approximates Ω.

corresponds to the amount of phytochrome (x) multiplied by its rate of activity (δ). If ($\delta x < 1$), the amount of phyB is a limiting factor and so the steady state depends on the total concentration of phyB (x). However, if δx is larger than 1, phyB is in excess. There is either a large amount of phyB available to bind PIF (x large), or the amount of time phyB spends in the complex (C) is small (δ large). In this case the steady state is controlled primarily by a factor $\left(\Omega \equiv \frac{1}{\mu} + \frac{1}{\delta}\right)$ (3.5). This means that either a slow rate of PIF tagging (μ) or of tagged PIF degradation (δ) would contribute to a high steady state of total PIF protein. The parameter Ψ (γx) represents the speed with which PIF is able to bind any available phyB. It is based on the tagging speed multiplied by the concentration of phyB ($\gamma \times x$). It is this parameter, rather than x or γ which is important in the steady state.

Table 3.5: Definition of Simplifications used in Modelling (Section 3.5)

Parameter	Definition
δx	$\delta \times x$
Ω	$\frac{1}{\mu} + \frac{1}{\delta}$
Ψ	$\gamma \times x$
O	Limit of Expansion

When the steady state is expanded around ($\Psi = \infty$) (3.5).

$$\lim_{t \to \infty} Y_{tot} = \Omega + \frac{1 - \Omega}{\Psi} + O\left[\frac{1}{\Psi^2}\right] \tag{3.5}$$

So for high values of Ψ, the steady state of PIF is controlled very strongly by the value Ω. As the experimentally observed steady state is about 20 % of the initial value, we therefore require that $\Omega \equiv \left(\frac{1}{\mu} + \frac{1}{\delta}\right) \approx 0.2$. So for this simple model, the steady state level of PIF is dependent equally on the tagging rate (δ) and the tagged pool degradation rate (μ). If both these parameters are too large, PIF degradation will be rapid and there will be no left over steady state. Several parameter sets are able to

accurately fit the PIF degradation mechanics using this model (Figure 3.10b).

3.5.2 Modelling a Change in Light Quality by Increasing Active phyB levels

Giving different intensities of red light pulse followed by a period of darkness, leads to different levels of PIF3 (Figure 3.7b). As these data were taken an hour after the light pulse, it is a reasonable assumption that phyB levels have not changed during this time period [84]. We can therefore treat the PIF3 data of Figure (3.7b) as the steady state of the system, described in (3.4). A light pulse of a given intensity will establish a certain % of P_{fr} which will stay relatively constant throughout the hour. The amount of PIF3 remaining after 1 hour can therefore be predicted from the P_{fr} % using (3.4).

To fit the parameters we add to the previous cost function a calculation for steady state PIF3 levels. In Figure (3.7b) the x axis represents the amount of active phyB. This can be simulated in our model by changing the value of x, such that for a data point representing 30% active phyB our steady state value of x is $0.3 \times x$. Levels of Y_{tot} from (3.4) are fitted to the actual data from Figure (3.7b). The resulting graph shows a very accurate fit to the data (Figure 3.11) showing this model is able to explain the sensitivity of the system to changes in active phytochrome. The system must however be expanded to simulate separate light conditions.

3.5.3 PIF Steady States In Constant Light

Following a light pulse, a certain proportion of phyB is activated which then affects PIF, leading to its degradation (Figure 3.7b). This behaviour has therefore been able to be described by this simple model. However under constant light conditions, phyB is in a state of dynamic equilibrium, switching between its active and inactive forms depending on the light conditions [16]. The conversion between the inactive phyB (P_r) and the active form (P_{fr}) is reversible and dependent on both the wavelength and intensity of light (3.6) (Figure 1.1).

$$P_r \underset{k_2}{\overset{k_1}{\rightleftharpoons}} P_{fr} \tag{3.6}$$

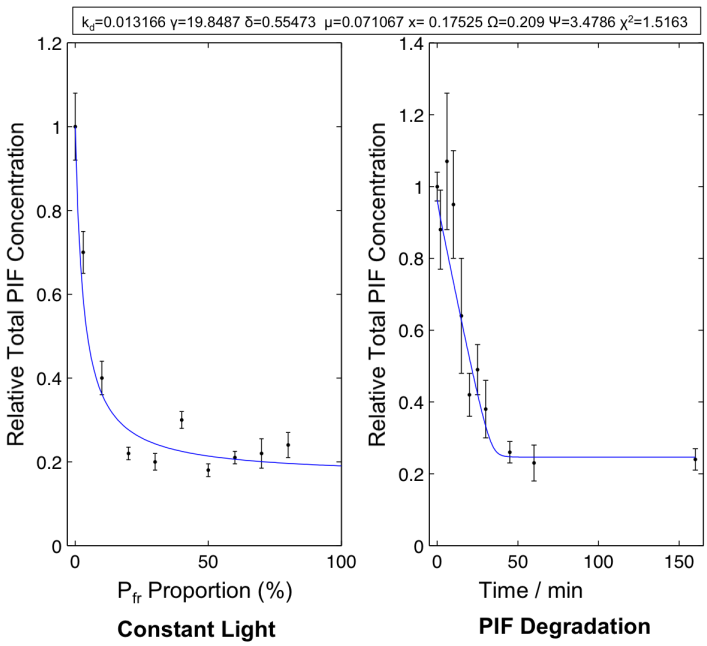

Figure 3.11: Fit of Model (Equations 3.4) to PIF3 Degradation Rate and Constant Light PIF3 Steady State

Simultaneous fit of the model to the PIF degradation mechanics shown in Figure (3.5) (right), and the steady state behaviour seen in Figure (3.7b), left.

The values of k_1 and k_2 shown in (3.6) have been calculated in a number of different wavelengths and fluences [12, 167]. These can therefore be inserted into a simple model. In order for there to be a difference between active and inactive forms of phyB a further equation must be added, representing active phyB (P_{fr}). As phyB is being held constant, a differential equation is not needed to describe inactive phyB (P_r), it is initially defined as the phyB not explained by the other equations. Active and inactive phyB can therefore be treated differently by the equation.

$$\begin{aligned} x &= \text{Total phyB} \\ P_r &= \text{Inactive phyB} \\ P_{fr} &= \text{Active phyB} \\ C &= PIF : phyB\text{complex} \end{aligned} \tag{3.7}$$

$$P_r \equiv (x - P_{fr} - C)$$

It is observed from Figures (3.7a, 3.7b) that a light pulse can cause a higher proportion of PIF to be degraded than constant light irradiated for 60 minutes. In order to try to explain this, the model is altered so that that phyB is able to convert back to its inactive form (with rate k_2) while in the complex with PIF. This is based on the experimentally observed phenomenon that phyB will separate from PIF3 in the presence of far red light [71]. The complex will only split up in this way in constant light, so this could explain the increased efficiency of a light pulse. The full equation set is shown below (3.8).

$$\begin{aligned} \dot{P_{fr}} &= k_1(x - P_{fr} - C) - k_2 P_{fr} - \gamma P_{fr} Y + \delta C \\ \dot{Y} &= 1 - Y - \gamma P_{fr} Y + k_2 C \\ \dot{C} &= \gamma P_{fr} Y - \delta C - k_2 C \\ \dot{Y_t} &= \delta C - \mu Y_t \end{aligned} \tag{3.8}$$

This new model is fitted to the data from Figures (3.7b, 3.7a & 3.7c) simultaneously

to estimate parameters. Now instead of estimating Figure (3.7b) by using the steady state equation, the light conditions used in the experiment are simulated, altering the values of k_1 and k_2 depending on the wavelength and fluence of light. Figure (3.12b) shows the fit of the model described in (3.8). It shows that the model can reproduce the result where a light pulse is more efficient at degrading PIF than constant light. This suggests that the separation of PIF from the complex on deactivation of phyB [71] could be significant in light signalling.

3.5.4 PhyB Degradation

The previous models have assumed constant phyB, which is likely a valid assumption for initial PIF degradation. However we now wish to include the long term degradation of phyB, to see if PIF dependent phyB destruction is consistent with the experimental data so far considered. PhyB synthesis and dark degradation must be introduced, with inactive phyB (P_r) created with rate α and degraded with rate β. These parameters now control the amount of phyB and so parameter x is no longer needed. The dark level of phyB is instead represented by the ratio of phyB synthesis to degradation ($\frac{\alpha}{\beta}$).

$$\begin{aligned}
\dot{P_r} &= \alpha - (\beta + k_1)P_r + k_2 P_{fr} \\
\dot{P_{fr}} &= k_1 P_r - (\beta + k_2)P_{fr} - \gamma(P_{fr} + P_y)Y \\
\dot{P_y} &= \delta C - \gamma P_y Y - (\beta + \nu)P_y \\
\\
\dot{Y} &= 1 - Y - \gamma(P_{fr} + P_y)Y + k_2 C \\
\dot{Y_t} &= \delta C - \mu Y_t \\
\\
\dot{C} &= \gamma(P_{fr} + P_y)Y - \delta C - k_2 C
\end{aligned} \tag{3.9}$$

To explain the slow, PIF dependent degradation, we reintroduce the tagged form of phyB (P_y), described in (S1.4). On exiting the complex, both PIF and phyB become tagged and they are degraded at rates μ and ν respectively. Figure (3.13b) shows the data can be explained by the model described in (3.9). We therefore find that the ideas of double tagging were consistent with all the data. The model is able to explain the counter-intuitive result of the difference between a light pulse and constant irradiation,

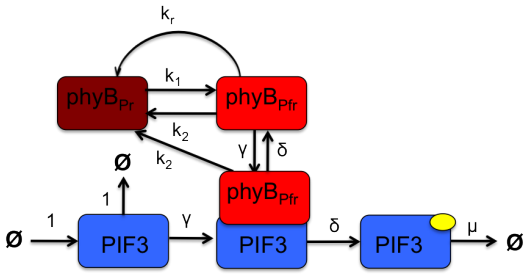

(a) (3.8)

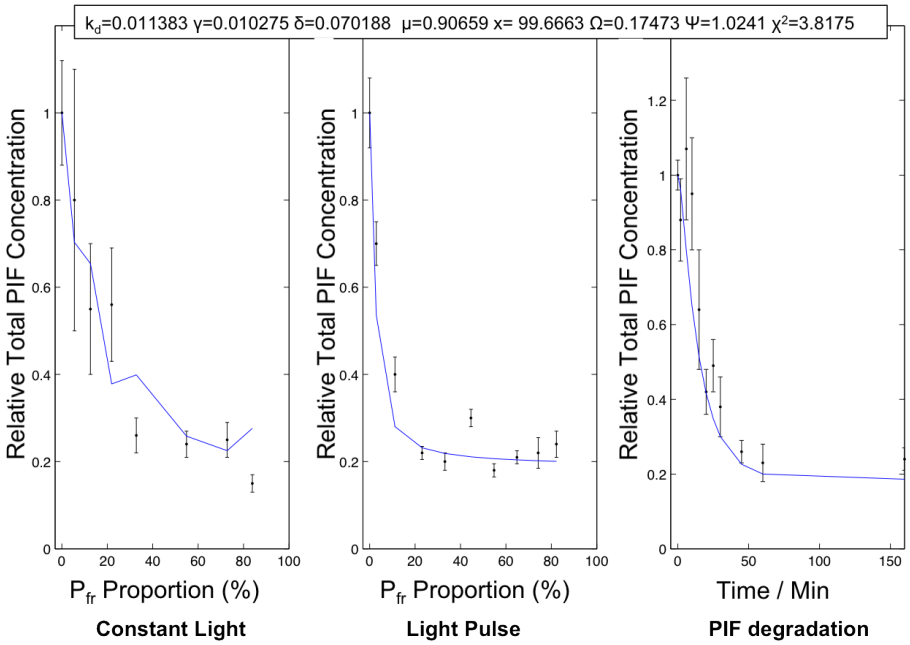

(b)

Figure 3.12: Fit of Model (Equations 3.8) to PIF3 Degradation Rate and Constant and Pulsed Light PIF3 Steady State

Model shown in (3.8) is fitted to the three data sets, shown in Figures (3.7c, 3.7a, 3.7b) Simultaneously

through complex separation. It should therefore be used to make predictions to test this hypothesis.

3.5.5 Parameter Estimation

Despite the relative simplicity of these models, the parameters of the system are non identifiable. Equally suitable parameter sets were found across the parameter space. Figures (3.14 & 3.15) give a representation of the spread of parameters found in the search method. Although there is a wide spread in the parameters found during optimisation, patterns of parameter distributions can be seen with a large number of iterations, particularly when only the accurate searches are looked at. The PIF turnover rate (k_d) appears the most identifiable, with accurate parameter sets generally clustered around a value of $0.01min^{-1}$ (Figure 3.14e, 3.14f), representing how important this parameter is to the steady state level of PIF. The most pronounced clustering is seen with the phyB relative dark level (Figures 3.15a, 3.15b). This is taken from dividing phyB synthesis (α) by phyB dark degradation (β). It is more sensible to look at this value than α or β individually as it shows the relationship between phyB and PIF levels. An accurate fit can be found with phyB either in excess or deficiency relative to PIF but not when they are at a similar level. As vastly different degradation mechanics are needed this may be one way of achieving it. This demonstrates that the differences in relative concentrations of the interacting signalling molecules could be important to function. Having phyB levels in excess would be one way of achieving transient PIF signalling alongside lasting phyB activity.

These data clusters raise the question of how the parameters interact to affect their relative levels. This can be investigated by looking at the correlation coefficients of the parameters in a heat map (Figure 3.16). Both the strongest positive and negative correlations involve the phyB degradation parameter ν. Changing this parameter has a large effect on both the rate of complex formation γ and the PIF3 turnover rate k_d. As both these factors relate to the degradation of phyB this is intuitive. There is much less data for phyB to fit to than the PIFs and so this parameter would be expected to

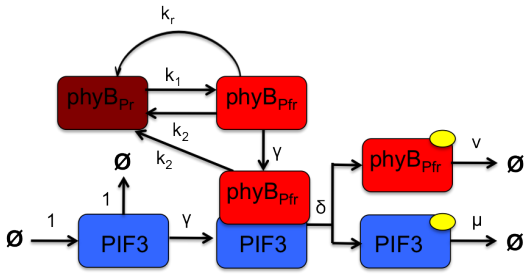

(a) 3.9

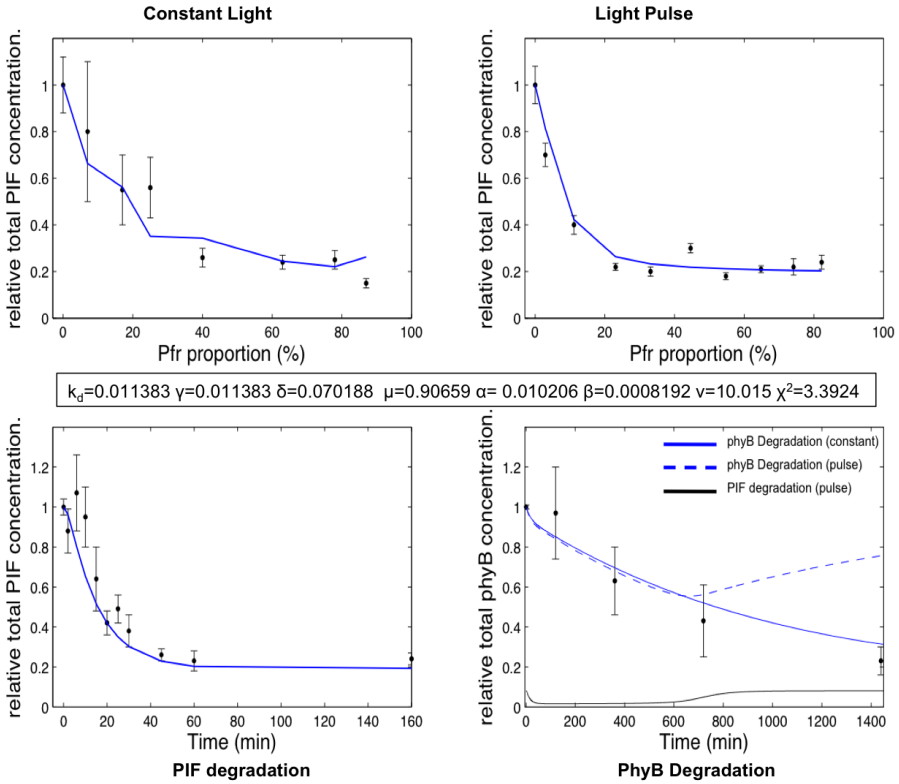

(b)

Figure 3.13: Fit of Model (Equations 3.9) to PIF3 Degradation Rate, Constant and Pulsed Light PIF3 Steady State and phyB Degradation Rate

Model shown in (3.9) is fitted to the four data sets, shown in Figure (3.7) simultaneously. The phyB degradation curve also shows behaviour of PIF and phyB following a 1 min light pulse.

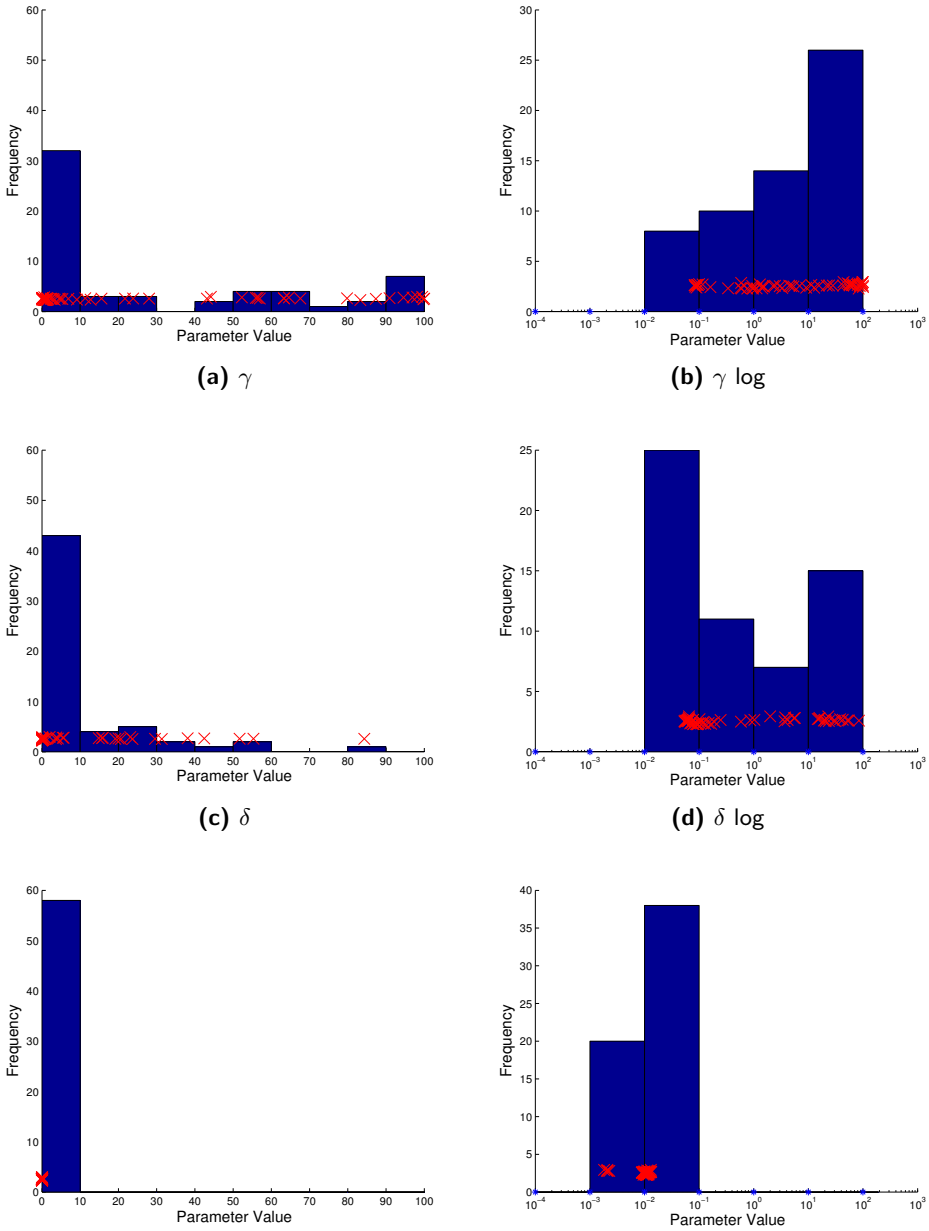

(a) γ **(b)** γ log

(c) δ **(d)** δ log

(e) k_d **(f)** k_d log

Figure 3.14: Distribution of Parameters γ, δ, k_d in 3.9

Histogram showing representative search of parameters used in model (3.9). (a,c,e) show a linear scale. (b,d,f) Log Scale. Accurate parameter sets ($\chi^2 < 3.5 = 58$ data sets) were used. Red Crosses Show the exact distribution of the parameters. Remaining parameters shown in Figure (3.15)

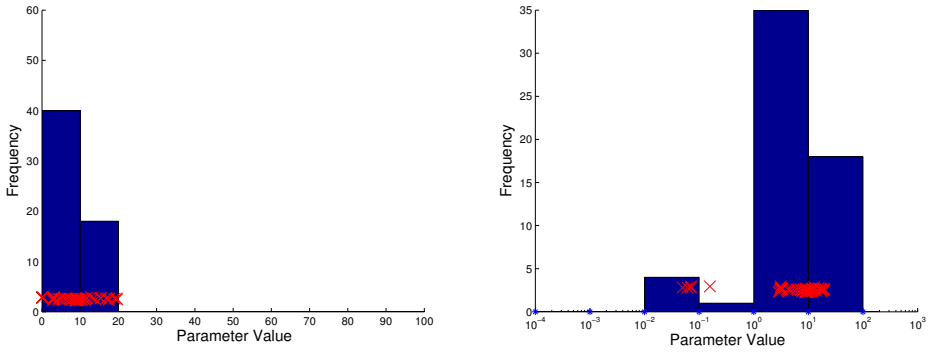

(a) x **(b)** x log

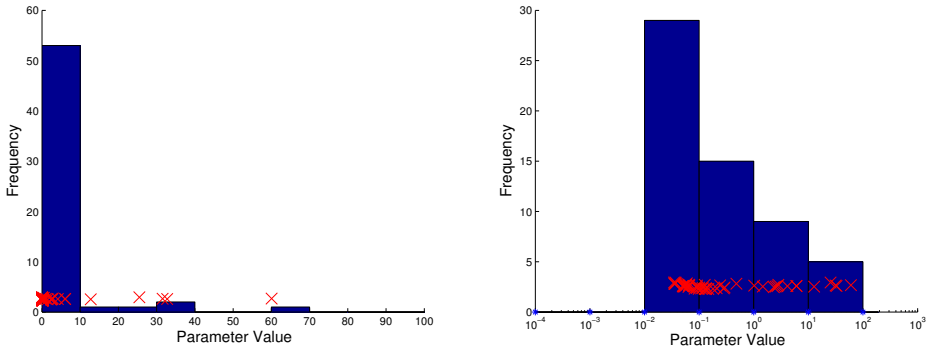

(c) μ **(d)** μ log

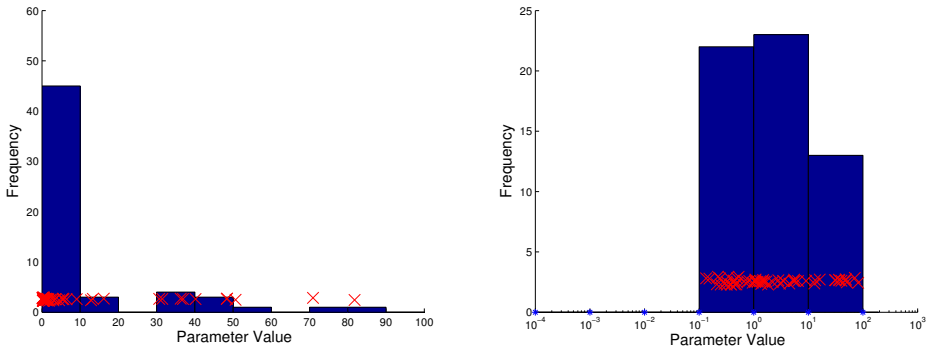

(e) ν **(f)** ν log

Figure 3.15: Distribution of Parameters x, μ, ν in 3.9

Histogram similar to Figure (3.14)

have a high degree of plasticity.

3.5.6 Complex Formation Rate (γ) Must be Low to Explain the Differences Between Light Conditions

Included in the heatmap (Figure 3.16) is the χ^2 measure of fit to the data. This shows that parameter γ has the largest affect on the fit of the model to the data. This is despite the large distribution of values leading to accurate parameters (Figure 3.14a, 3.14b). It was therefore investigated exactly how these models behaved under our different light conditions. Parameter sets of (3.9) with high values of γ fail to match the PIF degradation behaviour under constant light conditions (Figure 3.17). While other data is fitted accurately, there is no difference between light pulse and constant conditions, with the model too sensitive to low $P_{fr}\%$. With a high complex formation rate, the separation of the complex by light is not sufficiently strong to cause the difference in light conditions. It is therefore the case that the interaction of phyB and PIF3 must be relatively slow in order to signal differently in varying light conditions. This could be important to phytochrome signalling in response to fluence changes.

3.6 The Photo-Equilibrium Point can not Predict PIF3 Levels on its Own

The difference between the smooth results of the Light pulse and more jagged results in Continuous Light (Figures 3.12b, 3.13b) can be explained by the light conditions in the experiments. The seedlings experiencing a light pulse were only differentiated by a change in fluence. However, in Continuous Light the photoequilibrium point was altered with a series of different filters, effectively varying both the wavelength and fluence. Figure (3.18) shows the Constant light experiment from (Figures 3.12b, 3.13b) in a single graph. The blue line shows the simulation of the experimental light conditions, while the other lines show the same parameter set, if the light conditions were altered differently. For the green line, the light intensity is kept constant, and only the wavelength of light altered and the cyan and magenta lines show the results of keeping the cycling time and the time to equilibrium constant respectively.

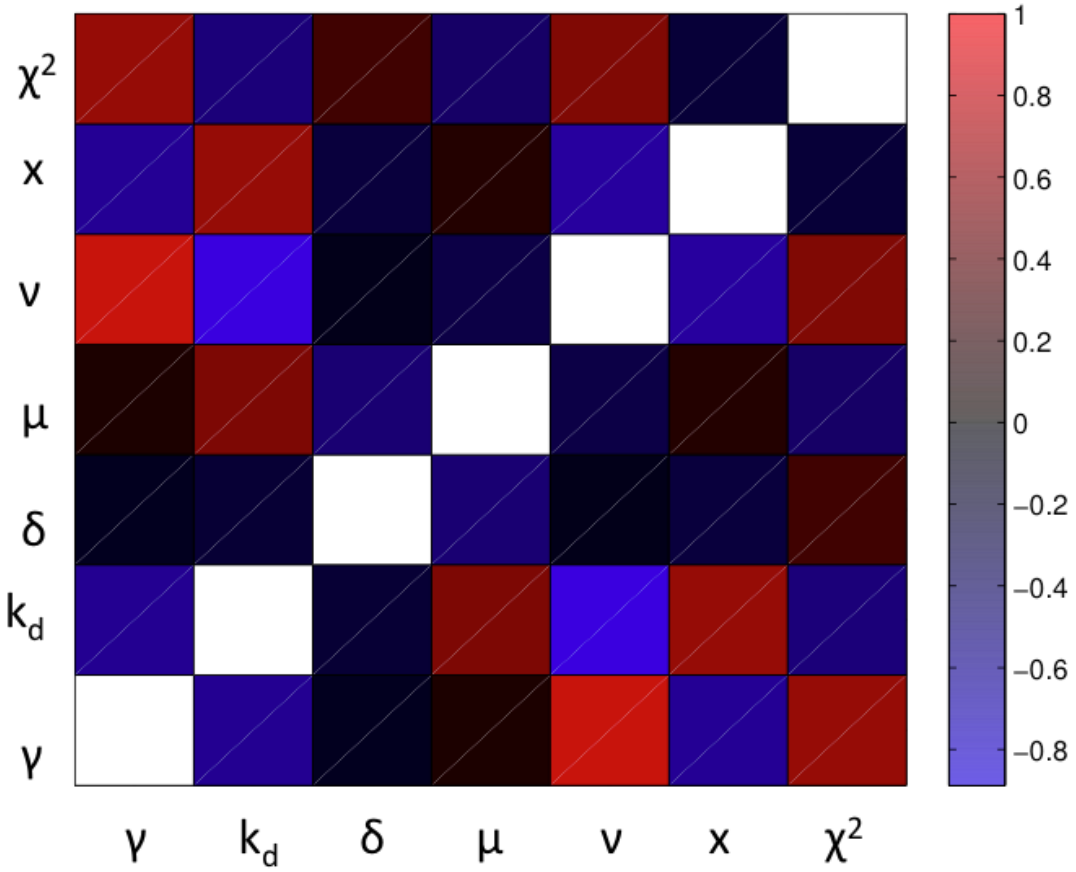

Figure 3.16: Heat map Representing Correlation Coefficients of Parameters Shown in (3.9)

A red square represents a positive correlation while a blue square represents a negative correlation with the brightness of these squares showing the strength of the correlation. The parameters are those previously described as $\gamma, k_d, \delta, \mu, \nu, x$ plus the value of χ^2 represented how strongly each of the parameters effect the fit to the data. Only the most accurate parameter sets ($\chi^2 < 3.5$) are selected for analysis (58 parameter sets) The distribution of these parameters was shown in Figures (3.14 & 3.15)

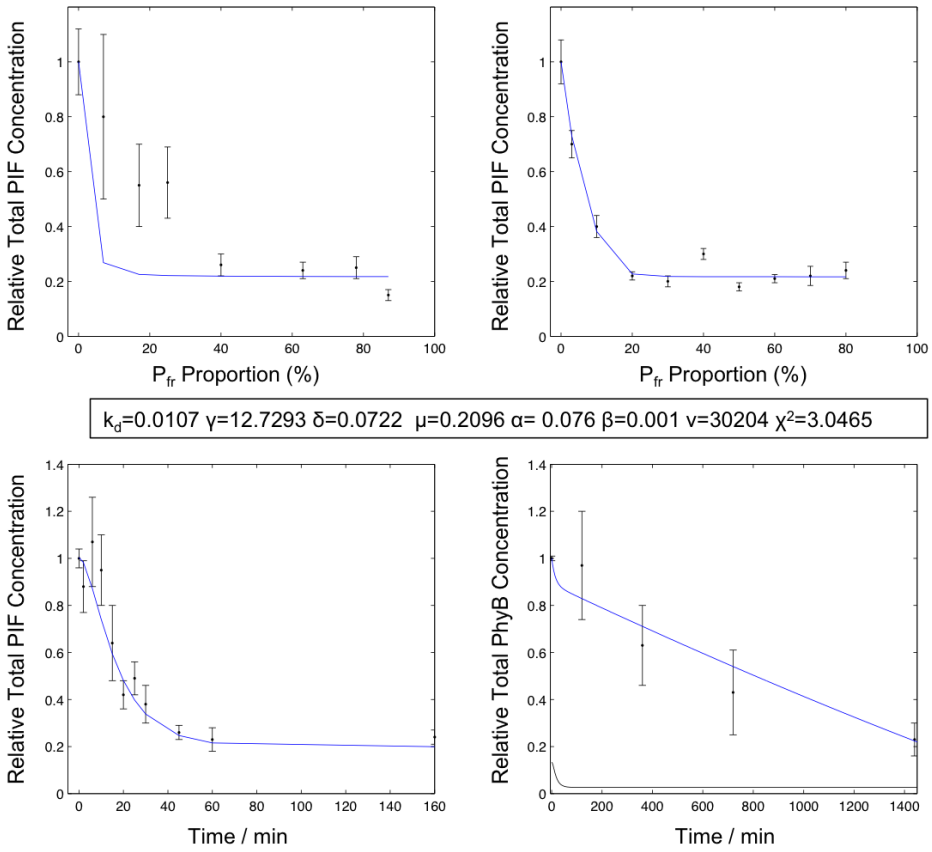

Figure 3.17: High Complex Formation Rate Removes the Constant Light Phenotype

Accurate ($\chi^2 < 3.5$) parameter sets from (3.9) with a high value of γ fail to recreate the constant light phenotype

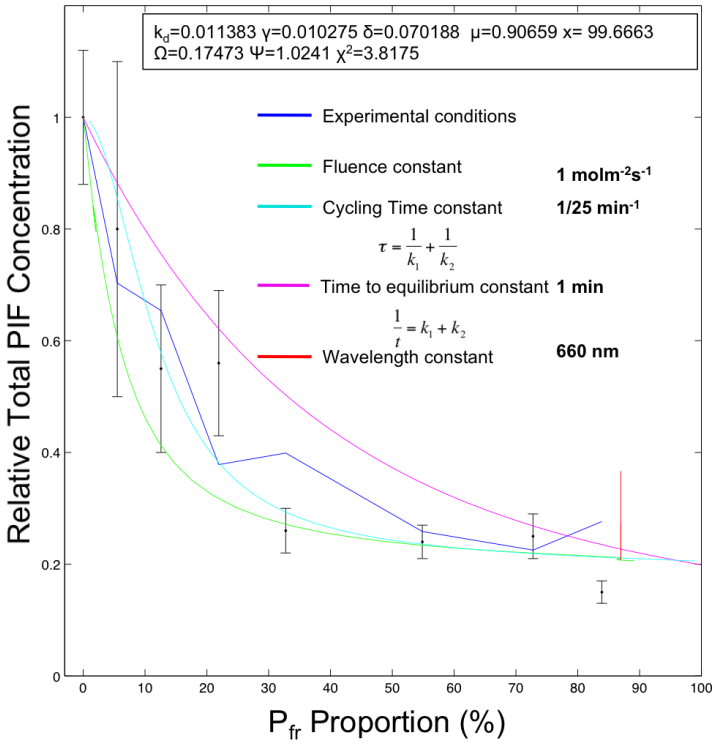

Figure 3.18: The Effect on (3.9) of Altering Light Conditions Smoothly

Constant Light conditions simulated by (3.9), with the Parameter set from the multi experiment fit shown in Figure (3.12b). Coloured lines show different ways of varying the light conditions, while the red line shows the effect of changing the fluence rate. This clearly shows that the P_{fr} proportion is not sufficient to explain PIF degradation mechanics.

This result shows that the P_{fr} proportion is not sufficient to explain the degradation rate of PIF3. In contrast to the experimental data, these other plots show a smooth relationship between the photo-equilibrium point and the final concentration of PIF3; they also vary between each other, and therefore we see the strange shape of the graph in Figures (3.12b, 3.13b) is a result of these changes in light condition. Other factors than the amount of active phyB are important for the PIF3 degradation rate. The effect of keeping the wavelength constant and varying the fluence is shown on the same graph (red), showing this effect simply. By definition, the photoequilibrium point in constant light is controlled only by the wavelength of light. However, the vertical line here shows that different PIF levels can be predicted from the same photoequilibrium point. This

shows that the steady state PIF levels predicted by the model is fluence rate dependent.

3.7 Model Predicts a High Intensity Response of PIF3 Levels

To observe the effect light intensity has on PIF3 we therefore plot steady state PIF3 levels against fluence rate, rather than the photo-equilibrium point. (Figure 3.19a). The graph has a minimum around ($0.1\mu molm^{-2}s^{-1}$), with high light intensities predicted to have higher levels of PIF3. This loss of degradation efficiency at high light intensities is counterintuitive and goes against the belief that an increase in light leads to an increase in phyB activity. This is related to the differences between constant and light pulse conditions. The separation of the PIF-phyB complex is dependent on the photoreversion parameter k_2, which is fluence rate dependent. Therefore for the same reason constant light has reduced efficiency, so does high intensity light. Figure (3.19a) shows the predicted effect at 660nm (red light). As the wavelength increases and we approach far red light, the absorption of P_{fr} increases (Figure 1.2) and therefore the strength of the parameter k_2. A more pronounced effect is seen at 690nm (Figure 3.19c), with PIF3 levels starting to rise at a lower light intensity. At wavelengths higher than 690nm, phyA has more of an effect and would therefore skew the response as it is also known to degrade PIF3 [81]. At wavelengths lower than 690nm phyA should only be acting through the VLFR mechanism and would not have a significant effect on PIF3 levels [30].

However, the high intensity PIF3 increase is lost in parameter sets unable to recreate the constant light phenotype (Figure 3.17, Figure 3.20). An increase in the complex formation rate γ, shown previously to provide oversensitivity to light, was found to strongly suppress the high intensity response (Figure 3.21a).

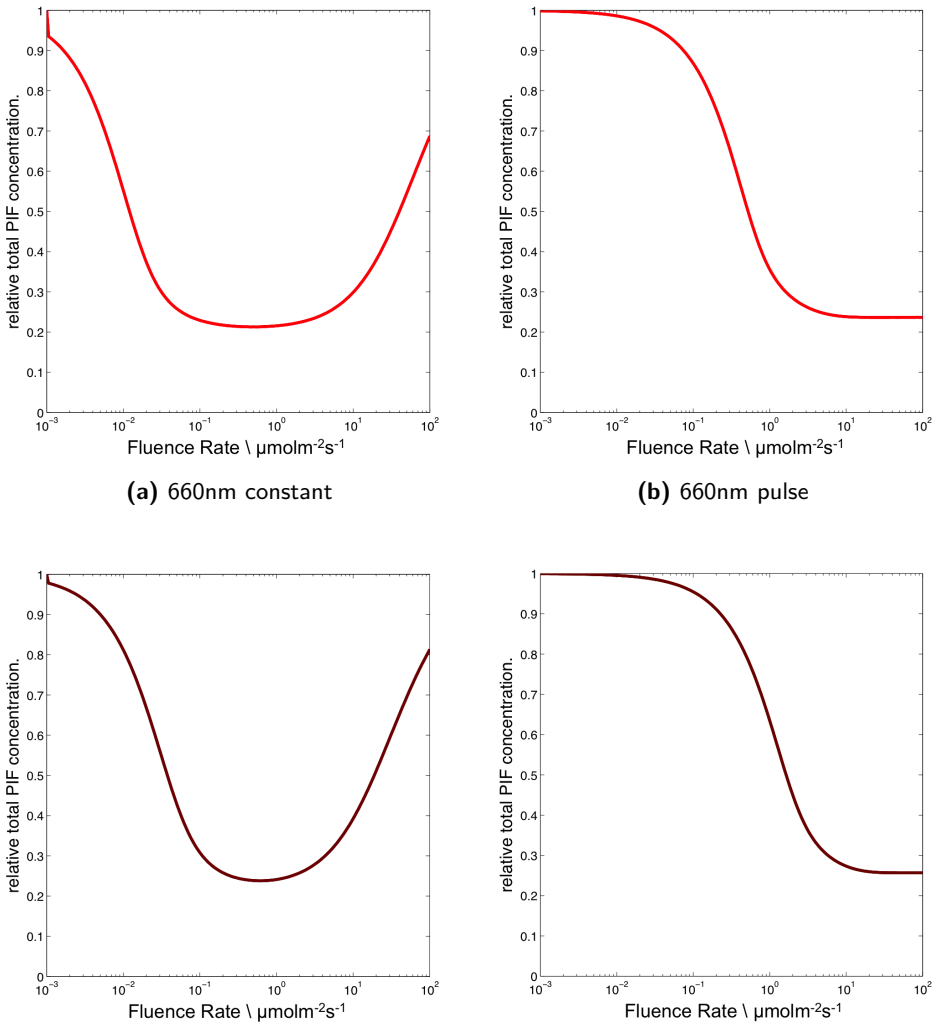

(a) 660nm constant

(b) 660nm pulse

(c) 690nm constant

(d) 690nm pulse

k_d=0.011383 γ=0.011383 δ=0.070188 μ=0.90659 α= 0.010206 β=0.0008192 ν=10.015 χ^2=3.3924

Figure 3.19: Simulated Fluence Response of PIF3 Levels in (3.9)

Predicted Fluence Response curve of steady state PIF3 levels an hour after illumination with 660 or 690nm light. Constant light conditions are shown on the left and the effect of a 1 minute light pulse is shown on the right

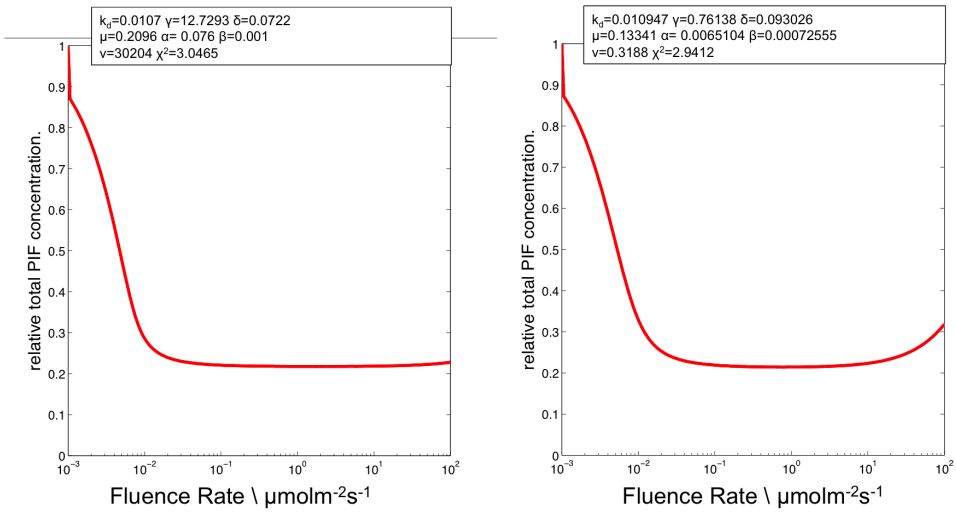

Figure 3.20: Parameter Sets Unable to Recreate the Constant Light Phenotype (γ high) do not show the high intensity phenotype

Intensity analysis repeated with parameter sets from Figures (3.17, S1.2) which were unable to distinguish between light pulse and constant light conditions. This phenotype is related to the high intensity response with this also lost in these parameter sets.

3.7.1 Sensitivity Analysis Confirms the Importance of Parameter γ to the High Light Intensity Response

To investigate how strongly the individual parameters contribute to model behaviour a simple sensitivity analysis was performed. Taking our most accurate parameter set as the starting value, the individual parameters were altered and the final fluence rate dependency graphs replotted in a sensitivity analysis (Figure 3.21). It is revealed that the PIF turnover parameter (k_d) and the tagged PIF degradation rate (δ) have a strong effect on the PIF steady state level, but it is the amount of active photoreceptor (x) and particularly the strength of the complex formation rate (γ) which contribute to the high intensity increase in PIF levels.

It is the PIF tagging rate (δ), which is shown to be the more important to the steady state through this analysis (Figure 3.21b). Although PIF synthesis k_d also has a significant effect, it is only through increasing the parameter than we see a large change in graph shape (Figure 3.21c). This analysis shows us that the tagging of PIF

is more important to its steady state than PIF synthesis rate. A dramatic decrease in PIF synthesis rate does not lead to a complete loss of PIF levels in red light (Figure 3.21a), and therefore we can conclude a large proportion of PIF present in constant red light has been present in the plant for some time. Upon transfer to light, PIF3 takes a few minutes to start to decrease in levels and this slow tagging step may be the reason for this (Figure 3.7c). The perturbation of complex formation rate (γ) confirms the importance of this parameter to the high intensity response (Figure 3.21a). Increasing the parameter suppresses the observed behaviour in high fluences and it is exaggerated by decreasing γ.

3.7.2 PIF3:LUC Levels do not Increase at High Fluence Rates

Model predictions were that levels of PIF protein would increase at high fluence rates due to increased separation of the PIF:phyB complex (Figure 3.19). These levels were tested in the lab through immunoblot of PIF3:PIF3:LUC seedlings grown in red light at a series of different light intensities. Blots were quantified relative to UGPase loading control. In contrast to predictions, the blots show there is no observed increase in PIF3 levels at light intensities over $1.4\mu molm^{-2}s^{-1}$. (Figure 3.22)

However, in the model, the synthesis of PIF3 is not dependent on external conditions, and this could be suppressing the result. We therefore retested the fluence response of PIF3 with the constitutively active 35S promoter, thought to be light insensitive [174]. If this line showed a rise in PIF3 levels at high fluences, it would suggest the reason we do not see the behaviour in PIF3:PIF3:LUC is due to altered PIF transcription at high fluence rates. Seedlings were grown in constant light for 4 days at different fluence rates. Again there is no observed increase in levels at high fluence rates (Figure 3.23). In order to explain this in relation to model predictions, this would suggest the complex formation rate (γ) is relatively high as shown in Figure (3.20). However, as these parameter sets do not show the difference in behaviour between pulsed and constant light samples (Figure 3.7), a further mechanism is needed to explain this.

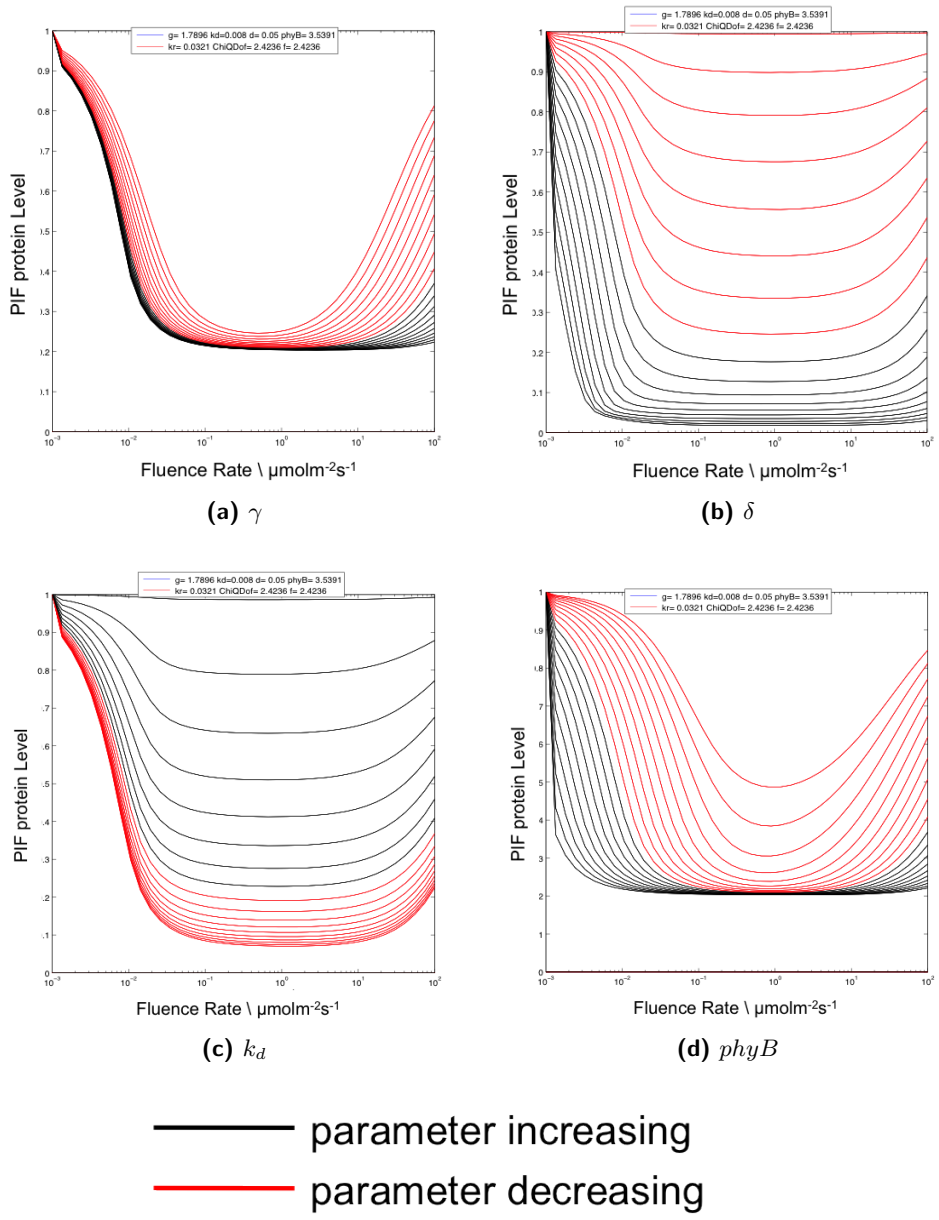

(a) γ **(b)** δ

(c) k_d **(d)** $phyB$

Figure 3.21: Sensitivity Analysis on Parameters γ,δ,k_d and x from Model (3.9).

The described parameter was either increased (black lines) or decreased (red lines) in a logarithmic scale. The fluence dependency graphs in constant red light replotted as in Figure 3.19a. Parameters k_d and δ are significant for PIF steady state in constant light, while $phyB$ and γ are more important for the fluence rate dependency of the response.

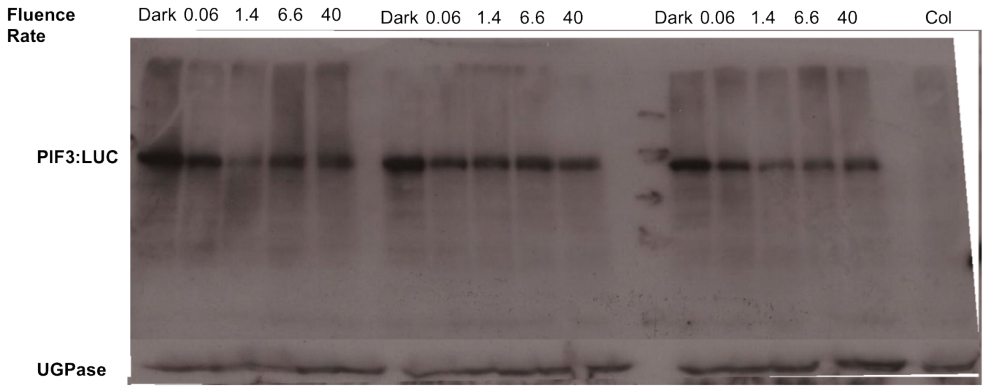

(a)

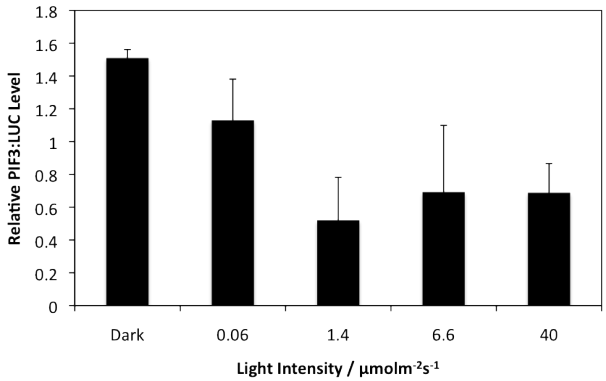

(b)

Figure 3.22: Immunoblots of PIF3:PIF3:LUC over a Fluence Curve

(a) Immunoblot from dark grown PIF3:LUC seedlings given 1 hour of Red Light (660nm), 22°C over a variety of different fluences. UGPase is included as a loading control. (b) Quantification from 3 separate experiments. PIF3 levels appear to be constant at light intensities higher than 1.4$\mu molm^{-2}s^{-1}$

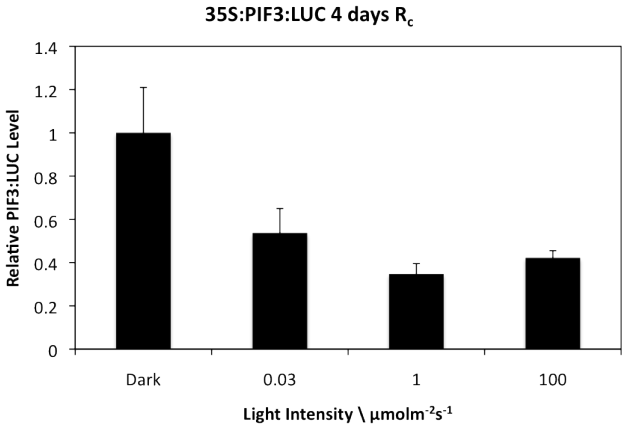

Figure 3.23: Luciferase Assay Confirms PIF3 Levels do not Increase at High Fluence Rates

This time seedlings were grown in constant red light for 4 days. PIF3 is overexpressed under the 35S promoter

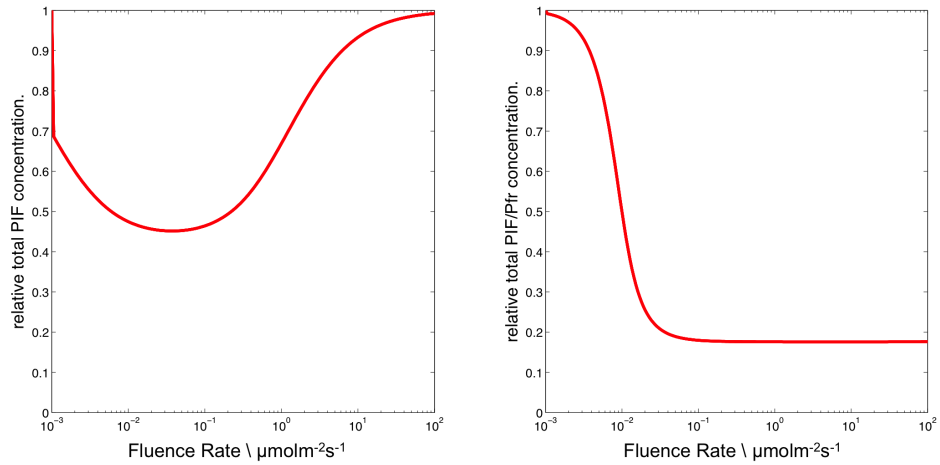

(a) Nuclear import (S1.15) **(b)** Phytochrome dimer (S1.13)

Figure 3.24: Predicted Fluence Response of PIF3 Levels of *Phytochrome Import* (S1.15) & *Phytochrome Dimer* (S1.13) Models

Effect of slowing down phyB signal transduction on fluence response curve. Nuclear import (S1.15) shows an enhanced response (a) but the inclusion of phyB dimerisation (S1.13) suppresses the response. (b). The phyB dimerisation model with these parameters was previously shown to maintain the constant light effect (Figure 3.25)

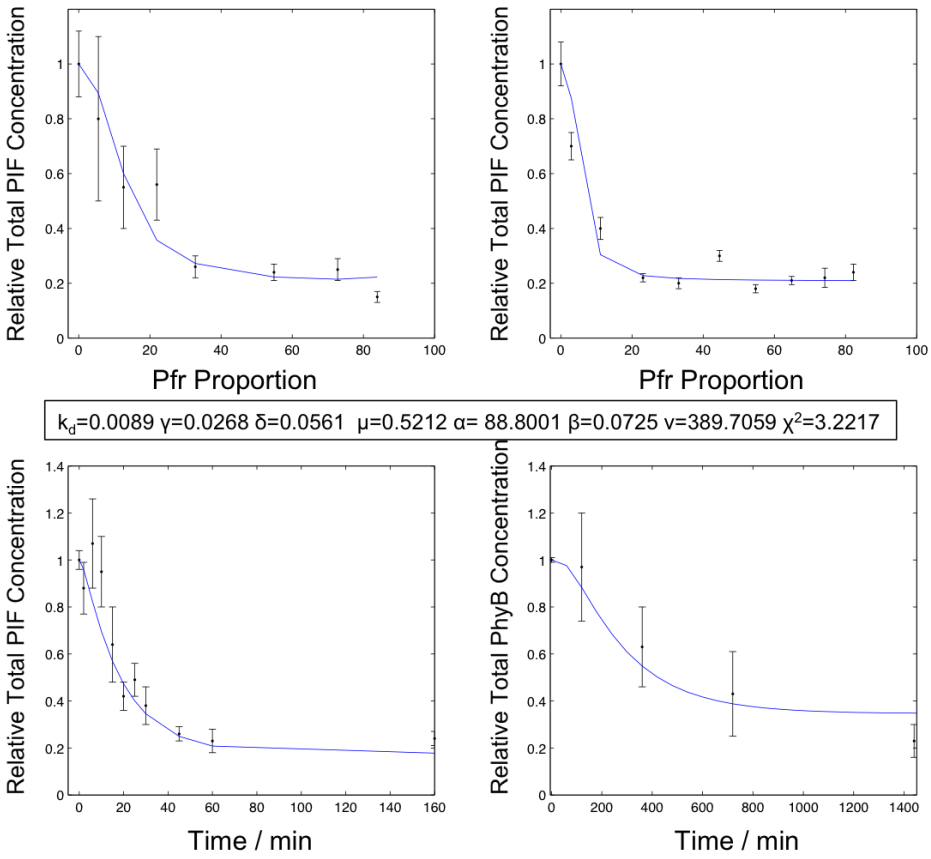

Figure 3.25: Fit of *PhyB Dimer* (S1.13) to PIF Degradation in Constant and Pulsed Light

The smoothing of the constant light data is possible by the introduction of phyB dimerisation.

3.8 Discussion

3.8.1 A Binding Cofactor or Tagging Step can Explain PIF and phyB Degradation Rates in Constant Conditions

We have modelled the simple red light signalling pathway in Arabidopsis, constructing a number of possible mechanisms able to explain the different degradation rates of phyB and PIF3. Though use of a cost function, accurate parameter sets were found for a number of these models. The complexity of these models meant the parameter sets were non-identifiable. However, using starting values from across the parameter space ensured the most accurate parameter sets were found. With a high degree of confidence we are therefore able to conclude that if a model is unable to fit the data, it is due to the failure of the model, rather than the incorrect parameter set. It was found initially that a simple model involving only PIF3 and phyB was incompatible with the degradation rates. It was therefore concluded that further components were needed to model the system.

Two models were able to recreate the data under constant and pulsed light conditions. One involved the binding of PIF3 by a protective Cofactor (*Protection*, Figure (3.3d), (S1.5)). The other achieved the mutual degradation by marking both PIF3 and phyB for degradation after the proteins bound to each other (*Double Tagging* Figure (3.3c), (S1.4)). Importantly, a short red light pulse is sufficient to cause PIF3 degradation and only these models were able to achieve this result.

3.8.2 Complex Separation is Needed to Explain the Increased Efficiency of Red Light Pulses

The models were subsequently compared to a number of quantitative data gathered by collaborators at the University of Freiburg. These included the counterintuitive result that a short pulse of red light can be more effective at degrading PIF3 than constant irradiation. When the *Protection* model (S1.5) was fitted to these data it was found to be over sensitive to light (Figure 3.9). The initial rate of PIF degradation was too great meaning a number of experimental results are incompatible with the model. The

Double Tagging model showed an accurate response to the majority of the data, but did not show this high efficiency of pulses on PIF3 degradation. Instead the model predicts the more intuitive interpretation that there is more degradation in constant light (Figure 3.8). This analysis therefore demonstrates there are additional factors the model needs to explain the behaviour under short pulses of light.

To explain these quantitative data, the model was therefore broken down and built up piecewise to explain the original data step by step, only including mutual degradation, when phyB degradation data was returned to constrain the model. The aim of this process was to find the minimum sized model able to explain all the data. In order to explain the higher efficiency of pulsed light relative to constant, the concept of complex separation was introduced, based off previous experimental observations [71]. This was able to explain the reported higher efficacy of pulsed light as the PIF:phyB complex will only separate in the presence of light. However, an unintuitive response was seen for the relationship between fluence rate and PIF levels.

3.8.3 Phytochrome is Dynamic Reversible Molecule, not a Light Switch

Modelling showed a separation between photoequilibrium point and output (Figure 3.18). The simulations shown in Figures (3.8, 3.9) did not use the photoequilibrium point to work out P_{fr} levels, but the light conditions directly. The resulting plot shows a relationship where the PIF3 steady state level is not directly dependent on the predicted P_{fr} %. The reason for this relationship is, that only photo-equilibrium point, and therefore wavelength (λ) is taken into account when calculating the P_{fr} %. Wavelength changes were achieved with different light filters. The intensity of light, which differs with these different filters is ignored in this plot. PhyB is well known to mediate fluence rate response in Arabidopsis seedlings [9, 118]. The concept of a photo-equilibrium point is therefore incorrect, as activation of phyB is dependent on the quantity as well as the quality of light. This result demonstrates that phyB should be considered as a dynamic molecule, converting between its active and inactive states and unable to be defined by a set wavelength of light. It has been observed that phyB deactivation (either by dark reversion or some other method) is necessary for fluence

response [16], but this is not sufficient to fully explain the sensitivity. There is further discussion on the molecular basis of fluence dependency in Section 4.3.1.

3.8.4 The Predicted Rise of PIF3 Levels in High Intensity Light

When the fluence dependency of the model was subsequently examined, this led to a counter-intuitive result. If the wavelength is kept constant, PIF3 levels are shown to increase at higher intensity light (Figure 3.19a). The light dependent separation of the PIF3 phyB complex can explain the increased efficiency of short pulses of light to PIF3 degradation. However, for the same reason the model shows increased PIF3 degradation at medium fluence rates. Molecular measurements proved this prediction to be incorrect with PIF3:LUC levels not increasing at high intensity light (Figures 3.22, 3.23).

Our analysis showed that this effect is dependent on the the strength of binding between phyB and PIF (γ). A large value of (γ) removes the high intensity effect, but also the increased PIF3 degradation under a light pulse (Figures 3.20a, 3.20b). Therefore explaining all the available data is inconsistent with the simple model. As PIF3 is known to separate from phyB in far red light it is a reasonable assumption to make that PIF3 will separate from P_r [71]. In high intensity light there should be reversion of phytochrome to its inactive form. The lack of rise in PIF3 levels therefore shows that either this dissociation rate is very low, or the plant has mechanisms to prevent PIF accumulation at high fluence rates. It has been postulated that one of the functions of nuclear speckles is to stabilise phyB, protecting it from dark reversion [16]. If instead they protected against photoreversion this would stop the increased phyB deactivation at high fluence rates.

3.8.5 PIF3 Degradation at High Light Intensities may be Through a Separate Mechanism

Factors other than phyB contribute to the degradation of PIF3. Aside from the other phytochromes which have a role in different light conditions, PIF3 activity is also

modified by the GA/DELLA pathway [175], while PIF4 and PIF5 are also known to be under transcriptional control of the clock [85, 89], and deactivated by HFR1 [80]. These factors are also all known to be light dependent, and may all be regulated by phyB [75]. These other light signalling pathways could provide a mechanism for phyB to dampen PIF levels at high fluence rates. In this sense, the classical method of phyB led PIF degradation is most important at lower light intensities, but is less efficient in high intensity light where a separate pathway is more important. Phytochrome A has previously been shown to be stabilised in very high intensity light, leading to a suppression of hypocotyl elongation in *phyB* null mutants [116]. In wild type seedlings, phyA may therefore be more active at degrading PIF3 in high intensity light. Recent work has found PIF3, and potentially other PIFs to be important for the transfer of phytochrome into the nucleus [55]. As nuclear phytochrome is thought to be unstable [84], this could be part of the control of PIF3 on phyB degradation. However this can not be the major function of the PIFs as we would expect the mutant phenotypes to be similar to phytochrome mutants while in reality the opposite is true.

3.8.6 PhyB Dimerisation Could be Suppressing High Fluence Rate Effects

Although the high fluence levels of PIF3 was an unintuitive prediction, it was based on known properties of the system components and therefore the fact that we did not see this effect is interesting. Some aspect of the system must be suppressing this response as based on the simple phyB PIF interactions described in the model (3.9) we would expect higher PIF levels at high light levels to be a serious problem. Sensitivity analysis (Figure 3.21) has shown that the level of phyB and the strength of the complex binding have the strongest effect on the high intensity response. A reduction in phytochrome binding can remove the response but at the cost of losing increased sensitivity to pulses of light (Figures 3.17,3.20).

The most obvious aspect missing in the model is any form of compartmentalisation. The proteins are free to interact at all times, while in reality we know phyB moves to the nucleus upon light activation [48]. In a computational sense this would have the

effect of slowing down the transmission of signal from light input to PIF degradation. A Phytochrome import model (S1) does not remove the high intensity effect (Figure 3.24a). Although the transduction of the light signal is slowed down, no effect is seen on the steady state. Treating phytochrome as a dimer would also slow down the transmission of the light signal (3.10). In this model, both monomers of phyB must be in the active form in order for it to enter the complex with PIF; the heterodimer $P_{fr}P_r$ is unstable however and and has an increased rate of dark reversion back to P_rP_r. The extreme sensitivity to changes in light input shown previously (Figure 3.18) suggests a lack of robustness in the model (3.9). The phyB dimer model changes light detection from a simple switch to a more transient process.

Table 3.6: Definition of the Dark Reversion Parameters

Parameter	Definition
k_R	$P_{fr}P_{fr} -> P_{fr}P_r$
k_r	$P_{fr}P_r -> P_rP_r$
$P_{fr}P_{fr}t$	Tagged PhyB

$$\begin{aligned}
\dot{P_rP_r} &= \alpha - (k_1+\beta)\,P_rP_r + (k_2+k_r)\,P_rP_{fr} \\
\dot{P_rP_{fr}} &= k_1\,(P_rP_r) - (k_1+k_2+k_r)\,P_rP_{fr} + (k_2+k_R)\,P_{fr}P_{fr} \\
\dot{P_{fr}P_{fr}} &= k_1P_rP_{fr} - (k_2+k_R+\gamma Y)\,P_{fr}P_{fr} \\
\dot{Y} &= k_d\,(1-Y) - \gamma Y P_{fr}P_{fr} + k_2C \\
\dot{C} &= \gamma P_{fr}P_{fr}Y - (\delta+k_2)\,C \\
\dot{Y_t} &= \delta C - \mu Y_t \\
\dot{P_{fr}P_{fr}t} &= \delta C - \nu P_{fr}P_{fr}^t
\end{aligned} \tag{3.10}$$

This does indeed reduce the extreme sensitivity to light, with the high fluence effect lost in the model (Figure 3.24b). This is achieved without the loss of constant light sensitivity previously seen for parameter sets showing this fluence response curve (Figure 3.25). Further, the response to the photo-equilibrium point is robust in R_c, showing a smooth curve, with this likely related to the loss of extreme sensitivity to

fluence. Dimerisation provides an adequate way for the system to be sensitive to short periods of red light but not overly sensitive to constant irradiation. The difference in behaviour between pulsed and constant light is not large in this model but an accurate fit to the data is found. That existing as a dimer could dampen the noise experienced by light conditions is a novel suggestion. Phytochrome may experience advantages of dimerisation beyond known functions such as heterogeneity [176].

By assuming the phyB dimer is only active when both monomers are active themselves however, changes the definition of the photo-equilibrium point. This may be an explanation for the data as it would explain why it appears that light pulses are more efficient at degrading PIF3 than constant light. Under this system, the activity of phytochrome is related to the proportion of $P_{fr}P_{fr}$ out of the dimres rather than the proportion of P_{fr} out of total monomers. However, it is not thought that both monomers have to be active for phytochrome to function properly and indeed, phyB can heterodimerise with other phytochromes such as phyD and phyE so this explanation would be surprising [45].

Chapter 4

Temperature Dependent Reversal of Red Light Response

Recent work has helped uncover mechanisms that illustrate how light and temperature control plant responses [93, 129]. Work from us and others has shown that these signals are not distinct, but interact and that functional light sensing machinery is important for the proper response of *Arabidopsis* to temperature [132, 137, 148]. This chapter examines the interaction between light and temperature on seedling growth. The Phytochrome Interacting Factors (PIF) transcription factors were revealed to be at the centre of a temperature dependent switch of light signalling. High temperatures lead to a reversal of light control on hypocotyl elongation. At 27$^{\circ}C$, an increase in red light leads to an increase hypocotyl length due to enhanced PIF activity. High temperature and high fluence rate interact at the PIF level to lead to increased hypocotyl elongation compared to seedlings grown at lower fluence rates at the same temperature. While phyB is important for the degradation of PIFs at low fluence rates, the high light intensity response in independent of the phytochromes. Evidence points to an apically derived signal interacting with the PIFs in high intensity light, most likely a product of photosynthesis.

Hypocotyls have emerged as a simple system for studying light and hormone sig-

nalling. The repression of hypocotyl elongation is a key element of photomorphogenesis and the final length is linked to the quantity and quality of light the seedling is exposed to [107, 124]. The length of the hypocotyl is well correlated to phyB activity [42], and it is well established as a read out of hormonal activity and temperature [93, 127]. The relative simplicity of the assay means more is known of hypocotyl elongation than any other system and is therefore ideal to study the interaction of light and temperature.

4.1 Introduction

4.1.1 The Interaction of Light and Temperature

Light and temperature are two of the most important factors in determining plant growth. As sessile autotrophs, maximising the amount of light absorbed is critical to a plants survival. Matching growth to the environmental conditions ensures *Arabidopsis* plants absorb enough energy from photosynthesis to support growth. Temperature is important to all organisms due to its effect on biochemical reaction rates. Yet, very little is known of how organisms perceive temperature molecularly. However, changes in ambient temperature can invoke dramatic alterations in a plant's physiology, and growth architecture, which is thought to maximise reproductive success in potentially stressful conditions [177].

For some responses, such as control of seedling elongation, light and temperature have been shown to have opposing effects. It is very well established that increased light fluence rates lead to a reduction in hypocotyl length and therefore seedling height [42, 62, 63, 163]. In natural environments, seedlings will grow longer under soil and heavily shaded conditions in search of light. An increase in temperature in contrast leads to an increase in hypocotyl elongation, coinciding with an increase in hypocotyl auxin and GA Levels [93, 127].

Importantly these external light and temperature signals have been shown to interact in the regulation of specific responses. In the dark there is no effect of temperature on final hypocotyl length in *Arabidopsis*. A difference in seedling phenotype is only

observed when seedlings are exposed to light [127, 178]. This suggests there is a level of molecular cross-talk between the light and temperature pathways. The red light photoreceptor, phytochrome B (phyB), has been identified as a likely site for this cross signalling. At cooler temperatures the *phyB* null mutant flowers with the same rosette number as wild type, while at 22 $^{\circ}C$ it is very early flowering [35]. When *phyB* deficient plants are grown at warmer temperatures a severe loss of biomass is seen, showing the photoreceptor is vital for biomass maintenance at warm temperatures [132].

4.1.2 PhyB Regulated Seedling Growth

In the early stages of *Arabidopsis* development, phyB is the most prominent of the red light receptors, as red light induced hypocotyl inhibition is severely attenuated in the *phyB* null mutant [9, 118]. In contrast, the *pif* mutants show the opposing phenotype, with shorter hypocotyls in red light [169]. Removing PIF1,3,4 & 5 (The *pifq* mutant) results in a constitutive photomorphogenic phenotype, with seedlings short in the dark [75, 96].

Hypocotyl length has long been seen as a read out of phyB activity, as there is a very strong correlation between phyB quantity and seedling length [42]. The response is controlled at least partly through the degradation and deactivation of the PIFs by phyB [87]. Upon light activation, phyB binds to PIF proteins leading to their subsequent phosphorylation, ubiquitination and degradation through the 26S proteosome [81, 83]. This degradation is based on the amount of active phyB (P_{fr}), and responds to external light conditions in a classical Low Fluence Response (LFR) [71, 95, 179] (see Section 1.1.5) . This degradation of PIF proteins leads to the change from skotomorphogenesis to photomorphogenesis, with the quadruple *pif1345* mutant (*pifq*) constitutively photomorphogenic [88].

However, a mutant form of PIF3 unable to bind phyA or phyB still causes a change in gene expression in response to red light [40]. The mutant PIF3 is stable [74] but mutants show hypocotyl elongation indistinguishable from a *pif3* mutant [40]. PhyB

has since been shown to sequester PIF from DNA, lowering its activity without needing to target the protein for degradation [180]. PhyB is able to affect PIF activity through other methods, such as manipulation of the GA hormone pathway and as an input to the circadian clock [75, 181, 182]. It is also thought that PIFs regulate growth through modulation of phyB levels [42], and it has been shown that PIF 3, 4 and 5 act additively to degrade phyB in a COP1 dependent manner [84]. The majority of PIF behaviour is as a transcription factor, although its affect on phyB levels is not through altered transcription [42]. This suggests the PIFs may have multiple functionality. [19, 40, 85].

4.1.3 Photohormones GA and Auxin Combine with PIF4 to Induce Temperature Induced Hypocotyl Elongation

Seedlings deficient in PIF have been shown to have severely reduced response to temperature [129]. The transcription, accumulation and phosphorylation of PIF4 has been shown to be temperature dependent [93, 132]. The binding of PIF4 to DNA is also dependent on temperature, suggesting that temperature could feed into light signalling through temperature dependent chromosome modification [137]. The *pif4* mutant does still have minor responses to temperature and there is a predicted function of PIF5 in temperature signalling [93].

The phytohormone auxin has been strongly implicated in the temperature response [127]. While large concentrations of exogenous auxin will lead to a decrease in hypocotyl length, lower concentrations cause increased hypocotyl elongation [136, 166]. Auxin signalling is known to contribute to temperature dependent hypocotyl elongation. A near complete loss of temperature response is observed in the largely auxin resistant *axr1-12* mutant, and mutants lacking auxin receptors, such as *tir1-3*, show significantly reduced temperature response [127]. An overlap of genes controlled by auxin and PIF4 & 5 has also previously been identified by microarray analysis [136]. The binding of PIF4 to Auxin biosynthesis genes *YUCCA8*, *TAA1* and *CYP79B2* was shown to be temperature dependent [146, 148]. This temperature dependent binding is also present on the auxin response gene *IAA29* [126]. The PIFs therefore are regulators of both auxin

levels and auxin response.

The regulation of seedling development by light and temperature is therefore part of a complicated system with many inputs and levels of control. At the heart of this system is the degradation of PIF by phyB but in some conditions this does not appear to be required for control of hypocotyl elongation [40]. This study seeks to uncover the mechanisms behind the light gating of temperature control [127] and the most important components of this system.

4.2 Results

4.2.1 High Temperatures Reverses the Seedling Growth Response: Hypocotyl Length Increases at High Fluence Rates in the Warm

A large body of literature has shown that an increase in red light intensity leads to the suppression of hypocotyl elongation [42, 68, 116, 163]. This idea is consistent with an increase in phytochrome activity, leading to a decrease in activity of the PIFs. We can replicate this behaviour when seedlings are grown at $17°C$ (Figure 4.1a). However, when plants are instead grown at elevated temperature ($27°C$), a reversal of this suppression is seen. Strikingly, increasing light intensity beyond 1.6 $\mu molm^{-2}s^{-1}$, does not suppress, rather it leads to a promotion of hypocotyl elongation (Figure 4.1b). This counter intuitive result suggests a switch in the behaviour between light signalling and physiological output at high temperatures. This observation suggests, at $27°C$ elongation is promoted at high fluence rates, either directly through deactivation of phyB or through a separate fluence dependent growth pathway. A similar requirement for high intensity light for the temperature response is seen with blue, white and red diurnal light. However the effect is strongest by far in constant red light (Figure S2.13).

If the difference between the warm and cool grown hypocotyls is plotted, a fluence dependency to the temperature effect is seen (Figure 4.2). This effect is nearly linear, so the importance of temperature is directly related to the amount of light received by the plant. With phytochrome previously shown to respond to light in a more logarith-

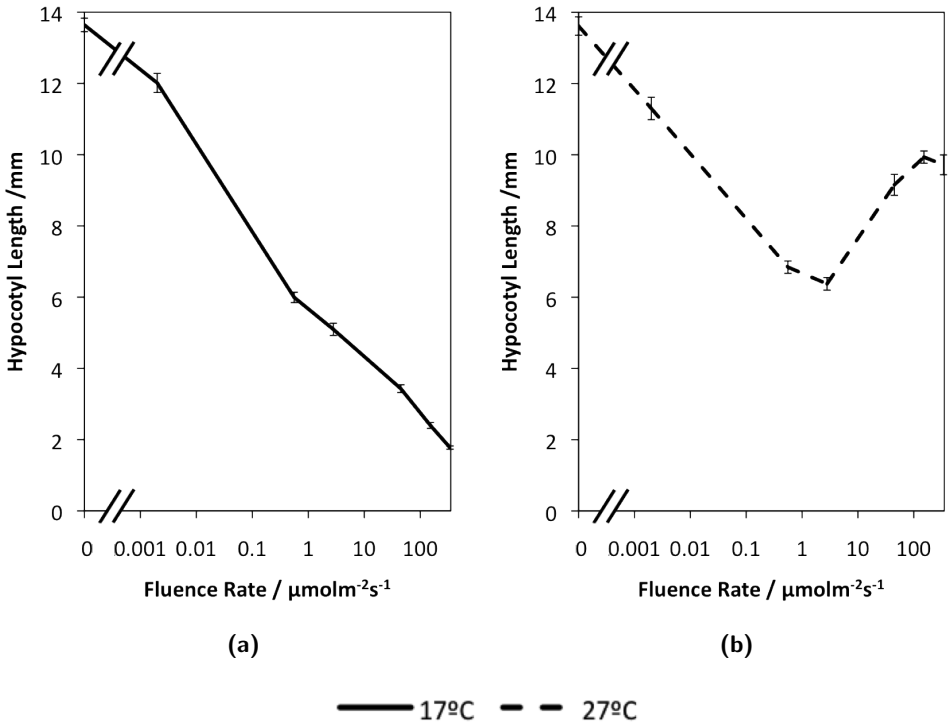

Figure 4.1: Fluence Response curve of Hypocotyl Length of Seedlings Grown at 17°C & 27°C

Hypocotyl length of 7 day old Seedlings of ecotype *Columbia* grown under a series of different red light intensities at 17 & 27°C. At 27°C increasing light intensity can cause an increase in hypocotyl elongation.

mic manner [16], this is consistent with a fluence rate specific signal that is activated in the warm.

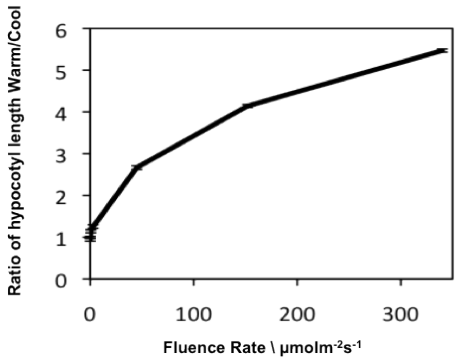

Figure 4.2: The Temperature Effect on Hypocotyl Growth is Roughly Linear

(Graph showing data from Figure (4.1). The ratio of hypocotyl length between warm grown and cool grown seedlings shows a fluence rate dependency on temperature effect

4.2.2 The Increase of Elongation in the Warm is Independent of Phytochromes

It was previously reported that at very high intensity light, *phyB* mutants show a suppression of hypocotyl length due to increased phytochrome A (phyA) activity [116]. We therefore reasoned that the effect on very high fluences may be a result of increased phyA signalling and set out to test this possibility by comparing the behaviour of *Col* wild type to *phyB* and *phyAB* null mutants at 17 & 27°C.

Inconsistent with the previous work, the *phyB* mutant does not show a strong suppression of hypocotyl length at very high fluence rates (Figure 4.3a) [116]. At very high intensity red light, a small suppression of hypocotyl length is observed compared to *phyAB*, but the effect is subtle. As the previous work was conducted in ecotype *Landsberg erecta* (*Ler*) we also ran the experiment with *Ler phyAB* alleles. This experiment yielded a similar result under our conditions (Figure S2.4). The data therefore indicate that at 17°C, phyB is the primary contributor to hypocotyl elongation over a broad fluence range.

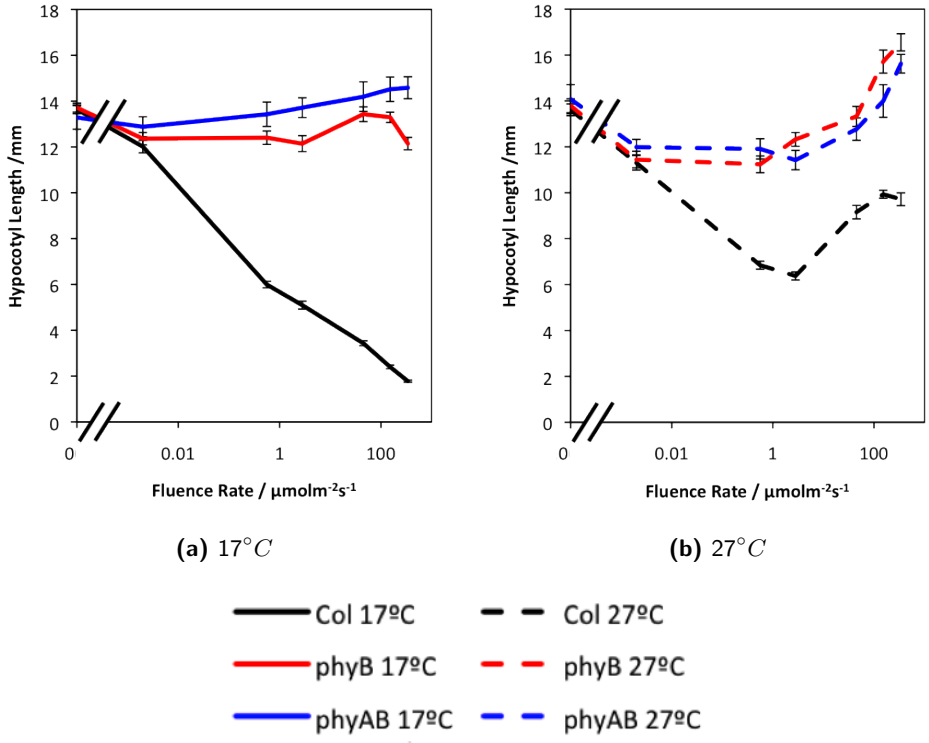

(a) 17°C **(b)** 27°C

Figure 4.3: Hypocotyl Phenotype of Phytochrome Mutants over a Fluence Curve at 17 & 27°C

A small phyA dependent reduction in hypocotyl length in response to fluence rate is seen in the cool. However, at 27°C, an increase in hypocotyl length is seen in *phyB* and *phyAB* similar to that of wild type, suggesting a phytochrome independent mechanism.

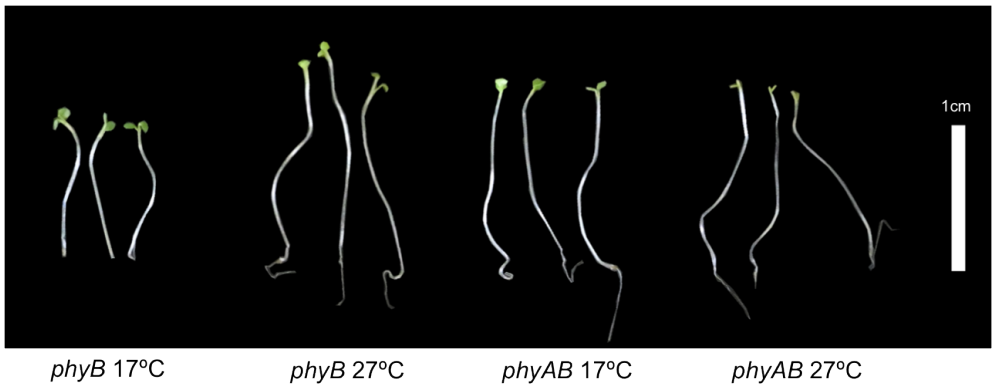

Figure 4.4: Photo of *phyB* and *phyAB* Mutants Grown at 342 $\mu molm^{-2}s^{-1}$, 17 & 27°C

In the warm, *phyB* and *phyAB* seedlings are constitutively long within a fluence rate range. However at very high intensity red light ($> 100\mu molm^{-2}s^{-1}$), an enhanced response is seen with greater hypocotyl elongation seen in high intensity light than darkness at $27°C$ (Figures 4.3b, 4.4). This suggests that while the suppression of hypocotyl growth seen in the cool is phytochrome dependent, this elongation in the warm may be independent of the photoreceptor. The other phytochrome single mutants (including *phyA*) all show a near wild type response in the warm, showing if there is a different signalling molecule, it is unlikely to be simply a different phytochrome (Figure S2.4, S2.9).

4.3 PhyB Properties: Analysis at Cool Temperatures

4.3.1 How Far can the Photoreceptor Confer Fluence Rate Sensitivity?

Although the suppression of hypocotyl length with increasing total fluence is well established [42, 68], this is inconsistent with what is known about the photoreceptor. PhyB is thought to only signal through an LFR which will saturate at high fluence rates. However, at $17°C$, continued fluence rate dependent suppression of hypocotyl length is observed in light intensities beyond $100\mu molm^{-2}s^{-1}$. The molecular mechanism of phyB activation is based on the dynamic equilibrium between its inactive and active forms, P_r and P_{fr}. The photoreceptor will convert from its inactive to active state based upon the quantity and quality of light it absorbs. The efficiencies of its photoconversion were calculated for different wavelengths previously and these were shown to be linearly dependent on the fluence rate (or photon flux) between approximately 1 and 10 $\mu molm^{-2}s^{-1}$ [12, 167, 183].

Using this knowledge of the photoreceptor, we therefore take a modelling approach to investigate if this is sufficient to explain the fluence rate control on hypocotyl elongation. The photoreceptor will reversibly convert between its inactive (P_r) and active (P_{fr}) forms dependent on the external light conditions (section 1.1.1) (Figure 4.5). This is modelled as a series of differential equations (4.1), with parameters k_1 and k_2 dependent on fluence rate (Table 4.1).

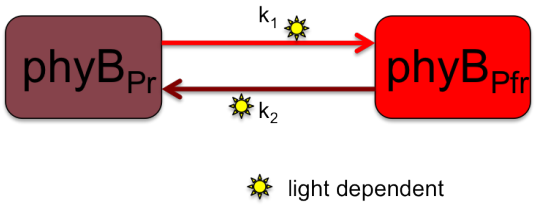

Figure 4.5: Cartoon of the Dynamic Reversibility of Phytochrome (Equation 4.1)

$$\begin{aligned} \dot{P_r} &= -P_r k_1 + P_{fr} k_2 \\ \dot{P_{fr}} &= +P_r k_1 - P_{fr} k_2 \end{aligned} \tag{4.1}$$

Table 4.1: Definition of the Parameters used in Section 4.3.1

Parameter	Definition
$\sigma_{r\lambda}$	Absorbance of P_r at wavelength λ
$\sigma_{fr\lambda}$	Absorbance of P_{fr} at wavelength λ
N_λ	Fluence rate at wavelength λ
k_1	$\sigma_{r\lambda} N_\lambda$ (Light dependent phyB activation)
k_2	$\sigma_{fr\lambda} N_\lambda$ (Light dependent phyB deactivation)
P_r	Inactive Phytochrome B
P_{fr}	Active Phytochrome B

As both the forward and reverse reactions of (4.1) are equally dependent on fluence rate, the steady state equations (4.2) are only dependent on the wavelength of light. This very simple model is therefore unable to recreate the fluence dependency observed in experimental data (Figure 4.6).

$$\begin{aligned} \lim_{t\to\infty} P_{fr} &= P_r \tfrac{k_2}{k_1} \\ &= P_r \tfrac{\sigma_{fr\lambda} N_\lambda}{\sigma_{r\lambda} N_\lambda} \\ &= P_r \tfrac{\sigma_{fr\lambda}}{\sigma_{r\lambda}} \end{aligned} \tag{4.2}$$

In (4.1) all the parameters are dependent on fluence rate. All the fluence dependent components therefore cancel in the steady state equations, leaving them only dependent on wavelength (4.2). For overall phytochrome activity to be dependent on fluence, it is therefore necessary to introduce non fluence dependent components. In the absence

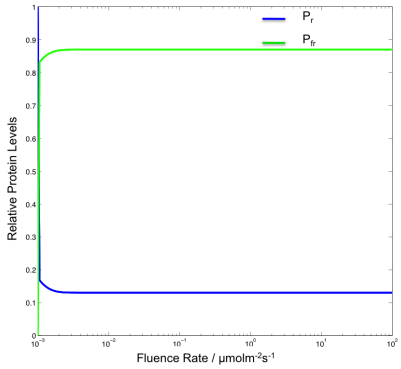

Figure 4.6: Simulated Relative Levels of P_r and P_{fr} from Equation (4.1) after 6 days of Constant Red Light over a Range of Light Intensities.

of light, P_{fr} will relax back to P_r in a process called dark reversion [17]. This is therefore introduced to the model. Dark reversion is notated by k_r and represents the non light dependent conversion from the active P_{fr} form to the inactive P_r form. This rate was calculated as $0.0321min^{-1}$ at 22 $°C$ [16] but is known to be temperature sensitive [145]. Light independent conversion back to P_r would introduce a level of fluence rate dependency. The higher the light intensity, the lower the relative contribution of dark reversion.

The introduction of synthesis and degradation of Phytochrome is a further way to add non fluence dependent components to the system. Phytochrome is synthesised in its inactive P_r state before converting to P_{fr}. The degradation of Phytochrome as P_{fr} would therefore apply fluence control on the system in a similar way to dark reversion, by reducing the pool of active Phytochrome in a fluence independent way. The modifications to the system are shown in equation (4.3) and P_{fr} steady state shown in (4.4).

Table 4.2: Definition of the Parameters used in Section 4.3.1

Parameter	Definition
k_r	Dark Reversion
α	P_r Synthesis
β	P_r Degradation
ν	P_{fr} Degradation

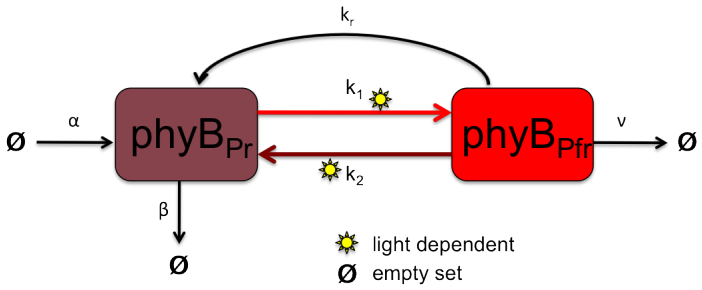

Figure 4.7: Cartoon of the Reversible Phytochrome Activation with non Fluence Dependent Components (Equation 4.3)

$$\begin{aligned} \dot{P_r} &= \alpha - P_r(k_1 + \beta) + P_{fr}(k_2 + k_r) \\ \dot{P_{fr}} &= +P_r k_1 - P_{fr}(k_2 + k_r + \nu) \end{aligned} \tag{4.3}$$

$$\begin{aligned} \lim t \to \infty P_{fr} &= \frac{\frac{js}{jd}}{\frac{\sigma_{fr}}{\sigma_r} + \frac{\nu + k_r}{\sigma_r N_\lambda} + \nu} \\ &= \frac{\frac{\alpha}{\beta}\sigma_r N_\lambda}{N_\lambda(\sigma_r \nu + \sigma_{fr}) + \nu + k_r} \end{aligned} \tag{4.4}$$

P_{fr} levels are now dependent on the fluence rate (N_λ) but in a non intuitive way. As N_λ is present on both the numerator and denominator, the amount of active photoreceptor reaches a maximum at $\frac{\alpha\sigma_r}{\beta(\sigma_r\nu+\sigma_{fr})}$. When plotted over a fluence curve on a logarithmic scale, a sigmoidal curve is seen, with the strongest fluence response seen in medium light intensities (Figure 4.8). So with this model it is possible to maintain a fluence response over about 2 orders of magnitude, with no phytochrome activity at 0.01 $\mu molm^{-2}s^{-1}$ and maximal activity at 1 $\mu molm^{-2}s^{-1}$. However, it has been shown that the hypocotyl phenotype is able to respond to different fluence rates over several orders of magnitude, so this model cannot account for the fluence rate control of hypocotyl elongation (Figure 4.1).

To observe whether this lack of fluence control is a function of the system as a whole or only the selected parameter set, a sensitivity analysis is performed. Individual parameters are altered and the resulting fluence dependency of P_{fr} plotted (Figure 4.9). Changing the phyB synthesis rate (α) or the P_{fr} degradation rate (ν) has no effect

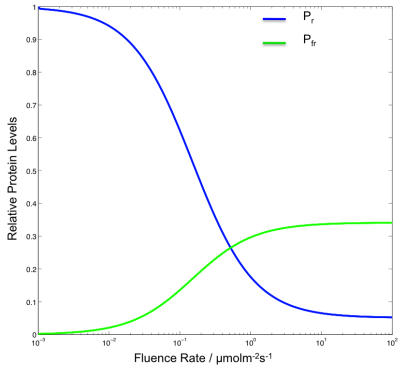

Figure 4.8: Simulated Relative Levels of P_r and P_{fr} from Equation (4.3) After 6 days of Constant Red Light Over a Range of Light Intensities.

on fluence dependency, only the amplitude of steady state P_{fr} (Figure 4.9a, 4.9c). By changing the values of P_r degradation (β) or dark reversion (k_r), the fluence dependency can be changed, but the range of control is not altered. So, if P_{fr} levels are sensitive to high intensity light, they are insensitive to low intensity light (Figure 4.9b, 4.9d). The parameters of light dependent parameters k_1 and k_2 are based on published values on the absorption spectra of phytochrome [183, 12, 167]. However, if these parameters are also allowed to vary, it does not increase the fluence dependency of the system (Figure S2.2).

An increase in phytochrome compartmentalisation does not improve the fluence rate dependency of P_{fr} as demonstrated in a the *Rausenberger 2010* Model [16]. The model, included phyB nuclear localisation and speckle formation, with nuclear phyB as the active signalling protein. When fitted to hypocotyl length, a sigmoidal curve is also seen. Analysis of this model is shown in Figure (S2.1), with no increase in fluence dependency observed.

The idea that phyB controls fluence dependent hypocotyl suppression in red light is well established [42]. This is because it is known to control hypocotyl elongation, and will respond to increasing fluence rates [16]. However, we have shown that the response of phyB alone is unable to confer the fluence sensitivity seen in hypocotyl control. This points to either the action of another red light receptor, possibly phyA [68], or a new

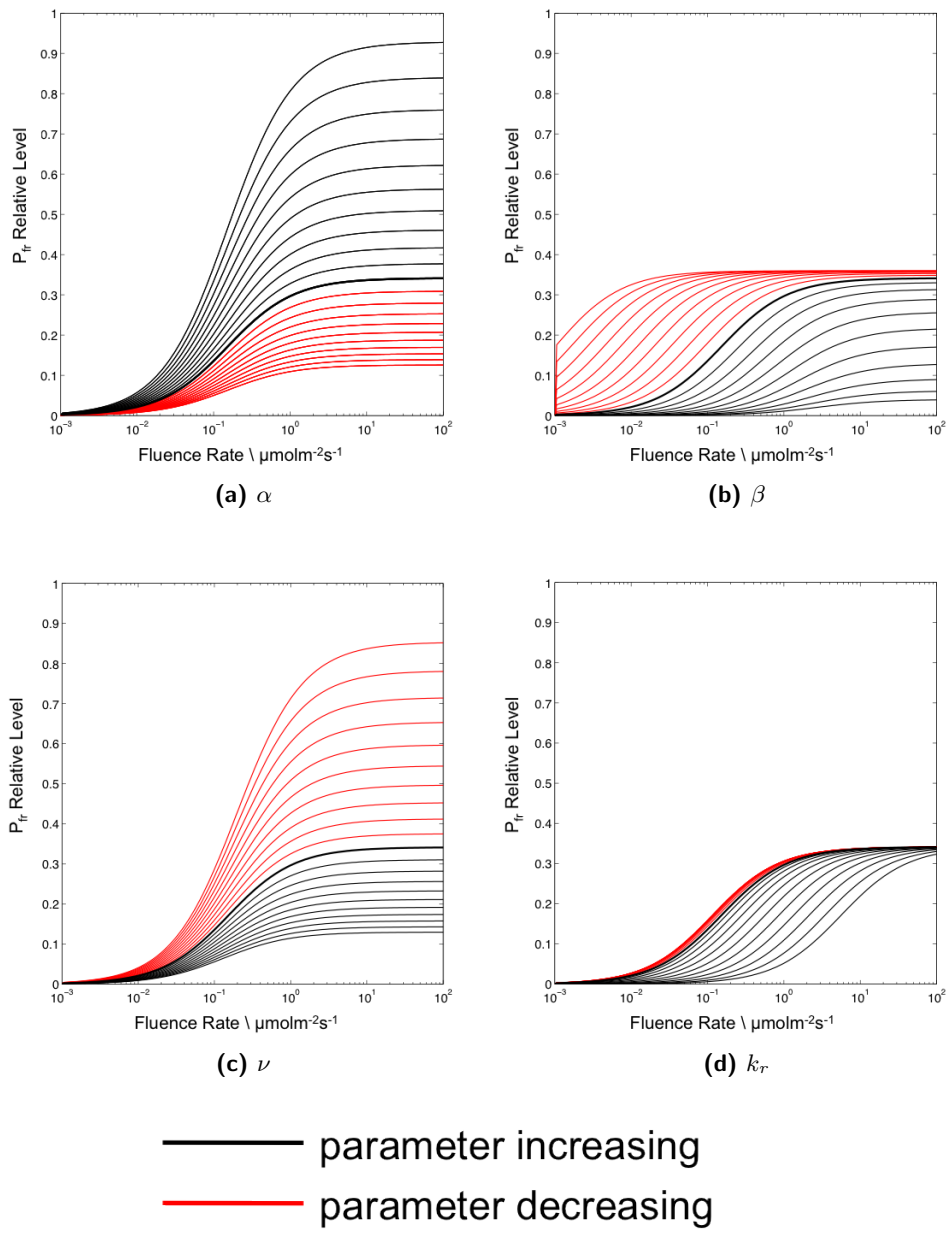

(a) α **(b)** β

(c) ν **(d)** k_r

Figure 4.9: Sensitivity Analysis Showing the Fluence Response of P_{fr} Steady State with Changing Parameter Sets

Parameters α (Figure 4.9a) and ν (Figure 4.9c) are increased or decreased in an exponential scale by a maximum of e^1; β (Figure 4.9b) and k_r (Figure 4.9d) by a maximum of e^5.

as yet undescribed form of phyB signalling, perhaps similar to the HIR described for phyA [30]. Suppression of hypocotyl elongation at high light intensities by phyA was previously described [116], but under our conditions the contribution from phyA was minor (Figure 4.3). Therefore we explored whether the persistent activity resulted from a phyB High Irradiance Response (HIR).

4.3.2 A High Irradiance Response Does not Contribute to Hypocotyl Elongation Suppression at 17°C

Normal phyB signalling is described as an LFR. This means it obeys the Bunsen-Roscoe law of reciprocity, with a plant only responding to the total fluence of light, irrespective of whether it is given in short high intensity pulses, or constant light of lower intensity [67]. A High Irradiance Response (HIR) occurs when the plant breaks this law of reciprocity, with an increased response to constant irradiation, that can not be recreated by the same quantity of light given in short light pulses [68] (section 1.1.5). Until now, phytochrome A has been the only light receptor described as signalling in an HIR [184], the characteristics of which rely on nuclear shuttling of the photoreceptor and its long term light instability [30]. To test if our observed phyB dependent behaviour was due to an HIR, seedlings were grown either in constant conditions or under short pulses of high intensity red light. The equivalent pulse to $40\mu molm^{-2}s^{-1}$ (R_c) of constant light was hourly pulses of $342\mu molm^{-2}s^{-1}$ for 7 minutes (R_p) .

At the lower end of the fluence range pulses are more effective than constant at suppressing hypocotyl elongation, however over the whole fluence range the effectiveness is broadly the same (Figure 4.10). As continuous light is not more potent than pulsed light at higher fluence rates, it suggests that phyB does not operate in an HIR in this range At even higher fluences a separation between the pulsed and constant conditions may be seen but we are limited by the power of our lights and unable to make that conclusion based on these data. However, at $12°C$, constant light does show slightly increased hypocotyl repression when compared to high intensity pulses, suggesting an HIR may be significant at very high light intensities (Figure S2.6).

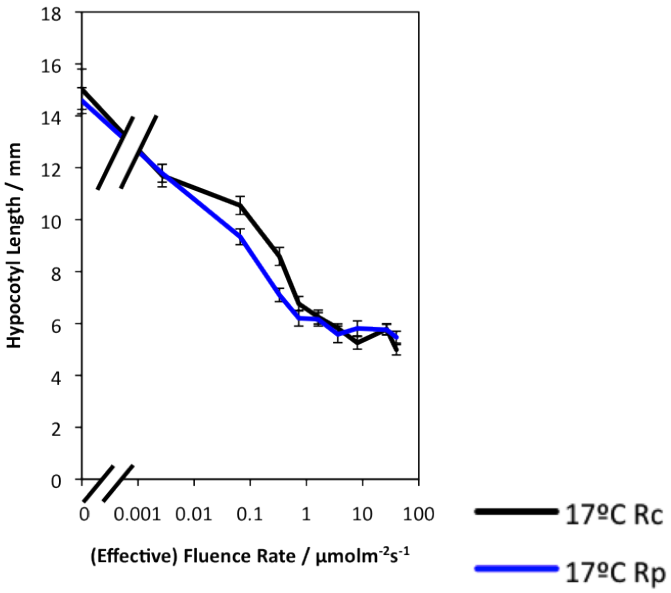

Figure 4.10: Affect of High Intensity Pulses Compared to Constant Light on Hypocotyl Length at $17°C$

Seedlings are either grown in constant conditions (Rc) or hourly pulses of 7 minutes high intensity light (Rp). Here the x-axis represents fluence rate for (Rc) and the effective fluence rate for Rp (pulsed fluence divided by 8.57)

To further test the notion that phyB may operate in an HIR we used the hyperactive *phyB-401* mutant. *phyB-401* is a mutant described as being unable to deactivate phytochrome B in far red light [25]. Phytochrome B has an altered structure in the PHY region of the protein and it is predicted to lose a section of the chromophore interacting tongue [163] (Section 1.3). This results in both the rate of photoreversion (k_2, (Table 4.1)) and dark reversion (k_r, (Table 4.2)) being severely reduced (Figure 4.11b). As a result this mutant is acutely sensitive to light, only requiring a light intensity of $0.001\mu molm^{-2}s^{-1}$ to see almost complete phyB dependent de-etiolation. In phyA, the HIR is dependent on cycling of the protein between its P_r and P_{fr} forms [30]. We should therefore be able to reduce the effect of an HIR by reducing the value of k_2 in *phyB-401*

We observe the previously described fluence response in phyB-401 at $17°C$, with extreme sensitivity to light followed by a lack of further response over the curve (Figure 4.12) [163]. However, at high intensity light the mutant shows a wild type re-

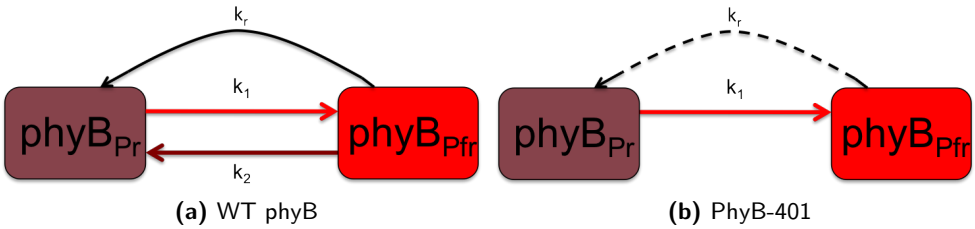

(a) WT phyB **(b)** PhyB-401

Figure 4.11: Cartoon Representation of phyB-401 Action Compared to Wild Type phyB

phyB-401 is extremely sensitive to light. Once activated, the photoreceptor is not deactivated by light and has a severely reduced dark reversion rate (k_r) [25, 163].

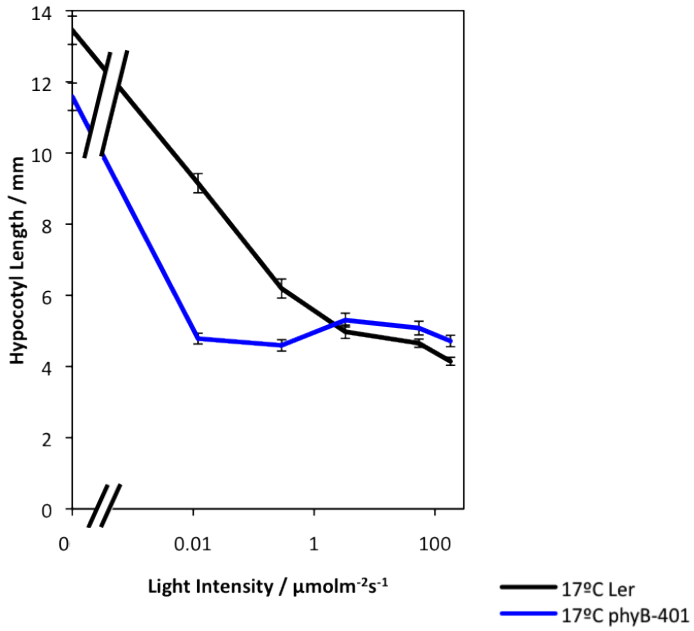

Figure 4.12: Hypocotyl Length of *phyB-401* Mutant Seedlings Grown at $17°C$

The phyB-401 grown at $17°C$ shows acute light sensitivity but no fluence rate dependence.

sponse, with a similar level of hypocotyl suppression in *phyB-401* as *Ler* wild type. The hypocotyl length in *phyB-401* is not fluence dependent over the range 0.01 $\mu molm^{-2}s^{-1}$ to 100$\mu molm^{-2}s^{-1}$, showing that phyB signalling is already saturated in the mutant at the very low fluence rate. This means maximal phyB signalling can be achieved by converting all P_r into P_{fr} which is consistent with an LFR. With previous data we conclude that the high intensity hypocotyl suppression is not the result of an HIR.

4.4 PhyB Can Still Repress Elongation at 27°C

4.4.1 Overexpressing PhyB Blocks the High Intensity Response

At both 17 and 27°C, there is an increase in hypocotyl length in the *phyB* mutant compared to wild type, showing phyB suppresses elongation in both the cool and the warm (Figure 4.3). However, a fluence dependent increase in hypocotyl length is still seen in plants deficient in phyB signalling at 27°C raising the possibility this may be phyB independent. A mutant line overexpressing phyB is known to reduce PIF levels and lead to a suppression of hypocotyl elongation [42]. If the high temperature elongation is phyB independent then it should be present even when the photoreceptor is overexpressed. We therefore look at the response of seedlings with PHYB expressed under the constitutively active 35S promoter over a fluence curve.

Seedlings containing PHYB:GFP were grown over the fluence curve at 17 & 27°C. PHYB:GFP was either transcribed under its own promoter (PHYB:PHYB:GFP) [185] or the overexpressing 35S Cauliflower Mosaic Virus promoter (35S:PHYB:GFP), both in a *phyB* background [163]. These lines are from different ecotypes, but it has been shown that both *Lansberg erecta* and *Columbia* have the same wild type phenotype (Figures 4.1, S2.4).

The previously described shape of fluence response of the mutants is seen at 17°C with the 35S overexpressor being sensitive to light and reducing to a very short hypocotyl in medium intensity light (Figure 4.13a). At 27°C however, the 35S overexpressor does not show the wild type phenotype. There is marginally increased suppression at low

light intensities but at high fluence rates, the hypocotyls are extremely short, with no difference in the transgenic line between 17 and 27°C (Figure 4.13). When PHYB is synthesised under its own promoter, a wild type effect is seen with an increase of hypocotyl elongation in the warm (Figure 4.13b). No evidence was found for a change in phyB transcription at different fluence rates and temperatures (Figure S2.7). It is therefore likely that the temperature effect requires limited levels of phyB.

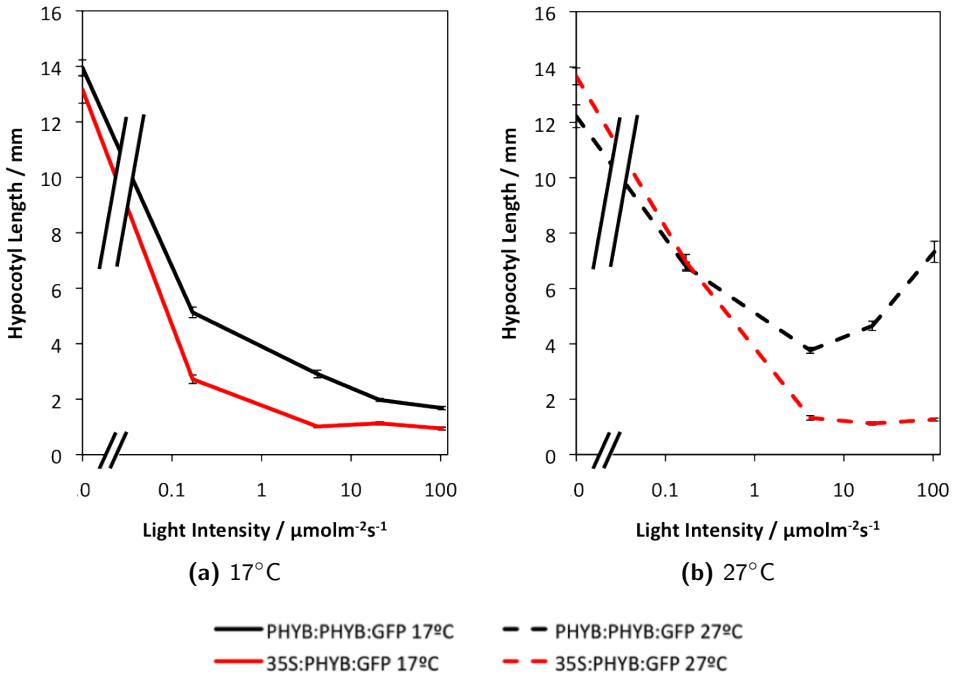

Figure 4.13: Hypocotyl Length of the PHYB overexpressor over a Fluence Curve at 17 & 27°C

4.4.2 PIF3 Protein Levels are Temperature Dependent but Do Not Change in High Fluence Rates

Vital to some of the functions of phyB is its ability to degrade the PIF family of transcription factors [75]. The activity of phyB can therefore be tested by looking at the levels of PIF3 protein over a fluence rate range at 17 and 27°C. Unlike PIF4 or PIF5, synthesis of PIF3 is not dependent on the clock and is therefore a better measure of phyB activity [19, 85]. If the activity of phyB is unchanged at the high fluences, we

would expect the degradation of PIF protein to also remain unchanged. PIF levels would be expected to decrease, consistent with an LFR but then stabilise at high light intensities. A quantitative PIF3:LUC experiment is therefore repeated at 17 and 27°C, to investigate if the fluence response of PIF3 is temperature sensitive (Figure 4.14). Both the acute and long term responses to fluence were investigated, with etiolated seedlings either given 1 hour of red light (Figure 4.14a), or seedlings grown in constant light for 4 days before harvest. (Figure 4.14b)

Consistent with previous results seen at 22 °C (Figure 3.23), PIF3 levels do not rise at high light intensities; and this is true both at 17°C & 27°C (Figure 4.14). There is a temperature dependent effect on PIF3, with levels higher at 17°C compared to 27°C. This is the opposite to that previously described for PIF4 [132, 140], and suggests that phyB is not less active at high temperatures. A similar analysis looked at the behaviour of 35S:PIF4:LUC over the same assay and again no fluence effect was seen. As reported previously, PIF4 levels were higher in the warm, but the levels did not increase at high light intensities at either temperature (Figure S2.10). These analyses suggest that the activity of phyB is not affected at high light intensities and this is true at both 17°C and 27°C. Therefore the temperature switch in behaviour does not result from reduced action by phyB on PIF degradation. As PIF levels do not change in response in high fluence rates, the effect we see in the warm is either PIF independent, or a result of a change in PIF activity independent of their levels. We therefore investigate if the high intensity response in the warm is due to a phyB independent, fluence rate response.

4.4.3 Pulses Eliminate the High Intensity Response at 27°C

At 17°C, analysis showed the suppression of hypocotyl elongation was consistent with a phyB LFR (Figure 4.10). However, as phyB will suppress hypocotyl length and degrade PIF at both 17 and 27°C, we looked to see if the warm behaviour could also be explained by an LFR.

At 27°C we observe a loss of the constant light wild type response, with no temper-

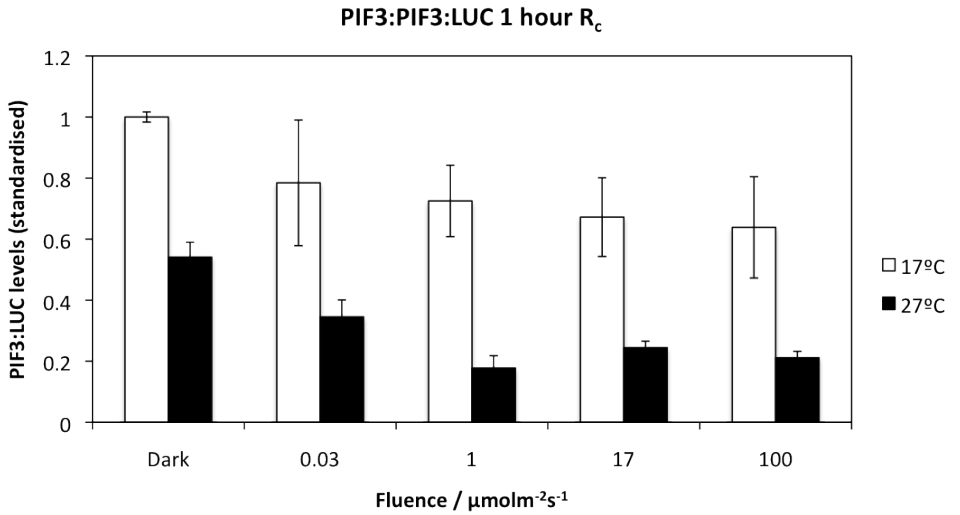

(a) PIF3:PIF3:LUC 1 hour

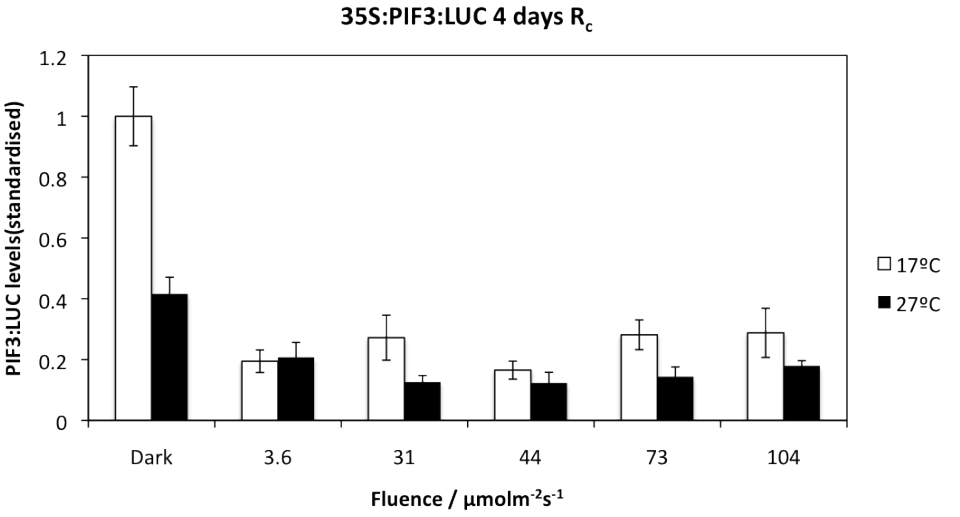

(b) 35S:PIF3:LUC 4 day

Figure 4.14: Destructive Assay Quantifying PIF3:LUC over a Fluence Curve

Levels of PIF3 in seedlings grown under different light intensities at 17°C & 27°C. Calculated by Luminescence values relative to total protein. Error bars represent standard error of the mean from 3 biological replicates.
(a) PIF3 transcribed on its own promoter, dark adapted seedlings given 1 hour of light.
(b) PIF3 transcribed on the 35S promoter. Seedlings grown in constant conditions for 4 days.

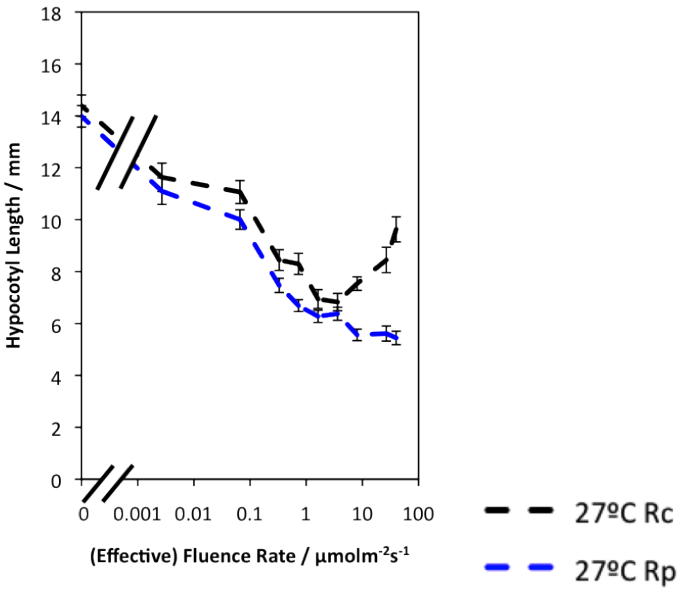

Figure 4.15: Affect of High Intensity Pulses Compared to Constant Light on Hypocotyl Length at $27°C$

Seedlings are either grown in constant conditions (Rc) or hourly pulses of 7 minutes high intensity light (Rp). Here the x-axis represents fluence rate for (Rc) and the effective fluence rate for Rp (pulsed fluence divided by 8.57)

ature effect of hypocotyl length at equivalent high fluence rates (Figure 4.15, 4.16). The pulses invoke a fluence dependent suppression of hypocotyl length throughout the LFR range before saturation at the higher light intensities. In order for high intensity light to increase seedling elongation in the warm, constant irradiance is required. At $27°C$, we see a loss of reciprocity showing the warm behaviour of hypocotyls is by definition the action of an HIR. As the response was previously described as phyB independent (Figure 4.3), this is not a phyB HIR, but a separate HIR dependent on external signals.

4.4.4 PhyB is Still Active at High Intensity Light in the Warm

If Wild Type phyB is losing activity at high fluences in the warm this should not be seen in the *phyB-401* mutant. We would expect a complete lack of fluence response in the mutant with seedlings short and de-etiolated in all light conditions. If however the effect is independent of phyB we would expect wild type hypocotyl elongation in the warm. At $27°C$, *phyB-401* shows the initial sensitivity to light at low intensities but at

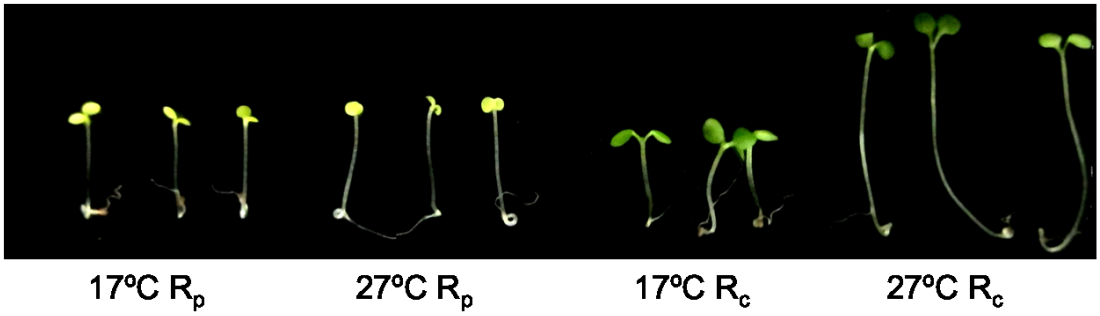

Figure 4.16: Photograph of Seedlings Grown in Constant Conditions (R_c) or Under High Intensity Pulses (R_p) at 17 or 27°C

Seedlings here were grown under the maximum light intensity ($R_c = 40\mu molm^{-2}s^{-1}, R_p = 342\mu molm^{-2}s^{-1}$). Seedlings are typical of all under the sample condition

the high fluence rates a return to wild type phenotype is seen. Increasing light intensity at 27°C leads to an increase in hypocotyl length as previously seen in WT (Figure 4.17). This therefore shows that the increased hypocotyl length in the warm is not due to the deactivation of phyB. Along with the slight rise seen in the *phyB* mutant at very high fluence rates (Figure 4.3), these data are consistent with the response being phyB independent.

This difference in phenotype between an overexpressing form of phyB (35S:PHYB:GFP, Figure (4.13)) and a hyperactive form (phyB-401, Figure (4.17)), suggests the absolute levels of phyB may be important. Both these lines show increased phyB activity but it is achieved differently. To test if the actual overexpression of phyB is contributing to the phenotype, we used a line overexpressing phyB-401 (35S:PHYB-401:GFP) [163]. If this line behaved as 35S:PHYB:GFP then the amount of phyB is important to the response.

The phyB-401 overexpressor also showed a removal of the temperature phenotype in high light with a very similar phenotype to the overexpressor of wild type phyB (Figure 4.18). This shows that the quantity of phyB is important for temperature induced elongation. PhyB is therefore active in both the warm and the cool and can act to repress hypocotyl length if it is overexpressed. However, in wild type seedlings this suppression of hypocotyl length is not seen in the warm.

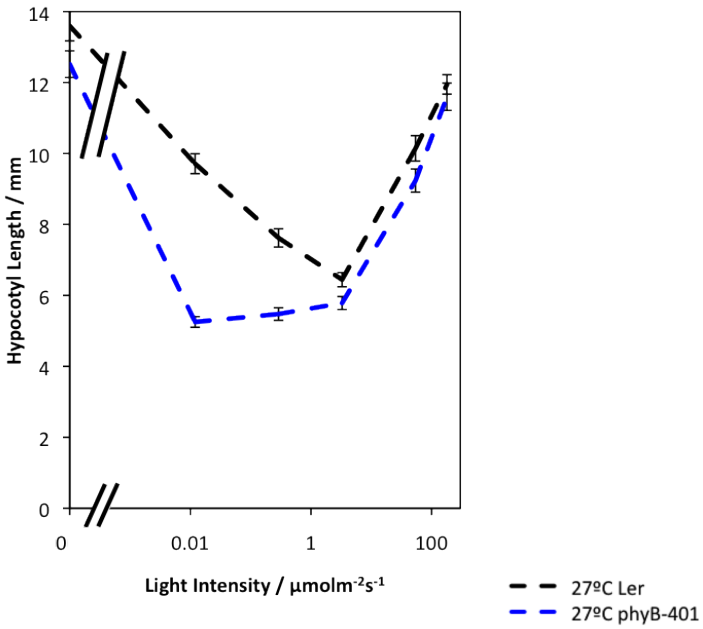

Figure 4.17: Hypocotyl Length of *phyB-401* Mutant Seedlings Grown at 27°C

At high intensity light at 27°C, the mutant relaxes back to *(Ler)* WT with a long hypocotyl at high fluence rates. Wild Type High Fluence phenotype is therefore not due to deactivation of phyB

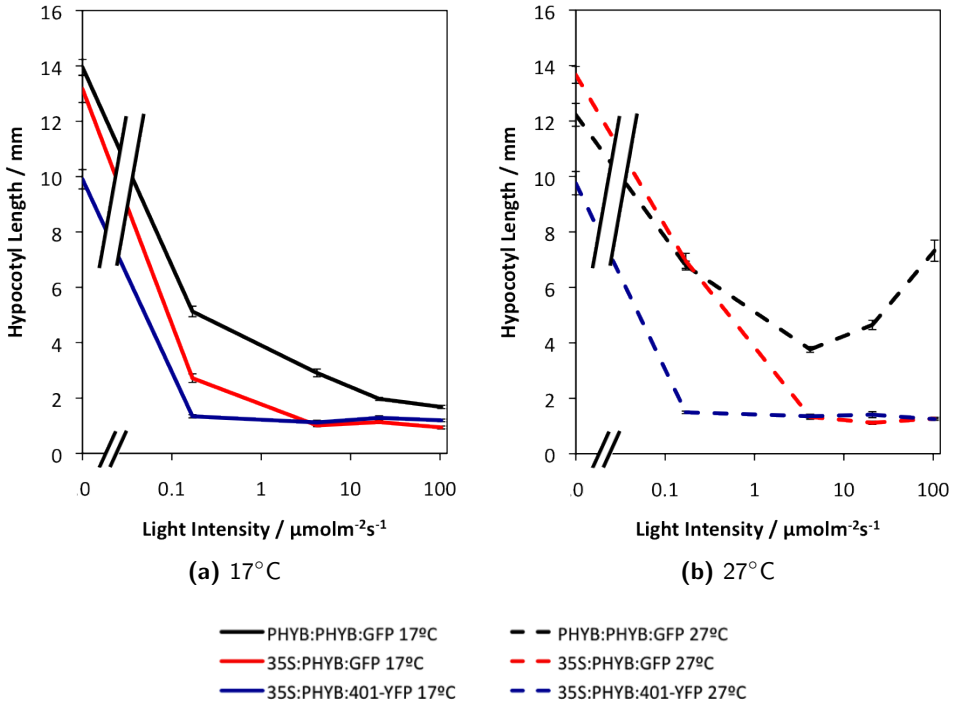

(a) 17°C **(b)** 27°C

Figure 4.18: Hypocotyl Length of PHYB-401 and PHYB Overexpressor over a Fluence Curve at 17 & 27°C

4.5 An Apically Derived Signal Can Explain High Fluence Rate Signalling

4.5.1 Understanding Seedling Growth at High Light Intensities

After cotyledon opening, *Arabidopsis* seedlings become photosynthetically active and send a hormone pulse to the rest of the seedling [186]. We therefore hypothesised that if the seedlings are more developed in higher intensity light, these plants may receive this auxin pulse earlier and therefore be longer simply as a result. To test this hypothesis, seedlings were grown at different intensity red light for 3-7 days to observe the growth response over time (Figure 4.19a, 4.20b). It had previously been observed that plants grown in higher intensity light had larger cotyledons [187]. Treatment with pulses leads to the reduction in cotyledon size relative to constant light, resulting in a loss of hypocotyl elongation in the warm (Figure 4.15). To investigate the hypothesis that a signal from the cotyledon corresponds to hypocotyl elongation, the cotyledon area was also measured and compared to hypocotyl growth over time (Figure 4.19c, 4.19d).

At all light intensities, the warm grown seedlings start to elongate earlier and are longer after 3 and 4 days even in the dark (Figure 4.20b). At medium light intensity (3.6 $\mu molm^{-2}s^{-1}$), and in the dark, the warm grown seedlings reach their maximum length after 5 days, so after 7 days of growth there is no longer an observable temperature effect. However, the high intensity light grown seedlings in the cool show virtually no elongation throughout the time series (Figure 4.19a). In contrast, the warm grown seedlings show immediate accelerated elongation followed by a further increase in growth after 6 days (Figure 4.20b). However, after only 4 days, a high intensity effect can already be seen in the warm, so an early auxin pulse can not explain the high light intensity effect (Figure 4.20b).

Cotyledon growth in high intensity light does not show the same level of temperature dependency as seen for hypocotyl growth. The warmer plants show increased cotyledon size after 3 and 4 days but this is no longer observed after 5 days. However, there is increased growth in the warm after 6 days, such that the temperature response returns in 7 day old seedlings (Figure 4.19d). This coincides with the second period of

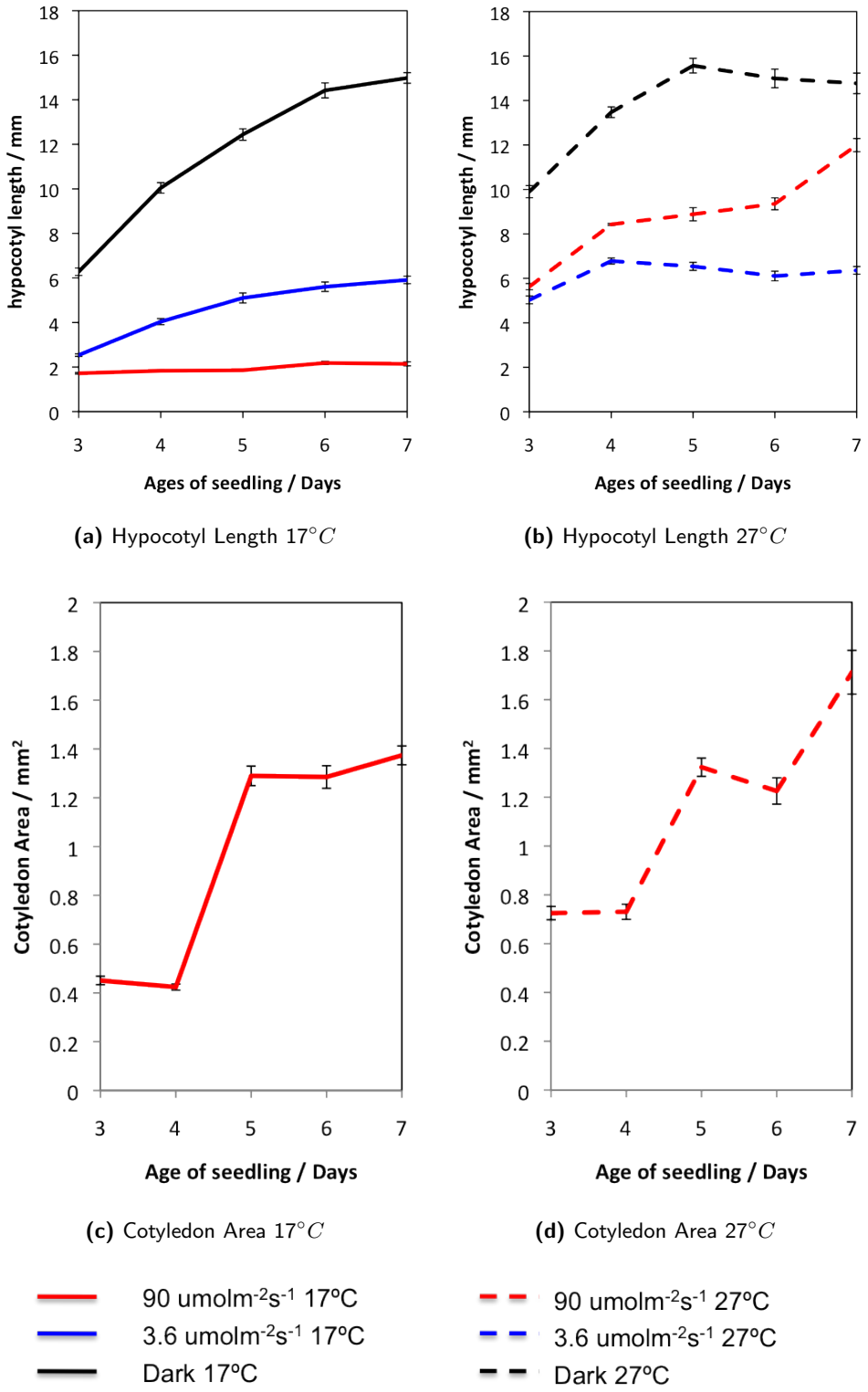

(a) Hypocotyl Length 17°C

(b) Hypocotyl Length 27°C

(c) Cotyledon Area 17°C

(d) Cotyledon Area 27°C

Figure 4.19: Seedling Growth of *Col* Wild Type at Different Light Intensities 17 & 27°C

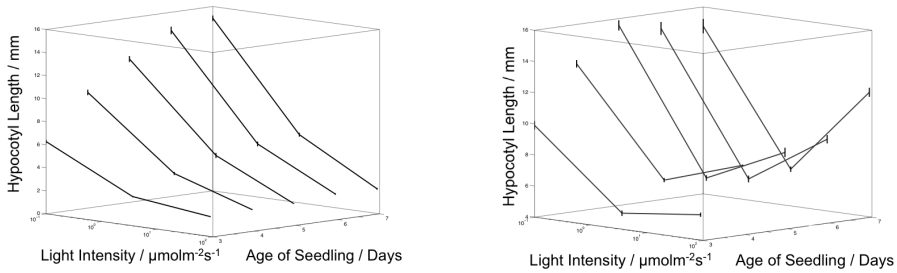

(a) $17°C$ **(b)** $27°C$

Figure 4.20: 3D graphs Showing A Change in Fluence Response Over Time

The reversal of fluence response in the warm can be seen to some extent after 3 days and it is certainly true after 4 days, before we have full photosynthetic activity

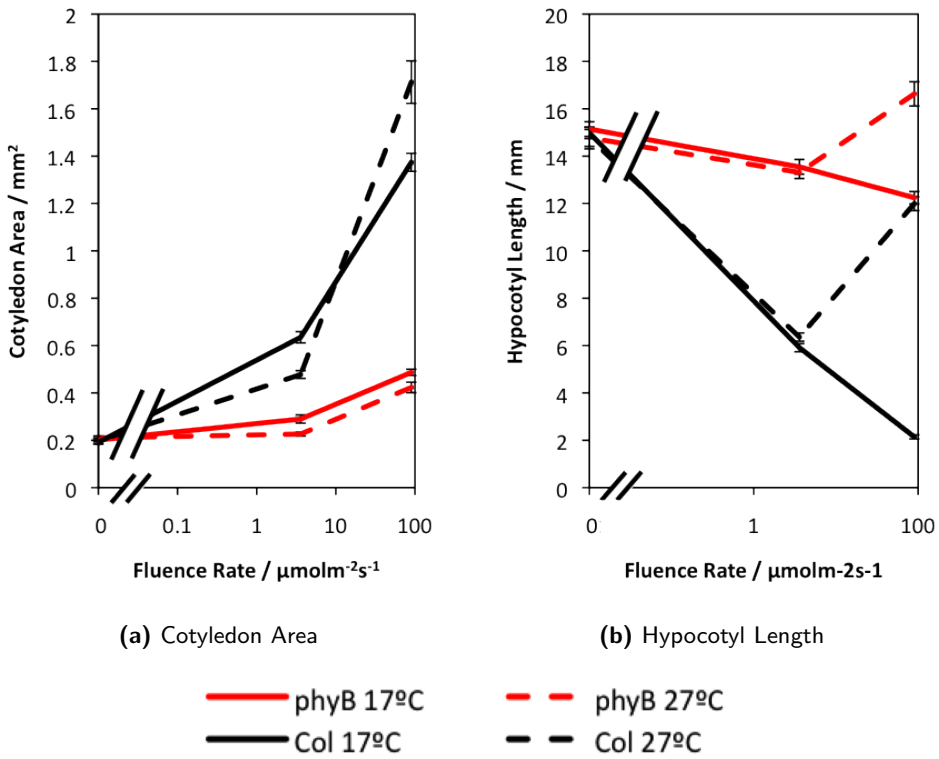

(a) Cotyledon Area **(b)** Hypocotyl Length

Figure 4.21: Fluence Response of Cotyledon Size Compared to Hypocotyl Length in *Col* and *phyB*

growth seen in hypocotyls in the warm, suggesting a coordination of growth between the two organs (Figure 4.20b). When cotyledon area is plotted on a fluence curve, it is apparent there is an increased fluence response at high temperatures (Figure 4.21). There is also a slight increase in cotyledon area with fluence rate in the *phyB* mutant which may be related to phyB independent growth in the warm.

In a previous study on hypocotyl growth in *Cucumis sativus*, cotyledons were shown to be needed for complete red light dependent suppression of hypocotyl growth, but not blue light dependent suppression [188]. This suggests that while the cryptochromes may signal exclusively in the hypocotyl to control blue light dependent hypocotyl suppression, the activity of phytochromes in the hypocotyl is not sufficient to explain red light dependent suppression, with an apical signal required. Although we are unable to perform the same experiment on *Arabidopsis*, our data shows a relationship between the pattern of cotyledon growth and hypocotyl temperature response. We are able to block this temperature response in hypocotyls by treatments that reduce cotyledon size, such as high intensity pulses (Figure 4.16).

4.5.2 Herbicide Norflurazon Blocks Temperature Dependent Hypocotyl Elongation at 27°C

To investigate the significance of the apical signalling to the response, seedlings were grown on media containing 5 μM of the herbicide norflurazon [165]. This chemical blocks the production of carotenoids leading to the destruction of chlorophyll through photobleaching [189, 190]. This stops photosynthesis and therefore cotyledons growth is retarded.

Strikingly, in $27°C$ grown seedlings, light promotion of hypocotyl elongation is lost on seedlings grown on norflurazon. Moreover, norflurazon application restores the classic fluence response seen at $17°C$ in warm grown seedlings (Figure 4.22). The temperature response is not lost however, with seedlings longer in the warm even when grown on the herbicide. This temperature effect is increased at higher fluences as observed

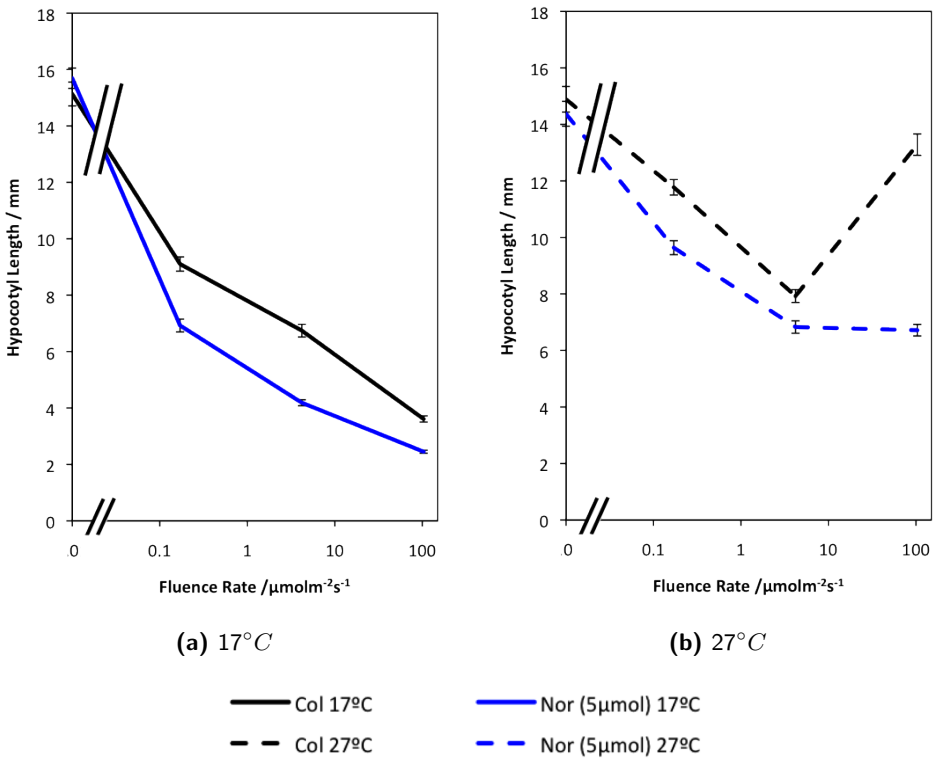

(a) 17°C **(b)** 27°C

Figure 4.22: Hypocotyl Phenotype of Wild Type Plants Grown on 5 μM Norflurazon at 17 & 27°C

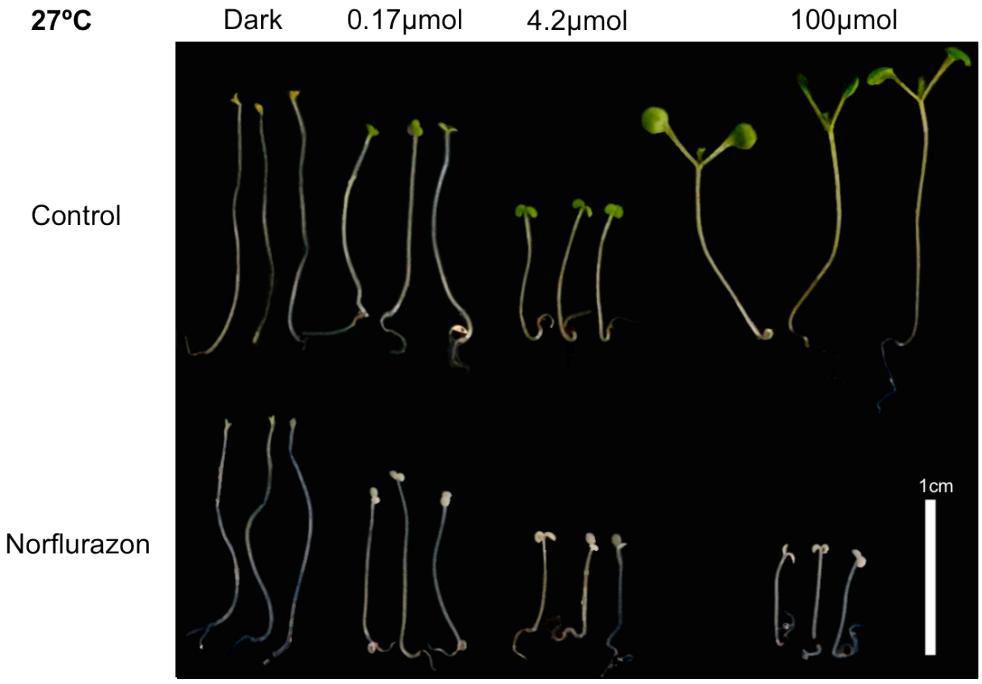

Figure 4.23: Photographs of Seedlings Grown at Increasing Fluence Rates at 27°C on or off Norflurazon

Seedlings grown on carotenoid inhibitor norflurazon (5μM) show reduced cotyledon development and lose High Fluence Growth in the Warm

in WT but the severity of this temperature effect is greatly reduced. The size of the cotyledons also shows no observable difference in response to fluence (Figure 4.23). Similar to treatment with high intensity pulses (Figure 4.15), norflurazon treatment abolishes the high fluence response in the warm. These data therefore show that phyB is still active across a fluence range at both 17 and 27°C. There is possibly a slight loss of phyB activity at higher temperatures, but it does not decrease at higher fluence rates. However, in the warm, a phyB independent high fluence rate response causes an increase in hypocotyl elongation that obscures the phyB effect. That the loss in hypocotyl elongation is accompanied by a loss in cotyledon growth suggests the high fluence response may be related to an apical signal and we therefore investigate if this signal may be auxin.

4.5.3 PIFs are Required for High Fluence Growth but this is not Driven by Auxin

That PIF4 is required for a temperature response is well established [129] and we would therefore expect high intensity growth to be largely lost in a *pif4* null mutant. However, there is also a predicted effect of PIF5 [93, 132], which may provide a level of temperature response in the absence of PIF4. Mutant seedlings were grown over the fluence range at 17 and 27°C to investigate this response.

A significant loss in the fluence response in the warm is seen in both *pif4* and *pif5*, although it is only completely abolished in a *pif45* double mutant. Here fluence dependent suppression of hypocotyl elongation is retained at 27°C (Figure 4.24b). PIF4 & 5 have previously been described as having a particularly important role at low light intensities, with mutants showing enhanced suppression of hypocotyl growth relative to wild type at lower light intensities [126]. Our data somewhat agrees with this in the cool (Figure 4.24a), but the opposite effect is seen at 27°C, with the effect of PIF4 and 5 most noticeable at high light intensities (Figures 4.24b, 4.24c).

That auxin signalling contributes to the temperature response is also known. Mutants deficient in auxin signalling, such as *tir1-3* and *axr1-12* have previously been

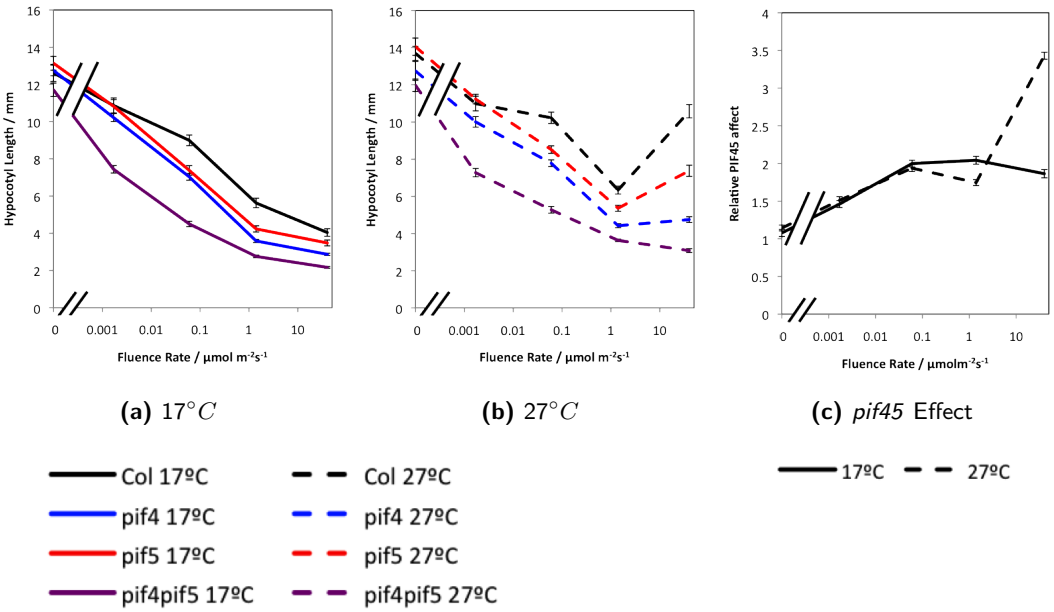

(a) 17°C **(b)** 27°C **(c)** *pif45* Effect

Figure 4.24: *pif4* and *pif5* Mutants Show a Reduced High Fluence Rate Effect

A suppression of the high fluence effect in the warm is seen in mutants of PIF4 and PIF5. The double *pif4pif5* mutant shows fluence rate dependent hypocotyl suppression in the warm.
(a) 17°C (b) 27°C (c) Length of *Col* Wild Type hypocotyls divided by *pif45* mutant show the relative effect that proteins have over a fluence curve *The experiment for this figure was performed by Henrik Johansson*

shown to have a reduced response to temperature in white light [127]. Microarray analysis has previously identified significant overlap between genes regulated by auxin and PIF4 & 5 [136], and PIF4 is known to bind the promoter of auxin response genes in a temperature dependent manner [126]. This lead to the hypothesis that the PIFs may be mediating the temperature based fluence response through auxin signalling.

PIF4 has previously been found to bind *YUCCA8* promoter [146] as well as promoters of other auxin biosynthesis genes, *TAA1* and *CYB79B2* [148] and so could be regulating growth directly through modulating auxin levels. However, as PIF levels do not increase at high fluences in the warm (Figure 4.14 S2.10), we are unable to explain the fluence response increase in hypocotyl length this way. However, auxin response genes are also dependent on the PIFs [146, 147, 148] and PIF4 binding has been shown directly on the auxin response gene *IAA29* [126]. We therefore hypothesised that PIF may also be necessary for the auxin response. In this sense, the higher the intensity of light, the more auxin is released by the cotyledon. It is however only in the warm that there is sufficient PIF 4 & 5 to interact with auxin and induce hypocotyl elongation.

To test this theory, Wild type and *pifq* mutants were treated with IAA for 2 hours and transcript measured by qPCR. The seedlings were grown in the warm at high intensity ($100\mu molm^{-2}s^{-1}$) red light in diurnal conditions for 6 days before transfer to constant light. Seedlings were moved to auxin or mock control at subjective dawn to coincide with peak expression of *PIF4* and *PIF5* [85]. If the auxin response is mediated through the PIFs we would expect there to be no response to increased gene expression in the *pifq* mutant. However, as native auxin levels would be much higher in the wild type [146, 148], if auxin is not signalling through the PIFs, we would therefore expect a stronger response to exogenous IAA on the quadruple mutant.

As previously reported, the expression of auxin responsive genes is dependent on the PIFs [80, 147, 148] (Figure 4.25). There is however still an observed auxin response in the *pifq* mutant, showing that auxin can promote its response genes independently of the PIFs. By Comparing the difference in expression between the IAA and solvent control treated samples, we can observe the fold effect of exogenous IAA. Using this

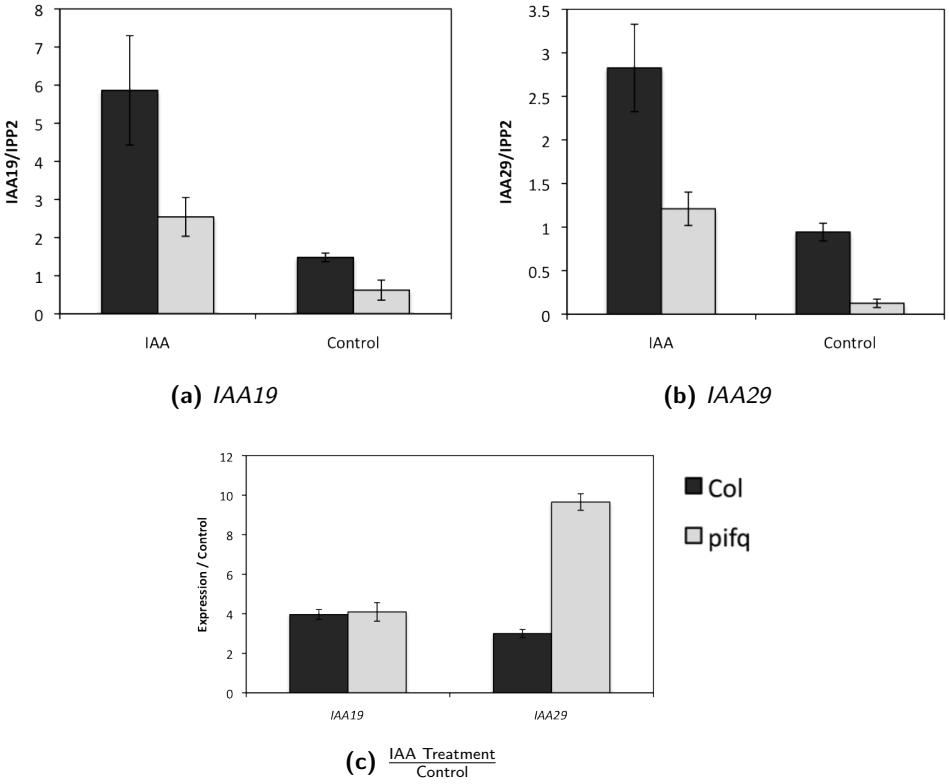

(a) *IAA19* **(b)** *IAA29*

(c) $\frac{\text{IAA Treatment}}{\text{Control}}$

Figure 4.25: Expression of Auxin Response Genes after Treatment with IAA on *Col* and *pifq* Compared to a Solvent Control. Error bars represent Standard Error of the Mean from 3 biological replicates.

comparison, *IAA29* is more responsive to auxin in *pifq* than *Col* and *IAA19* is equally responsive in the two backgrounds (Figure 4.25c). This suggests that the PIFs are not able to transduce an auxin effect. These data therefore show that PIF expression is not necessary for the auxin response. Although the PIFs are important in the regulation of these genes, they can not transduce an auxin signal onto gene expression. If our high irradiance response is coming from an apical signal, it is unlikely to be auxin transport.

4.5.4 PIF Activity is Promoted by Exogenous Sucrose and not Auxin

Seedlings grown on external sucrose show increased hypocotyl elongation in a manner dependent on GA and the PIFs [138, 191]. Sucrose promotes the stabilisation of PIF5 and leads to a longer period of growth, suggesting sucrose signalling could directly interact with light signalling [192]. It is therefore possible that *Arabidopsis* could be using sucrose directly as a measure of photosynthetic activity. The cotyledons have previously been shown to affect root growth by long distance sugar signalling [193]. With higher fluence rates leading to larger cotyledons and more photosynthetic activity, the levels of soluble sugar would be expected to be fluence dependent. If these are transferred to the hypocotyl, it could provide a mechanism for high fluence signalling.

At $27°C$, hypocotyls are constitutively long when grown on exogenous sucrose in a manner dependent on PIF4 and 5 (Figure S2.12b). We therefore looked to see if sucrose could directly alter the activity of PIFs. To test whether PIF activity was affected by sucrose, seedlings were treated with 2 % sucrose for 2 hours and harvested for RNA analysis alongside the test for auxin response (Figure 4.25). PIF activity was investigated by looking at the activity of PIF responsive gene *HFR1* in response to the treatment in either *Col* or *pifq*.

HFR1 expression is shown to be strongly induced by sucrose relative to Mock treatment but not IAA (Figure 4.26). Expression is strongly dependent on the PIFs, with the *pifq* mutant showing no increase of expression on sucrose. This is consistent with the stabilisation of PIFs by sucrose [192] and demonstrates that this can translate to an

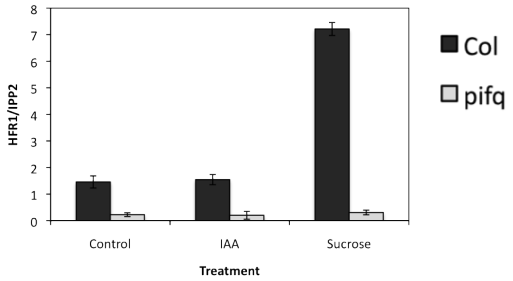

(a) *HFR1*

Figure 4.26: Effect of Exogenous Sucrose on Gene Expression

Expression of *HFR1* in response to IAA or Sucrose on *Col* or *pifq*. Error bars represent Standard Error of the Mean based on 3 biological replicates.

increase in PIF expression. These data suggest soluble sugars could be used as a signal for high photosynthetic activity and increased PIF activity at high light intensities. However more experiments would be required to verify these findings.

4.6 Discussion

4.6.1 PhyB Activation has a Limited Fluence Response

Hypocotyl length has been previously used as a read out of phyB activity, with hypocotyl length well correlated to phyB levels [42]. *phyB* null seedlings show greatly diminished Red Light fluence rate responses in their hypocotyl length, and the hypocotyl fluence rate response in wild type seedlings has previously been fitted to phyB activity [16]. We have shown that this level of fluence control is impossible based on current knowledge of the phyB protein. Using a modelling approach, the proportion of P_{fr} was shown to be only sensitive to increasing fluences over 2 orders of magnitude (Figure 4.8). Although this can provide a great deal of control on gene expression, the sensitivity is far less than *Arabidopsis* seedlings are capable of. We have shown the hypocotyl length of 7 day old seedlings grown in R_c is sensitive to over 4 orders of magnitude (Figure 4.1a).

This model prediction was supported by investigation of the behaviour of PIF3 protein in seedlings grown in increasing intensity red light. PIF3 levels are a better proxy

for phyB activity than hypocotyl length as the proteins are known to bind leading to PIF3 being tagged for degradation [81, 83]. We have shown that, unlike hypocotyl length, levels of PIF3 protein are only fluence rate dependent at the lower light intensities. There is no change in protein levels between 3 and $100\mu molm^{-2}s^{-1}$, and this is the case for both the acute and long term response (Figure 4.14). The fluence rate control of plant physiology can therefore not rest simply with the phyB signalling molecule. The phyB signalling component HMR accumulates in Red Light but reaches a plateau at only $0.2\mu molm^{-2}s^{-2}$ [64]. HMR is an important regulator of PIF degradation and this suggests phyB control is more important at lower fluence rates [63].

4.6.2 The Light Dependent Temperature Response is Actually Fluence Dependent

It has previously been reported that light is needed for *Arabidopsis* to show temperature dependent growth [127]. We observed that the normal fluence rate dependent suppression of hypocotyl length is reversed in the warm (Figure 4.1b). This is surprising, given that increased light is known to suppress hypocotyl elongation [169], but actually fits in well with this previous observation of temperature. However, instead of a light dependent binary switch of temperature dependence, we observe more of a gradual switch, with the higher the light intensity, the stronger the temperature effect. In constant red light this temperature effect is so strong that increasing light intensity can lead to an increase in hypocotyl elongation at $27°C$. If the temperature effect is defined as the fold difference between the $17°C$ and $27°C$ plants, we observe this is strongly dependent on the fluence rate of red light (Figure 4.2). The behaviour in hypocotyls is close to linear, with seedlings still responding to increased fluence rate above 100 $\mu molm^{-2}s^{-1}$. This is not consistent with phytochrome activity which responds to light with a logarithmic relationship (Figure 4.1a), suggesting the activity of another signal directly related to fluence rate. *Arabidopsis* may have a specific fluence rate dependent signalling molecule, but this would also be consistent with a product of photosynthesis. At ambient CO_2 levels, the photosynthetic activity of *Arabidopsis* has a near linear relationship with light intensity, before saturation at around 600 $\mu molm^{-2}s^{-1}$ in white light [194]. A photosynthate would therefore be able to confer

fluence rate sensitivity to very high light intensities.

4.6.3 Active PIF4 and 5 Protein and Low PhyB Levels are Required for the High Fluence Rate Response

PIF4 & 5 have previously been described as having a particularly important role at low light intensities, with mutants showing enhanced suppression of hypocotyl growth relative to wild type at lower light intensities [126]. Our data somewhat agrees with this in the cool (Figure 4.24a), but the opposite effect is seen at $27°C$, with the effect of PIF4 and 5 most noticeable at high light intensities (Figure 4.24b, 4.24c). As PIF levels do not change in high intensity light (Figures 4.14, S2.10), this suggests the increase in their activity is taking place downstream of the control on protein levels. This may be due to post translational modification, or interaction with a signalling molecule.

While the absence of PIF4 and 5 removes the high fluence rate response, the same is not true of seedlings deficient in phyB (Figure 4.3). As previously shown [42], the *phyB* null mutant shows no response to fluence rate at cooler temperatures, but in the warm a high intensity increase in hypocotyl length is observed in the mutant. The light intensity where this increase is first observed is around $40\mu molm^{-2}s^{-1}$; much higher than that seen for the wild type but the overall absolute increase in length in comparable (Figure 4.3b). The difference between the start of the response in the mutant and wild type may be due to the increased PIF levels in a *phyB* background. The similar increase in hypocotyl length in *phyB* and *Col* however suggests this fluence rate dependent effect is not related to the red light photoreceptor.

However, overexpressing phyB will completely remove the temperature dependent increase in hypocotyl elongation at high fluence rates (Figure 4.18b). This shows that phyB is still capable of suppressing growth in the warm. This is not however seen with hyperactive phyB-401 (Figure 4.17). Although higher levels of phyB can completely suppress PIF activity in the warm, this is not seen with WT phyB levels working at maximum efficiency. This suggests that the lower levels of phyB are necessary for

normal plant temperature signalling. In constant light, PIF levels do not completely degrade but are kept at a level approximately 20% of the dark [42]. These residual PIFs are known to be vital for *Arabidopsis* temperature signalling [129, 132, 148] and so it is important they are not degraded. This may therefore provide a reason for the degradation of phyB in constant light [84]. The limiting of long term phytochrome signalling is needed if there is to be efficient PIF signalling.

As overexpressing phyB or knocking out PIFs will remove the high intensity response, these components must be central to the control of the effect. PhyB was previously shown to be important to temperature compensation in 4 week old plants, in a manner dependent on its control of PIF4 [132]. Our analysis has confirmed that PIF4 is very important for the temperature response of *Arabidopsis* but that this occurs downstream of the photoreceptor. The strength of this temperature dependency also occurs in a fluence dependent way, independent of phyB (Figure 4.3). So although *phyB* mutants have an altered temperature response, the data suggests that this is largely due to the altered PIF levels in these plants. The temperature response is then feeding in at the PIF level, due to increased transcription and more efficient promoter binding of PIF4 at the higher temperatures [93, 137].

4.6.4 An Apically Derived High Fluence Response in the Warm

With phytochrome B ruled out, we investigated what could be the source of the high fluence rate dependent signalling observed in the warm. It was found that the high light intensity response in the warm is dependent on constant light. While high intensity light pulses were sufficient to give a normal fluence dependent response at $17°C$ (Figure 4.10), the same was not true at $27°C$, with no increase in hypocotyl elongation under pulsed light (Figure 4.15). Showing a similar loss in high temperature activity is the treatment of seedlings with herbicide norflurazon (Figure 4.22b). Under both these treatments the suppression of hypocotyl length with fluence is restored in the warm, showing the normal light signalling machinery is still active at $27°C$. However in the warm a separate high fluence rate signal masks this response, dramatically increasing

hypocotyl elongation in high intensity light. Consistent between the pulsed seedlings and those treated with norflurazon is that they both have much smaller, cotyledons than the control (Figures 4.16, 4.23). Due to the small cotyledon size and reduced levels of chlorophyll, these treated seedlings will be less photosynthetically active. This led to the hypothesis that the high fluence rate response in the warm could be due to an apically derived signal. As *pif4* mutants show a loss of temperature response without a noticeable change in cotyledon size [129], it was thought the high irradiance signal would interact with PIFs in order to induce hypocotyl elongation.

PIFs are known to interact with auxin signalling, binding to and regulating both auxin responsive and auxin biosynthesis genes [80, 146, 147, 148]. However, we found PIFs did not transduce an auxin response (Figure 4.25). Exogenous auxin did not require the presence of PIFs to increase target gene expression in the warm, confirming previous results seen in the cool [166]. We are therefore able to rule out auxin as the apical signal. However, the increase of PIF activity after treatment with sucrose gave preliminary evidence that this could be the relevant high fluence rate signal (Figure 4.26). Sucrose is a suitable small signalling molecule as it's production is directly related to photosynthesis and therefore its presence is a sign that the plant is photosynthetically active. Glucose is the best known sugar signalling molecule, signalling largely via hexokinase to affect plant growth, however disaccharides such as sucrose have also been shown to alter gene expression [195, 196]. Sucrose is known to induce hypocotyl growth and for this to be strongly related to the PIFs [138, 192]. It has also been demonstrated as a long distance signalling molecule between cotyledons and roots [193]. This would therefore provide a mechanism for fluence dependency as the greater the amount of light, the more effective photosynthesis would be and so the greater the flux of soluble sucrose. The sugar would then be transported to the hypocotyls where they cause an increase in hypocotyl elongation, but only in the warm where there is sufficient PIF activity.

Recent work has implicated brassinosteroids (BR) in the control of seedling elongation [139, 140]. Increased addition of exogenous brassinolide (BL, the most active brassinosteroid) leads to increased hypocotyl elongation in a dose dependent manner.

This is partly dependent on the PIFs and high temperature hypocotyl elongation was also shown to require both PIF4 and BR signalling. As BR have previously been implicated in sugar signalling [197], they are a potential candidate for mediating the signal of high photosynthetic activity. An interaction between BR, at high light intensity, and PIF4 and 5, at high temperature, would then lead to increased hypocotyl elongation.

4.6.5 Transduction of External Light Conditions to Seedling Architecture

Is is not surprising that there are several levels of control in how a seedling will respond to changes in light conditions. That temperature would feed into the system directly is also intuitive as there is much more information in the interaction between light and temperature than either of the conditions alone. We have uncovered a mechanism where warm ambient temperature affects the development of a seedling directly related to the intensity of light (Figure 4.1, 4.2). We have shown that the characteristics of phytochrome are insufficient for it to confer fluence sensitivity over the known intensity range and that hypocotyl elongation in the warm is phyA and phyB independent (Figure 4.3). The high temperature response has been linked to the photosynthetic activity of the plant, with sucrose the most likely candidate as a high fluence rate signal, interacting with PIFs to promote hypocotyl elongation.

At low fluences, the degradation of the PIFs by phyB is most important to their function, but this saturates at a relatively low light intensity, with further changes in activity a result of an apically derived High fluence signal. In fact, at higher fluences the PIF dependent degradation of phyB will limit its signalling. That the temperature induced growth is dependent on PIF4 was already known [129], and we found this effect to be fluence dependent (Figure 4.24c). The Temperature affect on PIF is independent of phyB, and auxin is acting downstream mediating some of the PIFs responses. High fluence effects appear to be coming from an apical signal, as blocking cotyledon growth will also block warm hypocotyl growth. Soluble sugars, or another photosynthate are the most promising candidate for this signal. Given the known effect of brassinosteroids on PIF mediated growth [140, 139], and their implication in sugar

signalling [197], these may provide a downstream signal of photosynthetic activity. We therefore propose a high light intensity dependent control of growth, independent of the photoreceptor which interacts with PIFs to induce increased elongation at high fluence rates in the warm (Figure 4.27).

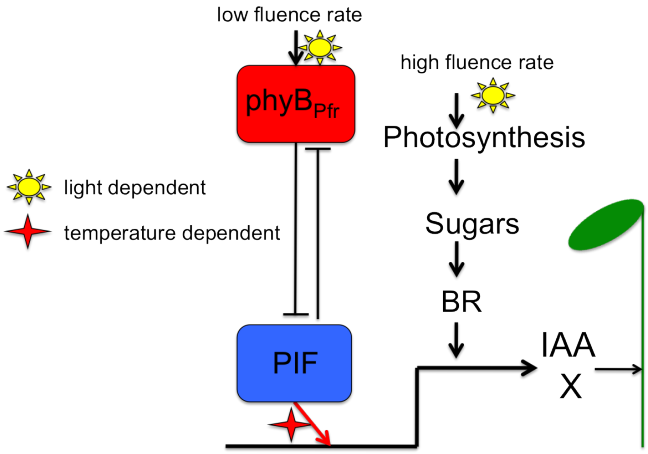

Figure 4.27: Dual Regulation at Low Fluence Rates and High Fluence Rates Converge of the PIFs

Chapter 5

Convergence of Temperature and Light Regulate Adult Plant Architecture and Physiology

5.1 Introduction

In the previous chapter (Chapter 4), the interaction of temperature and light was explored using mutant seedlings. It was shown that temperature will feed in independent of the photoreceptor, affecting PIFs directly. The phenotype of *phyB* mutants was therefore explained as due to the increased PIFs in the mutant. In this chapter, we investigate if this behaviour is conserved in adult plants. The majority of studies on the response of light signalling mutants to temperature has been performed on seedlings [93, 129]. It is however unclear if everything reported at the seedling stage is followed through to the adult and a comprehensive study of the adult plant response to temperature does not exist at this stage. PhyB has previously been described as a key regulator in temperature compensation in adult plants, due to the reduced plant biomass of the *phyB* mutant grown at $28°C$ [132]. Based on seedling phenotypes we would predict this is due to the high PIF levels in the mutant.

5.1.1 The Effect of Photoreceptors on Temperature Control

Plants deficient in the light receptor phytochrome B (phyB) have an early flowering phenotype [43, 198]. This is only observed in warm ambient temperatures however, as no change of flowering time is seen at $16°C$ [35]. In contrast, phytochrome A (phyA) promotes flowering and *phyA* mutants have a slightly late flowering phenotype in short days which is not temperature dependent between 16 and $22°C$ [35, 198]. *phyB* mutants have been shown to have longer petioles, increased leaf angle and reduced biomass compared to wild type when plants are grown at temperatures of $28°C$ and higher, implicating phyB as important to temperature compensation in WT plants [132, 199]. In response to warm temperature, wild type plants show an increase in petiole angle, but this is delayed in *phyA* and *phyAB* mutants, before eventually reverting to a wild type phenotype [199]. PhyA and phyB have also been previously shown to repress each others signalling [200, 201], so it is possible some phenotypes of *phyB* mutants are due to enhanced phyA function.

5.1.2 Phenotypes of Adult *pif* Mutants

The phytochrome signalling partner, PIF4 has been shown to operate in a temperature dependent manner in the regulation of hypocotyl length, petiole length and petiole angle [129]. In wild type plants an increase in temperature can promote flowering in short days [128], a response strongly dependent on PIF4. At high temperatures, PIF4 is able to bind the floral promoter FT with greatly enhanced efficiency. The protein is likely prevented from binding in the cool by the DELLA proteins, as a quintuple *della* mutant will flower early at $12°C$ [137]. The behaviour correlates with the temperature dependent flowering of the *phyB* mutant [35]. In low temperatures where there is no PIF4 activity, phytochrome does not affect flowering, while in higher temperatures, the enhanced PIF4 levels in a *phyB* mutant are able to induce flowering through FT. Part of the phyB control on biomass is also through the degradation of PIF4, as the *pif4* mutation will partially rescue the severely depleted biomass in a *phyBhfr1* background [132]. PIF5 has also been implicated in the temperature response in hypocotyl growth, but to a lesser role than PIF4 [93]. Whether this is retained in adult plants is not known.

5.1.3 The Control of Plant Architecture by the Circadian Clock

Transcription of *PIF4* and *PIF5* is under the control of the circadian clock, a series of transcriptional feedback loops that interact to produce an approximately 24 hour rhythm [85, 106]. The clock acts to coordinate *Arabidopsis* growth and development with the day night cycle and allows response to the changes in day length associated with the seasons. A clock with a period that does not match the external environment causes reduced biomass in the plant [152] and importantly the clock is buffered to temperature, with very little change in period across an ambient range (see section 1.4.5). However, reduced clock function has been shown to have a positive effect in barley grown at high latitudes (large increase in changes of day length) [202]. *CIRCADIAN CLOCK ASSOCIATED 1* (CCA1) is a component of the morning loop of the circadian clock [106]. Overexpressing CCA1 leads to an arrhythmic clock [164] but also the loss of rhythmic *PIF4* and *PIF5* transcription [85]. *PIF* transcript production is not suppressed in subjective night, leading to increased hypocotyl and petiole elongation in the mutant [91, 92]. However, despite increased *PIF* levels, the *CCA1-OX* transgenic line is late flowering in both long and short days [164, 203]. This is largely due to decreased levels of *CONSTANS* (*CO*) in the mutant [203]. *CO* is known to promote FT and is degraded by phyB and stabilised by phyA [43, 44].

In short photoperiods, *Arabidopsis* has an extended vegetative phase. The transition to the reproductive phase, known as bolting, is strongly delayed leading to plants with a much higher number of rosette leaves than those grown in photoperiods with more than 12 hours light [130]. However, high temperature is able to override this response to as great an extent as long days [128]. This is strongly dependent on PIF4 [137] and also greatly enhanced in a *phyB* mutant [35]. The temperature dependent flowering of a number of mutants, crosses and transgenic lines was therefore investigated in 10:14 photoperiods at 17 or 27 $^{\circ}C$. These lines, *phyB*, *pif45*, *pif45phyB*, *phyAB*, *CCA1-OX*, *CCA1-OXphyB* have altered phyB and PIF levels and their analysis will help to learn more of the temperature control of physiology, particularly with regard

to the light signalling pathway.

5.2 Results

5.2.1 The Effect of Temperature on Flowering Time and Leaf Emergence in Light Signalling Mutants

First the leaf production rate was analysed in mutants in comparison to wild type. At 17°C, *phyB*, *pif45phyB*, *phyAB* and *CCA1-OX*, have a wild type leaf emergence phenotype of approximately 5.5 new leaves per week (Figure 5.1a, 5.1d). A slight delay is observed in the production of leaves in the *pif45* mutant (Figure 5.1a), resulting in a slightly later flowering time but the same number of rosette leaves at bolting (Figure 5.2b). This shows that although PIF4 and 5 have previously been described as important in warm temperatures, they also have a function in the cool [93, 129]. A wild type leaf emergence rate is however seen in *pif45phyB*, showing phyB is required for the response and suggesting PIFs may act through phyB in the cool. Like *pif45*, a delay of growth is also observed in *CCA1-OXphyB* plants at 17°C. While both *phyB* and *CCA1-OX* have wild type leaf emergence, *CCA1-OXphyB* shows a delayed initial rate of leaf emergence before an increase in the later part of the vegetative phase, eventually flowering with a similar number of leaves to wild type (Figures 5.1d, 5.2b).

At 27°C, *phyAB*, *pif45* and *pif45phyB* plants showed a wild type leaf emergence phenotype of approximately 4.5 new leaves a week (Figure 5.1b). So in terms of leaf emergence, PIF4 and 5 appear to only have a function at cooler temperatures. At 27°C, *phyB* flowers with approximately 5 rosette leaves and so the leaf emergence phenotype of this mutant can not be observed. *CCA1-OX* plants have a slow rate of leaf emergence at 27 °C which is conserved in *CCA1-OXphyB*, showing the importance of a rhythmic clock to leaf emergence is temperature dependent.

High temperatures are able to elicit similar effects as long days in the promotion of flowering [128], but this effect is largely lost in the absence of PIF4 [137]. This work confirms this finding as the *pif45* mutant has highly delayed flowering in the

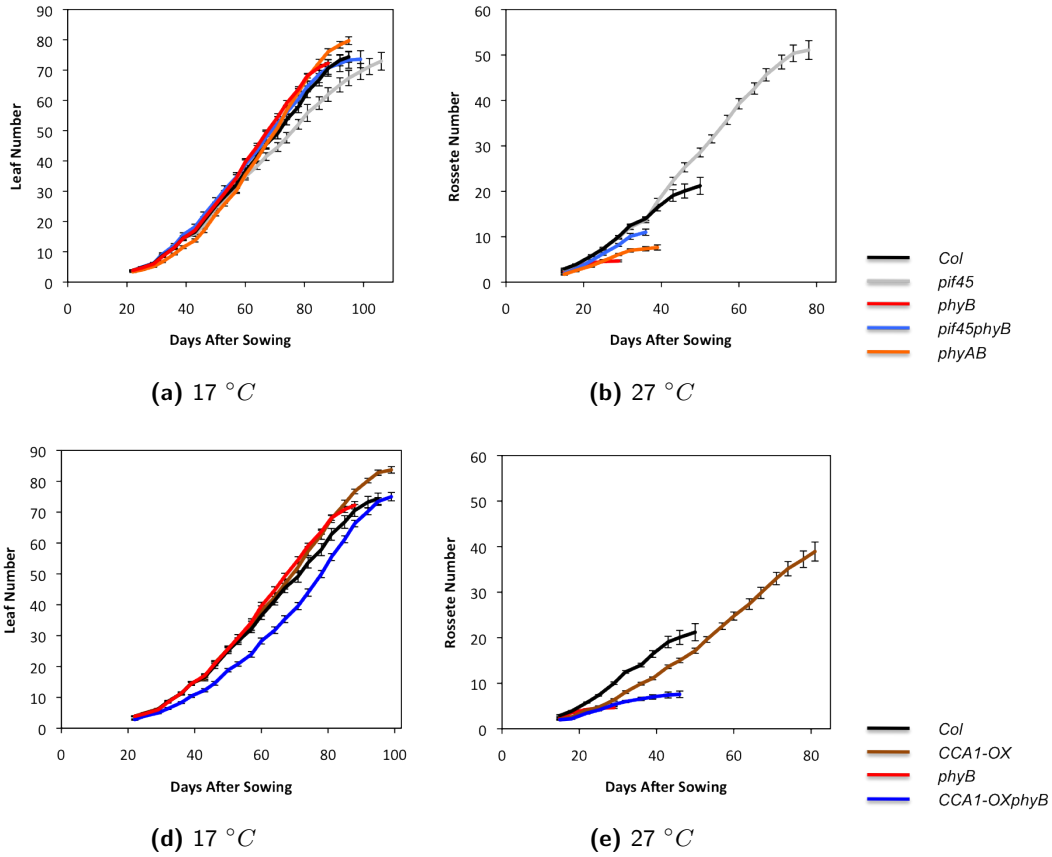

(a) 17 $^{\circ}C$ **(b)** 27 $^{\circ}C$

(d) 17 $^{\circ}C$ **(e)** 27 $^{\circ}C$

Figure 5.1: Leaf Emergence Phenotypes of Mutant Plants Grown at 17 and 27 $^{\circ}C$

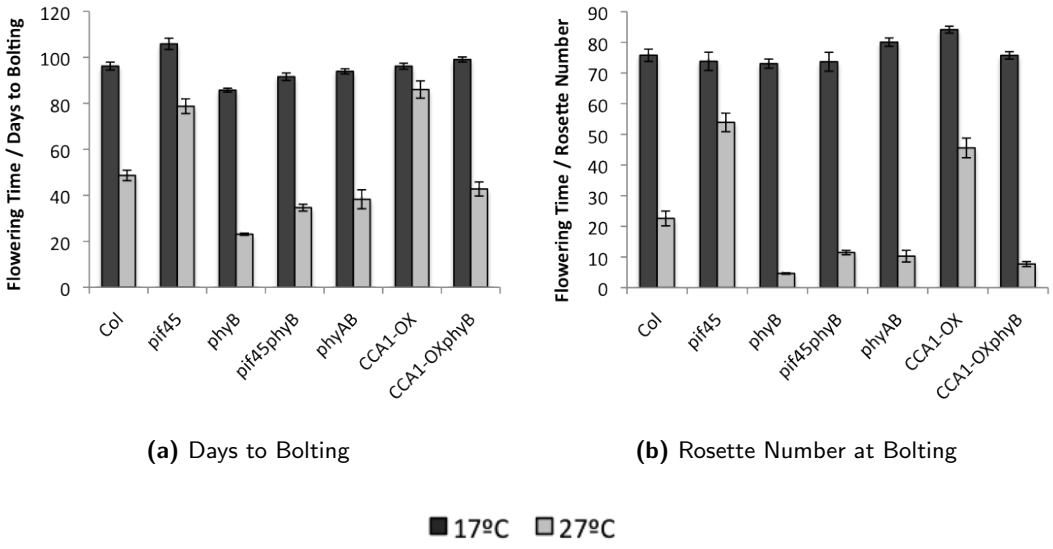

(a) Days to Bolting **(b)** Rosette Number at Bolting

Figure 5.2: Flowering Time of Mutant Plants Grown at 17 and 27 $^{\circ}C$

warm when compared to wild type (Figure 5.2). Consistent with previous literature, *phyB* mutants show an increased importance of the temperature control of flowering time [35]. However, as the *pif45phyB* triple mutant flowers at a similar time and with comparable leaf number to the single *phyB* mutant, this implies that *phyB* is largely epistatic to *pif45* for this response. PhyB therefore appears to be required for the *pif45* flowering phenotype. The *phyAB* double mutant is early flowering at 27 $^{\circ}C$ but this is less severe than seen for *phyB* (Figure 5.2). Similar to *pif45phyB*, the *phyAB* mutant shows a slightly reduced temperature effect compared to *phyB* (Figure 5.2). This may be additive, as the *phyA* single mutant has a slight late flowering phenotype [198, 204], and the effect of phyA might be greater in a *phyB* background due to the mutual repression by the photoreceptors [200, 201]. Like *pif45*, the CCA1 overexpressor also shows strongly delayed flowering at $27^{\circ}C$, not observed at $17^{\circ}C$, showing the previously reported flowering phenotype of the transgenic line is temperature sensitive (Figure 5.2) [164, 203]. The *CCA1-OXphyB* line produces an inflorescence meristem (bolts) with a similar number of rosette leaves to the *phyB* mutant, appearing to show that phyB is required for the *CCA1-OX* phenotype. However, this does not lead to flowering and the stem bifurcates leading to several rosettes in a loss of Shoot Apical Meristem (SAM) Identity (Figures S3.2g, S3.3).

5.2.2 PIF4 & 5 Promote Growth at Low Temperatures and Contribute to Phytochrome Signalling in the Warm

We wished to investigate the impact of temperature on the growth and development of our mutant and transgenic lines. Upon bolting, at $17^{\circ}C$, and at seed formation at $27^{\circ}C$, plants were harvested and individual rosette leaves weighed and measured to characterise the adult phenotypes. The total size of the leaves were also quantified, with the total leaf length, petiole length and leaf diameter measured. A value for the thickness of the leaf was calculated by taking the ratio of the leaf area divided by the mass (Figure 5.3c). Due to the large number of leaves at $17^{\circ}C$, the first rosettes had been overly shaded and had tended to reach senescence. There is therefore little data on these early leaves.

Wild Type plants show an increase in leaf size and mass with temperature (Figure 5.4b), and this is due to both an increase in leaf length and width (Figure 5.3a, 5.3b). In the warm an increase in petiole length is also seen (Figure 5.3d), consistent with previous reports [129].

At $17°C$, *phyB*, *pif45phyB*, *CCA1-OX* and *CCA1-OXphyB*, have a leaf weight distribution similar to the wild type phenotype (Figures 5.5a, 5.5d). Consistent with the slow leaf emergence, *pif45* mutants showed leaves of a lower biomass, confirming the PIFs do have a function at lower temperatures (Figure 5.4a). The mutant also has a lower overall biomass and leaves with shorter petioles (Figures 5.6 5.3d), leaving the plant with a visibly reduced rosette size (Figure 5.7d). The low biomass of *pif45* is rescued in the *pif45phyB* mutant, which shows wild type leaf and total biomass at $17°C$, similar to the *phyB* single mutant (Figures 5.5a, 5.4a, 5.6a). As *phyB* is epistatic to *pif45* in this response it implies phyB is required for the reduced biomass of the *pif45* mutant in the cool. The leaves of the *phyAB* mutant show greatly enhanced growth, with significantly higher mass than any other mutant at $17°C$ (Figure 5.5a). As the *phyB* single mutant does not show a strong phenotype compared to wild type, this suggests that phyA is acting to constrain the growth of *Arabidopsis* in the cool.

Inconsistent with previous reports, there is no noticeable petiole lengthening in *phyB* and *CCA1-OX* lines. This is due to the age of plants used in the study and the leaves selected for analysis. Younger *phyB* and *CCA1-OX* plants did have visually longer petioles than *Col* (Figure S3.4) and by comparing all the leaves of the adult plants, it is apparent that the oldest leaves of *phyB* and *CCA1-OX* have longer petioles than the equivalent *Col* leaves (Figures S3.10b, S3.11b, S3.12). However, leaves in the middle of the rosette showed similar petiole length.

In contrast to the data at $17°C$, *pif45* plants do not show reduced leaf size when grown at $27°C$ (Figure 5.5b), showing this effect is specific to the cool. The leaves still show reduced petiole length, but their area and mass are similar to wild type, as is the overall biomass of the plant (Figures 5.4a, 5.4b, 5.6a). Therefore PIF4 and 5 are

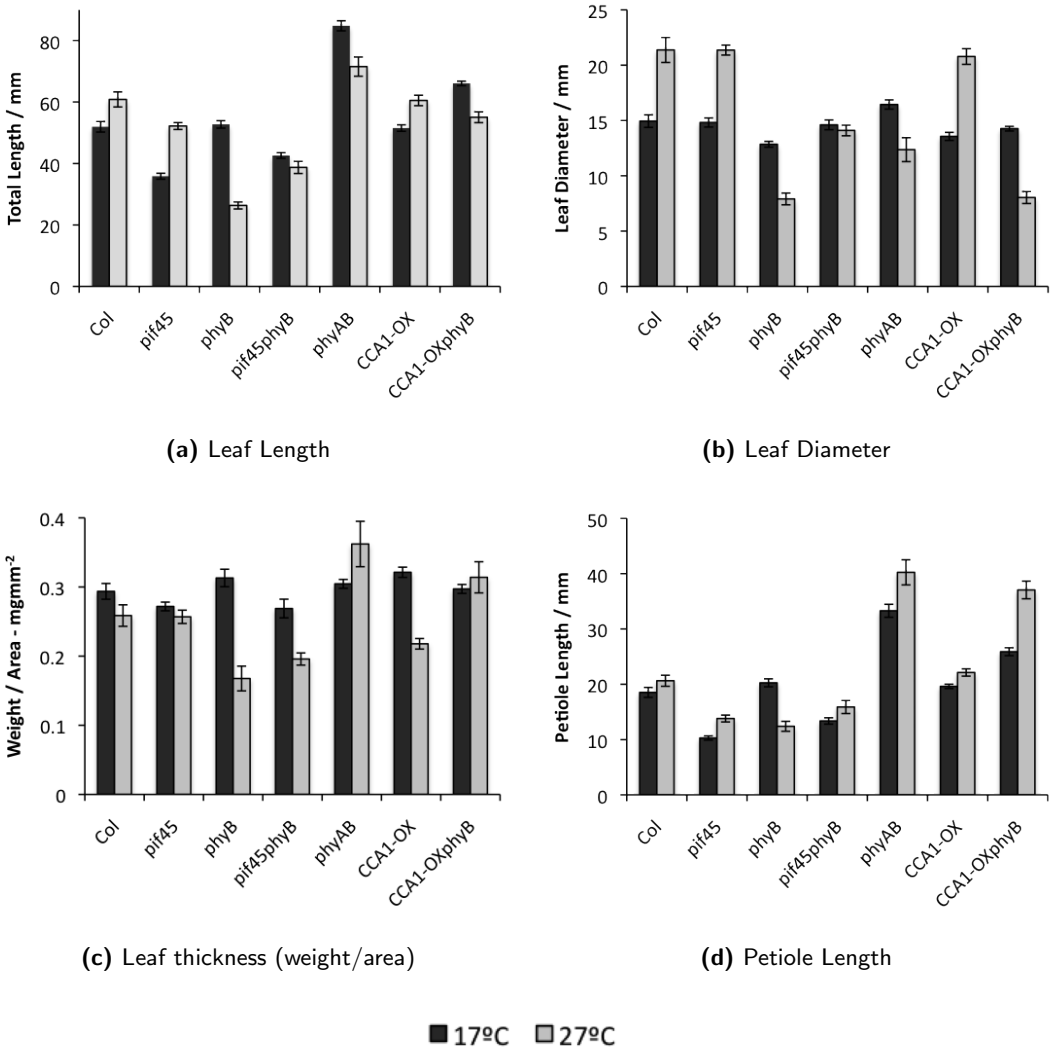

(a) Leaf Length

(b) Leaf Diameter

(c) Leaf thickness (weight/area)

(d) Petiole Length

Figure 5.3: Length, Leaf Diameter and Approximate Thickness of Leaves of Mutants Grown at 17 and 27$^{\circ}C$

Leaves in the centre of the rosette were selected for average analysis. At 17$^{\circ}C$, leaves 20-22 were used, while at 27 $^{\circ}C$ leaves 4-6 were used due to the much lower leaf number at this temperature

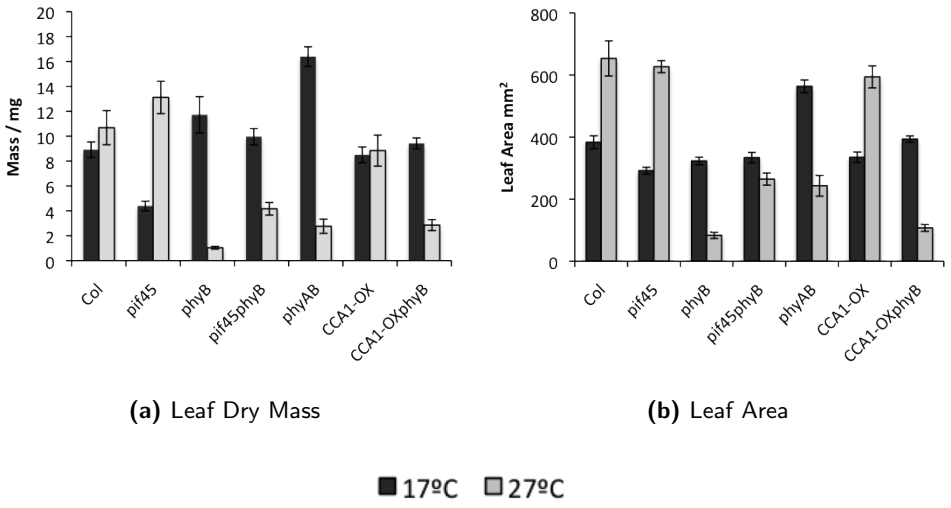

(a) Leaf Dry Mass **(b)** Leaf Area

Figure 5.4: Size and Mass of Leaves Grown at 17 and 27°C

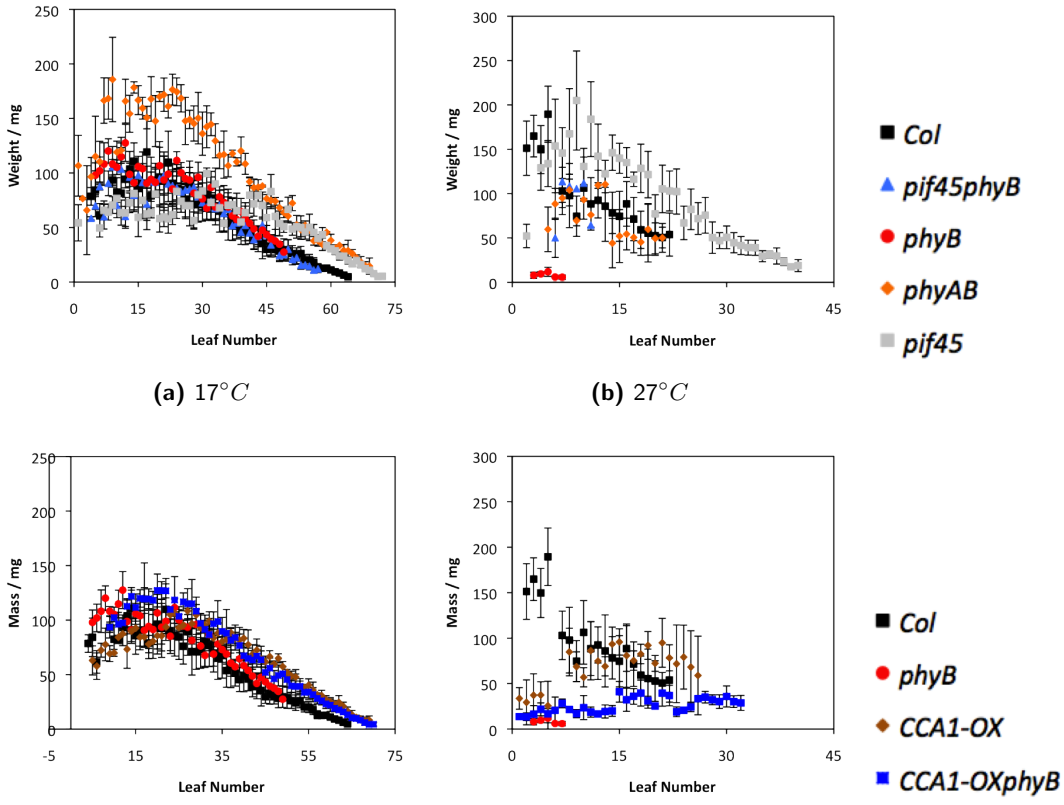

(a) 17°C **(b)** 27°C

(d) 17 °C **(e)** 27 °C

Figure 5.5: Distribution of Fresh Leaf Mass of Individual Mutants

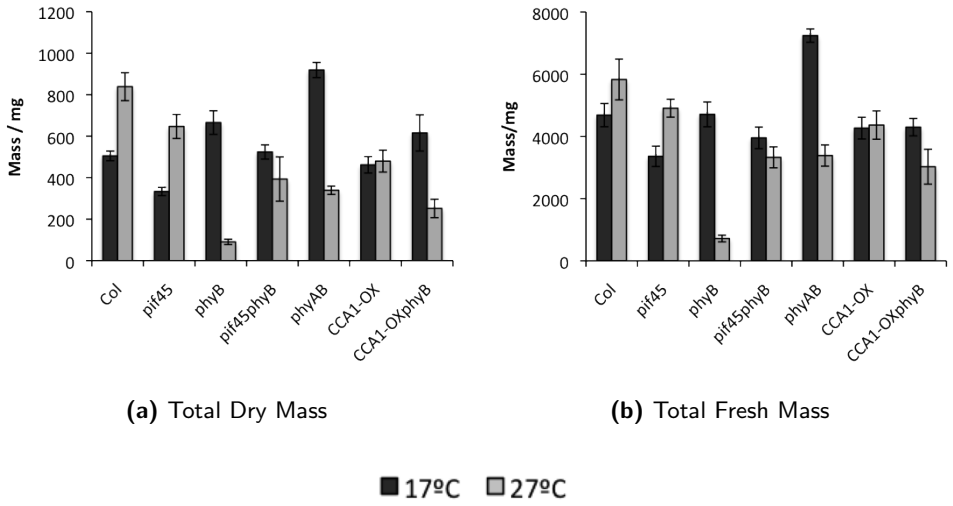

(a) Total Dry Mass **(b)** Total Fresh Mass

Figure 5.6: Fresh and Dry Biomass of Plants Grown 17 and 27 $^{\circ}C$

only needed for Wild Type leaf growth at lower temperatures. Consistent with previous reports, *phyB* mutants showed severely reduced biomass when grown in the warm [132], and as expected this is correlated to reduced leaf mass and size (Figures 5.4a, 5.4b, 5.6a, 5.8c). In the opposite response to PIF4 and 5, phyB appears to only be important to biomass production at the warmer temperatures. The *pif45phyB* mutant shows reduced leaf growth and biomass at 27$^{\circ}C$ compared to wild type, but shows a partial rescue of the *phyB* single mutant (Figures 5.5b, 5.6a, 5.8e). This suggests that the very small leaves of *phyB* at 27$^{\circ}C$ is partly due to its the high level of PIFs in the mutant. *phyAB* plants show reduced leaf size and total biomass at 27$^{\circ}C$ compared to Wild Type, while maintaining long petioles (Figures 5.5b, 5.6a, 5.3d, 5.8b). However, when compared to the *phyB* single mutant, this is a similar response to that seen at 17$^{\circ}C$, with an increase in biomass seen compared to *phyB* in both temepratures. In a *phyB* background, phyA is acting to restrain leaf growth in a temperature independent manner.

The *CCA1-OX* single mutant, produced leaves of a similar size and mass to wild type at 27$^{\circ}C$ (Figures 5.5e, 5.4a 5.4b). Although the *CCA1-OXphyB* plants bolted with an average of only 8 rosette leaves, many more were counted when the plant was harvested. The loss of SAM identity in the mutant meant it produced up to four

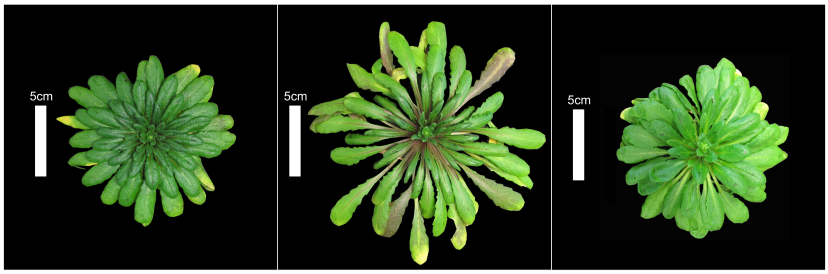

(a) *Col* **(b)** *phyAB* **(c)** *phyB*

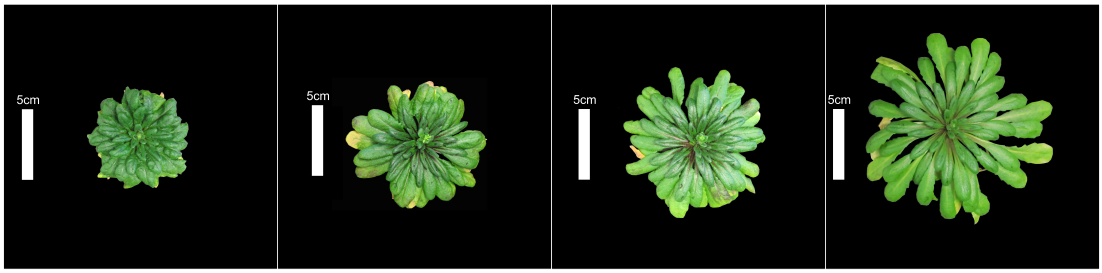

(d) *pif45* **(e)** *pif45phyB* **(f)** *CCA1-OX* **(g)** *CCA1-OXphyB*

Figure 5.7: Photograph of Rosettes of Mutant Plants Grown at 17°C

Scale Bar Represents 5cm

(a) *Col* **(b)** *phyAB* **(c)** *phyB*

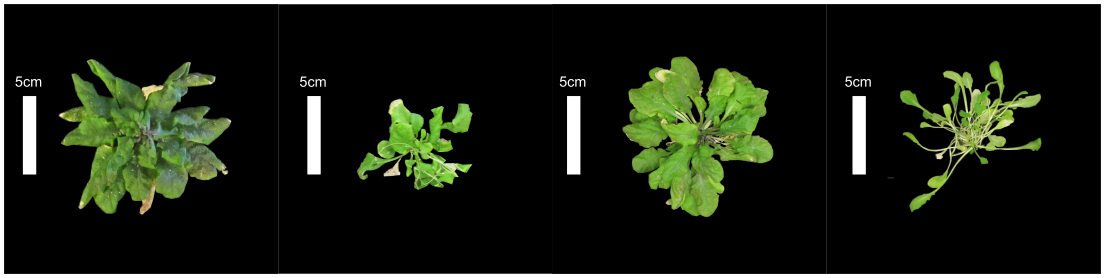

(d) *pif45* **(e)** *pif45phyB* **(f)** *CCA1-OX* **(g)** *CCA1-OXphyB*

Figure 5.8: Photograph of Rosettes of Mutant Plants Grown at 27°C

Scale Bar Represents 5cm

separate rosettes (Figure S3.3). Shortly after stem bifurcation [205], one of the rosettes bolted, but another continued to produce leaves which is the reason for this discrepancy. Therefore, although the *CCA1-OXphyB* plant appears to rescue the low biomass of the *phyB* mutant (Figure 5.6a), this is almost entirely due to the greatly increased leaf number of the transgenic line. Similar to wild type plants, at $27°C$, removing phyB in a *CCA1-OX* background leads to a dramatic reduction in leaf size and weight (Figures 5.4a, 5.4b). However, compared to *phyB*, *CCA1-OXphyB* plants do show a slight rescue of the small leaf size phenotype, suggesting the input from phyB into the clock may contribute to this process.

5.3 Discussion

5.3.1 Phytochrome and the PIFs Affect Plant Architecture Through Mutually Dependent Control

PhyB has previously been implicated in the regulation of plant responses to temperature. A *phyB* mutant shows early flowering at $22°C$ but this is completely lost if the temperature is dropped to $16°C$ [35]. PhyB is also known to be important in maintaining plant biomass at warmer temperatures, acting at least partly by restraining PIF4 activity [132]. As PIF4 has been identified as a key regulator of the temperature induction of flowering in short days [137] it was postulated that phyB could be affecting temperature dependent flowering through degradation of PIF4 and PIF5. However, we found that the removal of phyB substantially reduced the late flowering phenotype of *pif45* at $27°C$ (Figure 5.2). This is inconsistent with the idea that PIFs transduce the temperature effect through their binding to FT in the warm [137]. In the absence of the photoreceptor, temperature dependent flowering returns in plants lacking PIF4, implicating a phyB, PIF4 and PIF5 independent pathway in the temperature control of flowering time. Previously, floral repressors *FLOWERING LOCUS C* (*FLC*) and *FLOWERING LOCUS M* (*FLM*) were shown to be involved in the thermal induction of flowering time, upstream of FT [128]. These may provide temperature dependent flowering in the absence of PIF4.

As the delay of flowering in the *pif45* mutant is strongly dependent on phyB, this

suggests the PIFs are transducing their flowering time effect through the photoreceptor. Previously, *phyB* was shown to be epistatic to *pif7* when comparing hypocotyl length in constant red light grown seedlings [42] and this analysis suggests the feedback of PIF on phyB activity is an important factor in light signalling. PhyB levels are known to be higher in a *pif45* mutant [84], and these increased levels may be causing the delay in flowering time in the warm. However, plants overexpressing phyB are also known to flower early [206] so it is not the high levels of phyB alone that delay flowering time. The increase in phyB levels in *pif45* is far less than that seen in *PHYB-OX* however, and the overexpressor is also known to have a shorter free running period than wild type [207]. As the *phyB* mutant and the *PHYB-OX* line both flower early, we can not be sure what the affect of slightly modifying phyB levels would be. Alternatively, the PIFs may be affecting phyB activity rather than levels, increasing the efficiency phyB is able to degrade CO protein.

At $27°C$, the severe loss of biomass in *phyB* [132] can be partly rescued in the *pif45phyB* background (Figures 5.5b 5.4b, 5.3, 5.6, S3.2). This suggests that the very low biomass in *phyB* is partly due to the increased PIF levels in the mutant [87]. The degradation of PIFs by phyB is an important part of photomorphogenesis [88], and these data suggest this may also be part of leaf growth. Light is known to be required for leaf formation and these results suggest phytochrome PIF signalling is one way this is achieved [208]. The *pif45* mutant grown at $27°C$ shows leaf growth similar to that of wild type, suggesting PIF4 and 5 do not effect leaf growth in wild type plants in the warm.

However, at $17°C$, the *pif45* mutant shows a reduction in leaf emergence relative to wild type (Figure 5.1a). The size and mass of the leaves and overall plant biomass is also reduced in *pif45* mutants grown in the cool, but this is lost in the *pif45phyB* triple mutant (Figures 5.5a 5.4b, 5.3, 5.6). Similar to flowering time at $27°C$, phyB is required for the phenotype of *pif45* at $17°C$. Previously, PIF4 and PIF5 have been described as important to signalling in high temperatures [129, 93] but we have shown they also have a role in plant biomass production at cooler temperatures. Again, this may be related to the feedback on phyB. Slightly higher levels of phyB in *pif45* would

lead to lower levels of other transcription factors such as PIF3 which may be important at lower temperatures.

5.3.2 PhyA Dependent Plant Growth Suppression

While phyA and phyB have similar behaviours in the transfer from dark to light, these diverge in adult plants, having for example opposite activity on CO, and therefore flowering time [130]. Relative to *phyB*, the *phyAB* mutant did show a slight delay of flowering time (Figure 5.2) without a rescue of the wild type phenotype, consistent with the phytochromes having opposite effects on CO protein directly. However, the most dramatic effect of the *phyAB* mutant was in the increased biomass of the plant (Figure 5.6). When compared to the *phyB* single mutant a large increase is seen in both temperatures, suggesting that in the absence of phyB, phyA acts to constrain growth. This is particularly apparent in the leaves, which are longer, wider and heavier in *phyAB*, with much longer petioles (Figures 5.4, 5.3). PhyB has been shown to repress phyA [201], so the dramatic reduction in biomass of *phyB* may be partly due to the increased activity of phyA. However, at $17°C$, *phyB* plants have a wild type phenotype, suggesting no gain of phyA function in the cool (Figure 5.7c). The increased size of *phyAB* in the cool (Figure 5.7b) suggests phyA may be constraining growth of *Arabidopsis* independent of phyB. This increased growth is particularly apparent with regard to leaf size, with the double mutant producing very long leaves with elongated petioles (Figure 5.3). However without the single *phyA* mutant to compare to we can only make limited conclusions.

A previous study showed reduced biomass and petiole length in *phyAB* compared to *phyB*, in plants grown at $20°C$ [34]. These data were however obtained in *Landsberg erecta* (*Ler*), which is thought to have a stronger phyA effect than *Columbia* [116] (Section 4.2.2). We therefore hypothesise that the increased importance of phyA in *Ler* causes this severe loss of growth in the ecotype. Alternatively, this may be a day length or temperature specific effect, as the previous study was run in 8:16 photoperiods at $20°C$. However, this is only slightly different from our conditions so it is possibly a

combination of these factors.

5.3.3 High PIF Transcript in *CCA1-OX* Does not Correlate With Reduced Biomass

The temperature phenotype of *CCA1-OX* was studied as the transgenic line loses the rhythmic control of *PIF4* and *PIF5* [85]. The *CCA1-OX* transgenic line has an arrhythmic clock, and therefore its growth patterns are regulated solely by the light dark cycle. Other than the previously described late flowering phenotype [203] (Figure 5.2), *CCA1-OX* plants showed wild type development at both temperatures (Figures 5.4a, 5.4b, 5.6, 5.7f, 5.8f). The expression of *PIF4* and *PIF5* is increased in *CCA1-OX* [85]. However the plant does not show the decreased biomass at $27°C$ associated with high PIF levels [132, 137]. This either suggests that increased transcription of *PIF4* and *PIF5* in the mutant does not translate to increased PIF protein, or that increased PIF levels are not sufficient to reduce plant biomass.

CCA1-OXphyB plants would be expected to have very high PIF levels [85, 87], but an enhancement of the *phyB* mutant is not observed in this line. Rosette leaves are instead slightly larger in the mutant compared to *phyB* at $27°C$ (Figure 5.5e). In a similar manner to *pif45*, *CCA1-OX* can slightly rescue the *phyB* phenotype when plants are grown at $27°C$. While the mutants have different levels of *PIF* expression, they have both lost the rhythmic expression of *PIF4* and *PIF5* RNA. This may suggest a large part of the way phyB controls growth in high temperature is through maintaining the photoperiodic control of growth [19]. The *CCA1-OXphyB* plants were also observed to have a severe loss of SAM identity, with the stem bifurcating leading to the formation of several rosettes (Figure S3.3). This phenotype has been previously seen in mutants deficient in cell cycle control [205, 209]. In mammals, the cell cycle is known to be entrained by the circadian clock, so the loss of rhythmic and photoperiodic control in *CCA1OXphyB* may be the reason for this phenotype [210, 211]. As the response is temperature dependent it may also be expected that the high levels of PIF4 PIF5 in *CCA1-OXphyB* have a role in the loss of SAM identity.

5.3.4 PhyB is at the Centre of *Arabidopsis* Temperature Compensation, Integrating Many Pathways

The importance of phyB in the correct architecture to high temperatures was already known [132] and we have shown this to be implicated through the control of many different pathways. The previously described impact on PIF4 activity is confirmed, due to the increase in size of *pif45phyB* relative to *phyB* (Figure 5.3, 5.6) [137]. However the flowering response appears to act in the opposite direction, with PIFs affecting phyB action to bring about early flowering in the warm (Figure 5.2). PIF4 and 5 also appear to be dependent on phyB in the control of growth at $17°C$. A dramatic increase in biomass relative to *phyB* can also be achieved by knocking out phyA (Figures 5.6, S3.2b), showing that the photoreceptors antagonise each other in response to temperature. The control of total biomass was also shown to be closely related to flowering time, with artificially delayed flowering leading to increased biomass even in the *phyB* background. PhyB therefore controls biomass in the warm through at least two different mechanisms. Maintaining leaf biomass through action on the PIFs and maintaining leaf number through coordination with the clock of flowering time. The control of PIFs on flowering time occurs at least partly through phyB, possibly affecting its interaction with the clock. Similar to their behaviour in seedlings [42, 40], under some conditions PIFs appear to control growth through modulating phyB activity.

Chapter 6

Discussion

Recent publications have shown that Phytochrome control of light signalling appears far less intuitive than previously thought. Following the discovery of PIF3, a transcription factor binding partner for phyB [70], the main route of phytochrome signal transduction seemed clear. After activation by light, phytochrome would trigger the degradation of PIF transcription factors, effecting a downstream change in transcription and the target physiological response [10]. However, recent results have suggested that phyB-PIF signal transduction is not a simple linear response as previously thought. For instance, under continuous irradiation, PIF3, PIF4 and PIF7 appear to control hypocotyl growth by modulating phyB levels [42]. The data therefore suggests phyB and PIF negatively regulate each other, but this moves us away from the original receptor effector hypothesis. To take this forward, in this thesis I have considered in detail the dynamic interaction between Phytochrome and the PIFs. As both phyB and PIF4 have been strongly implicated in temperature signalling [93, 129, 132], I have also determined the impact of temperature on the system, uncovering a novel interaction between high intensity light, temperature and the light signalling components.

While, the transfer to light leads to a rapid decrease in levels of PIF protein [61, 87], the degradation of phyB occurs over a much slower time scale [84]. A minimal model was constructed to explain these relative degradation rates, which was then expanded to explain the behaviour of PIF3 protein under various red light conditions (Figure 3.13). However, after fitting to the data, the model predicted that more PIF3 protein

would be present in seedlings grown in high intensity light compared to low intensity light (Figure 3.19a). PIF3 is a strong promoter of hypocotyl elongation [88], and this result would therefore predict an increase in hypocotyl elongation in plants grown at high fluence rates. When seedlings were grown at lower temperatures, consistent with previous reports, we observed a suppression of hypocotyl elongation in increasing fluence rate red light (Figure 4.1a) [116, 163]. However, at $27°C$, an increase of hypocotyl elongation was observed in high intensity light ($> 1.6\mu molm^{-2}s^{-1}$)(Figure 4.1b) and we postulated that this light dependent elongation was a result of elevated PIF levels, as predicted by the model. However, it was found that PIF3 protein levels did not accumulate with increasing fluence rates at any temperature studied (Figures 3.22, 4.14).

By analysing the fluence dependency of phyB, we found it to be unable to induce signalling throughout the fluence rate range (Section 4.3.1). While physiological outputs of seedlings are sensitive to fluence rate changes over several orders of magnitude [42], a change in the proportion of P_{fr} can only be explained over a 100 fold change in light intensity (Figure 4.9). A phyB independent suppression of hypocotyl length in very high intensity red light has previously been reported [116]. Under our conditions this is more subtle than seen previously in the cool, but at $27°C$ high fluence rates led to increased hypocotyl elongation in *phyB* mutants at $27°C$ (Figure 4.3b). The high intensity response was also observed in hyperactive *phyB-401* seedlings, showing the increased growth is not due to a loss of phyB activity at the high fluence rates (Figure 4.17).

As modelling and experiments showed the fluence rate signal that promoted hypocotyl growth in the warm was independent of phyB, we postulated that the high fluence rate signal could be a product of photosynthesis. As photosynthesis in *Arabidopsis* has been shown to respond to increasing intensities of light up to $600\mu molm^{-2}s^{-1}$ [194], this would provide a sensor for high light beyond what is achievable by phytochrome B. While phyB will be important in the initial sensing of light and therefore the formation of the photosynthetic machinery [212], in wild type plants the responses to high intensity light would be due to a photosynthate. In this sense, the plants are not responding directly to high intensity light but to a secondary response such as high levels of soluble

sugars.

In support of this argument, when seedlings were grown on the photosynthesis inhibiting herbicide norflurazon, the light induced hypocotyl elongation at $27°C$ was abolished (Figure 4.22). In addition, exogenous sucrose was shown to stimulate PIF activation of target *HFR1*. Sucrose is known to increase hypocotyl elongation and does so in a PIF dependent way [138, 192]. Sucrose has also been shown to act as a direct signalling molecule, transducing information from the cotyledon to the roots [193] and exogenous sucrose can enhance gene expression in a dose dependent manner [196]. Brassinosteroids have previously been suggested to integrate light and sugar signalling [197], and also light and temperature signalling [139, 140] so this hormone could provide the mechanism for the interaction of high intensity light and temperature.

That, light and temperature converge on seedling hypocotyl growth was previously known [127], but the fluence rate dependence of the response is a novel finding from this study (Figure 4.1b). At $27°C$ a switch in the control of hypocotyl elongation is observed, with an increase in fluence rate only suppressing hypocotyl length until approximately $1.6\mu molm^{-2}s^{-1}$. Beyond this point, increasing light intensity leads to increased hypocotyl length. The effect of temperature on hypocotyl length was calculated as almost linearly dependent on the fluence rate (Figure 4.2). This therefore suggests a dual light effect on hypocotyl elongation. At lower fluence rates, activated phytochrome will induce photomorphogenesis by degrading transcription factors such as the PIFs. However, there is likely a second signal for seedling elongation directly related to the photosynthetic activity of the plant. In high temperatures this signal becomes active, inducing hypocotyl elongation in a manner dependent on PIF4.

PIF4 has been reported to control temperature induced changes in architecture beyond the seedling stage, affecting the increased petiole length and early flowering response of warm grown plants [129, 137]. We looked to characterise the behaviour of light signalling mutants grown at elevated temperatures to test if conclusions formed from seedling behaviour were consistent with adult mutants. As plants deficient in PIF4 showed virtually no temperature response to flowering, we questioned whether

phyB control of adult plant architecture was through the degradation of PIF4. In terms of flowering time this was not observed. The late flowering time phenotype of *pif45* can be largely explained by the presence of phyB, as when phyB is removed this is greatly attenuated (Figure 5.2) [84]. This result was not expected given than PIF4 is known to bind the FT promoter in a temperature dependent way [137], but as the PIFs and particularly PIF4 have a huge variety of ways to signal [75, 77, 87, 137, 148], it is perhaps not surprising. While direct binding to FT is likely part of the control PIF4 has on flowering time, our evidence suggests the early flowering phenotype of the *pif4* mutant is partly due to increased phyB activity.

While PIF4 and PIF5 has previously been implicated in the control of growth in the warm [93, 129], we found the *pif45* mutants to have decreased leaf production rate and biomass at $17°C$, showing the proteins also have a function in the cool (Figures 5.1a, 5.6). Interestingly, this was also lost in *pif45phyB*, showing phyB is required for this response. Although we found the control of biomass in the warm to be partly due to the degradation of PIFs by phyB, the control of biomass in the cool appears to act largely through PIF feedback on phyB. This result is similar to that observed for flowering time in the warm, as well as results previously described for hypocotyl elongation [40, 42].

So while the temperature dependent growth of seedlings is very strongly dependent on PIF4 and PIF5, adult plants are able to respond to temperature in a manner independent of PIF4 and 5. Due to the dynamic and complex nature of light signalling, it is not always clear what the effect of an individual mutation would be. *pif4* mutants will have decreased PIF4 activity but also higher phyB levels. In turn this means the suppression of the other PIF proteins will be higher. The *pif45phyB* mutant would therefore be expected to have greater activity of phyA, PIF1 and PIF3, amongst other factors, and these will all contribute to the phenotype [83, 86, 201]. The regulation of adult growth therefore appears to be far more complicated than what is seen in seedlings, with many more processes to coordinate and the added complication here of comparing white and red light. However, *pif45* and *pif45phyB* seedlings do show a slight response to temperature, showing they are not the only temperature dependent

transcription factors (Figures 4.24, S2.11). In the *pif45phyB* mutant these could be the cause of the accelerated flowering.

The mutual, reciprocal regulation by phyB and the PIFs is unintuitive and appears to vary dependent on the conditions. We have expanded this knowledge to adult plants, with leaf biomass seemingly based on phyB regulation of PIF at warmer temperatures, but PIF regulation of phyB in the cool. This system still requires extensive study but based on our hypocotyl analysis we have shown how external signals can interact with the core complex. PhyB and PIF, together collaborate signals such as high photosynthetic activity and temperature to lead to changes in physiological output. In reality, a very large number of components with be involved in light and temperature signalling. PhyB and the PIFs should therefore not be thought of as receptor and effector, but as components of a system coordinating a plants response to the external environment.

Bibliography

[1] J. Medina, R. Catalá, and J. Salinas. The cbfs: Three arabidopsis transcription factors to cold acclimate. *Plant Science*, 180(1):3–11, 2011.

[2] R. Mittler, A. Finka, and P. Goloubinoff. How do plants feel the heat? *Trends in Biochemical Sciences*, 2012.

[3] E. Liscum, D.W. Hodgson, and T.J. Campbell. Blue light signaling through the cryptochromes and phototropins. So that's what the blues is all about. *Plant Physiology*, 133(4):1429–1436, 2003.

[4] P. Gyula, E. Schafer, and F. Nagy. Light perception and signalling in higher plants. *Current Opinion in Plant Biology*, 6(5):446–452, 2003.

[5] S. McCoshum and J.Z. Kiss. Green light affects blue-light-based phototropism in hypocotyls of Arabidopsis thaliana 1. *The Journal of the Torrey Botanical Society*, 138(4):409–417, 2011.

[6] S. Frechilla, L.D. Talbott, R.A. Bogomolni, and E. Zeiger. Reversal of blue light-stimulated stomatal opening by green light. *Plant and Cell Physiology*, 41(2):171–176, 2000.

[7] T. Zhang, S.A. Maruhnich, and K.M. Folta. Green light induces shade avoidance symptoms. *Plant Physiology*, 157(3):1528–1536, 2011.

[8] M. Chen and J. Chory. Phytochrome signaling mechanisms and the control of plant development. *Trends in Cell Biology*, 2011.

[9] H. Okamoto, M. Matsui, and X.W. Deng. Overexpression of the heterotrimeric g-protein alpha-subunit enhances phytochrome-mediated inhibition of hypocotyl elongation in arabidopsis. *Science's STKE*, 13(7):1639, 2001.

[10] P.H. Quail et al. Phytochrome photosensory signalling networks. *Nature Reviews Molecular Cell Biology*, 3(2):85–93, 2002.

[11] SE Braslavsky, W. Gärtner, and K. Schaffner. Phytochrome photoconversion. *Plant, Cell & Environment*, 20(6):700–706, 1997.

[12] AL Mancinelli. The physiology of phytochrome action. In R.E. Kendrick and GHM Kronenberg, editors, *Photomorphogenesis in Plants*. Kluwer Academic Publishers, 1994.

[13] A.T. Ulijasz, G. Cornilescu, C.C. Cornilescu, J. Zhang, M. Rivera, J.L. Markley, and R.D. Vierstra. Structural basis for the photoconversion of a phytochrome to the activated Pfr form. *Nature*, 463(7278):250–254, 2010.

[14] M. Furuya and P.S. Song. 4.3 assembly and properties of holophytochrome. *Photomorphogenesis in Plants*, page 105, 1994.

[15] R.E. Kendrick and W.S. Hillman. Dark reversion of phytochrome in Sinapis alba L. *Plant Physiology*, 46(4):596, 1970.

[16] J. Rausenberger, A. Hussong, S. Kircher, D. Kirchenbauer, J. Timmer, F. Nagy, E. Schäfer, and C. Fleck. An integrative model for phytochrome B mediated photomorphogenesis: from protein dynamics to physiology. *PloS one*, 5(5):e10721, 2010.

[17] U. Sweere, K. Eichenberg, J. Lohrmann, V. Mira-Rodado, I. Baurle, J. Kudla, F. Nagy, E. Schafer, and K. Harter. Interaction of the response regulator ARR4 with phytochrome B in modulating red light signaling. *Science's STKE*, 294(5544):1108, 2001.

[18] T. Kunkel, V. Speth, C. Büche, and E. Schäfer. In vivo characterization of phytochrome-phycocyanobilin adducts in yeast. *Journal of Biological Chemistry*, 270(34):20193–20200, 1995.

[19] J. Soy, P. Leivar, N. González-Schain, M. Sentandreu, S. Prat, P.H. Quail, and E. Monte. Phytochrome-imposed oscillations in PIF3-protein abundance regulate hypocotyl growth under diurnal light-dark conditions in Arabidopsis. *The Plant Journal*, 2012.

[20] A. Nagatani. Phytochrome: structural basis for its functions. *Current Opinion in Plant Biology*, 13(5):565–570, 2010.

[21] Y. Oka, T. Matsushita, N. Mochizuki, T. Suzuki, S. Tokutomi, and A. Nagatani. Functional analysis of a 450–amino acid N-terminal fragment of phytochrome B in Arabidopsis. *The Plant Cell*, 16(8):2104, 2004.

[22] N.C. Rockwell, Y.S. Su, and J.C. Lagarias. PHYTOCHOME STRUCTURE AND SIGNALING MECHANISMS. *Annual review of Plant Biology*, 57:837, 2006.

[23] E.A. Kikis, Y. Oka, M.E. Hudson, A. Nagatani, and P.H. Quail. Residues clustered in the light-sensing knot of phytochrome B are necessary for conformer-specific binding to signaling partner PIF3. *PLoS genetics*, 5(1):e1000352, 2009.

[24] L.O. Essen, J. Mailliet, and J. Hughes. The structure of a complete phytochrome sensory module in the Pr ground state. *Proceedings of the National Academy of Sciences*, 105(38):14709, 2008.

[25] T. Kretsch, C. Poppe, and E. Schäfer. A new type of mutation in the plant photoreceptor phytochrome B causes loss of photoreversibility and an extremely enhanced light sensitivity. *The Plant Journal*, 22(3):177–186, 2000.

[26] S. Mathews, M. Lavin, and R.A. Sharrock. Evolution of the phytochrome gene family and its utility for phylogenetic analyses of angiosperms. *Annals of the Missouri Botanical Garden*, pages 296–321, 1995.

[27] S. Mathews and RA Sharrock. Phytochrome gene diversity. *Plant Cell and Environment*, 20(6):666–671, 1997.

[28] Y.J. Han, H.S. Kim, Y.M. Kim, A.Y. Shin, S.S. Lee, S.H. Bhoo, P.S. Song, and J.I. Kim. Functional characterization of phytochrome autophosphorylation in plant light signaling. *Plant and Cell Physiology*, 51(4):596–609, 2010.

[29] R.J. Staneloni, M.J. Rodriguez-Batiller, D. Legisa, M.R. Scarpin, A. Agalou, P.D. Cerdán, A.H. Meijer, P.B.F. Ouwerkerk, and J.J. Casal. Bell-like homeodomain selectively regulates the high-irradiance response of phytochrome A. *Proceedings of the National Academy of Sciences*, 106(32):13624–13629, 2009.

[30] J. Rausenberger, A. Tscheuschler, W. Nordmeier, F. Wüst, J. Timmer, C. Fleck, and A. Hiltbrunner. Photoconversion and Nuclear Trafficking Cycles Determine Phytochrome As Response Profile to Far-Red Light. *Cell*, 146:813–825, 2011.

[31] K.A. Franklin and P.H. Quail. Phytochrome functions in Arabidopsis development. *Journal of experimental botany*, 61(1):11, 2010.

[32] L. Hennig, W.M. Stoddart, M. Dieterle, G.C. Whitelam, and E. Schäfer. Phytochrome e controls light-induced germination of arabidopsis. *Plant Physiology*, 128(1):194–200, 2002.

[33] K.A. Franklin. Shade avoidance. *New Phytologist*, 179(4):930–944, 2008.

[34] P.F. Devlin, K.J. Halliday, N.P. Harberd, and G.C. Whitelam. The rosette habit of Arabidopsis thaliana is dependent upon phytochrome action: novel phytochromes control internode elongation and flowering time. *The Plant Journal*, 10(6):1127–1134, 1996.

[35] K.J. Halliday, M.G. Salter, E. Thingnaes, and G.C. Whitelam. Phytochrome control of flowering is temperature sensitive and correlates with expression of the floral integrator FT. *The Plant Journal*, 33(5):875–885, 2003.

[36] S. Robert, G. Mouille, and H. Höfte. The mechanism and regulation of cellulose synthesis in primary walls: lessons from cellulose-deficient arabidopsis mutants. *Cellulose*, 11(3):351–364, 2004.

[37] B. Wenden, L. Kozma-Bognár, K.D. Edwards, A.J.W. Hall, J.C.W. Locke, and A.J. Millar. Light inputs shape the Arabidopsis circadian system. *The Plant Journal*, 66(3):480–491, 2011.

[38] J.W. Reed, A. Nagatani, T.D. Elich, M. Fagan, and J. Chory. Phytochrome A and phytochrome B have overlapping but distinct functions in Arabidopsis development. *Plant Physiology*, 104(4):1139–1149, 1994.

[39] B. Strasser, M. Sánchez-Lamas, M.J. Yanovsky, J.J. Casal, and P.D. Cerdán. Arabidopsis thaliana life without phytochromes. *Proceedings of the National Academy of Sciences*, 107(10):4776–4781, 2010.

[40] B. Al-Sady, E.A. Kikis, E. Monte, and P.H. Quail. Mechanistic duality of transcription factor function in phytochrome signaling. *Proceedings of the National Academy of Sciences*, 105(6):2232, 2008.

[41] L. Hennig, C. Poppe, S. Unger, and E. Schäfer. Control of hypocotyl elongation in Arabidopsis thaliana by photoreceptor interaction. *Planta*, 208(2):257–263, 1999.

[42] P. Leivar, E. Monte, B. Al-Sady, C. Carle, A. Storer, J.M. Alonso, J.R. Ecker, and P.H. Quail. The Arabidopsis phytochrome-interacting factor PIF7, together with PIF3 and PIF4, regulates responses to prolonged red light by modulating phyB levels. *The Plant Cell Online*, 20(2):337, 2008.

[43] F. Valverde, A. Mouradov, W. Soppe, D. Ravenscroft, A. Samach, and G. Coupland. Photoreceptor regulation of constans protein in photoperiodic flowering. *Science's STKE*, 303(5660):1003, 2004.

[44] P.D. Cerdán and J. Chory. Regulation of flowering time by light quality. *Nature*, 423(6942):881–885, 2003.

[45] R.A. Sharrock and T. Clack. Heterodimerization of type II phytochromes in Arabidopsis. *Proceedings of the National Academy of Sciences of the United States of America*, 101(31):11500, 2004.

[46] H. Li, J. Zhang, R.D. Vierstra, and H. Li. Quaternary organization of a phytochrome dimer as revealed by cryoelectron microscopy. *Proceedings of the National Academy of Sciences*, 107(24):10872, 2010.

[47] T. Clack, A. Shokry, M. Moffet, P. Liu, M. Faul, and R.A. Sharrock. Obligate heterodimerization of Arabidopsis phytochromes C and E and interaction with the PIF3 basic helix-loop-helix transcription factor. *The Plant Cell Online*, 21(3):786–799, 2009.

[48] C. Fankhauser and M. Chen. Transposing phytochrome into the nucleus. *Trends in Plant Science*, 13(11):596–601, 2008.

[49] A. Nagatani. Light-regulated nuclear localization of phytochromes. *Current Opinion in Plant Biology*, 7(6):708–711, 2004.

[50] Y. Jiao, O.S. Lau, and X.W. Deng. Light-regulated transcriptional networks in higher plants. *Nature Reviews Genetics*, 8(3):217–230, 2007.

[51] A. Hiltbrunner, A. Viczián, E. Bury, A. Tscheuschler, S. Kircher, R. Tóth, A. Honsberger, F. Nagy, C. Fankhauser, and E. Schäfer. Nuclear accumulation of the phytochrome a photoreceptor requires fhy1. *Current Biology*, 15(23):2125–2130, 2005.

[52] A. Hiltbrunner, A. Tscheuschler, A. Viczián, T. Kunkel, S. Kircher, and E. Schäfer. Fhy1 and fhl act together to mediate nuclear accumulation of the phytochrome a photoreceptor. *Plant and Cell Physiology*, 47(8):1023–1034, 2006.

[53] J. Rösler, I. Klein, and M. Zeidler. Arabidopsisfhl/fhy1 double mutant reveals a distinct cytoplasmic action of phytochrome a. *Proceedings of the National Academy of Sciences*, 104(25):10737, 2007.

[54] K. Sakamoto and A. Nagatani. Nuclear localization activity of phytochrome B. *The Plant Journal*, 10(5):859–868, 1996.

[55] A. Pfeiffer, M.K. Nagel, C. Popp, F. Wüst, J. Bindics, A. Viczián, A. Hiltbrunner, F. Nagy, T. Kunkel, and E. Schäfer. Interaction with plant transcription factors can mediate nuclear import of phytochrome B. *Proceedings of the National Academy of Sciences*, 109(15):5892–5897, 2012.

[56] R. Yamaguchi, M. Nakamura, N. Mochizuki, S.A. Kay, and A. Nagatani. Light-dependent translocation of a phytochrome B-GFP fusion protein to the nucleus in transgenic Arabidopsis. *The Journal of Cell Biology*, 145(3):437–445, 1999.

[57] P. Gil, S. Kircher, E. Adam, E. Bury, L. Kozma-Bognar, E. Schäfer, and F. Nagy. Photocontrol of subcellular partitioning of phytochrome-B: GFP fusion protein in tobacco seedlings. *The Plant Journal*, 22(2):135–145, 2000.

[58] M. Chen. Phytochrome nuclear body: an emerging model to study interphase nuclear dynamics and signaling. *Current Opinion in Plant Biology*, 11(5):503–508, 2008.

[59] E. Monte, J.M. Tepperman, B. Al-Sady, K.A. Kaczorowski, J.M. Alonso, J.R. Ecker, X. Li, Y. Zhang, and P.H. Quail. The phytochrome-interacting transcription factor, PIF3, acts early, selectively, and positively in light-induced chloroplast development. *Proceedings of the National Academy of Sciences of the United States of America*, 101(46):16091, 2004.

[60] M. Chen, R. Schwab, and J. Chory. Characterization of the requirements for localization of phytochrome b to nuclear bodies. *Proceedings of the National Academy of Sciences*, 100(24):14493, 2003.

[61] D. Bauer, A. Viczián, S. Kircher, T. Nobis, R. Nitschke, T. Kunkel, K.C.S. Panigrahi, É. Ádám, E. Fejes, E. Schäfer, et al. Constitutive photomorphogenesis 1 and multiple photoreceptors control degradation of phytochrome interacting factor 3, a transcription factor required for light signaling in Arabidopsis. *The Plant Cell Online*, 16(6):1433–1445, 2004.

[62] T. Matsushita, N. Mochizuki, and A. Nagatani. Dimers of the N-terminal domain of phytochrome B are functional in the nucleus. *Nature*, 424(6948):571–574, 2003.

[63] M. Chen, R.M. Galvão, M. Li, B. Burger, J. Bugea, J. Bolado, and J. Chory. Arabidopsis hemera/ptac12 initiates photomorphogenesis by phytochromes. *Cell*, 141(7):1230–1240, 2010.

[64] R.M. Galvão, M. Li, S.M. Kothadia, J.D. Haskel, P.V. Decker, E.K. Van Buskirk, and M. Chen. Photoactivated phytochromes interact with hemera and promote its accumulation to establish photomorphogenesis in arabidopsis. *Genes & Development*, 26(16):1851–1863, 2012.

[65] J.J. Casal, R.A. Sánchez, and J.F. Botto. Modes of action of phytochromes.

[66] J.J. Casal and H. Boccalandro. Co-action between phytochrome b and hy4 in arabidopsis thaliana. *Planta*, 197(2):213–218, 1995.

[67] A.C. McCormac, D. Wagner, M.T. Boylan, P.H. Quail, H. Smith, and G.C. Whitelam. Photoresponses of transgenic arabidopsis seedlings expressing introduced phytochrome b-encoding cdnas: evidence that phytochrome a and phytochrome b have distinct photoregulatory functions. *The Plant Journal*, 4(1):19–27, 1993.

[68] MA Mazzella, TM Alconada Magliano, and JJ Casal. Dual effect of phytochrome a on hypocotyl growth under continuous red light. *Plant, Cell & Environment*, 20(2):261–267, 1997.

[69] S. Schmidt, H. Drumm-Herrel, R. Oelmüller, and H. Mohr. Time course of competence in phytochrome-controlled appearance of nuclear-encoded plastidic proteins and messenger rnas. *Planta*, 170(3):400–407, 1987.

[70] M. Ni, J.M. Tepperman, and P.H. Quail. PIF3, a phytochrome-interacting factor necessary for normal photoinduced signal transduction, is a novel basic helix-loop-helix protein. *Cell*, 95(5):657–667, 1998.

[71] M. Ni, J.M. Tepperman, and P.H. Quail. Binding of phytochrome B to its nuclear signalling partner PIF3 is reversibly induced by light. *Nature*, 400(6746):781, 1999.

[72] E. Huq and P.H. Quail. PIF4, a phytochrome-interacting bHLH factor, functions as a negative regulator of phytochrome B signaling in Arabidopsis. *The EMBO journal*, 21(10):2441–2450, 2002.

[73] E. Huq, B. Al-Sady, M. Hudson, C. Kim, K. Apel, and P.H. Quail. Phytochrome-interacting factor 1 is a critical bHLH regulator of chlorophyll biosynthesis. *Science's STKE*, 305(5692):1937, 2004.

[74] R. Khanna, E. Huq, E.A. Kikis, B. Al-Sady, C. Lanzatella, and P.H. Quail. A novel molecular recognition motif necessary for targeting photoactivated phytochrome signaling to specific basic helix-loop-helix transcription factors. *The Plant Cell Online*, 16(11):3033–3044, 2004.

[75] P. Leivar and P.H. Quail. PIFs: pivotal components in a cellular signaling hub. *Trends in Plant Science*, 2010.

[76] J.F. Martínez-García, E. Huq, and P.H. Quail. Direct targeting of light signals to a promoter element-bound transcription factor. *Science*, 288(5467):859, 2000.

[77] G. Toledo-Ortiz, E. Huq, and P.H. Quail. The Arabidopsis basic/helix-loop-helix transcription factor family. *The Plant Cell Online*, 15(8):1749–1770, 2003.

[78] S.V. Kumar and P.A. Wigge. H2A. Z-containing nucleosomes mediate the thermosensory response in Arabidopsis. *Cell*, 140(1):136–147, 2010.

[79] C.D. Fairchild, M.A. Schumaker, and P.H. Quail. HFR1 encodes an atypical bHLH protein that acts in phytochrome A signal transduction. *Genes & development*, 14(18):2377–2391, 2000.

[80] P. Hornitschek, S. Lorrain, V. Zoete, O. Michielin, and C. Fankhauser. Inhibition of the shade avoidance response by formation of non-dna binding bhlh heterodimers. *The EMBO journal*, 28(24):3893–3902, 2009.

[81] E. Park, J. Kim, Y. Lee, J. Shin, E. Oh, W.I. Chung, J.R. Liu, and G. Choi. Degradation of phytochrome interacting factor 3 in phytochrome-mediated light signaling. *Plant and Cell Physiology*, 45(8):968–975, 2004.

[82] B. Al-Sady, W. Ni, S. Kircher, E. Schäfer, and P.H. Quail. Photoactivated phytochrome induces rapid PIF3 phosphorylation prior to proteasome-mediated degradation. *Molecular Cell*, 23(3):439–446, 2006.

[83] B. Phee, J. Kim, D. Shin, J. Yoo, K. Park, Y. Han, Y. Kwon, M. Cho, J. Jeon, S. Bhoo, et al. A novel protein phosphatase indirectly regulates phytochrome-interacting factor 3 via phytochrome. *Biochem. J*, 415:247–255, 2008.

[84] I.C. Jang, R. Henriques, H.S. Seo, A. Nagatani, and N.H. Chua. Arabidopsis PHYTOCHROME INTERACTING FACTOR Proteins Promote Phytochrome B Polyubiquitination by COP1 E3 Ligase in the Nucleus. *The Plant Cell Online*, 22(7):2370, 2010.

[85] K. Nozue, M.F. Covington, P.D. Duek, S. Lorrain, C. Fankhauser, S.L. Harmer, and J.N. Maloof. Rhythmic growth explained by coincidence between internal and external cues. *Nature*, 448(7151):358–361, 2007.

[86] H. Shen, L. Zhu, A. Castillon, M. Majee, B. Downie, and E. Huq. Light-induced phosphorylation and degradation of the negative regulator PHYTOCHROME-INTERACTING FACTOR1 from Arabidopsis depend upon its direct physical interactions with photoactivated phytochromes. *The Plant Cell Online*, 20(6):1586–1602, 2008.

[87] S. Lorrain, T. Allen, P.D. Duek, G.C. Whitelam, and C. Fankhauser. Phytochrome-mediated inhibition of shade avoidance involves degradation of growth-promoting bHLH transcription factors. *The Plant Journal*, 53(2):312–323, 2008.

[88] P. Leivar, E. Monte, Y. Oka, T. Liu, C. Carle, A. Castillon, E. Huq, and P.H. Quail. Multiple phytochrome-interacting bhlh transcription factors repress premature seedling photomorphogenesis in darkness. *Current Biology*, 18(23):1815–1823, 2008.

[89] T. Yamashino, A. Matsushika, T. Fujimori, S. Sato, T. Kato, S. Tabata, and T. Mizuno. A link between circadian-controlled bhlh factors and the aprr1/toc1 quintet in arabidopsis thaliana. *Plant and Cell Physiology*, 44(6):619–629, 2003.

[90] D.A. Nusinow, A. Helfer, E.E. Hamilton, J.J. King, T. Imaizumi, T.F. Schultz, E.M. Farré, and S.A. Kay. The elf4-elf3-lux complex links the circadian clock to diurnal control of hypocotyl growth. *Nature*, 475(7356):398–402, 2011.

[91] Y. Niwa, T. Yamashino, and T. Mizuno. The circadian clock regulates the photoperiodic response of hypocotyl elongation through a coincidence mechanism in arabidopsis thaliana. *Plant and Cell Physiology*, 50(4):838–854, 2009.

[92] T. Ruts, S. Matsubara, A. Wiese-Klinkenberg, and A. Walter. Aberrant temporal growth pattern and morphology of root and shoot caused by a defective circadian clock in arabidopsis thaliana. *The Plant Journal*, 2012.

[93] J.A. Stavang, J. Gallego-Bartolomé, M.D. Gómez, S. Yoshida, T. Asami, J.E. Olsen, J.L. García-Martínez, D. Alabadí, and M.A. Blázquez. Hormonal regulation of temperature-induced growth in arabidopsis. *The Plant Journal*, 60(4):589–601, 2009.

[94] S. Mathews. Evolutionary studies illuminate the structural-functional model of plant phytochromes. *The Plant Cell Online*, 22(1):4–16.

[95] G. Bae and G. Choi. Decoding of light signals by plant phytochromes and their interacting proteins. *Annu. Rev. Plant Biol.*, 59:281–311, 2008.

[96] P. Leivar, J.M. Tepperman, E. Monte, R.H. Calderon, T.L. Liu, and P.H. Quail. Definition of early transcriptional circuitry involved in light-induced reversal of pif-imposed repression of photomorphogenesis in young arabidopsis seedlings. *The Plant Cell Online*, 21(11):3535–3553, 2009.

[97] D.E. Richards, K.E. King, T. Ait-Ali, and N.P. Harberd. How gibberellin regulates plant growth and development: a molecular genetic analysis of gibberellin signaling. *Annual review of Plant Biology*, 52(1):67–88, 2001.

[98] A.L. Silverstone, H.S. Jung, A. Dill, H. Kawaide, Y. Kamiya, and T. Sun. Repressing a repressor: gibberellin-induced rapid reduction of the rga protein in arabidopsis. *The Plant Cell Online*, 13(7):1555–1566, 2001.

[99] M. De Lucas, J.M. Davière, M. Rodríguez-Falcón, M. Pontin, J.M. Iglesias-Pedraz, S. Lorrain, C. Fankhauser, M.A. Blázquez, E. Titarenko, and S. Prat. A molecular framework for light and gibberellin control of cell elongation. *Nature*, 451(7177):480–484, 2008.

[100] S. Feng, C. Martinez, G. Gusmaroli, Y. Wang, J. Zhou, F. Wang, L. Chen, L. Yu, J.M. Iglesias-Pedraz, S. Kircher, et al. Coordinated regulation of Arabidopsis thaliana development by light and gibberellins. *Nature*, 451(7177):475–479, 2008.

[101] H. Wang, L.G. Ma, J.M. Li, H.Y. Zhao, and X.W. Deng. Direct interaction of arabidopsis cryptochromes with cop1 in light control development. *Science's STKE*, 294(5540):154, 2001.

[102] H.Q. Yang, R.H. Tang, and A.R. Cashmore. The signaling mechanism of arabidopsis cry1 involves direct interaction with cop1. *The Plant Cell Online*, 13(12):2573–2587, 2001.

[103] X.L. Liu, M.F. Covington, C. Fankhauser, J. Chory, and D.R. Wagner. Elf3 encodes a circadian clock–regulated nuclear protein that functions in an arabidopsis phyb signal transduction pathway. *The Plant Cell Online*, 13(6):1293–1304, 2001.

[104] J.W. Reed, P. Nagpal, R.M. Bastow, K.S. Solomon, M.J. Dowson-Day, R.P. Elumalai, and A.J. Millar. Independent action of elf3 and phyb to control hypocotyl elongation and flowering time. *Plant Physiology*, 122(4):1149–1160, 2000.

[105] E. Kolmos, E. Herrero, N. Bujdoso, A.J. Millar, R. Tóth, P. Gyula, F. Nagy, and S.J. Davis. A reduced-function allele reveals that early flowering3 repressive action on the circadian clock is modulated by phytochrome signals in arabidopsis. *The Plant Cell Online*, 23(9):3230–3246, 2011.

[106] A. Pokhilko, A.P. Fernández, K.D. Edwards, M.M. Southern, K.J. Halliday, and A.J. Millar. The clock gene circuit in arabidopsis includes a repressilator with additional feedback loops. *Molecular Systems Biology*, 8(1), 2012.

[107] E.M. Josse and K.J. Halliday. Skotomorphogenesis: the dark side of light signalling. *Current Biology*, 18(24):R1144–R1146, 2008.

[108] J. Bou-Torrent, I. Roig-Villanova, and J.F. Martínez-García. Light signaling: back to space. *Trends in Plant Science*, 13(3):108–114, 2008.

[109] T.W. McNellis, A.G. von Arnim, T. Araki, Y. Komeda, S. Miséra, and X.W. Deng. Genetic and molecular analysis of an allelic series of cop1 mutants suggests functional roles for the multiple protein domains. *The Plant Cell Online*, 6(4):487–500, 1994.

[110] M.T. Osterlund, C.S. Hardtke, N. Wei, and X.W. Deng. Targeted destabilization of hy5 during light-regulated development ofarabidopsis. *Nature*, 405:462–466, 2000.

[111] U. Hoecker. Regulated proteolysis in light signaling. *Current Opinion in Plant Biology*, 8(5):469–476, 2005.

[112] C. Yi and X.W. Deng. Cop1–from plant photomorphogenesis to mammalian tumorigenesis. *Trends in Cell Biology*, 15(11):618–625, 2005.

[113] A.G. von Arnim and X.W. Deng. Light inactivation of arabidopsis photomorphogenic repressor cop1 involves a cell-specific regulation of its nucleocytoplasmic partitioning. *Cell*, 79(6):1035–1045, 1994.

[114] H.E. Boccalandro, M.C. Rossi, Y. Saijo, X.W. Deng, and J.J. Casal. Promotion of photomorphogenesis by cop1. *Plant Molecular Biology*, 56(6):905–915, 2004.

[115] S. Laubinger, K. Fittinghoff, and U. Hoecker. The spa quartet: a family of wd-repeat proteins with a central role in suppression of photomorphogenesis in arabidopsis. *The Plant Cell Online*, 16(9):2293–2306, 2004.

[116] K.A. Franklin, T. Allen, and G.C. Whitelam. Phytochrome a is an irradiance-dependent red light sensor. *The Plant Journal*, 50(1):108–117, 2007.

[117] B. Liu, Z. Zuo, H. Liu, X. Liu, and C. Lin. Arabidopsis cryptochrome 1 interacts with spa1 to suppress cop1 activity in response to blue light. *Genes & Development*, 25(10):1029–1034, 2011.

[118] D. Staiger, L. Allenbach, N. Salathia, V. Fiechter, S.J. Davis, A.J. Millar, J. Chory, and C. Fankhauser. The arabidopsis srr1 gene mediates phyb signaling and is required for normal circadian clock function. *Genes & development*, 17(2):256, 2003.

[119] H.Q. Yang, Y.J. Wu, R.H. Tang, D. Liu, Y. Liu, and A.R. Cashmore. The c termini of arabidopsis cryptochromes mediate a constitutive light response. *Cell*, 103(5):815–827, 2000.

[120] P.D. Duek and C. Fankhauser. Hfr1, a putative bhlh transcription factor, mediates both phytochrome a and cryptochrome signalling. *The Plant Journal*, 34(6):827–836, 2003.

[121] Q. Zhou, P.D. Hare, S.W. Yang, M. Zeidler, L.F. Huang, and N.H. Chua. Fhl is required for full phytochrome a signaling and shares overlapping functions with fhy1. *The Plant Journal*, 43(3):356–370, 2005.

[122] A. Castillon, H. Shen, and E. Huq. Blue light induces degradation of the negative regulator phytochrome interacting factor 1 to promote photomorphogenic development of arabidopsis seedlings. *Genetics*, 182(1):161–171, 2009.

[123] X. Kang and M. Ni. Arabidopsis short hypocotyl under blue1 contains spx and exs domains and acts in cryptochrome signaling. *The Plant Cell Online*, 18(4):921–934, 2006.

[124] J.J Casal. Shade Avoidance. *The Arabidopsis Book*, e0157(doi: 10.1199/tab.0157).

[125] H. Smith and GC Whitelam. The shade avoidance syndrome: multiple responses mediated by multiple phytochromes. *Plant, Cell & Environment*, 20(6):840–844, 1997.

[126] P. Hornitschek, M.V. Kohnen, S. Lorrain, J. Rougemont, K. Ljung, I. López-Vidriero, J.M. Franco-Zorrilla, R. Solano, M. Trevisan, S. Pradervand, et al. Phytochrome interacting factors 4 and 5 control seedling growth in changing light conditions by directly controlling auxin signaling. *The Plant Journal*, 2012.

[127] W.M. Gray, A. Östin, G. Sandberg, C.P. Romano, and M. Estelle. High temperature promotes auxin-mediated hypocotyl elongation in Arabidopsis. *Proceedings of the National Academy of Sciences*, 95(12):7197, 1998.

[128] S. Balasubramanian, S. Sureshkumar, J. Lempe, and D. Weigel. Potent induction of arabidopsis thaliana flowering by elevated growth temperature. *PLoS Genetics*, 2(7):e106, 2006.

[129] M.A. Koini, L. Alvey, T. Allen, C.A. Tilley, N.P. Harberd, G.C. Whitelam, and K.A. Franklin. High temperature-mediated adaptations in plant architecture require the bHLH transcription factor PIF4. *Current Biology*, 19(5):408–413, 2009.

[130] Y.H. Chew, A.M. Wilczek, M. Williams, S.M. Welch, J. Schmitt, and K.J. Halliday. An augmented arabidopsis phenology model reveals seasonal temperature control of flowering time. *New Phytologist*, 2012.

[131] F. Turck, F. Fornara, and G. Coupland. Regulation and identity of florigen: Flowering locus t moves center stage. *Annu. Rev. Plant Biol.*, 59:573–594, 2008.

[132] J. Foreman, H. Johansson, P. Hornitschek, E.M. Josse, C. Fankhauser, and K.J. Halliday. Light receptor action is critical for maintaining plant biomass at warm ambient temperatures. *The Plant Journal*, 65(3):441–452, 2011.

[133] K. Sidaway-Lee, E.M. Josse, A. Brown, Y. Gan, K.J. Halliday, I.A. Graham, and S. Penfield. Spatula links daytime temperature and plant growth rate. *Current Biology*, 20(16):1493–1497, 2010.

[134] W.D. Teale, I.A. Paponov, and K. Palme. Auxin in action: signalling, transport and the control of plant growth and development. *Nature Reviews Molecular Cell Biology*, 7(11):847–859, 2006.

[135] S. Abel and A. Theologis. Early genes and auxin action. *Plant Physiology*, 111(1):9, 1996.

[136] K. Nozue, S.L. Harmer, and J.N. Maloof. Genomic analysis of circadian clock-, light-, and growth-correlated genes reveals phytochrome-interacting factor5 as a modulator of auxin signaling in arabidopsis. *Plant Physiology*, 156(1):357–372, 2011.

[137] S.V. Kumar, D. Lucyshyn, K.E. Jaeger, E. Alós, E. Alvey, N.P. Harberd, and P.A. Wigge. Transcription factor pif4 controls the thermosensory activation of flowering. *Nature*, 2012.

[138] Z. Liu, Y. Zhang, R. Liu, H. Hao, Z. Wang, and Y. Bi. Phytochrome interacting factors (pifs) are essential regulators for sucrose-induced hypocotyl elongation in arabidopsis. *Journal of Plant Physiology*, 2011.

[139] E. Oh, J.Y. Zhu, and Z.Y Wang. Interaction between BZR1 and PIF4 integrates brassinosteroid and environmental responses. *Nature Cell Biology*, (doi:10.1038/ncb2545), 2012.

[140] M.Y. Bai, J.X. Shang, E. Oh, M. Fan, Y. Bai, R. Zentella, T.P. Sun, and Z.Y Wang. Brassinosteroid, gibberellin and phytochrome impinge on a common transcription module in Arabidopsis. *Nature Cell Biology*, (doi:10.1038/ncb2546), 2012.

[141] J.R. Ecker et al. The ethylene signal transduction pathway in plants. *Science*, 268(5211):667, 1995.

[142] J. Smalle, M. Haegman, J. Kurepa, M. Van Montagu, and D.V.D. Straeten. Ethylene can stimulate arabidopsis hypocotyl elongation in the light. *Proceedings of the National Academy of Sciences*, 94(6):2756, 1997.

[143] J.M. Alonso, T. Hirayama, G. Roman, S. Nourizadeh, and J.R. Ecker. Ein2, a bifunctional transducer of ethylene and stress responses in arabidopsis. *Science*, 284(5423):2148–2152, 1999.

[144] S. Zhong, H. Shi, C. Xue, L. Wang, Y. Xi, J. Li, P.H. Quail, X.W. Deng, and H. Guo. A molecular framework of light-controlled phytohormone action in¡ i¿ arabidopsis¡/i¿. *Current Biology*, 2012.

[145] E. Schäfer and W. Schmidt. Temperature dependence of phytochrome dark reactions. *Planta*, 116(3):257–266, 1974.

[146] J. Sun, L. Qi, Y. Li, J. Chu, and C. Li. Pif4–mediated activation of yucca8 expression integrates temperature into the auxin pathway in regulating arabidopsis hypocotyl growth. *PLoS Genetics*, 8(3):e1002594, 2012.

[147] A. Kunihiro, T. Yamashino, N. Nakamichi, Y. Niwa, H. Nakanishi, and T. Mizuno. Phytochrome-interacting factor 4 and 5 (pif4 and pif5) activate the homeobox athb2 and auxin-inducible iaa29 genes in the coincidence mechanism underlying photoperiodic control of plant growth of arabidopsis thaliana. *Plant and Cell Physiology*, 52(8):1315–1329, 2011.

[148] K.A. Franklin, S.H. Lee, D. Patel, S.V. Kumar, A.K. Spartz, C. Gu, S. Ye, P. Yu, G. Breen, J.D. Cohen, et al. Phytochrome-interacting factor 4 (pif4) regulates auxin biosynthesis at high temperature. *Proceedings of the National Academy of Sciences*, 108(50):20231–20235, 2011.

[149] E. Thingnaes, S. Torre, A. Ernstsen, and R. Moe. Day and night temperature responses in arabidopsis: effects on gibberellin and auxin content, cell size, morphology and flowering time. *Annals of botany*, 92(4):601–612, 2003.

[150] M.A. Blázquez, J.H. Ahn, and D. Weigel. A thermosensory pathway controlling flowering time in arabidopsis thaliana. *Nature genetics*, 33(2):168–171, 2003.

[151] J.H. Lee, S.J. Yoo, S.H. Park, I. Hwang, J.S. Lee, and J.H. Ahn. Role of svp in the control of flowering time by ambient temperature in arabidopsis. *Genes & development*, 21(4):397, 2007.

[152] A.N. Dodd, N. Salathia, A. Hall, E. Kévei, R. Tóth, F. Nagy, J.M. Hibberd, A.J. Millar, and A.A.R. Webb. Plant circadian clocks increase photosynthesis, growth, survival, and competitive advantage. *Science's STKE*, 309(5734):630, 2005.

[153] P.A. Salomé and C.R. McClung. Pseudo-response regulator 7 and 9 are partially redundant genes essential for the temperature responsiveness of the arabidopsis circadian clock. *The Plant Cell Online*, 17(3):791–803, 2005.

[154] E. Boikoglou, Z. Ma, M. von Korff, A.M. Davis, F. Nagy, and S.J. Davis. Environmental memory from a circadian oscillator: The arabidopsis thaliana clock differentially integrates perception of photic vs. thermal entrainment. *Genetics*, 189(2):655–664, 2011.

[155] K.D. Edwards, J.R. Lynn, P. Gyula, F. Nagy, and A.J. Millar. Natural allelic variation in the temperature-compensation mechanisms of the arabidopsis thaliana circadian clock. *Genetics*, 170(1):387–400, 2005.

[156] A. Mehra, M. Shi, C.L. Baker, H.V. Colot, J.J. Loros, and J.C. Dunlap. A role for casein kinase 2 in the mechanism underlying circadian temperature compensation. *Cell*, 137(4):749–760, 2009.

[157] P.D. Gould, J.C.W. Locke, C. Larue, M.M. Southern, S.J. Davis, S. Hanano, R. Moyle, R. Milich, J. Putterill, A.J. Millar, et al. The molecular basis of temperature compensation in the arabidopsis circadian clock. *The Plant Cell Online*, 18(5):1177–1187, 2006.

[158] P.A. Salomé, D. Weigel, and C.R. McClung. The role of the arabidopsis morning loop components cca1, lhy, prr7, and prr9 in temperature compensation. *The Plant Cell Online*, 22(11):3650–3661, 2010.

[159] E.M. Farré, S.L. Harmer, F.G. Harmon, M.J. Yanovsky, and S.A. Kay. Overlapping and distinct roles of prr7 and prr9 in the arabidopsis circadian clock. *Current Biology*, 15(1):47–54, 2005.

[160] A.B. James, N.H. Syed, S. Bordage, J. Marshall, G.A. Nimmo, G.I. Jenkins, P. Herzyk, J.W.S. Brown, and H.G. Nimmo. Alternative splicing mediates responses of the arabidopsis circadian clock to temperature changes. *The Plant Cell Online*, 24(3):961–981, 2012.

[161] J.W. Reed, P. Nagpal, D.S. Poole, M. Furuya, and J. Chory. Mutations in the gene for the red/far-red light receptor phytochrome b alter cell elongation and physiological responses throughout arabidopsis development. *The Plant Cell Online*, 5(2):147–157, 1993.

[162] R. Khanna, Y. Shen, C.M. Marion, A. Tsuchisaka, A. Theologis, E. Schäfer, and P.H. Quail. The basic helix-loop-helix transcription factor pif5 acts on ethylene biosynthesis and phytochrome signaling by distinct mechanisms. *The Plant Cell Online*, 19(12):3915–3929, 2007.

[163] É. Ádám, A. Hussong, J. Bindics, F. Wüst, A. Viczián, M. Essing, M. Medzihradszky, S. Kircher, E. Schäfer, and F. Nagy. Altered Dark-and Photoconversion of Phytochrome B Mediate Extreme Light Sensitivity and Loss of Photoreversibility of the phyB-401 Mutant. *PLoS ONE*, 6(11):e27250, 2011.

[164] Z.Y. Wang and E.M. Tobin. Constitutive expression of the *CIRCADIAN CLOCK ASSOCIATED 1* (*CCA1*) gene disrupts circadian rhythms and suppresses its own expression. *Cell*, 93(7):1207–1217, 1998.

[165] G. Saini, R. Meskauskiene, W. Pijacka, P. Roszak, L.L.E. Sjögren, A.K. Clarke, M. Straus, and K. Apel. happy on norflurazon(hon) mutations implicate perturbance of plastid homeostasis with activating stress acclimatization and changing nuclear gene expression in norflurazon-treated seedlings. *The Plant Journal*, 65(5):690–702, 2011.

[166] E.J. Chapman, K. Greenham, C. Castillejo, R. Sartor, A. Bialy, T. Sun, and M. Estelle. Hypocotyl transcriptome reveals auxin regulation of growth-promoting genes through ga-dependent and-independent pathways. *PloS one*, 7(5):e36210, 2012.

[167] J.M. Kelly and J.C. Lagarias. Photochemistry of 124-kilodalton avena phytochrome under constant illumination in vitro. *Biochemistry*, 24(21):6003–6010, 1985.

[168] K.A. Franklin, U. Praekelt, W.M. Stoddart, O.E. Billingham, K.J. Halliday, and G.C. Whitelam. Phytochromes b, d, and e act redundantly to control multiple physiological responses in arabidopsis. *Plant Physiology*, 131(3):1340–1346, 2003.

[169] P. Leivar, E. Monte, M.M. Cohn, and P.H. Quail. Phytochrome signaling in green arabidopsis seedlings: Impact assessment of a mutually negative phyb–pif feedback loop. *Molecular Plant*, 2012.

[170] T.F. Coleman and Y. Li. An interior trust region approach for nonlinear minimization subject to bounds. 1993.

[171] T.F. Coleman and Y. Li. On the convergence of interior-reflective newton methods for nonlinear minimization subject to bounds. *Mathematical programming*, 67(1):189–224, 1994.

[172] M. Stein. Large sample properties of simulations using latin hypercube sampling. *Technometrics*, pages 143–151, 1987.

[173] S.J. Gould and S. Subramani. Firefly luciferase as a tool in molecular and cell biology. *Analytical biochemistry*, 175(1):5–13, 1988.

[174] Y. Shen, S. Feng, L. Ma, R. Lin, L.J. Qu, Z. Chen, H. Wang, and X.W. Deng. Arabidopsis fhy1 protein stability is regulated by light via phytochrome a and 26s proteasome. *Plant Physiology*, 139(3):1234–1243, 2005.

[175] D. Alabadí, J. Gallego-Bartolomé, L. Orlando, L. García-Cárcel, V. Rubio, C. Martínez, M. Frigerio, J.M. Iglesias-Pedraz, A. Espinosa, X.W. Deng, et al. Gibberellins modulate light signaling pathways to prevent arabidopsis seedling de-etiolation in darkness. *The Plant Journal*, 53(2):324–335, 2008.

[176] N.J. Marianayagam, M. Sunde, and J.M. Matthews. The power of two: protein dimerization in biology. *Trends in biochemical Sciences*, 29(11):618–625, 2004.

[177] A. Samach and P.A. Wigge. Ambient temperature perception in plants. *Current Opinion in Plant Biology*, 8(5):483–486, 2005.

[178] F. VASSEUR, F. PANTIN, and D. VILE. Changes in light intensity reveal a major role for carbon balance in arabidopsis responses to high temperature. *Plant, Cell & Environment*, 2011.

[179] J. Shin, K. Kim, H. Kang, I.S. Zulfugarov, G. Bae, C.H. Lee, D. Lee, and G. Choi. Phytochromes promote seedling light responses by inhibiting four negatively-acting phytochrome-interacting factors. *Proceedings of the National Academy of Sciences*, 106(18):7660, 2009.

[180] E. Park, J. Park, J. Kim, A. Nagatani, J.C. J. Clark Lagarias, and G. Choi. Phytochrome B inhibits binding of Phytochrome-Interacting Factors to their target promoters. *The Plant Journal*, (Accepted Article):doi: 10.1111/j.1365–313X2012.05114, 2012.

[181] P. Achard, L. Liao, C. Jiang, T. Desnos, J. Bartlett, X. Fu, and N.P. Harberd. Dellas contribute to plant photomorphogenesis. *Plant Physiology*, 143(3):1163–1172, 2007.

[182] S. Hanano, M.A. Domagalska, F. Nagy, and S.J. Davis. Multiple phytohormones influence distinct parameters of the plant circadian clock. *Genes to Cells*, 11(12):1381–1392, 2006.

[183] J.C. Lagarias, J.M. Kelly, K.L. Cyr, and W.O. Smith Jr. Comparative photochemical analysis of highly purified 124 kilodalton oat and rye phytochromes in vitro. *Photochemistry and Photobiology*, 46(1):5–13, 1987.

[184] G. Toledo-Ortiz, Y. Kiryu, J. Kobayashi, Y. Oka, Y. Kim, H.G. Nam, N. Mochizuki, and A. Nagatani. Subcellular sites of the signal transduction and degradation of phytochrome a. *Plant and Cell Physiology*, 51(10):1648–1660, 2010.

[185] M. Endo, S. Nakamura, T. Araki, N. Mochizuki, and A. Nagatani. Phytochrome b in the mesophyll delays flowering by suppressing flowering locus t expression in arabidopsis vascular bundles. *The Plant Cell Online*, 17(7):1941–1952, 2005.

[186] K.J. Halliday, J.F. Martínez-García, and E.M. Josse. Integration of light and auxin signaling. *Cold Spring Harbor perspectives in Biology*, 1(6), 2009.

[187] S. Penfield, E.M. Josse, R. Kannangara, A.D. Gilday, K.J. Halliday, and I.A. Graham. Cold and light control seed germination through the bhlh transcription factor spatula. *Current Biology*, 15(22):1998–2006, 2005.

[188] M. Black and J.E. Shuttleworth. The role of the cotyledons in the photocontrol of hypocotyl extension in cucumis sativus l. *Planta*, 117(1):57–66, 1974.

[189] D. Chamovitz, I. Pecker, and J. Hirschberg. The molecular basis of resistance to the herbicide norflurazon. *Plant Molecular Biology*, 16(6):967–974, 1991.

[190] J. Breitenbach, C. Zhu, and G. Sandmann. Bleaching herbicide norflurazon inhibits phytoene desaturase by competition with the cofactors. *Journal of agricultural and food chemistry*, 49(11):5270–5272, 2001.

[191] Y. Zhang, Z. Liu, L. Wang, S. Zheng, J. Xie, and Y. Bi. Sucrose-induced hypocotyl elongation of arabidopsis seedlings in darkness depends on the presence of gibberellins. *Journal of Plant Physiology*, 167(14):1130–1136, 2010.

[192] J.L. Stewart, J.N. Maloof, and J.L. Nemhauser. Pif genes mediate the effect of sucrose on seedling growth dynamics. *PLoS One*, 6(5):e19894, 2011.

[193] S. Kircher and P. Schopfer. Photosynthetic sucrose acts as cotyledon-derived long-distance signal to control root growth during early seedling development in arabidopsis. *Proceedings of the National Academy of Sciences*, 109(28):11217–11221, 2012.

[194] M.E. Salvucci, A.R. Portis Jr, and W.L. Ogren. Light and CO_2 response of ribulose-1, 5-bisphosphate carboxylase/oxygenase activation in arabidopsis leaves. *Plant Physiology*, 80(3):655, 1986.

[195] M. Ramon, F. Rolland, and J. Sheen. Sugar sensing and signaling. *The Arabidopsis Book/American Society of Plant Biologists*, 6, 2008.

[196] F. Rook, F. Corke, R. Card, G. Munz, C. Smith, and M.W. Bevan. Impaired sucrose-induction mutants reveal the modulation of sugar-induced starch biosynthetic gene expression by abscisic acid signalling. *The Plant Journal*, 26(4):421–433, 2001.

[197] A. Laxmi, L.K. Paul, J.L. Peters, and J.P. Khurana. Arabidopsis constitutive photomorphogenic mutant, bls1, displays altered brassinosteroid response and sugar sensitivity. *Plant Molecular Biology*, 56(2):185–201, 2004.

[198] A. Giakountis, F. Cremer, S. Sim, M. Reymond, J. Schmitt, and G. Coupland. Distinct patterns of genetic variation alter flowering responses of arabidopsis accessions to different daylengths. *Plant Physiology*, 152(1):177–191, 2010.

[199] M. Van Zanten, L.A.C.J. Voesenek, A.J.M. Peeters, and F.F. Millenaar. Hormone-and light-mediated regulation of heat-induced differential petiole growth in arabidopsis. *Plant Physiology*, 151(3):1446–1458, 2009.

[200] P.D. Cerdán, M.J. Yanovsky, F. Reymundo, A. Nagatani, R.J. Staneloni, G.C. Whitelam, and J.J. Casal. Regulation of phytochrome b signaling by phytochrome a and fhy1 in arabidopsis thaliana. *The Plant Journal*, 18(5):499–507, 1999.

[201] L. Hennig, C. Poppe, U. Sweere, A. Martin, and E. Schäfer. Negative interference of endogenous phytochrome b with phytochrome a function in arabidopsis. *Plant Physiology*, 125(2):1036–1044, 2001.

[202] S. Faure, A.S. Turner, D. Gruszka, V. Christodoulou, S.J. Davis, M. von Korff, and D.A. Laurie. Mutation at the circadian clock gene early maturity 8 adapts domesticated barley (hordeum vulgare) to short growing seasons. *Proceedings of the National Academy of Sciences*, 2012.

[203] S.X. Lu, C.J. Webb, S.M. Knowles, S.H.J. Kim, Z. Wang, and E.M. Tobin. Cca1 and elf3 interact in the control of hypocotyl length and flowering time in arabidopsis. *Plant Physiology*, 158(2):1079–1088, 2012.

[204] M.A. Mazzella, D. Bertero, and J.J. Casal. Temperature-dependent internode elongation in vegetative plants of arabidopsis thaliana lacking phytochrome b and cryptochrome 1. *Planta*, 210(3):497–501, 2000.

[205] H.M.O. Leyser and IJ Furner. Characterisation of three shoot apical meristem mutants of arabidopsis thaliana. *Development*, 116(2):397–403, 1992.

[206] D.J. Bagnall, R.W. King, G.C. Whitelam, M.T. Boylan, D. Wagner, and P.H. Quail. Flowering responses to altered expression of phytochrome in mutants and transgenic lines of arabidopsis thaliana (l.) heynh. *Plant Physiology*, 108(4):1495–1503, 1995.

[207] A. Hall, L. Kozma-Bognár, R.M. Bastow, F. Nagy, and A.J. Millar. Distinct regulation of cab and phyb gene expression by similar circadian clocks. *The Plant Journal*, 32(4):529–537, 2002.

[208] S. Yoshida, T. Mandel, and C. Kuhlemeier. Stem cell activation by light guides plant organogenesis. *Genes & Development*, 25(13):1439–1450, 2011.

[209] Y. Liu, W. Ye, B. Li, X.J. Zhou, Y. Cui, M.P. Running, and K. Liu. Ccs52a2/fzr1, a cell cycle regulator, is an essential factor for shoot apical meristem maintenance in arabidopsis thaliana. *BMC Plant Biology*, 12(1):135, 2012.

[210] C. Gérard and A. Goldbeter. Entrainment of the mammalian cell cycle by the circadian clock: Modeling two coupled cellular rhythms. *PLoS Computational Biology*, 8(5):e1002516, 2012.

[211] J.S. Pendergast, M. Yeom, B.A. Reyes, Y. Ohmiya, and S. Yamazaki. Disconnected circadian and cell cycles in a tumor-driven cell line. *Communicative & integrative Biology*, 3(6):536, 2010.

[212] J. Moon, L. Zhu, H. Shen, and E. Huq. Pif1 directly and indirectly regulates chlorophyll biosynthesis to optimize the greening process in arabidopsis. *Proceedings of the National Academy of Sciences*, 105(27):9433, 2008.

Appendix S1

Models, Parameters and Figures related to Chapter 3

Derivation of PhyB Degradation Rate

For the following equation (S1.1) phyB is represented by x, and the dark dependent and light dependent degradation steps represented by κ and σ respectively.

$$\begin{aligned}
Darkness \xrightarrow{\kappa} \quad x \quad &\xrightarrow{\kappa} \\
Light \xrightarrow{\kappa} \quad x \quad &\xrightarrow{\kappa+\sigma} \\
\tfrac{dx}{dt} &= \kappa - (\kappa+\sigma)\, x \\
\tfrac{dx}{dt} + (\kappa+\sigma)\, x &= \kappa \\
\tfrac{d}{dt}\left(e^{(\kappa+\sigma)t}x\right) &= \kappa e^{(\kappa+\sigma)t} \\
e^{(\kappa+\sigma)t}x &= \tfrac{\kappa}{\kappa+\sigma}e^{(\kappa+\sigma)t} + c\text{: } x = 1 \text{ when } t = 0 \\
x &= \tfrac{\kappa}{\kappa+\sigma} + \tfrac{\sigma}{\kappa+\sigma}e^{-(\kappa+\sigma)t} \\
x &= \tfrac{\kappa}{\kappa+\sigma}\left(1 + \tfrac{\sigma}{\kappa}e^{-(\kappa+\sigma)t}\right)
\end{aligned} \tag{S1.1}$$

Based on calculated values of phyB degradation [16, 84], values of κ and σ are calculated as $0.00061 min^{-1}$ and $0.0024 min^{-1}$ .This means in the darkness, 0.061% of phyB is turned over every minute and there is an additional effect where 0.24% of phyB is lost due to red light.

Simple Mutual Degradation

$$\begin{aligned}
\dot{P}_r &= \alpha - (k_1+\beta)\, P_r + (k_2+k_r)\, P_{fr} \\
\dot{P_{fr}} &= k_1 P_r - (k_2 + k_r + \nu PIF)\, P_{fr} \\
\dot{PIF} &= k_d - PIF\,(k_d + \mu P_{fr})
\end{aligned} \tag{S1.2}$$

Indirect phyB Degradation

$$\begin{aligned} \dot{P_r} &= \alpha - (k_1 + \beta)\, P_r + (k_2 + k_r)\, P_{fr} \\ \dot{P_{fr}} &= k_1 P_r - (k_2 + k_r + \nu X)\, P_{fr} \\ \dot{PIF} &= k_d - PIF\,(k_d + \mu P_{fr}) \\ \dot{X} &= x_s - X\,(x_d + x_t PIF) \end{aligned} \tag{S1.3}$$

Double Tagging

$$\begin{aligned} \dot{P_r} &= \alpha - (k_1 + \beta)\, P_r + (k_2 + k_r)\, P_{fr} \\ \dot{P_{fr}} &= k_1 P_r - (k_2 + k_r + \gamma PIF)\, P_{fr} \\ \dot{PIF} &= k_d - PIF\,(k_d + \gamma P_{fr}) \\ \dot{P_{fr}*} &= \gamma P_{fr} PIF - \nu P_{fr} \\ \dot{P_{fr}*} &= \gamma P_{fr} PIF - \mu PIF \end{aligned} \tag{S1.4}$$

PIF Protection

$$\begin{aligned} \dot{P_r} &= \alpha - (k_1 + \beta)\, P_r + (k_2 + k_r)\, P_{fr} \\ \dot{P_{fr}} &= k_1 P_r - (k_2 + k_d + k_r + \nu PIF)\, P_{fr} \\ \dot{PIF} &= k_d - PIF\,(k_d + \gamma X + \mu P_{fr}) + \rho C \\ \dot{X} &= x_s - X\,(x_d + \gamma PIF) + \rho C \\ \dot{C} &= \gamma PIFX - \rho C \end{aligned} \tag{S1.5}$$

Phytochrome Support

$$\begin{aligned} \dot{P_r} &= \alpha - (k_1 + \beta)\, P_r + (k_2 + k_r)\, P_{fr} \\ \dot{P_{fr}} &= k_1 P_r - (k_2 + k_d + k_r + \gamma X) + \rho C \\ \dot{PIF} &= k_d - PIF\,(k_d + \mu P_{fr}) \\ \dot{X} &= x_s - X\,(x_d + \gamma P_{fr}) + \nu PIF \\ \dot{C} &= \gamma P_{fr} X - \rho C + \nu PIF \end{aligned} \tag{S1.6}$$

PIF homodimers

$$\begin{aligned} \dot{P_r} &= \alpha - (k_1 + \beta)\, P_r + (k_2 + k_r)\, P_{fr} \\ \dot{P_{fr}} &= k_1 P_r - (k_2 + k_d + k_r + \nu PIF)\, P_{fr} \\ \dot{PIF} &= k_d - PIF\,(k_d + \gamma PIF) + \rho PIF : PIF \\ \dot{PIF : PIF} &= \gamma PIF^2 - (\rho + \mu)\, PIF : PIF \end{aligned} \tag{S1.7}$$

PIF heterodimers

$$
\begin{aligned}
\dot{P_r} &= \alpha - (k_1 + \beta) P_r + (k_2 + k_r) P_{fr} \\
\dot{P_{fr}} &= k_1 P_r - (k_2 + k_d + k_r + \nu PIF + p_{t1} P1) P_{fr} \\
\dot{PIF} &= k_d - PIF (k_d + \gamma (P1 + PIF)) + \rho (2PIF : PIF + PIF : P1) \\
\dot{P1} &= k_{d1} - P1 (k_{d1} + \gamma (P1 + PIF)) + \rho (2P1 : P1 + PIF : P1) \\
PIF \dot{:} PIF &= \gamma PIF^2 - (\rho + \mu P_{fr}) PIF : PIF \\
P1 \dot{:} P1 &= \gamma P1^2 - (\rho) P1 : P1 \\
\dot{PIF} : P1 &= \gamma PIF * P1 - (\rho + \mu P_{fr}) PIF : P1
\end{aligned}
\tag{S1.8}
$$

PIF labile heterodimers

$$
\begin{aligned}
\dot{P_r} &= \alpha - (k_1 + \beta) P_r + (k_2 + k_r) P_{fr} \\
\dot{P_{fr}} &= k_1 P_r - (k_2 + k_d + k_r + \nu PIF + p_{t1} P1 + p_{t2} P2) P_{fr} \\
\dot{PIF} &= k_d - PIF (k_d + \gamma (P1 + P2 + PIF)) \\
&+ \rho (2PIF : PIF + PIF : P1 + PIF : P2) \\
\dot{P1} &= k_{d1} - P1 (k_{d1} + \gamma (P1 + P2 + PIF)) \\
&+ \rho (2P1 : P1 + PIF : P1 + P1 : P2) \\
\dot{P2} &= k_{d2} - P2 (k_{d2} + \gamma (P1 + P2 + PIF)) \\
&+ \rho (2P2 : P2 + PIF : P2 + P1 : P2) \\
PIF \dot{:} PIF &= \gamma PIF^2 - (\rho + \mu P_{fr}) PIF : PIF \\
P1 \dot{:} P1 &= \gamma P1^2 - (\rho) P1 : P1 \\
P2 \dot{:} P2 &= \gamma P2^2 - (\rho) P2 : P2 \\
\dot{PIF} : P1 &= \gamma PIF * P1 - (\rho + \mu P_{fr}) PIF : P1 \\
\dot{PIF} : P2 &= \gamma PIF * P2 - (\rho + \mu P_{fr}) PIF : P2 \\
P1 \dot{:} P2 &= \gamma P1 * P2 - (\rho + \mu P_{fr}) P1 : P2
\end{aligned}
\tag{S1.9}
$$

Early PIF3 degradation over Time

$$
\begin{aligned}
\dot{Y} &= 1 - Y - \gamma(x - C)Y \\
\dot{C} &= \gamma(x - C)Y - \delta C \\
\dot{Y_t} &= \delta C - \mu Y_t
\end{aligned}
\tag{S1.10}
$$

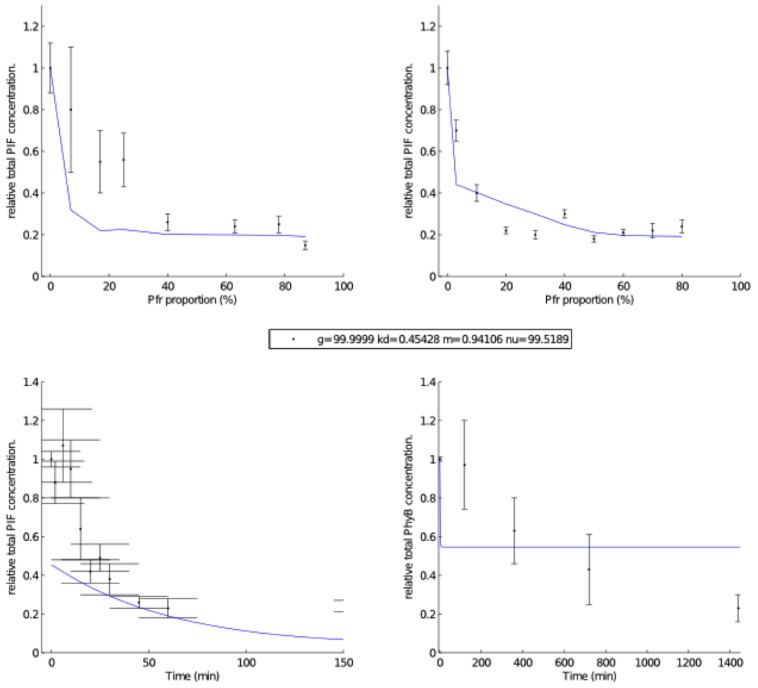

(a) Double Tagging

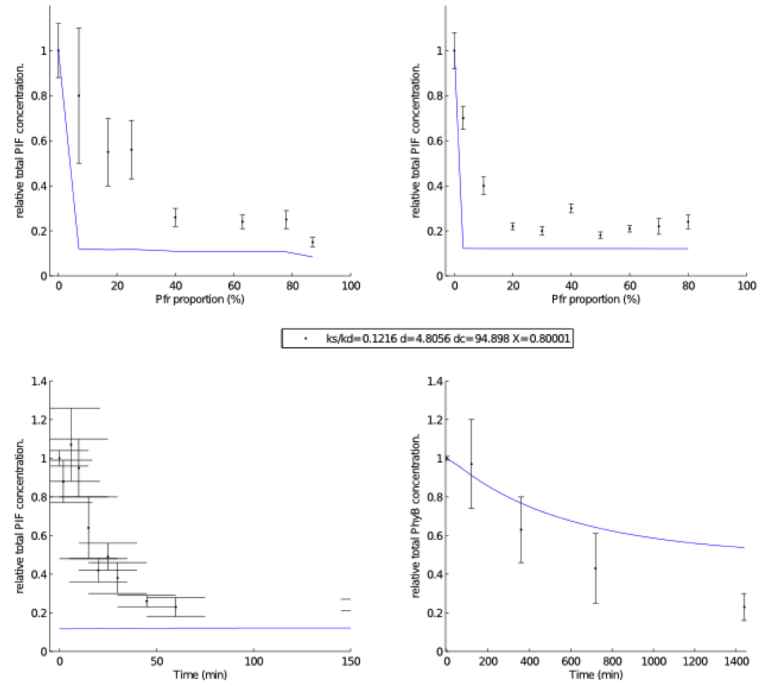

(b) protection

Figure S1.1: Multi Experiment Fit of (a). *Double Tagging* (S1.4) (b).*Protection* (S1.5) Models to Quantitative Data Shown in Figure (3.7).

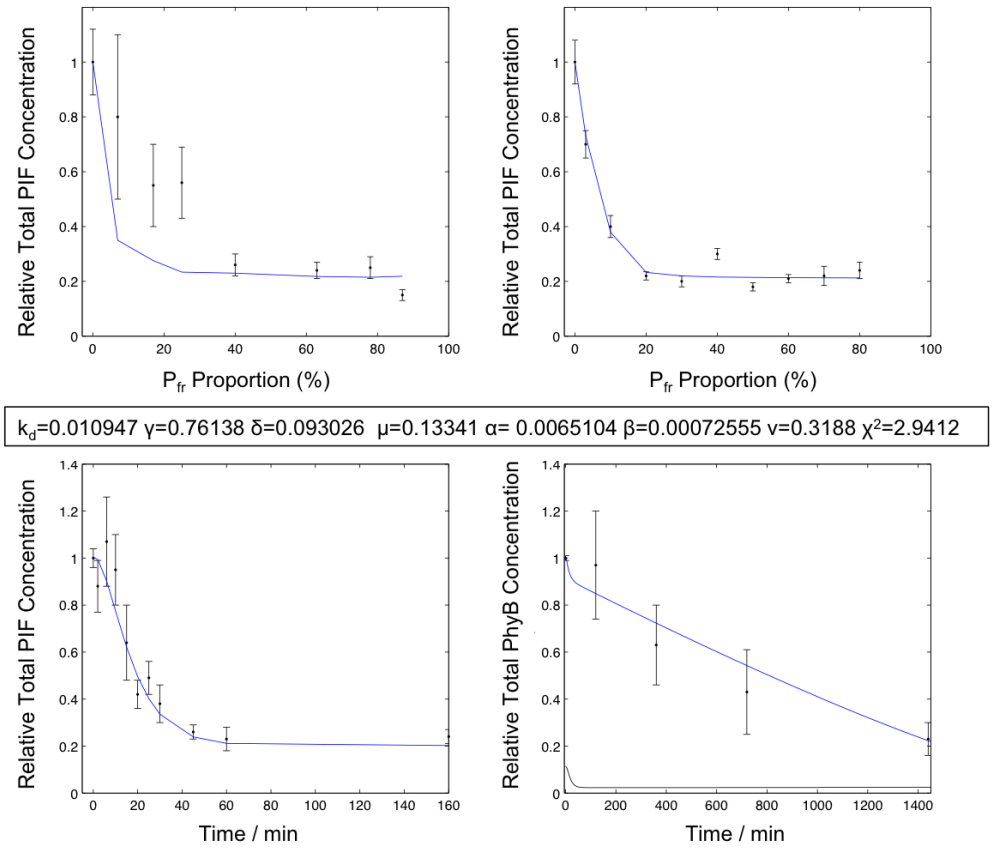

Figure S1.2: Complex Formation Rate (γ) Will Remove Constant Light Phenotype even if it is relatively low (0.76))

Repeat of plot from Figure (3.17) with a different parameter set. Parameter (γ) is much lower than previously but still removes the constant light phenotype.

$$
\begin{aligned}
\lim_{t\to\infty} Y &= \frac{-\delta+\gamma-\delta\gamma phyB+\sqrt{4\delta\gamma+(\delta-\gamma+\delta\gamma phyB)^2}}{2\gamma} \\
\lim_{t\to\infty} C &= \frac{1+\frac{\delta}{\gamma}+\delta phyB-\frac{\sqrt{4\delta\gamma+(\delta-\gamma+\delta\gamma phyB)^2}}{\gamma}}{2\delta} \\
\lim_{t\to\infty} Y_t &= \frac{1+\frac{\delta}{\gamma}+\delta phyB-\frac{\sqrt{4\delta\gamma+(\delta-\gamma+\delta\gamma phyB)^2}}{\gamma}}{2\mu} \\
\lim_{t\to\infty} Y_{tot} &= \tfrac{1}{2\delta\gamma\mu}[\gamma\mu-\delta^2(\mu-1)(1+\gamma phyB)-\delta\sqrt{4\delta\gamma+(\delta-\gamma+\delta\gamma phyB)^2} \\
&\quad -\mu\sqrt{4\delta\gamma+(\delta-\gamma+\delta\gamma phyB)^2}+\delta\mu\sqrt{4\delta\gamma+(\delta-\gamma+\delta\gamma phyB)^2} \\
&\quad +\delta(\mu+\gamma(\mu phyB+\mu+1))]
\end{aligned}
\tag{S1.11}
$$

PIF degradation in Time, Pulsed and Constant Light

$$
\begin{aligned}
\dot{P_{fr}} &= k_1(phyB-P_{fr}-C)-k_2P_{fr}-\gamma P_{fr}Y+\delta C \\
\dot{Y} &= 1-Y-\gamma P_{fr}Y+k_2C \\
\dot{C} &= \gamma P_{fr}Y-\delta C-k_2C \\
\dot{Y_t} &= \delta C-\mu Y_t
\end{aligned}
\tag{S1.12}
$$

Phytochrome Dimers

$$
\begin{aligned}
\dot{P_{fr}P_r} &= k_1(phyB-P_{fr}P_r-P_{fr}P_{fr}-C)-dd(k_1+k_2)P_{fr} \\
\dot{P_{fr}P_{fr}} &= dd(k_1P_{fr}P_r)-k2P_{fr}P_{fr}-\gamma P_{fr}P_{fr}Y+\delta C \\
\dot{Y} &= 1-Y-\gamma P_{fr}P_{fr}Y+k_2C \\
\dot{C} &= \gamma P_{fr}P_{fr}Y-(\delta+k_2)C \\
\dot{Y_t} &= \delta C-\mu Y_t
\end{aligned}
\tag{S1.13}
$$

Modified Double Tagging

$$\begin{aligned}
\dot{P}_r &= \alpha - (\beta + k_1)P_r + k_2 P_{fr} \\
\dot{P_{fr}} &= k_1 P_r - (\beta + k_2)P_{fr} - \gamma(P_{fr} + P_y)Y \\
\dot{P}_y &= \delta C - \gamma P_y Y - (\beta + \nu)P_y \\
\\
\dot{Y} &= 1 - Y - \gamma(P_{fr} + P_y)Y + k_2 C \\
\dot{Y}_t &= \delta C - \mu Y_t \\
\\
\dot{C} &= \gamma(P_{fr} + P_y)Y - \delta C - k_2 C
\end{aligned} \tag{S1.14}$$

Phytochrome Import

$$\begin{aligned}
\dot{P}_r &= -\left(k_1 + \beta\right) P_r + \left(k_2 + k_r\right) P_{fr} + \alpha \\
\dot{P_{fr}} &= k_1 P_r - \left(k_2 + k_r + \beta\right) P_{fr} - k_{in} P_{fr} \\
\dot{P_{fr}^n} &= k_1 P_r^n - \left(k_2 + k_r + \beta\right) P_{fr}^n - \gamma P_{fr}^n PIF + k_{in} P_{fr} \\
\dot{P_r^n} &= -\left(k_1 + \beta\right) P_r^n + \left(k_2 + k_r\right)\left(P_{fr}^n\right) \\
\dot{PIF} &= k_d\left(1 - PIF\right) - \gamma\left(P_{fr}^n + P_{fr}^t\right) PIF + \left(k_2 + k_r\right) C \\
\dot{C} &= \gamma P_{fr}^n PIF - \left(\delta + k_2 + k_r\right) C \\
\dot{PIF^t} &= \delta\left(C + PIF^t P_{fr} + PIF P_{fr}^t + PIF^t P_{fr}^t\right) - \left(\mu + \gamma\left(P_{fr}^t + P_{fr}^n\right)\right) PIF^t \\
\dot{P_{fr}^t} &= \delta\left(C + PIF^t P_{fr} + PIF P_{fr}^t + PIF^t P_{fr}^t\right) - \left(\nu + \gamma\left(PIF^t + PIF\right)\right) P_{fr}^t \\
\dot{PIF^t P_{fr}} &= \gamma P_{fr}^t PIF - \delta PIF^t P_{fr} - \left(k_2 + k_r\right) PIF^t P_{fr} \\
\dot{PIF P_{fr}^t} &= \gamma P_{fr}^n PIF^t - \delta PIF P_{fr}^t \\
\dot{PIF^t P_{fr}^t} &= \gamma P_{fr}^t PIF^t - \delta PIF^t P_{fr}^t
\end{aligned} \tag{S1.15}$$

Table S1.1: Parameter set of (S1.10) plotted in Figure (3.10b): PIF3 degradation

Parameter	Value
γ	2.5801
k_d	0.013264
δ	0.1126
μ	0.11352
x	10.7154

Table S1.2: Parameter set of (S1.11) plotted in Figure (3.11): PIF3 degradation and Steady State

Parameter	Value
γ	19.8487
k_d	0.013166
δ	0.55473
μ	0.071067
x	0.17525

Table S1.3: Parameter set of (4.4) plotted in Figure (3.12b): PIF3 degradation, Pulsed and Constant Light

Parameter	Value
γ	0.010275
k_d	0.011383
δ	0.070188
μ	0.90659
$phyB$	99.6663

Table S1.4: Parameter set of (3.9) plotted in Figure (3.13): Modified Double Tagging

Parameter	Value
γ	0.082203
k_d	0.011383
δ	0.070188
μ	0.90659
α	0.010206
β	0.0008192
x	12.4584961
ν	10

Table S1.5: Parameter set of (S1.13) plotted in Figure (3.25): PhyB Dimer

Parameter	Value
γ	0.92875
k_d	0.011788
δ	0.089038
μ	0.16346
x	82.8721

Table S1.6: Mathematical Description of Constant Light Conditions

$P_{fr}\%$	λ	Fluence ($\mu molm^{-2}s^{-1}$)	k_1	k_2
0	Dark	0	0	0
7	725	6.8	0.012	0.158
17	716	2.4	0.070	0.350
25	708	5.9	0.043	0.127
40	703	2.3	0.177	0.261
63	692	2.3	0.184	0.109
78	699	5.0	0.218	0.061
87	685	1.4	1.775	0.273

Table S1.7: Mathematical Description of Pulsed Light Conditions

$P_{fr}\%$	λ	Fluence ($\mu molm^{-2}s^{-1}$)	k_1	k_2
0	Dark	0	0	0
3	660	0.1	0.025	0.003
10	660	0.4	0.101	0.013
20	660	0.9	0.227	0.030
30	660	1.4	0.354	0.047
40	660	2.1	0.530	0.070
50	660	2.9	0.732	0.097
60	660	4.0	1.010	0.134
70	660	5.6	1.414	0.187
80	660	8.5	2.147	0.285

Appendix S2

Supplementary Figures Related to Chapter 4

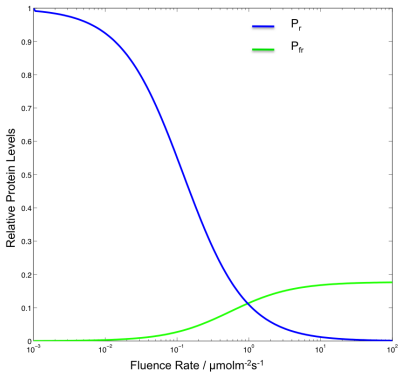

Figure S2.1: Fluence Rate Dependency of Rauserberger 2010 Model

Phytochrome P_r to P_{fr} % from a previously described model of Phytochrome Nuclear Compartmentalisation [16]

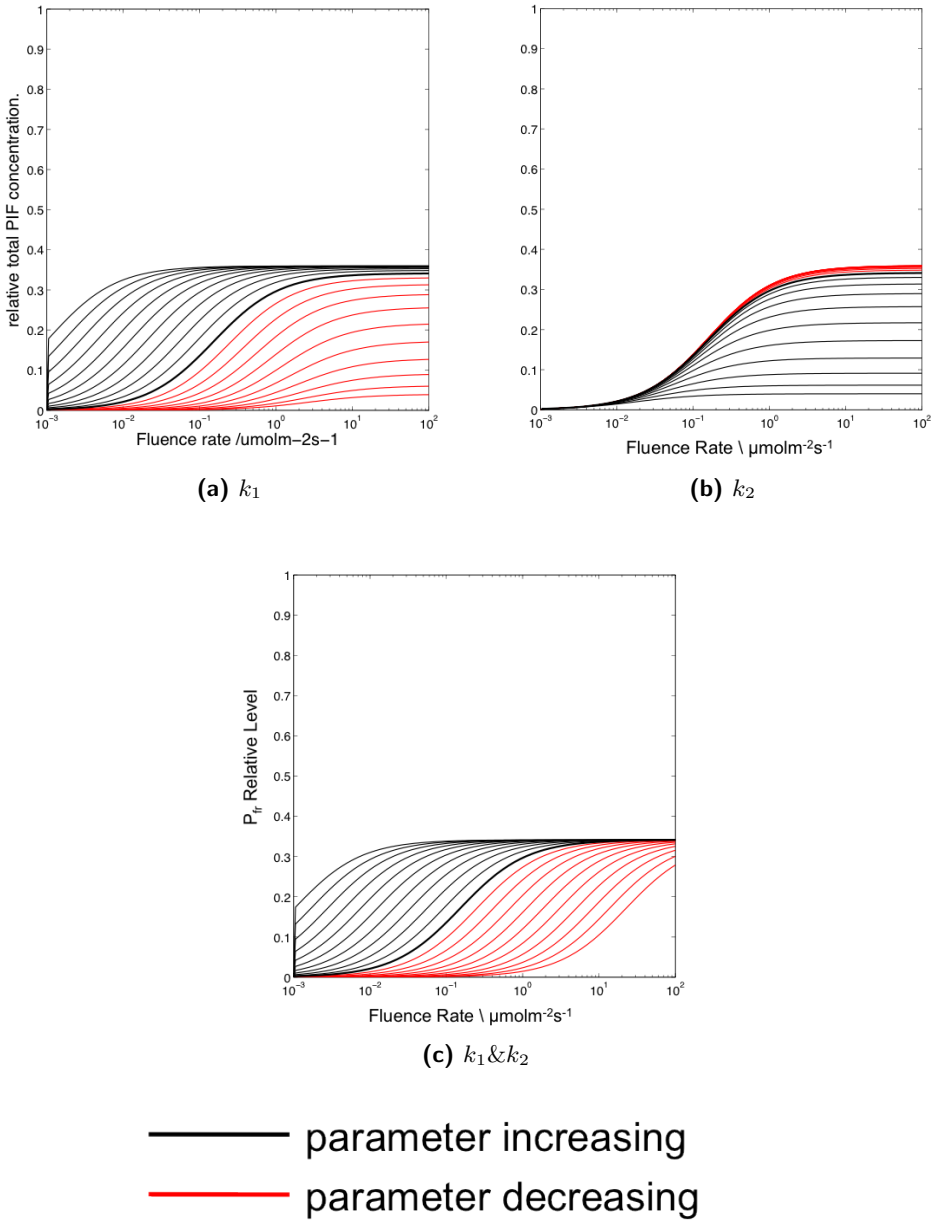

(a) k_1 **(b)** k_2

(c) k_1&k_2

Figure S2.2: Fluence Dependency of P_{fr} Levels if phyB Photoconversion Parameters k_1 and k_2 are Allowed to Vary

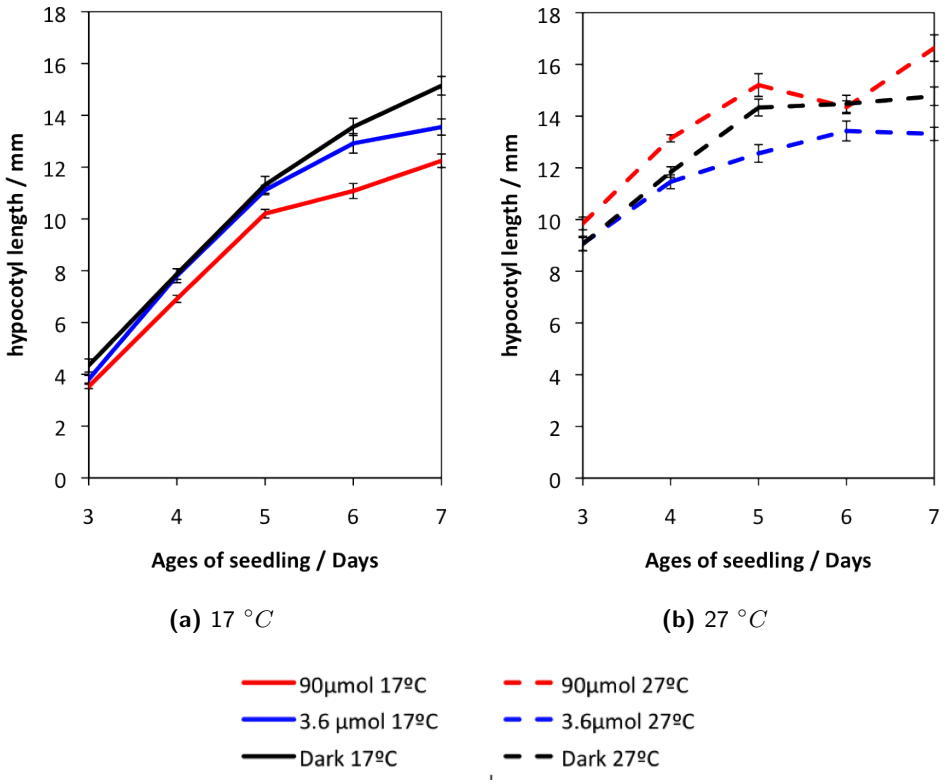

(a) 17 $^{\circ}C$ **(b)** 27 $^{\circ}C$

Figure S2.3: Hypocotyl Growth of *phyB* Mutant at Different Light Intensities 17 & 27 $^{\circ}C$

The *phyB* mutant shows temperature dependent growth early on but this is lost in early seedlings. The 5 day old phenotype seen previously in not repeated in Columbia [116]

.

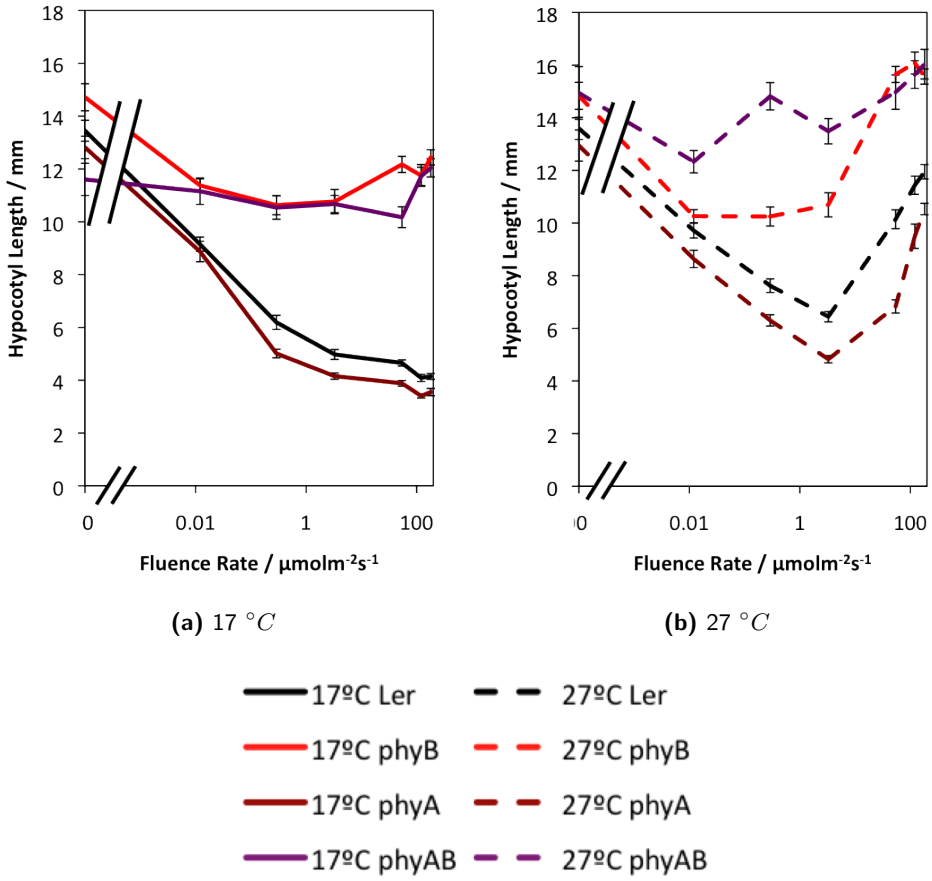

(a) 17 $^{\circ}C$ **(b)** 27 $^{\circ}C$

Figure S2.4: Hypocotyl Phenotype of Phytochrome Mutants in *Landsberg erecta* over a Fluence Curve at 17 & 27 $^{\circ}C$

High Intensity response of phyAB in 17 & 27 $^{\circ}C$ shows no phytochrome A high intensity effect.

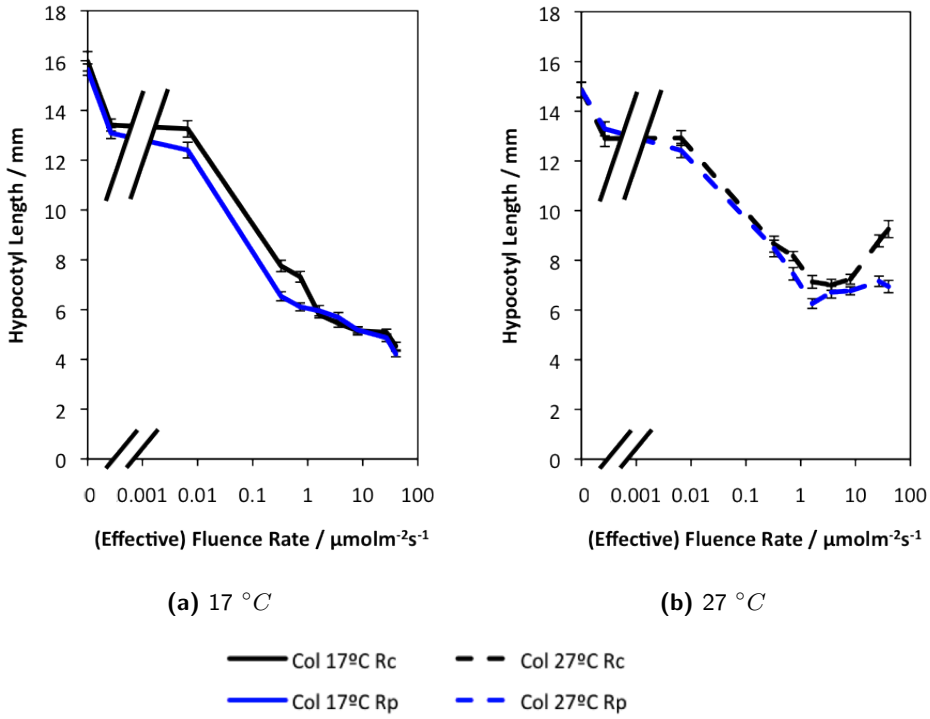

(a) 17 $^{\circ}C$ **(b)** 27 $^{\circ}C$

Figure S2.5: High Intensity Pulses Given Every 10 Minutes can Produce a Partial HIR

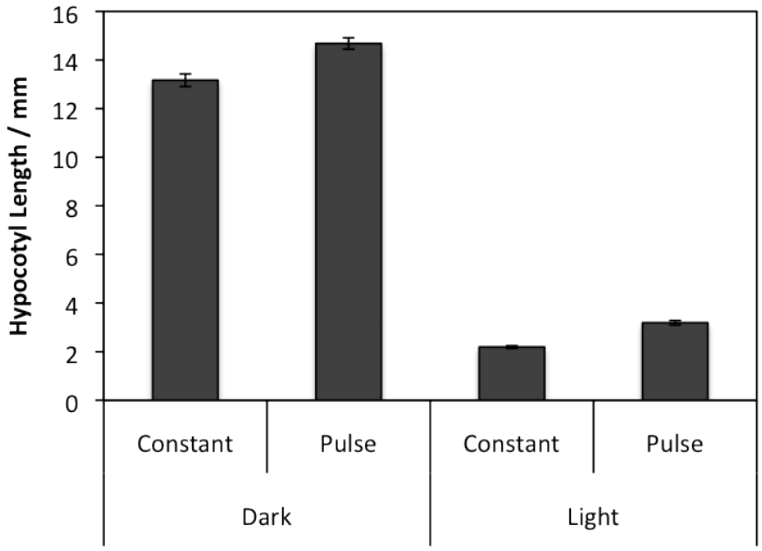

Figure S2.6: Hypocotyl Length of 11 day old Seedlings Grown at 12$^{\circ}C$ Under Constant Light or High Intensity Light Pulses.

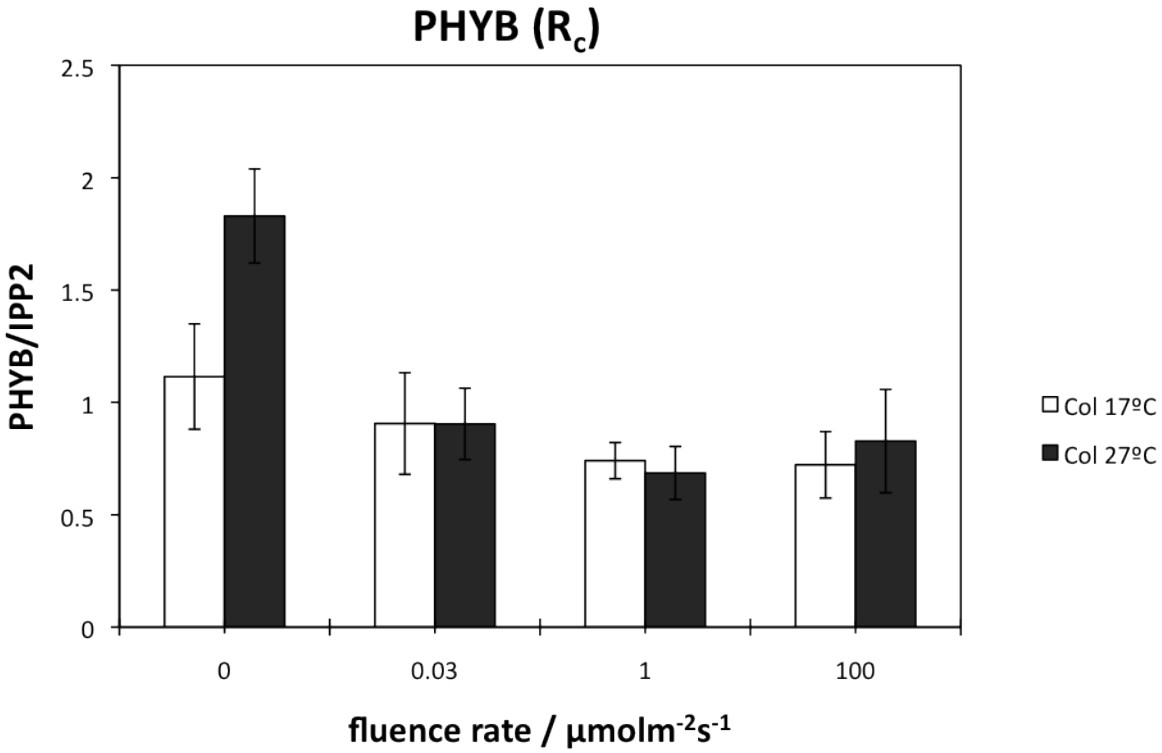

Figure S2.7: phyB RNA levels from seedlings grown for 7 days in different fluence rates at 17°C and 27°C

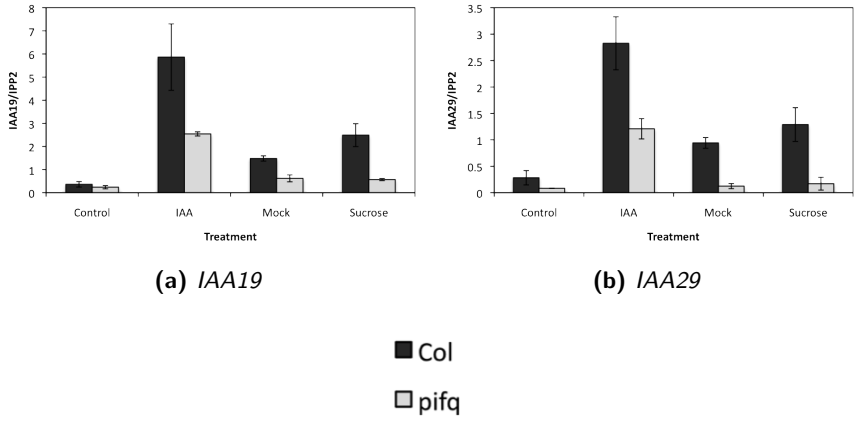

(a) *IAA19* **(b)** *IAA29*

Figure S2.8: Expression of Auxin Response Genes after Treatment with IAA or Sucrose on *Col* and *pifq* Compared to a Solvent Mock Treatment

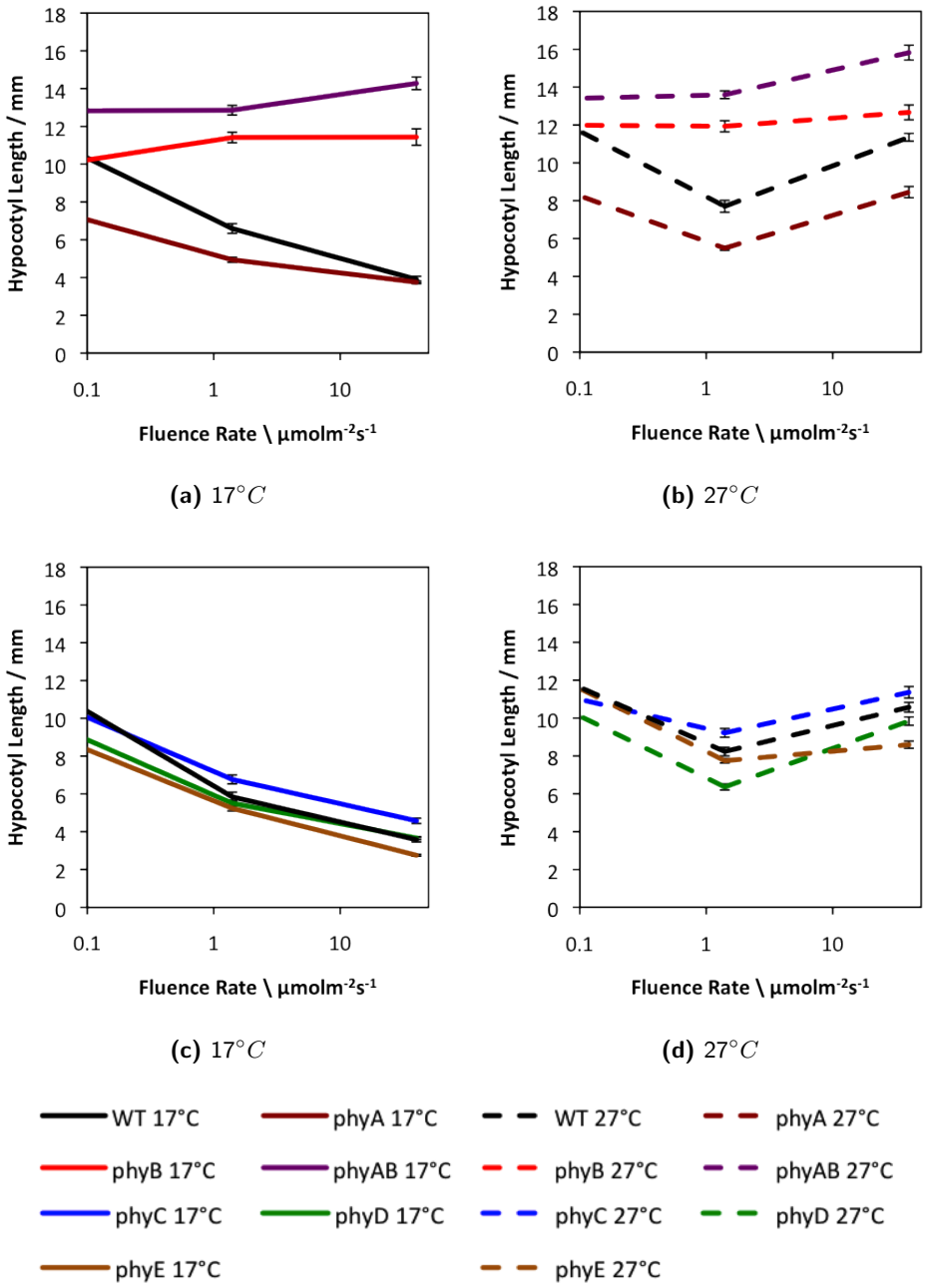

(a) $17°C$ **(b)** $27°C$

(c) $17°C$ **(d)** $27°C$

Figure S2.9: Hypocotyl Phenotype of Phytochrome Mutants over a Fluence Curve at 17 & $27°C$

(a,b) *phyA*, *phyB*, *phyAB*
(c,d) *phyC*, *phyD*, *phyE*
Experiments for these figures were done by Henrik Johansson

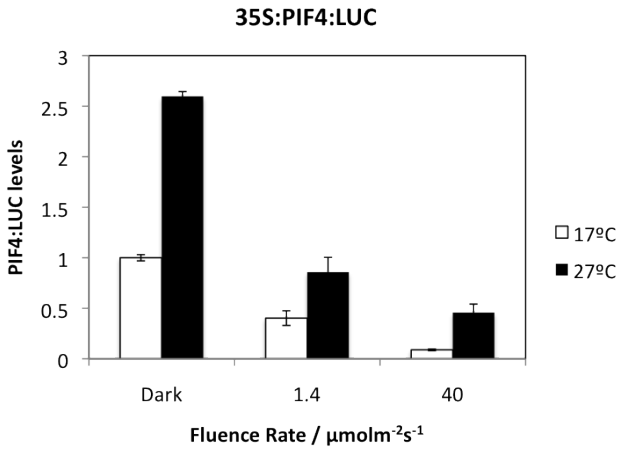

Figure S2.10: PIF4 LUC Levels over a Fluence Curve

Quantitive measurement of 35S:PIF4:LUC grown at 17 or 27°C over a fluence curve. There is a degradation of the protein relative to fluence with an increase in levels at high temperature.
Experiments for these figures were done by Henrik Johansson

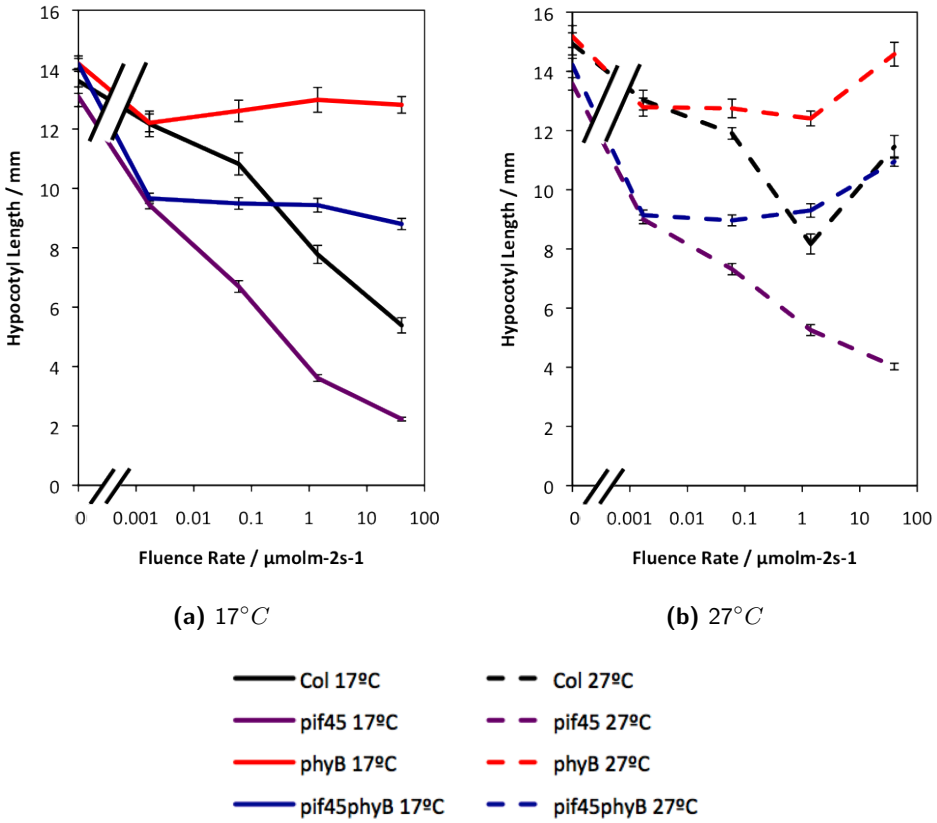

(a) $17°C$ **(b)** $27°C$

Figure S2.11: Hypocotyl Length of *pif45phyB* Triple Mutants Grown at 17 and $27°C$

Experiments for these figures were done by Henrik Johansson

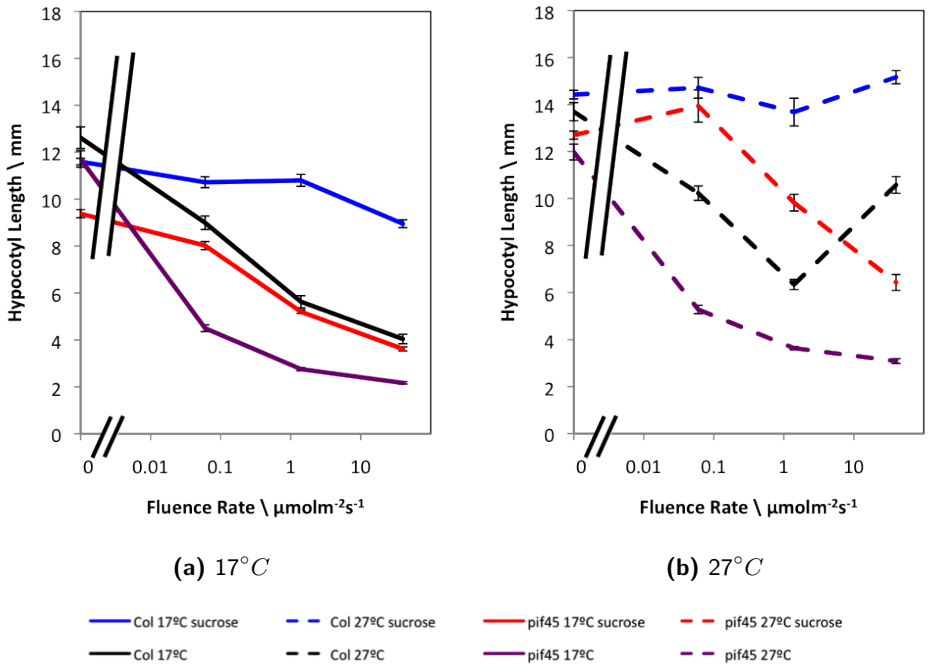

(a) $17^{\circ}C$ **(b)** $27^{\circ}C$

Figure S2.12: Seedlings Treated with Sucrose Compared to Previous Experiment of no Sucrose (Figure 4.24)

Experiments for these figures were done by Henrik Johansson

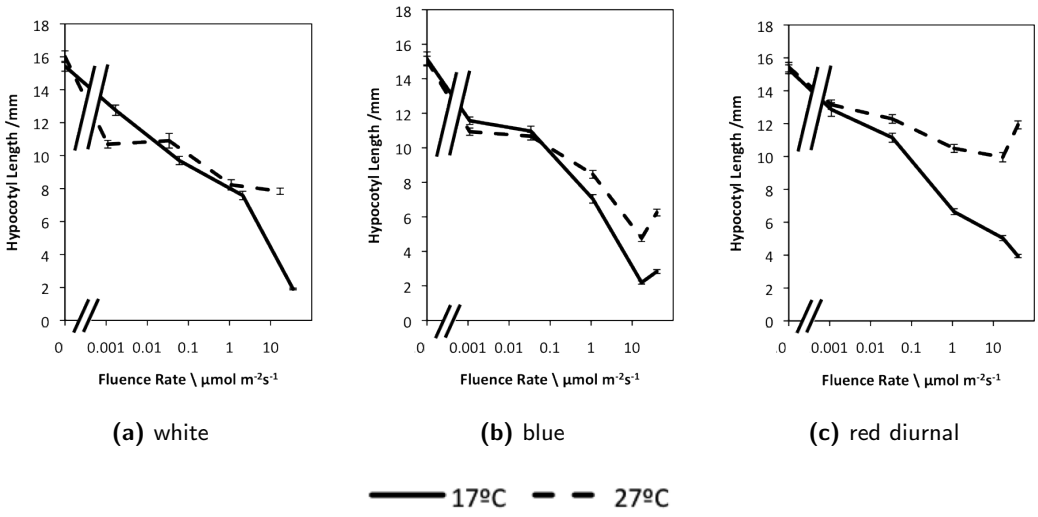

(a) white **(b)** blue **(c)** red diurnal

Figure S2.13: Temperature Effect in Constant white, blue and red Diurnal Light

Experiments for these figures were done by Henrik Johansson

Appendix S3

Supplementary Figures Related to Chapter 5

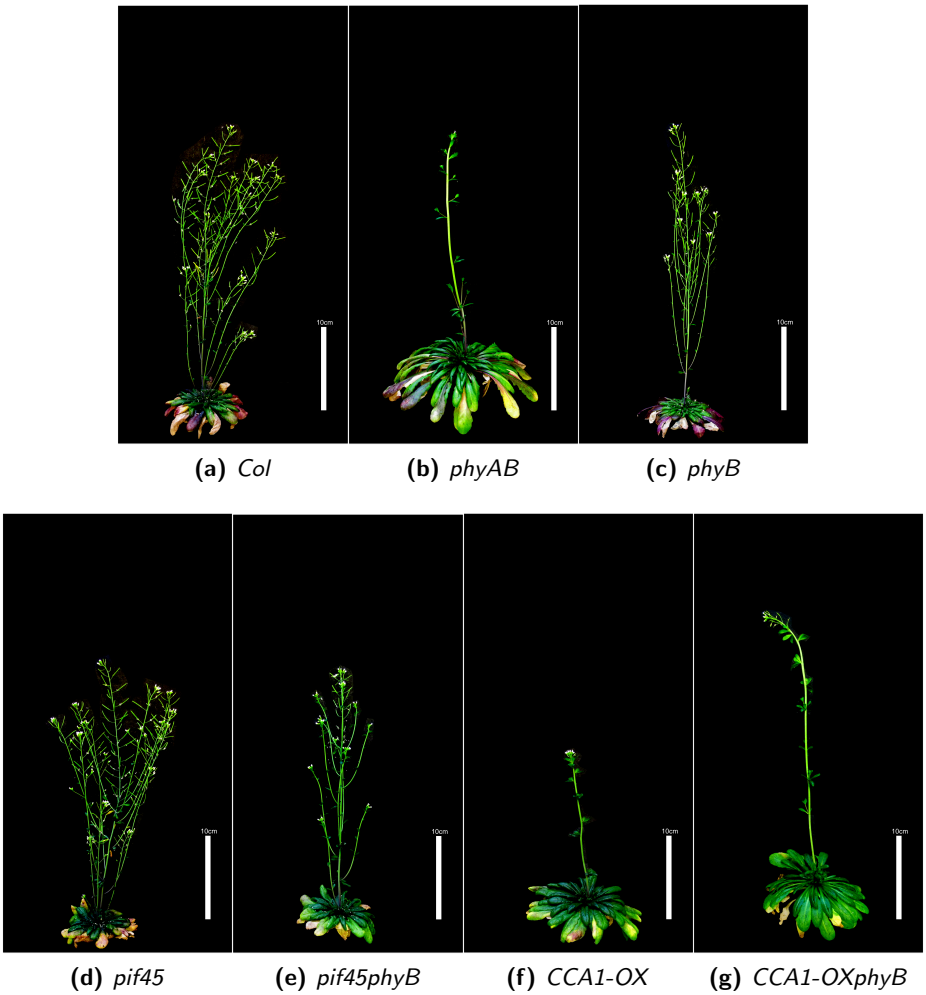

(a) *Col* **(b)** *phyAB* **(c)** *phyB*

(d) *pif45* **(e)** *pif45phyB* **(f)** *CCA1-OX* **(g)** *CCA1-OXphyB*

Figure S3.1: Photograph of 122 day old Mutant Plants Grown at 17 $^{\circ}C$

Scale Bar Represents 10cm

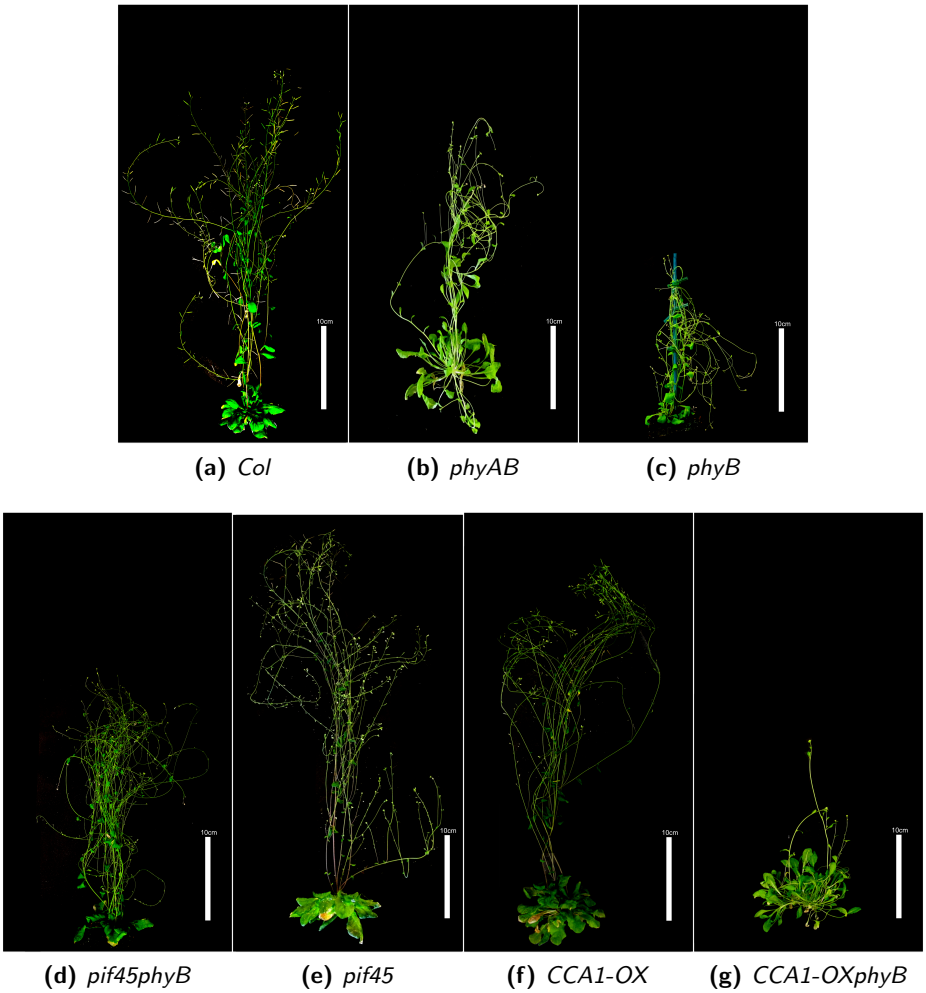

(a) *Col* **(b)** *phyAB* **(c)** *phyB*

(d) *pif45phyB* **(e)** *pif45* **(f)** *CCA1-OX* **(g)** *CCA1-OXphyB*

Figure S3.2: Photograph of Mutant Plants Grown at 27 $^{\circ}C$

Scale Bar Represents 10cm

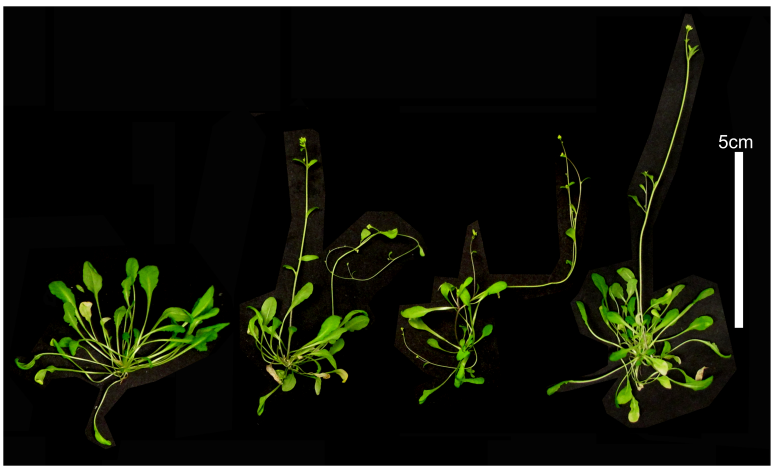

Figure S3.3: Separated Rosettes of a Single *CCA1-OXphyB* Plant (Figure S3.2g) Showing Severe Loss of Shoot Apical Meristem Identity

Scale Bar Represents 5cm

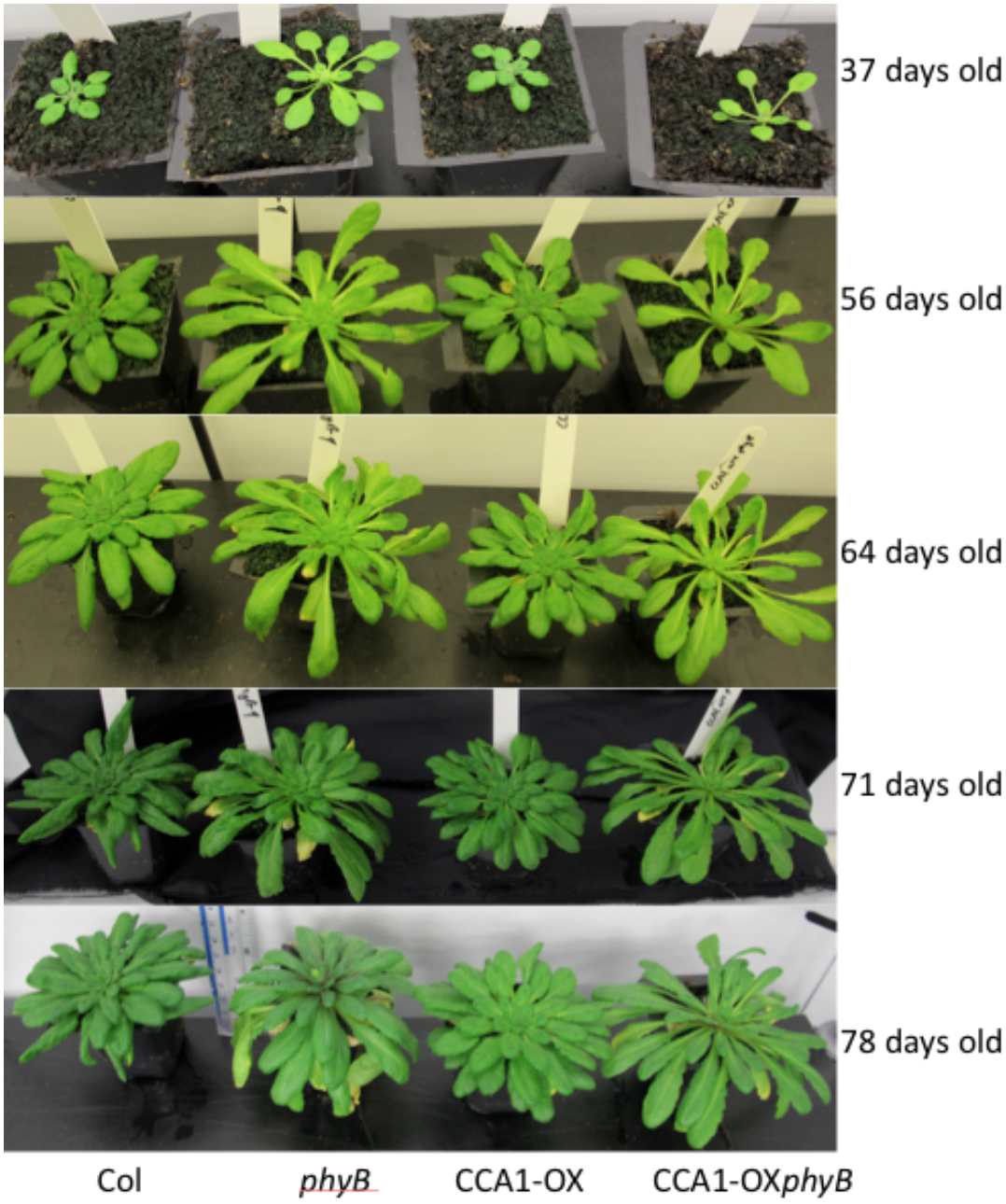

Figure S3.4: Growth Phenotypes of *Col*, *phyB*, *CCA1-OX* and *CCA1-OXphyB* Mutants Grown at 17°C

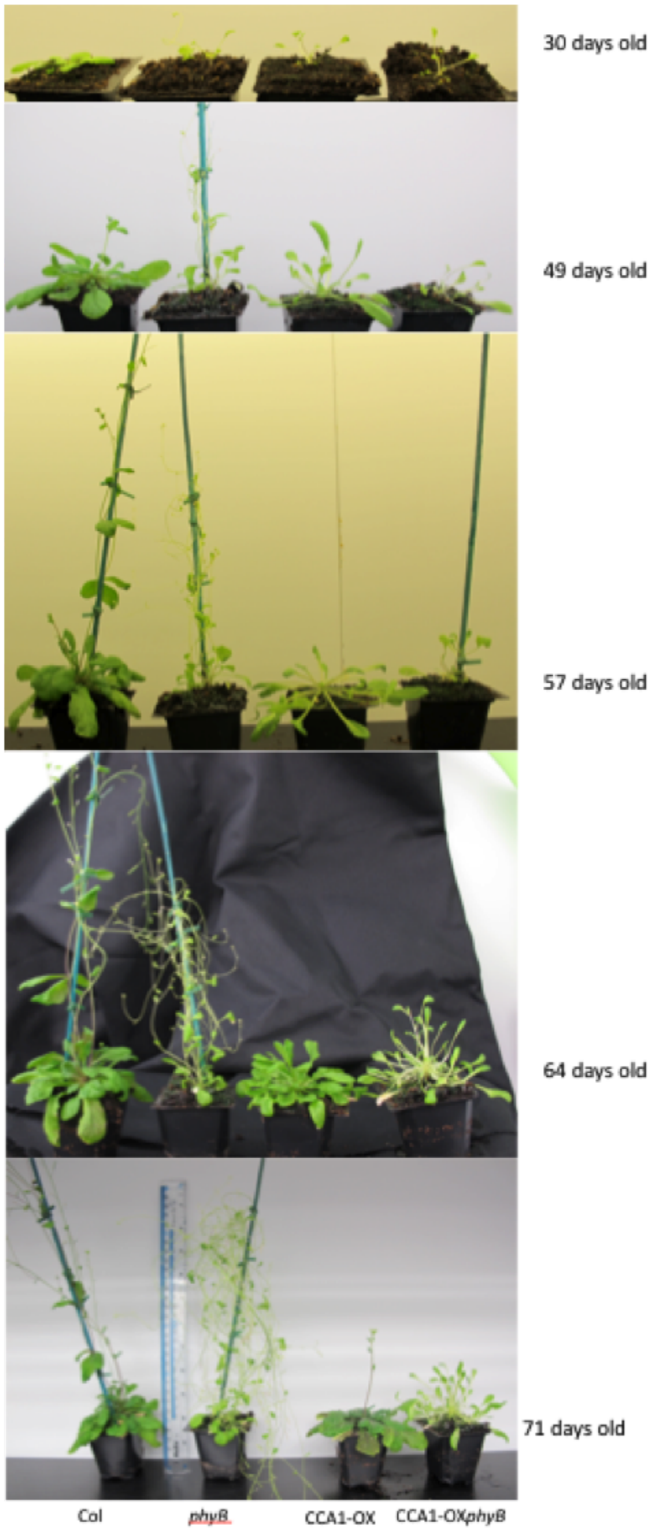

Figure S3.5: Growth Phenotypes of *Col*, *phyB*, *CCA1-OX* and *CCA1-OXphyB* Mutants Grown at 27°C

Figure S3.6: Growth Phenotypes of *Col*, *phyB*, *pif45* and *pif45phyB* Mutants Grown at $17°C$

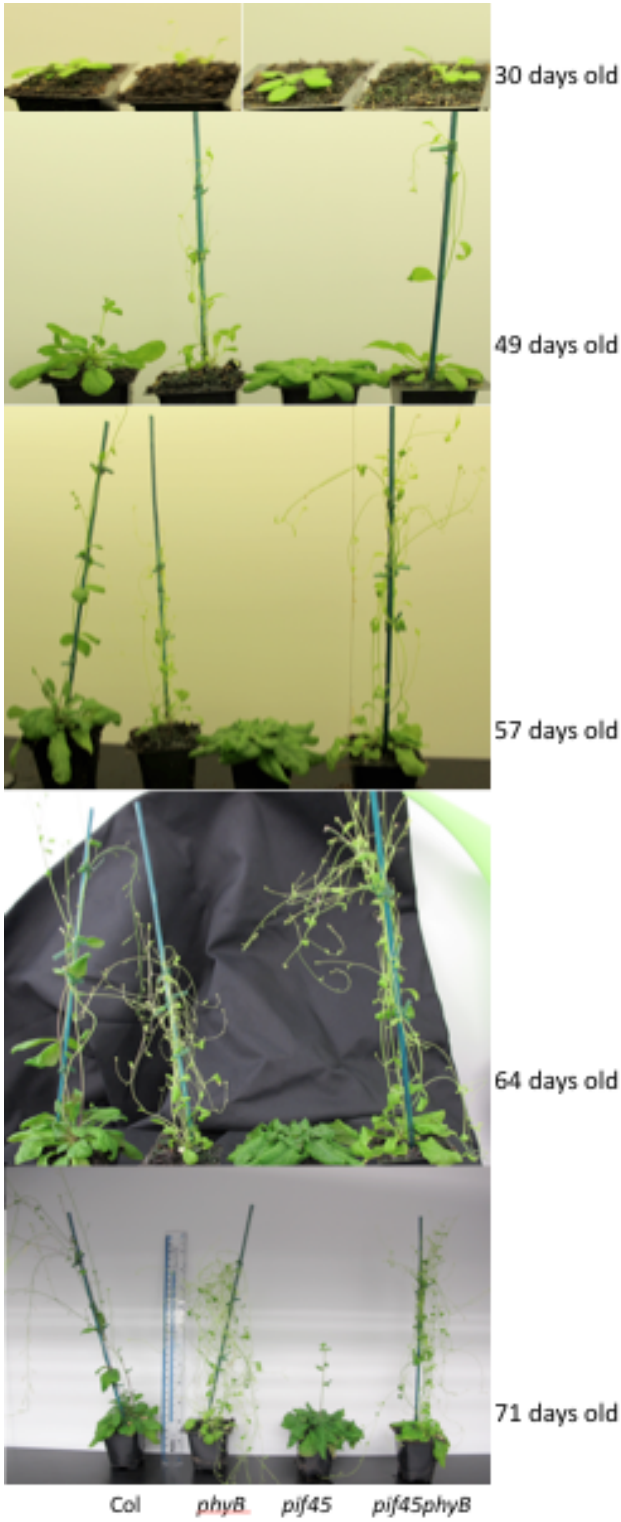

Figure S3.7: Growth Phenotypes of *Col*, *phyB*, *pif45* and *pif45phyB* Mutants Grown at $27°C$

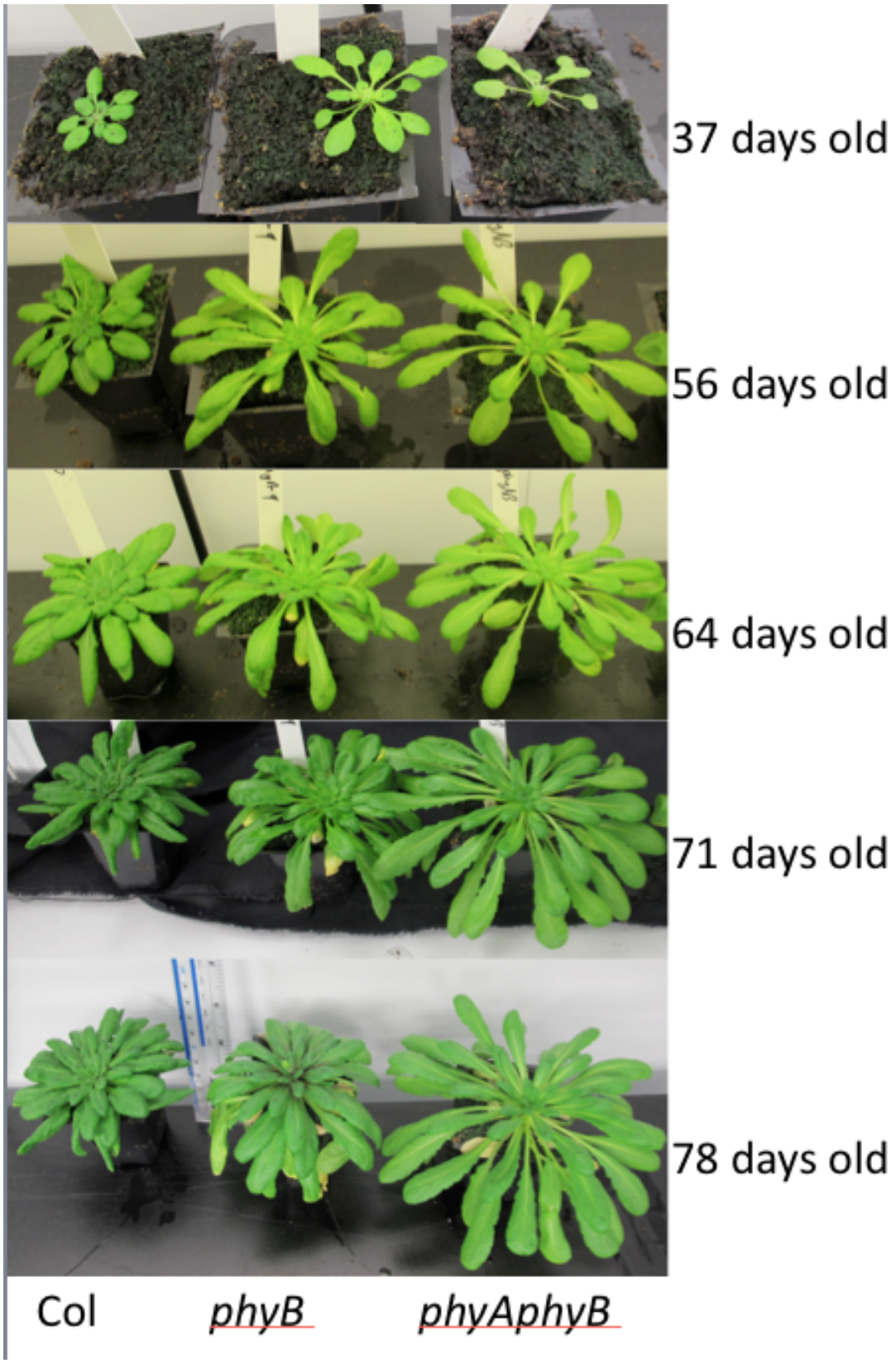

Figure S3.8: Growth Phenotypes of *Col*, *phyB* and *phyAB* Mutants Grown at 17°C

Figure S3.9: Growth Phenotypes of *Col*, *phyB* and *phyAB* Mutants Grown at 27°C

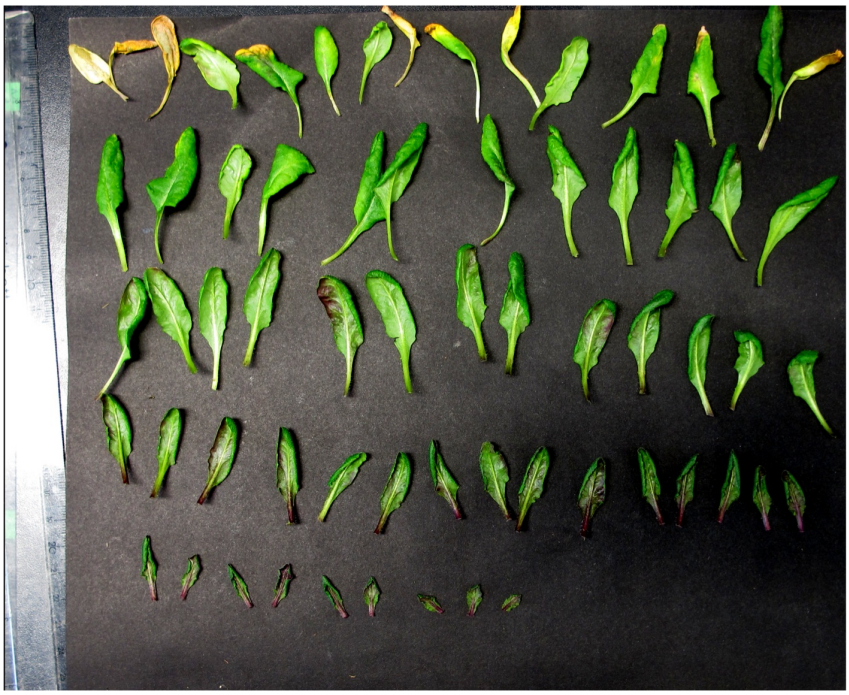

(a) 17°C

(b) 27°C

Figure S3.10: Photo of Leaves of *Col* Plants Grown at 17 and 27°C

(a) 17°C

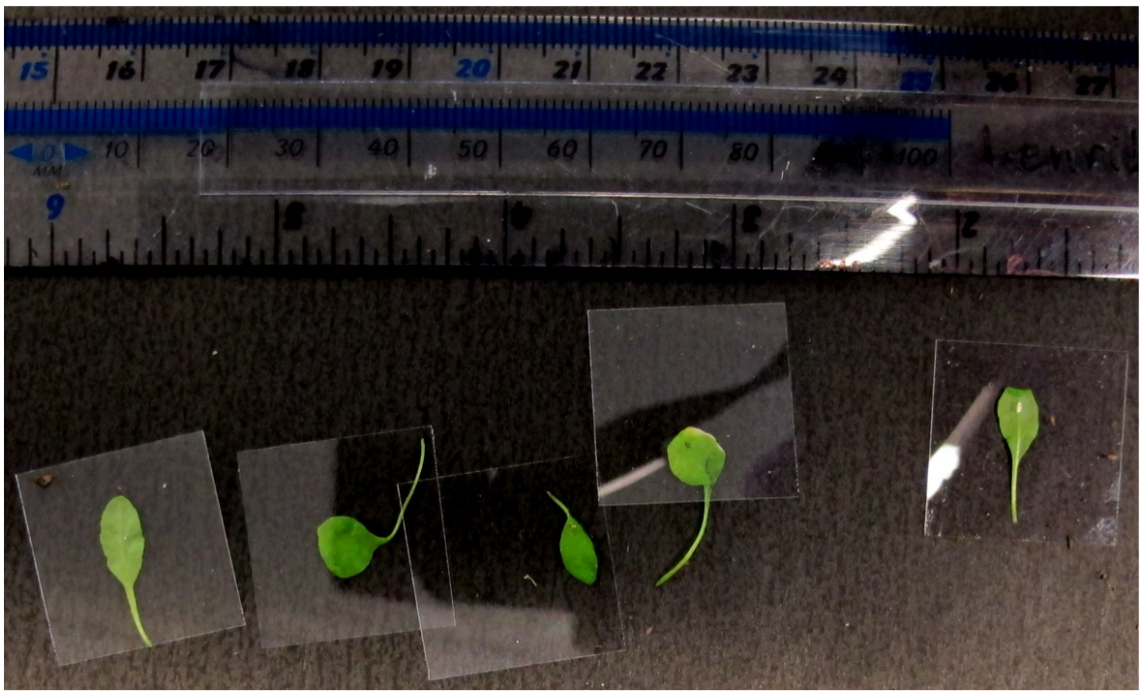

(b) 27°C

Figure S3.11: Photo of Leaves of *phyB* Plants Grown at 17 and 27°C

(a) 17°C

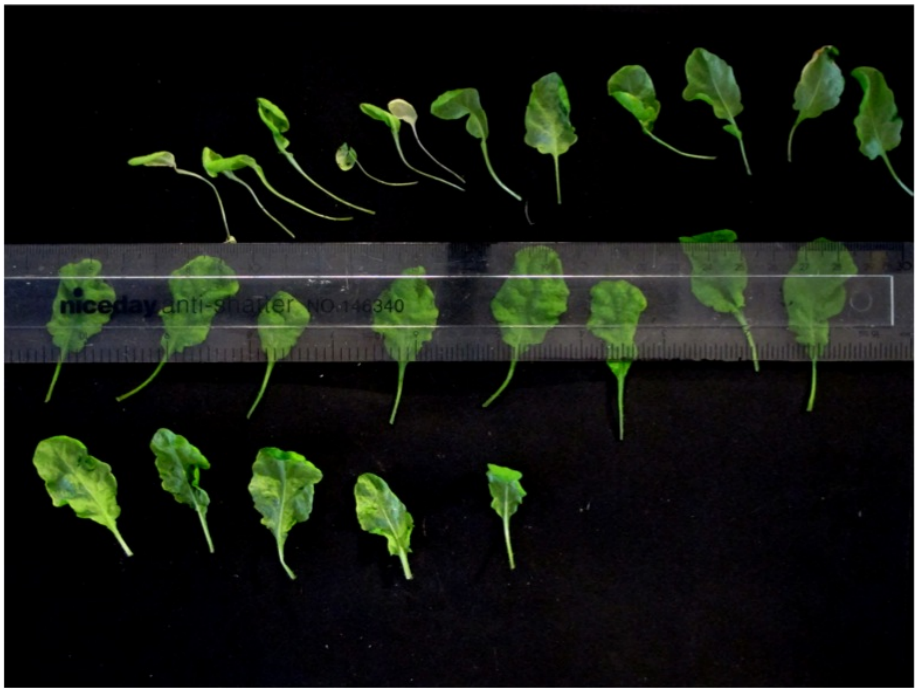

(b) 27°C

Figure S3.12: Photo of Leaves of *CCA1-OX* Plants Grown at 17 and 27°C